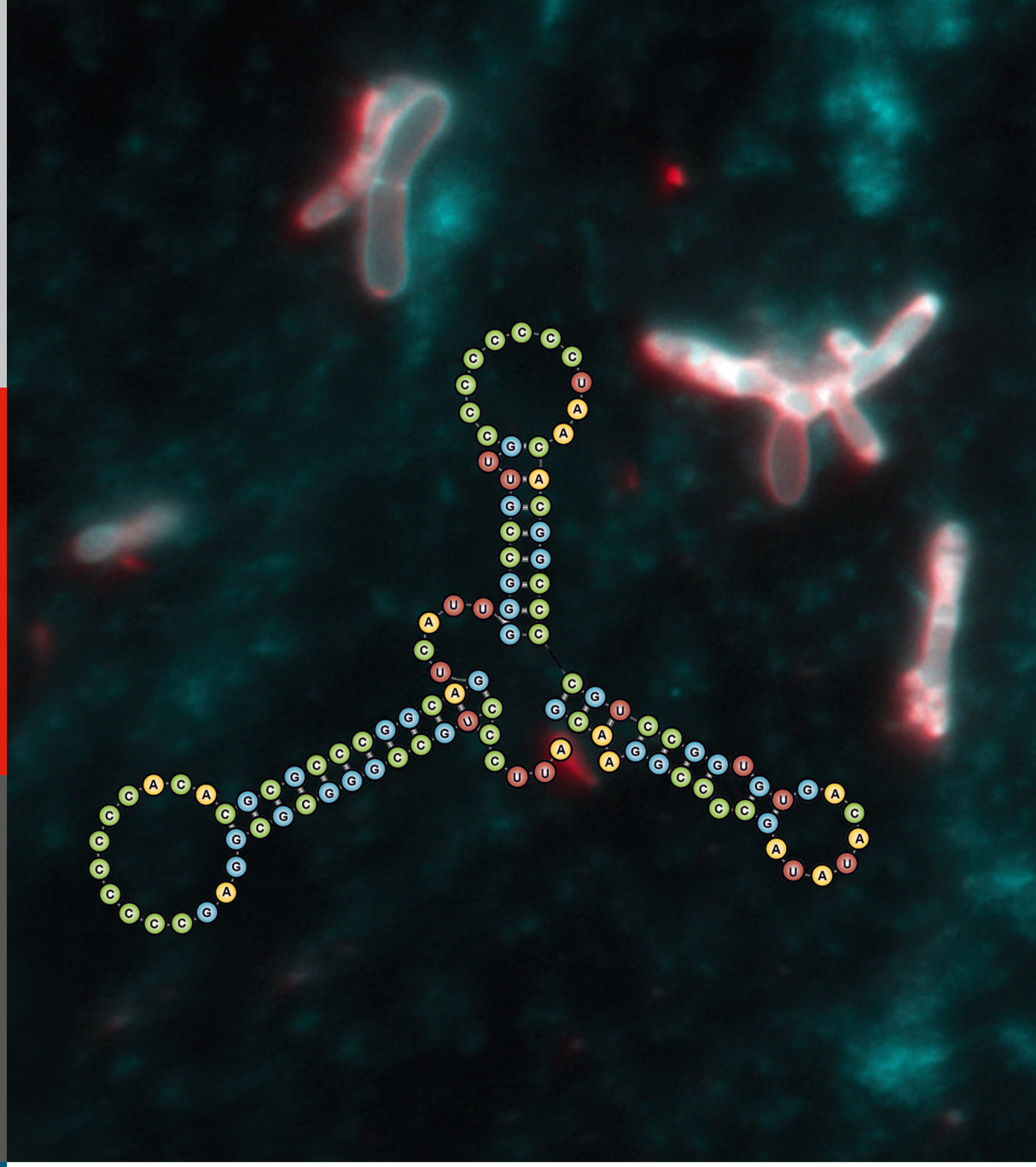

The 6C RNA of *Corynebacterium glutamicum*

Jennifer Pahlke

Member of the Helmholtz Association

JÜLICH
FORSCHUNGSZENTRUM

Schriften des Forschungszentrums Jülich
Reihe Gesundheit / Health Band / Volume 76

Forschungszentrum Jülich GmbH
Institute of Bio- and Geosciences (IBG)
Biotechnology (IBG-1)

The 6C RNA of *Corynebacterium glutamicum*

Jennifer Pahlke

Schriften des Forschungszentrums Jülich
Reihe Gesundheit / Health

Band / Volume 76

ISSN 1866-1785

ISBN 978-3-95806-003-6

Bibliographic information published by the Deutsche Nationalbibliothek.
The Deutsche Nationalbibliothek lists this publication in the Deutsche Nationalbibliografie; detailed bibliographic data are available in the Internet at http://dnb.d-nb.de.

Publisher and Distributor: Forschungszentrum Jülich GmbH
Zentralbibliothek
52425 Jülich
Tel: +49 2461 61-5368
Fax: +49 2461 61-6103
Email: zb-publikation@fz-juelich.de
www.fz-juelich.de/zb

Cover Design: Grafische Medien, Forschungszentrum Jülich GmbH

Printer: Grafische Medien, Forschungszentrum Jülich GmbH

Schriften des Forschungszentrums Jülich
Reihe Gesundheit / Health, Band / Volume 76

D 61 (Diss. Düsseldorf, Univ., 2014)

ISSN 1866-1785
ISBN 978-3-95806-003-6

The complete volume is freely available on the Internet on the Jülicher Open Access Server (JuSER) at www.fz-juelich.de/zb/openaccess

Content

Abbreviations

Amp^R	ampicillin resistance
ATCC	American Type Culture Collection
BHI(S)	brain heart infusion (+Sorbitol)
BSA	bovine serum albumine
bidist.	bidistilled
bp	base pair(s)
cDNA	complementary deoxyribonucleic acid
DAPI	4'-6-diamidino-2-phenylindole
DIG	digoxigenin
DIG-11-dUTP	digoxigenin-11-2'-deoxy-uridine-5'- triphosphate
DMSO	dimethylsulfoxide
dNTP	deoxynucleoside triphosphate
ds	double-stranded
DTT	dithiothreitol
Δ	delta
EDTA	ethylenediaminetetraacetic acid
e.g.	example given
et al.	*et alii* (latin: and others)
EtOH	ethanol
Fig.	figure
g	standard gravity (9.81 m s^{-2})
i.e.	id est (latin: that is)
IGR	intergenic region
IPTG	isopropyl-thio-β-D-galactopyranosid
Kan^R	kanamycin resistance
LB	Luria Bertani
MALDI	matrix-assisted laser desorption ionisation
MCS	multiple cloning site
MWCO	molecular weight cut-off
MOPS	3-morpholinopropanesulfonic acid
MS	mass spectrometry
mRNA	messenger ribonucleic acid
μ	growth rate
NaOAc	sodium acetate
NAD(H)	nicotinamide adenine dinucleotide (reduced)

OD_{600}	optical density at 600 nm
PAGE	polyacrylamide-gel electrophoresis
PBS	phosphate buffered saline
PCR	polymerase chain reaction
pH	negative decimal logarithmic value of hydrogen ion concentration
rpm	rounds per minute
rRNA	ribosomal ribonucleic acid
SDS	sodium dodecylsulfate
sec	second(s)
ss	single-stranded
TAE	tris-acetate/ EDTA buffer
TCA	trichloric acid
TE	tris base – EDTA
TEA	triethanolamine
TEMED	N,N,N',N'-tetramethylethylendiamin
Tm	melting temperature of DNA
TNIG	tris base– NaCl – imidazol – glycerol
TOF	time of flight
Tris	tris-(hydroxymethyl)-aminomethane
Triton X-100	4-octylphenolpolyethoxylat
TSS	transcriptional start site
tRNA	transfer ribonucleic acid
U	enzymatic activity (µmol per minute)
UV	ultraviolet
vol	volume
v/v	volume per volume
wt	wild type
w/v	weight per volume

Summary

The 6C RNA family is a class of small RNAs (sRNAs) with as yet unknown function present and conserved within the phylum *Actinobacteria*, including the Gram-positive soil bacterium *Corynebacterium glutamicum*. In this work studies were conducted to characterize properties of the 6C RNA from *C. glutamicum* ATCC 13032 and to shed light on possible physiological roles in this species. The following results were obtained:

(i) The 6C RNA was found to be present in *C. glutamicum* throughout growth in CGXII medium with glucose and exhibited RNA level changes not greater than two-fold. RNA stability tests using rifampicin revealed a 6C RNA half-life of >120 min, showing that it is a very stable sRNA. Quantitation of the 6C RNA transcripts yielded about 325 and about 260 molecules per cell in the exponential and in the stationary growth phase, respectively, which is much more compared to numbers of individual mRNAs.

(ii) 6C RNA pull-down experiments using crude protein extracts of *C. glutamicum* revealed 3-phosphoglycerate kinase (PGK) as a candidate protein interaction partner. However, an interaction of 6C RNA with purified PGK could not be confirmed yet by electrophoretic mobility shift assays, possibly indicating that a further factor is required.

(iii) The 6C RNA is not essential for *C. glutamicum* and the growth of a 6C RNA deletion mutant was very similar to the wild type under various cultivation conditions tested, except when treated with the SOS response-inducing antibiotic mitomycin C (MMC), which caused a growth defect of the Δ6C RNA mutant. Reporter fusion constructs with promoters of the LexA-regulated genes *recA*, *recN*, *cglIM* and *dnaE2* indicated that the SOS response level in the Δ6C RNA mutant is lower in the stationary growth phase compared to the wild type. This leads to the suggestion that the 6C RNA might be involved in the SOS response or plays a more general role in the stress defense of *C. glutamicum.* Complementation studies of the Δ6C RNA mutant by plasmid-born expression of the 6C RNA from its native promoter revealed an unexpected and exceptional growth phenotype in the presence of MMC. Quantitation of 6C RNA revealed an about five-fold increased level in the complemented strain.

(iv) The increased 6C RNA level resulted in an elongated cell shape under standard conditions and a dramatically branched cell shape in the presence of MMC, indicating that the 6C RNA might be involved in the regulation of cell division in *C. glutamicum*.

(v) 6C RNA deletion as well as 6C RNA overexpression led to changes in the global mRNA expression profile. Notably, the WhiB-like transcriptional regulator WhcD had a decreased mRNA level in the 6C RNA overproducer. WhcD is homologous to the septation and cell division-related regulator WhmD in *Mycobacterium smegmatis*. A Δ*whcD* mutant showed a reduced growth and a strongly altered cell morphology resembling that of the 6C RNA overproducer in the presence of MMC. Thus, the homologous proteins indeed seem to be functionally equivalent in both actinobacteria. These results suggest that the 6C RNA may have an impact on the expression of *whcD* or its mRNA stability, thereby playing a role in some aspect of septation and cell division in *C. glutamicum.*

Zusammenfassung

Die 6C RNA Familie ist eine Klasse von kleinen RNAs mit bisher unbekannter Funktion. Sie ist im Phylum *Actinobacteria*, einschließlich des Vertreters *Corynebacterium glutamicum*, einem Gram-positiven Bodenbakterium, hoch konserviert. In dieser Arbeit wurden Untersuchungen durchgeführt, um die 6C RNA in *C. glutamicum* ATCC 13032 zu charakterisieren, und Hinweise auf ihre physiologische Rolle in dieser Spezies zu erhalten.
Folgende Ergebnisse wurden erhalten:

(i) Die 6C RNA ist während des gesamten Wachstumsverlaufs in CGXII-Medium mit Glukose exprimiert, und zeigte nur geringe Veränderungen des RNA-Spiegels, die nicht größer als 2-fach waren. RNA-Stabilitätstests mit Rifampicin ergaben, dass die 6C RNA eine Halbwertszeit von mindestens 120 Minuten hat und dem zufolge, eine sehr stabile kleine RNA ist. Quantifizierungen der 6C RNA ergaben ca. 325 Moleküle pro Zelle in der exponentiellen und ca. 260 Moleküle pro Zelle in der stationären Wachstumsphase. Das ist viel mehr als die Menge an individueller mRNAs.

(ii) Durch 6C RNA Affinitätsxperimente mit Proteinrohextrakten von *C. glutamicum* wurde das Protein 3-Phosphoglycerat-Kinase (PGK) als ein möglicher Interaktionspartner der 6C RNA indentifiziert. Durch Gelretardationsstudien konnte eine Interaktion von 6C RNA mit aufgereinigter PGK bisher jedoch noch nicht bestätigt werden. Möglicherweise ist ein weiterer Faktor für die Interaktion nötig.

(iii) Die 6C RNA ist nicht essentiell für *C. glutamicum* und das Wachstum einer 6C RNA-Deletionsmutante war unter verschiedensten getesteten Bedingungen wie das des Wildtyps. Nur die Zugabe des Antibiotikums Mitomycin C (MMC), welches die SOS-Antwort auslöst, führte zu einem Wachstumsdefekt der ∆6C Mutante. Reporterfusionskonstrukte mit Promotoren der durch LexA regulierten Gene *recA*, *recN*, *cglIM* and *dnaE2* zeigten, dass die SOS-Antwort in der ∆6C Mutante in der stationären Phase im Vergleich zum Wildtyp niedriger ist. Dieses Ergebnis führt zu der Annahme, dass die 6C RNA möglicherweise in der SOS-Antwort involviert ist, oder eventuell eine generelle Rolle in der Stressabwehr von *C. glutamicum* spielen könnte. Komplementationsexperimente mit plasmidbasierter Expression der 6C RNA von ihrem nativen Promotor in der ∆6C Mutante zeigten einen unerwarteten und einzigartigen Wachstumsphänotyp in Anwesenheit von MMC. Die Quantifizierung der 6C RNA ergab einen ca. fünf-fach höheren RNA-Spiegel in dem komplementierten Stamm.

(iv) Der erhöhte 6C RNA-Spiegel führte zu einer verlängerten Zellform unter Standardbedingungen und zu einer stark verzweigten Zellmorphologie in Anwesenheit von MMC. Dies zeigt, dass die 6C RNA in der Zellteilung von *C. glutamicum* involviert sein könnte.

(v) Die Deletion sowie die Überexpression der 6C RNA führten zu Veränderungen im globalen Genexpressionsprofil. Bei Überexpression der 6C RNA war die verringerte Expression von *whcD* auffällig, welches für einen WhiB-ähnlichen Transkriptionsfaktor kodiert. WhcD ist homolog zu dem Septierungs- und Zellteilungs-assoziierten Regulator WhmD in *Mycobacterium smegmatis.* Eine ∆*whcD*-Mutante zeigte ein verringertes

Wachstum und eine stark veränderte Zellmorphologie, welche sehr ähnlich zu der Morphologie des 6C RNA-Überpoduzenten in Anwesenheit von MMC ist. Dies zeigt, dass die beiden homologen Proteine tatsächlich in beiden Actinobakterien funktional equivalent zu sein scheinen. Diese Ergebnisse lassen darauf schließen, dass die 6C RNA einen Einfluss auf die Expression von *whcD* oder seiner mRNA Stabilität haben könnte, und damit eine gewisse Rolle in der Septierung und Zellteilung in *C. glutamicum* spielen könnte.

1 Introduction

1.1 *Corynebacterium glutamicum*, a model organism of biotechnological relevance

Corynebacterium glutamicum is a Gram-positive rod-shaped soil bacterium which was isolated in 1957 by Kinoshita and coworkers in a screening for glutamic acid producing bacteria from a soil sample collected at Ueno Zoo in Tokyo (Japan) (Kinoshita, 1957, Udaka, 1960). It is a non-sporulating, non-pathogenic bacterium and a model microorganism for important related pathogenic species, in particular *Corynebacterium diphtheriae* and *Mycobacterium tuberculosis*. Both *Corynebacteriaceae* and *Mycobacteriaceae* belong to the order *Corynebacteriales* (Gao & Gupta, 2012). *C. glutamicum* is of very high industrial importance and has the GRAS status (generally recognized as save). It is mainly used for the large-scale industrial production of the flavour enhancer L-glutamate (2.93 mio t/a) and the feed additive L-lysine (1.95 mio t/a) (http://www.ajinomoto.com/en/ir/). Besides amino acid production, *C. glutamicum* also offers promising capabilities for the production of a variety of compounds ranging from organic acids such as succinate (Okino*, et al.*, 2008, Litsanov*, et al.*, 2012, Litsanov*, et al.*, 2012, Wieschalka*, et al.*, 2013) over biofuels (Inui*, et al.*, 2004, Smith*, et al.*, 2010, Blombach*, et al.*, 2011) to heterologous proteins (Meissner*, et al.*, 2007).

A free-living organism like *C. glutamicum* needs to be able to respond to different environmental conditions and this is usually achieved by a large repertoire of regulatory proteins. The circular chromosome of *C. glutamicum* comprises 3.3 Mbp and contains more than 3,000 annotated protein coding sequences (Ikeda & Nakagawa, 2003, Kalinowski*, et al.*, 2003). The annotation assignments and several studies revealed the presence of proteins involved in protein phosphorylation and pupylation, transcriptional regulators including two-component systems, as well as small RNAs (sRNAs), all together indicating manifold regulation on different levels in *C. glutamicum*.

Transcriptional as well as posttranslational regulation mechanisms have been studied and elucidated in the last years, among them protein phosphorylation is a key mechanism for the regulation of cellular activities. Phosphorylation of proteins on L-serine and L-threonine residues by protein kinases is an abundant covalent modification. For *C. glutamicum* four seronine/threonine protein kinases (STPK), namely PknA, PknB, PknG, and PknL (Fiuza*, et al.*, 2008a, Schultz*, et al.*, 2009) and a few STPK substrates are known so far. The first STPK substrate identified in *C. glutamicum* was OdhI which was shown to be phosphorylated by all four STPK (Niebisch*, et al.*, 2006, Schultz*, et al.*, 2009) Moreover, the cell division protein FtsZ (Schultz, Niebisch et al. 2009), MurC, a ligase essential for peptidoglycan biosynthesis (Fiuza*, et al.*, 2008b), and the cytoskeletal protein RsmP, regulating rod-shaped morphology of *C. glutamicum* (Fiuza*, et al.*, 2010) were convincingly

shown to be STPK substrates. Beside phosphorylation, pupylation is another posttranscriptional modification of proteins present in *C. glutamicum* (Küberl*, et al.*, 2014). Pupylation was originally identified in *M. tuberculosis* (Pearce*, et al.*, 2008) and is functionally related to eukaryotic ubiquitination. The prokaryotic ubiquitin-like protein (Pup) has been shown to target proteins for degradation via the proteasome in mycobacteria (Pearce*, et al.*, 2008, Striebel*, et al.*, 2014). Recently, 55 pupylated proteins have been detected in the proteasome-free *C. glutamicum* (Küberl*, et al.*, 2014). However, the regulatory roles of puyplation in *C. glutamicum* remain to be further investigated.

About 5% (159 genes) of the protein coding genes in *C. glutamicum* encode a variety of transcriptional regulators, including sigma subunits (factors) of RNA polymerase, two-component signal transduction systems and DNA binding transcriptional regulators (Schröder & Tauch, 2010). *C. glutamicum* has seven sigma subunits (factors) of RNA polymerase: the primary sigma factor SigA, the primary-like SigB and five alternative sigma factors (SigC, SigD, SigE, SigH and SigM) (Pátek & Nešvera, 2011). *C. glutamicum* also possesses 13 two-component signal transduction systems and the role of five has already been elucidated: they are involved in citrate utilization, in osmoregulation and cell wall homeostasis, in the adaption to phosphate starvation, in the adaptation to copper stress and in heme homeostasis (Bott & Brocker, 2012). The regulators of *C. glutamicum* can be divided into three groups: (i) 'global regulators' that control more than 20 target genes belonging to a minimum of four different functional categories, (ii) 'master regulators' that control a large number of functionally related genes belonging to a corresponding functional module, and (iii) 'local regulators' which control a small group of functionally related genes and tend to be clustered with their target genes (Brinkrolf*, et al.*, 2010).

The only global regulator of *C. glutamicum*, termed GlxR, belongs to the Crp -family. A total of 215 potential GlxR binding sites were predicted bioinformatically based on current experimental data (Kohl & Tauch, 2009). However, recently, in a ChIP-chip experiment 209 potential target regions were detected genome-wide (Toyoda*, et al.*, 2011). Among these, 94 new GlxR-binding regions, that have not been previously predicted, were identified (Toyoda*, et al.*, 2011). More recently, additional 21 GlxR binding sites were identified, which were not previously reported (Jungwirth*, et al.*, 2012).

11 regulators were classified as master regulators (including SigB and SigH), which control the expression of a number of functionally related genes. The remaining regulators are classified as local regulators, which control the expression of a small numer of genes. The transcriptional regulatory network of *C. glutamicum* is characterized by overlaps of regulons controlling gene expression (Brinkrolf*, et al.*, 2010).

Recently, RNA sequencing revealed that *C. glutamicum* is also well equipped with sRNAs potentially fulfilling regulatory roles (Mentz*, et al.*, 2013). High throughput short-read

sequencing and mapping of libraries prepared from a pool of isolated small RNA fractions yielded more than 800 sRNAs (Mentz, Neshat et al. 2013). These potential sRNAs were classified into untranslated regions (UTRs) of mRNAs (316), *cis*-antisense sRNAs (543), and *trans*-encoded sRNAs (262) including the 6C RNA (Mentz, Neshat et al. 2013). For 77 *trans*-encoded sRNAs significant sequence and secondary structure conservation was found by a computational approach using a whole genome alignment with the closely related species *C. efficiens* YS-314 and *C. diphtheriae* NCTC 13129 (Mentz, Neshat et al. 2013). The only experimentally analysed sRNA in *C. glutamicum* so far is ArnA (Zemanová*, et al.*, 2008). The ArnA RNA is located in the chromosomal intergenic region cg1934-cg1935, which is within the CGP3 prophage region (Frunzke*, et al.*, 2008, Baumgart*, et al.*, 2013) and its transcription was increased after heat shock (Zemanová*, et al.*, 2008). Moreover, the transcriptional start point of an additional species of ArnA RNA was detected after heat shock (Zemanová*, et al.*, 2008). The stress-response σ factor SigH was found to be involved in the synthesis of these ArnA RNAs (Zemanová*, et al.*, 2008). Both ArnA RNAs are in antisense direction to and overlap with the 5`-untranslated region of the transcript of the cg1935 gene coding for a transcriptional regulator of the GntR family (Frunzke*, et al.*, 2008). These results lead to the suggestion that the small ArnA RNAs may have a regulatory function (Zemanová*, et al.*, 2008).

1.2 Small RNAs in bacteria

The term small RNAs (sRNAs) derives from the small size of these RNAs from about 50 to 300 nt (Storz*, et al.*, 2011) up to 500 nt (RNAIII of *Staphylococcus aureus* (Boisset*, et al.*, 2007). Since these RNAs usually do not encode for proteins, the term “non-coding RNAs” (ncRNAs) can also be used. Most of the sRNAs are encoded in the intergenic regions (IGR) of the chromosome. sRNAs were shown to modulate a wide range of physiological responses. They can act on the level of transcription, translation and on mRNA stability (Waters & Storz, 2009, Liu & Camilli, 2010, Storz*, et al.*, 2011).

sRNAs can be classified into two major groups: (i) the base-pairing sRNAs and (ii) the sRNAs that act by protein binding. Recently, a new class of RNAs was discovered that are called “clustered regularly interspaced short palindromic repeats” (CRISPRs). CRISPRs are widespread in the genomes of many bacteria and almost all archaea (reviewed in Sorek*, et al.*, 2008). Although the CRISPR systems, composed of the CRISPR arrays and the CAS (CRISPR associated) genes, which encode for the Cas proteins, are wide-spread, they vary greatly among microbial species (reviewed in (Sorek*, et al.*, 2008). However, they have all in common that they are a defence system that protects bacteria and archaea from mobile genetic elements, such as plasmids, bacteriophages and transposable elements (reviewed in (van der Oost*, et al.*, 2009). These CRISPR arrays are composed of an up to 550 bp leader

sequence followed by direct repeats that are separated by similarly sized non-repetitive spacers (reviewed in Sorek, Kunin et al. 2008). CRISPRs acquire phage-derived spacers that provide immunity, presumably by CRISPR-mediated degradation of phage mRNA or DNA. Resistance is acquired by incorporating short stretches of invading DNA sequences into genomic CRISPR loci (Barrangou*, et al.*, 2007). These integrated sequences are thought to function as a genetic memory that prevents the host from being infected by viruses containing this recognition sequence (Brouns*, et al.*, 2008). The new spacers are inserted at the beginning of the array. The repeat-spacer array is transcribed into a long RNA, and the repeats enable the formation of a secondary structure (reviewed in Sorek, Kunin et al. 2008). The cascade complex of Cas proteins recognizes the sequence or structure of the repeats and processes the RNA into a single repeat-spacer unit (crRNAs) (Brouns et al 2008). The single stranded small crRNAs, complexed with additional Cas proteins, base pair with phage nucleic acids, leading to their degradation (Brouns*, et al.*, 2008).

The group of sRNAs that act by base-pairing with their target mRNAs is much broader than the group that acts by modulating protein activity. Base-pairing sRNAs are usually divided into *cis*-acting and *trans*-acting antisense RNAs. In the following, the role of sRNAs in gene regulation by base pairing is described.

1.2.1 *Cis*-encoded antisense RNAs

Cis-encoded RNAs are highly structured molecules with one to four stem loops (Brantl, 2007). These antisense RNAs are encoded at the same DNA locus as their target and show perfect complementarity to it (reviewed in (Brantl, 2007). Many *cis*-encoded sRNAs were found on plasmids, phages and transposons. *Cis*-encoded antisense RNAs of these mobile genetic elements regulate replication and thereby control copy numbers of plasmids, in phages they are involved in the switch from lysogeny to the lytic cycle and in case of transposons they control the transposition frequency of the transposon (reviewed in (Brantl, 2007). Plasmid-encoded antisense RNAs that are involved in replication, conjugation or segregation stability are expressed constitutively and are mostly unstable, whereas chromosomally encoded RNAs have a variable half live (reviewed in Brantl, 2007).

Cis-encoded antisense RNAs employ different modes of action to regulate their target. Some of them will be discussed in the following by some examples. *Cis*-encoded antisense RNAs can act by transcription attenuation, translation inhibition, inhibition of primer maturation and by influencing mRNA stability (Figure 1). The pT181 staphylococcal plasmid is an example for replication control by attenuation. In this case the antisense RNA blocks expression of the plasmid-encoded initiator protein (RepC) by inducing premature termination (attenuation) of the initiator mRNA by promoting the formation of a termination-causing hairpin just 5' to the initiator start codon (Novick*, et al.*, 1989). An example for

translation inhibition is the *hok*/*sok* locus of plasmid R1 in *E. coli*, which mediates plasmid stabilization by killing of plasmid-free segregants (Nielsen*, et al.*, 1991). The Sok (`suppression of killing`) RNA inhibits the synthesis of a toxin that kills plasmid-free cells. This highly toxic protein is encoded by the *hok* (`host killing` protein) gene and damages the cell membrane (Gerdes & Molin, 1986). The Sok RNA indirectly regulates the *hok* translation by inhibiting *mok* (`mediation of killing`) translation (Nielsen, Thorsted et al. 1991). The ORF of the *mok* gene overlaps with almost the entire *hok* gene. Thus, efficient translation of the *hok* gene is dependent on translation of the *mok* gene. The Sok RNA is less stable than the *hok* mRNA (Gerdes*, et al.*, 1997), thus in plasmid-free cells the Sok RNA is rapidly degraded, whereas the stable *hok* mRNA is translated and the toxin causes irreversible damage to the cell membrane and is thus lethal to host cells. This way of regulation enables efficient plasmid stabilization (reviewed in (Gerdes*, et al.*, 1997). A further example for a *cis*-encoded sRNA, was discovered on plasmid ColE1 (Tomizawa*, et al.*, 1981). ColE1 requires a plasmid-encoded replication primer that is synthesized as a 550 nt pre-primer (RNAII). In case of ColE1 the binding of the sRNA (RNA I) leads to the inhibition of preprimer (RNA II) maturation by causing downstream alterations in the secondary structure of the preprimer. These changes in the secondary structure prevent the formation of RNA-DNA hybrids at the replication origin so that the preprimer can not be cleaved by RNAase H to form the functional replication primer (Tomizawa, 1986), thus replication can not take place.

Also a number of chromosomally *cis*-encoded sRNAs have been found so far. Research on *cis*-acting RNAs revealed that they can act as antitoxins. One example is RatA from *Bacillus subtilis*, which regulates the toxin TxpA (Silvaggi*, et al.*, 2005). The *txpA* and *ratA* genes are in convergent orientation and overlap by about 75 nucleotides, such that the 3`-region of *ratA* is complementary to the 3`-region of *txpA* (Silvaggi*, et al.*, 2005). Deletion of *ratA* led to an increase of the *txpA* mRNA level. It is suggested that the RatA RNA blocks the accumulation of the mRNA for the toxin TxpA by annealing to the 3`-end of the *txpA* mRNA, thereby triggering its degradation (Silvaggi*, et al.*, 2005) (see also Figure 1). There is also an example known in which the sRNA has a stabilizing effect on its target mRNA, namely, the *E. coli* GadY/*gadX* system. The gene encoding the sRNA GadY is located between and opposite to two genes encoding for transcriptional regulators of the acid response, namely *gadX* and *gadW.* The expression of GadY RNA is highly induced during stationary phase (Opdyke*, et al.*, 2004). GadY base pairs with the *gadXW* mRNA and confers increased stability to the *gadX* and *gadW* mRNA.

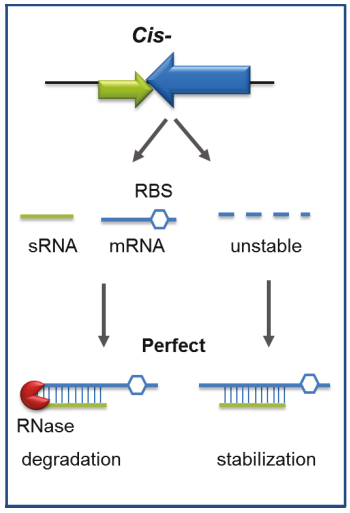

Figure 1 Examples for the mode of action of *cis*-encoded sRNAs. *Cis*-encoded sRNAs bind perfectly to their mRNA target. Binding of the *cis*-encoded sRNA can for example lead to degradation or to the stabilization of the respective mRNA target (modified from Liu and Camilli, 2010).

1.2.2 *Trans*-encoded antisense RNAs

The majority of sRNAs are *trans*-acting, which means they exhibit only short and imperfect base-pairing with their target mRNA and are encoded elsewhere on the bacterial genome as their target (reviewed in (Waters & Storz, 2009). The region of potential base pairing between the *trans*-encoded sRNA and its targets typically encompasses about 10 to 25 nucleotides (nt), but only a core of nucleotides seems to be critical for the actual regulation (Waters & Storz, 2009, Storz*, et al.*, 2011). Due to the only partial complementarity to their target, *trans*-encoded sRNAs can have several targets. This fact adds a notable level of complexity to gene transcription regulation (Papenfort & Vogel, 2009). One example for an sRNA that has several targets is RyhB of *E. coli*. RyhB is involved in the regulation of at least seven genes, of which six encode proteins required for iron transport and storage. Thus RyhB provides a mechanism for the cell to down-regulate iron-storage proteins and nonessential iron containing proteins when iron is limiting (Massé & Gottesman, 2002). RyhB itself is negatively regulated by the ferric uptake regulator protein, Fur (Massé & Gottesman, 2002).

The most important mechanism used by *trans*-encoded antisense RNAs is inhibition of translation. Translation of the target mRNA can be inhibited by blocking the ribosomal binding site (RBS) and thus inhibiting association with the small ribosomal subunit and consequently translation initiation (Figure 2). The interaction of the sRNA with its target mRNA can also entail degradation of the mRNA by RNase III (Boisset*, et al.*, 2007) or RNase E (Morita*, et al.*, 2005), thereby preventing translation of the respective mRNA.

Furthermore, gene expression can also be activated by sRNAs (reviewed in (Fröhlich & Vogel, 2009) (Figure 2). One example for an sRNA that activates translation by base-pairing is DsrA in *E. coli* (Sledjeski & Gottesman, 1995), which acts as positive regulator of *rpoS* mRNA. The *rpoS* encodes for the stationary phase sigma factor σ^S. By pairing of DsrA to a self-inhibitory *rpoS* hairpin, the RBS of the *rpoS* mRNA is uncaged and translation can occur (Majdalani*, et al.*, 1998, Sledjeski*, et al.*, 2001).

Often the chaperon protein Hfq is required for the function and/or stability of *trans*-encoded sRNAs (Brennan & Link, 2007). Hfq was identified in *E. coli* as host factor required for initiation of plus-strand synthesis by the replicase of the Qß RNA bacteriophage (Franze de Fernandez*, et al.*, 1968). Hfq is a homohexamer that is similar to the eukaryotic RNA-binding Sm and Sm-like proteins involved in splicing (Valentin-Hansen*, et al.*, 2004). The repetition of identical binding pockets on the Hfq hexamer suggests that the binding surface can accommodate more than one RNA target (Valentin-Hansen*, et al.*, 2004). This would allow simultaneous binding of two RNA strands. Thus, Hfq could promote the interaction between these strands, which is particularly important in sRNA/target mRNA interactions. Indeed, for many bacteria it has been shown that the protein Hfq cooperates in intermolecular base pairing between the sRNA and its target mRNA to provide regulatory activity (Zhang*, et al.*, 1998, Møller*, et al.*, 2002, Brennan & Link, 2007). Notably, in some bacteria, like *Streptomyces coelicolor* and *C. glutamicum*, no Hfq protein or homologous protein could be identified, yet (Sun*, et al.*, 2002, Vockenhuber*, et al.*, 2011). This leads to the question if these bacteria employ a novel RNA chaperon, which is functionally equivalent to the Hfq protein, or if the sRNAs of these species do not require such a protein for their functionality. In other bacteria, like *Bacillus anthracis* and *Ralstonia metallidurans*, even two distinct copies of Hfq were found (Sun*, et al.*, 2002).

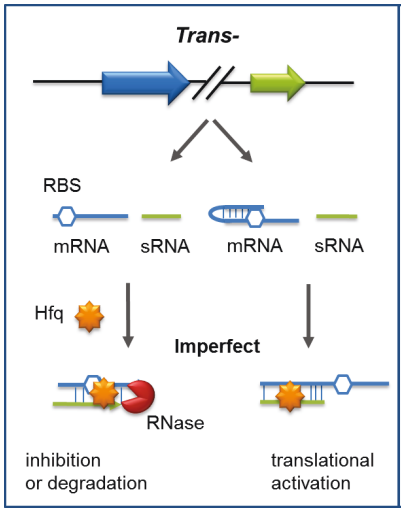

Figure 2 Examples for the mode of action of *trans*-encoded sRNAs. *Trans*-encoded sRNAs bind imperfectly to their mRNA target, mostly with the help of the Hfq protein. Binding of the *trans*-encoded sRNA leads either to inhibition of translation by blocking the ribosomal binding site (RBS) or to silencing by degradation of the mRNA by RNases, or to the activation of translation for example by abolishing self-inhibitory hairpins (modified from Liu and Camilli, 2010).

1.2.3 sRNAs that modulate protein activity

Beside base pairing antisense RNAs, also some protein-binding sRNAs are known. This class of sRNAs can be divided into (i) sRNAs with intrinsic activity (RNaseP), (ii) sRNAs that contribute to a ribonucleoprotein particle (4.5S and tmRNA) and (iii) sRNAs which exert their regulatory function by mimicking structures of other nucleic acids (reviewed in (Waters & Storz, 2009) (Figure 3). One example of (iii) is the *E. coli* CsrB RNA which modulates the activity of CsrA (reviewed in (Babitzke*, et al.*, 2009). CsrA is a small RNA-binding protein which is the effector of the carbon storage regulator (csr), which was identified as global regulator system that controls bacterial gene expression on the post-transcriptional level. Glycogen synthesis and catabolism, gluconeogenis, glycolysis, adherence, biofilm formation and motility are modulated by CsrA (reviewed in (Romeo, 1998). CsrA blocks translation and causes rapid mRNA degradation (Liu & Romeo, 1997). CsrB possesses several binding sites for CsrA and thus serves as a competitor for CsrA mRNA targets, especially when the CsrB level increases. The *csrB* gene expression is activated by the BarA-UvrY two-component system when the bacterial cultures approach the stationary phase (Mondragón*, et al.*, 2006). A second sRNA, namely CsrC, functions analogous to CsrB (Weilbacher*, et al.*, 2003).

Another example in the group of sRNAs that modulate protein activity is the 6S RNA of *E. coli*. The 6S RNA binds to the holoenzyme of RNA polymerase (RNAP) (Wassarman & Storz, 2000, Steuten*, et al.*, 2013). It has been shown that the level of 6S RNA increases in

the stationary growth phase (Wassarman & Storz, 2000). The 6S RNA is characterized by its secondary structure that consists of a central bulge flanked by two irregular stem structures and mimics the conformation of DNA during transcription initiation (open promoter DNA). In *E. coli* the 6S RNA inhibits transcription of many genes during the stationary phase due to its high concentration and affinity for the σ^{70}-RNAP holoenzyme (Trotochaud & Wassarman, 2004, Cavanagh, *et al.*, 2008, Neusser, *et al.*, 2010). Additionally it was shown that the 6S RNA acts as a template for the synthesis of small de novo transcription products, termed pRNAs (Wassarman & Saecker, 2006, Gildehaus, *et al.*, 2007). The synthesis of pRNAs leads to the release of RNAP-bound 6S RNA during outgrowth from the stationary phase (Wassarman & Saecker, 2006, Wurm, *et al.*, 2010, Steuten & Wagner, 2012).

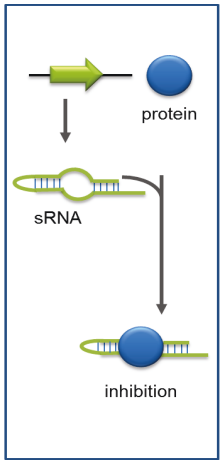

Figure 3 Example for the mode of action of sRNAs that act by protein binding. sRNAs that act by modulating protein activity often mimic the conformation of a double-stranded DNA (modified from Liu and Camilli, 2010).

Regulatory RNAs are often the small players in the back, mostly showing up when environmental conditions change. Every bacterium has its own set of sRNAs which is most likely perfectly adapted to the habitat of the respective organism. Many regulatory RNAs are involved in complex cell processes, like virulence (Boisset, *et al.*, 2007), stress response to e.g. iron limitation (RyhB) (Geissmann & Touati, 2004, Massé, *et al.*, 2005), oxidative stress (OxyS) (Altuvia, *et al.*, 1998), sugar-phosphate stress (SgrS) (Vanderpool & Gottesman, 2004, Kawamoto, *et al.*, 2005), acid stress (GadY) (Tramonti, *et al.*, 2008), temperature (DsrA) (Sledjeski, *et al.*, 1996) or outer membrane composition (MicA, MicF, MicC, RybB, OmrA/OmrB) (reviewed in (Vogel & Papenfort, 2006). In contrast to the wealth of knowledge on sRNAs from other bacteria, for *C. glutamicum* the roles and mechanisms of all detected sRNA candidates still need to be elucidated.

1.3 The 6C RNA family

The 6C RNA family is a class of sRNAs present and conserved in many *Actinomycetales* genera. The name 6C RNA originates from the two predicted stem-loops, each containing a stretch of six or more conserved cytosine residues (Figure 4). In the RNA-families (Rfam) online database, which collects non-coding RNA families, for the 6C RNA family overall 150 species of actinobacteria are listed (Gardner*, et al.*, 2009, Burge*, et al.*, 2013). From these 150 species, 20 species are present in the seed sequence alignment (Figure 5), which includes sequences with the highest similarity to the consensus motif (Figure 4) (http://rfam.sanger.ac.uk/family/RF01066).

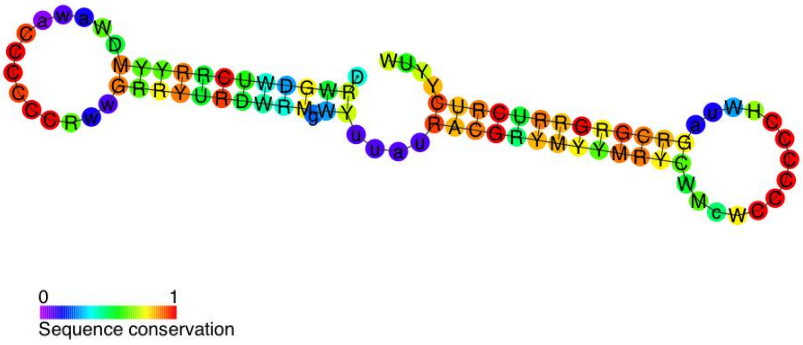

Figure 4 Consensus motif of the 6C RNA family. The sequence conservation is indicated by colours: red means very high conservation and blue to violet means very low conservation. Taken from (http://rfam.sanger.ac.uk/family/RF01066) (Gardner*, et al.*, 2009, Burge*, et al.*, 2013).

Figure 5 6C RNA family seed sequence alignment. The conserved six cytosine residues in the 6C RNA sequences are highlighted in grey. The species in which more than six consecutive cytosine residues are found, in at least one loop region, are underlined. The additional cytosine residues in these species are highlighted in yellow. Modified from (http://rfam.sanger.ac.uk/family/RF01066).

Notably, *C. glutamicum* is the only species in the seed sequence alignment of the 6C RNA family in which even eight consecutive cytosine residues are present in both predicted stem-loops (Figure 5 and Figure 6).

The 6C RNA was originally found in *Streptomyces coelicolor* (Swiercz*, et al.*, 2008). In this species three transcripts with a size of about 67, 90 and 130 nt, respectively, were detected. These transcripts were were found to have a shared common core sequence, but different 5`- and 3`-ends (Swiercz*, et al.*, 2008). The expression of the transcripts was observed on both minimal and rich media. However, the expression profile of the two shorter transcripts in particular, suggests that they are upregulated later in development, at a time that corresponds to spore formation (Swiercz*, et al.*, 2008). However, not all actinobacteria in which the 6C RNA sequence motif is conserved form spores. Therefore, the 6C RNA expression changes might not be primarily related to sporulation but rather reflect a general dormancy or metabolic slow-down response (Swiercz*, et al.*, 2008).

In *C. glutamicum* the 6C RNA motif is located in the intergenic region of cg0360 and cg0362 (genome position 314,705 to 314,782 bp) (Kalinowski*, et al.*, 2003). Recently, the start and stop of the 6C RNA transcript in *C. glutamicum* was published to be at position 314,679 bp and 314,787 bp, resulting in a size of 109 bp (Mentz*, et al.*, 2013). Based on this size, the secondary structure prediction of the 6C RNA transcript of *C. glutamicum* suggests two prominent stem-loops and one minor stem (Figure 6).

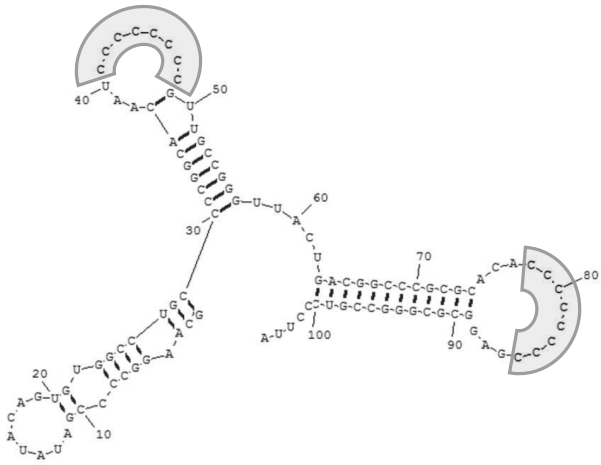

Figure 6 Predicted secondary structure of the 6C RNA in *C. glutamicum*. The secondary structure of the 6C RNA was predicted using the program RNA structure 4.2 (Mathews*, et al.*, 1999). The eight cytosine residues in the conserved stem-loops are indicated by grey regions.

1.4 Aims of this work

The first aim of this work was to characterize the 6C RNA in *C. glutamicum*. For this purpose, investigations on the 6C RNA expression level during the course of growth, the number of 6C RNA molecules per cell, and on the stability of this sRNA were performed. Additionally, it should be analysed if the 6C RNA expression is regulated by one or more transcriptional regulators.

A second topic of this work addressed the question of the physiological role of the 6C RNA in *C. glutamicum*. It was checked whether the deletion of the 6C RNA has any effects on *C. glutamicum* under standard conditions as well as under different stress conditions. For this purpose, two Δ6C RNA mutant variants were constructed and characterized. In case that the Δ6C RNA mutants should have a phenotype under a certain condition, this should be analysed in more detail.

A third aim was to identify putative targets of the 6C RNA in *C. glutamicum*. Therefore, a target search was performed on the mRNA level as well as on the protein level. For the mRNA target search a global transcriptome analysis of the 6C RNA deletion mutant and of a 6C RNA overexpression strain should be performed. RNA pull-down experiments with *in vitro* generated 6C RNA should be used to identify putative protein targets. If one or more genes or proteins should be assumed as good 6C RNA target candidates, further experiments should be performed to confirm these assumptions.

2 Materials and Methods

2.1 Buffers and antibiotics

All chemicals were obtained from Merck AG (Darmstadt, Germany), Fluka (Steinheim, Germany), Sigma-Aldrich (Taufkirchen, Germany), Carl Roth GmbH & Co. KG (Karlsruhe, Germany), Roche Diagnostics GmbH (Mannheim, Germany) and GE Healthcare (München, Germany).

All solutions were solved in H_2O bidist. if not otherwise stated.

Ampicillin	50 mg ml^{-1} (sterile-filtered)
Biotin	200 mg l^{-1} (sterile-filtered)
Carbenicillin	50 mg ml^{-1} (sterile-filtered)
Glucose	40% (w/v) (autoclaved)
Kanamycin	50 mg ml^{-1} (sterile-filtered)
Mitomycin C	1.5 mM (2 mg Mitomycin C and 48 mg NaCl in 4 ml)
Rifampicin	50 mg ml^{-1} in methanol
5x ASSC	0.75 M NaCl, 75 mM tri-Na citrate, 10 mM NaOH, pH 11.5
Blocking solution	1% (w/v) Blocking reagent in maleic acid buffer
Buffer D	20 mM Tris-HCl (pH 7.5), 6% (v/v) glycerol, 0.1 M KCl, 0.2 mM EDTA
B+W buffer	10 mM Tris-HCl (pH 7.5), 2 M NaCl
100x Denhardt`s solution	2% (w/v) BSA, 2% (w/v) Ficoll 400, 2% (w/v) polyvinyl pyrrolidone
Detection buffer	100 mM Tris-HCl, 100 mM NaCl, 50 mM $MgCl_2$ x 6 H_2O, pH 9.5
Elution buffer	TGED buffer, 2 M NaCl
Enzymatic lysis buffer	20 mM Tris-HCl (pH 8.0), 2 mM EDTA, 1.2% (v/v) Triton X -100
10x FA buffer	200 mM MOPS, 50 mM sodium acetate, 20 mM EDTA, pH 7.0
1x FA running buffer	100 ml FA buffer (10x), 20 ml formaldehyde (37%), 880 ml H_2O
Hybridisation buffer	50% (v/v) formamide, 5x SSC, 3x Denhardt`solution, 0.5% (v/v) SDS, 0.2% (v/v) sodiumlauryl sarcosinate, 5% (v/v) dextran sulfate
Maleic acid buffer	100 mM maleic acid, 150 mM NaCl, pH 7.5
NNGx buffer	50 mM NaH_2PO_4 (pH 8.0), 300 mM NaCl, 5% (v/v) glycerol, x mM imidazole

PBS	137 mM NaCl, 2.7 mM KCl, 4.3 mM Na_2HPO_4, 1.4 mM KH_2PO_4, pH 7.4
Proteinase K solution	20 mg ml^{-1}
RamA binding buffer	10 mM Tris-HCl (pH 8.0), 1 mM EDTA, 10% (v/v) glycerol, 1 mM DTT, 250 mM NaCl
RamA storage buffer	50 mM Tris-HCl (pH 7.4), 100 mM NaCl, 10 mM $MgCl_2$, 1 mM EDTA, 1 mM DTT, 10% (v/v) glycerol
SDS	10 % (w/v)
20x SSC	3 M NaCl, 300 mM tri-Na citrate, pH 7.0
Strip-Puffer	20 mM Tris-HCl (pH 7.9), 500 mM NaCl, 100 mM $Na_2EDTA \times 2H_2O$
50x TAE-buffer	242 g Tris-HCl, 57.1 ml acetic acid, 14.7 g EDTA (pH 8.0)
0.5x TBE buffer	44.5 mM Tris-borate, 1 mM EDTA (pH 8.3)
TE buffer	10 mM Tris-HCl (pH 8.0), 1 mM $Na_2EDTA \times 2\ H_2O$
TG buffer	1 mM Tris-HCl (pH 7.5), 10% (v/v) glycerol
Tris buffer	50 mM Tris-HCl (pH 7.5)
TNIGx+-Puffer	20 mM Tris-HCl, 300 mM NaCl, 5% (v/v) glycerol, pH 8.0, x mM imidazol
TGED buffer	20 mM Tris-HCl (pH 7.5), 10% (v/v) glycerol, 0.1 M NaCl, 1 mM EDTA, 0.01% Triton X-100, 1 mM DTT (freshly added)
Wash buffer	0.3% (w/v) Tween 20 in maleic acid buffer
6x DNA loading buffer	40% (w/v) sucrose, 0.25% (w/v) bromophenol blue
5x RNA loading buffer	30% (v/v) formamide, 20% (v/v) glycerol, 40% (v/v) 10x FA buffer, 2.7% (v/v) formaldehyde, 4 mM EDTA (pH 8.0), 10 µg/ml ethidium bromide, 0.6% (w/v) bromophenol blue
DAPI	1 µg ml^{-1} in 50% (v/v) glycerol
Nil Red	0.5 mg ml^{-1} in DMSO

2.2 Culture media

The components for complex media were obtained from Difco Laboratories (Detroit, USA).

The following media were used:

BHI medium: 37 g l^{-1} brain heart infusion

BHIS medium: 37 g l^{-1} brain heart infusion, 91 g l^{-1} sorbitol

CGXII medium: 42 g l^{-1} MOPS, 20 g l^{-1} $(NH_4)_2SO_4$, 5 g l^{-1} urea, 1 g l^{-1} KH_2PO_4, 1 g l^{-1} K_2HPO_4, 0.25 g l^{-1} $MgSO_4$ x 7 H_2O, 10 mg l^{-1} $CaCl_2$, the pH was adjusted to 7.0 with KOH. After autoclaving, 1 ml l^{-1} biotin (0.2 g l^{-1}), 1 ml l^{-1} protocatechuic acid (30 g l^{-1} solved in 1M NaOH, sterile filtered), 1 ml trace element solution (see below) and 40 g l^{-1} glucose were added to the medium.

LB medium: 5 g l^{-1} yeast extract, 10 g l^{-1} tryptone, 10 g l^{-1}NaCl

TB medium: 24 g l^{-1} yeast extract, 12 g l^{-1} tryptone, 0.4% (v/v) glycerol, 0.5% (w/v) glucose and after autoclaving the medium 2.31 g l^{-1} KH_2PO_4 and 12.54 g l^{-1} K_2HPO_4 were added.

Trace element solution: 10 g l^{-1} $FeSO_4$ x 7 H_2O, 10 g l^{-1} $MnSO_4$ x H_2O, 1 g l^{-1} $ZnSO_4$ x 7 H_2O, 0.2 g l^{-1} $CuSO_4$ x 5 H_2O, 20 mg l^{-1} $NiCl_2$ x 6 H_2O, to dissolve acidify in HCL (pH 1.0).

For agar plates, 18 g l^{-1} agar was added to the medium before autoclaving.

Kanamycin (25 µg ml^{-1} for *C. glutamicum* or 50 µg ml^{-1} for *E. coli*) or Carbenicillin (100 µg ml^{-1} for *E. coli*) were added to the culture medium or the agar plates to select the respective *E. coli* and *C. glutamicum* strains.

2.3 Oligonucleotides

Oligonucleotides were synthesized by Eurofins MWG Operon (Ebersberg, Germany) or Biolegio (Nijmegen, Netherlands) and are listed in Table 1.

Table 1 Oligonucleotides used in this work. The recognition sites for endonucleases introduced with the oligonucleotides are underlined. The complementary sequences of the overlap extension PCR oligonucleotides are highlighted in bold. The core T7 RNA polymerase binding site is highlighted in bold and underlined. Italic sequences are identical to the sequence of the biotin primer.
iP= including promoter sequence, IV Trans = in vitro transcription.

Name	DNA Sequence (5´ - 3´)	Restriction site
Construction of the Δ6C mutant		
Delta 6C-1	TTTAAGTCGACAGTGACCACCGAATGCATGG	SalI
Delta 6C-2	**CCCATCCACTAAACTTAAACA**AGGCCACACTGTATATCGGG	-
Delta 6C-3	**TGTTTAAGTTTAGTGGATGGG**CTTATTTTCTAAACTAGTGCCCTTAG	-
Delta 6C-4	AATTTGAATTCCAGTTGTTTGTCATCTCTGCC	EcoRI
Construction of the Δ6CiP mutant		
Delta 6CiP-2	**CCCATCCACTAAACTTAAACA**GAATAACACGAATACTTAACAGTGTGG	-
Delta 6CiP-3	**TGTTTAAGTTTAGTGGATGGG**TTTCTAAACTAGTGCCCTTAGCAG	-
Delta 6CiP-4	AATTTGAATTCGTTGTTTGTCATCTCTGCCTAAAGC	EcoRI
Construction of the ΔOP_cg0362 mutant		
Delta OP_cg0362-1	TTTAACCTGCAGGCTTAATTGCAGGGCTTCGACAG	SbfI
Delta OP_cg0362-2	**CCCATCCACTAAACTTAAACA**GATGGTGTTCATGGCACCTAC	-
Delta OP_cg0362-3	**TGTTTAAGTTTAGTGGATGGG**ACCGTCACCGTTCGTGGACAAGAAG	-
Delta OP_cg0362-4	AATTTGAATTCCCTATGCCAGAAGTGACACGGACATC	EcoRI
Construction of the Δ*whcD* mutant		
Delta whcD-1	CGTTAAGCTTGCACTGCTTATACTTGTAGGGAGTG	HindI
Delta whcD-2	**CCCATCCACTAAACTTAAACA**CTTTGCAGATACGTCCCCAGCTG	-
Delta whcD-3	**TGTTTAAGTTTAGTGGATGGG**GAACGTGAGCGCCGCCGCCTG	-
Delta whcD-4	GCTTGGATCCGATTCCAGGATCTCTAGCGTGGC	BamHI
Construction of pAN6 derivatives		
OPcg0362-fw	TTTAACATATGTTGAAAGCACGTAAGCCTCAGGCCACAGTAG	NdeI
OPcg0362-rv	AATTTGAATTCTCATAAAGGTCCTGCTTTTGCGTGGGCTTC	EcoRI
whcD-fw	TTTAACTGCAGATGGAAGATTCAGCTGGGGACGTATCTGC	PstI
whcD-rv	AATTTGCTAGCTTACGAAATTTCGCGTTTCAGGCGGCG	NheI
Construction of pEKEx2 derivatives		
6C RNA-fw	TTTAAGTCGACGTTTGATATGCCATAATTTCAGGTGC	SalI
6C RNA-rv	AATTTGAATTCCAGAAAATCTGCTAAGGGCACTAG	EcoRI
Construction of pJC1 derivatives		
6C RNA-Prom-fw	TTTAAGGATCCTGGCAACTTTCCAAGACTGAG	BamHI
6C RNA-Prom-rv	AAATTGTCGACCACAGAAAATCTGCTAAGGGCA	SalI
Construction of pUCBM21 derivatives for in vitro transcription		
IV Trans 6C RNA-fw	TCTAGA**TAATACGACTCACTATA**GGCAAGGCCCCGATATACAGTG	XbaI
IV Trans 6C RNA-rv	AGATTATAAGGGACGGCCCGCGCCT	PsiI
Amplification of ss dig-labeled complementary DNA probe		
NB_fw	TGGCGTTTGATATGCCATAATTTCAGGTGC	-
NB_rv	ACAGAAAATCTGCTAAGGGCACTAGTTTAG	-

Name	DNA Sequence (5´ - 3´)	Restriction site
Amplification of PCR product for DNA affinity chromatography		
6C_Promotor_fw	CGTAGGCGTAGGTGGAACTC	-
6C_Promotor_rv	*GAGGAGTCGTCGATGTGGAGACC*CACACTGTATATCGGGGCCTT	-
Biotin-Primer	BITEG-GAGGAGTCGTCGATGTGGAGACC	-
Amplification of PCR product for electrophoretic mobility shift assays		
6C_Promotor_rv_2	GCACCTGAAATTATGGCATATC	-
Pgi_Promotor_fw JP	CCTACCTTCTCGATCCCTTCTC	-
Pgi_Promotor_rv JP	CCTGGGTGGTCGAAATGTC	-
aceb1 (Gerstmeir, *et al.*, 2004)	TCAAGTCGACTTCCTTAAGTGCTGATTCG	SalI
acebR4 (Gerstmeir, *et al.*, 2004)	CGGGATCCCGCTCCTTTTAAAGCATGGG	BamHI
Oligonucleotides for sequencing/verification of integration or deletion of DNA sequences		
Δ6C and Δ6CiP mutant mutant		
Delta 6C-left	TGCCGACAGCTTCCAACATG	-
Delta 6C-right	CTCATCAGGAGTGCTCGGCA	-
ΔOP_cg0362 mutant		
Delta OP_cg0362-left	CGATGGGTTCCACCAGTTCTTTC	-
Delta OP_cg0362-right	GAAGCTCGAGATTGAAGGGCTGTTG	-
ΔwhcD mutant		
Delta whcD-left	GTTTCCGTCGAGCGCGAAACCTTCC	-
Delta whcD-right	CGAATATGCGTAGGTGAGGGTTGCGAC	-
Oligonucleotides for colony-PCR and sequencing of pK19*mobsacB* derivatives		
M13-control-fw	CGCCAGGGTTTTCCCAGTCAC	-
M13-control-rv	AGCGGATAACAATTTCACACAGGA	-
rsp	CACAGGAAACAGCTATGACCATG	-
univ	CGCCAGGGTTTTCCCAGTCACGAC	-
Oligonucleotides for colony-PCR and sequencing of pJC1 derivatives		
pJC1-for	CGCGAGGGCGATCAGCGACGC	-
pJC1-rev-neu2	TGCAACTTTATCCGCCTCCAT	-
Oligonucleotides for colony-PCR and sequencing of pAN6 and pEKEx2 derivatives		
pEKEX-fw-2	CGGCGTTTCACTTCTGAGTTCGGC	-
pEKEX-rv-2	GATATGACCATGATTACGCCAAGC	-

2.4 Bacterial strains and plasmids

All strains used or constructed during this work are listed in Table 2.

Table 2 Bacterial strains used or constructed in this work and their relevant characteristics.

Strain	Relevant characteristics	Source or Reference
***C. glutamicum* strains**		
ATCC 13032	biotin-auxotrophic wild type	(Abe*, et al.*, 1967)
Δ6C	ATCC 13032 derivative with deletion of the 6C RNA conserved motif (+28 to +101 bp from 6C RNA TSS) located in the IGR of *cg0360* and *cg0362*	This work
Δ6CiP	ATCC 13032 derivative with deletion of the 6C RNA gene including the 6C RNA promoter region (-58 to +106 bp from the 6C RNA TSS)	This work
ΔOPcg0362	ATCC 13032 derivative with in-frame deletion of the operon OP_cg0362 (*cg0362-cg0369*)	This work
Δ*whcD*	ATCC 13032 derivative with in-frame deletion of the *whcD* gene (*cg0850*)	This work
MV-ValLeu33	ATCC 13032 derivative with deletion of *ltbR* and *leuA*, with chromosomal integration of *leuA*_B018 (feedback resistant 2-Isoproplymalatesynthase) under control of the *tuf* promoter into the Δ*leuA* locus and with chromosomally integrated mutations into *ilvN* coding for amino acid exchanges G20D, I21D, and I22F	(Vogt*, et al.*, 2014)
DM1800	ATCC 13032 derivative *pyc*^{P485S}, *lys*^{CT311I}	(Georgi*, et al.*, 2005)
***E. coli* strains**		
DH5α	F^- Φ80*dlac*Δ (*lacZ*)M15 Δ (*lacZYA-argF*) U169 *endA1 recA1 hsdR17* (r_K^-, m_K^+) *deoR thi-1 phoA supE44* λ^- *gyrA96 relA1; strain for cloning*	(Hanahan, 1983)
BL21(DE3)	*F- ompT hsdS B(r B- m B-) gal dcm (λcIts857 ind1 Sam7 nin5 lacUV5 -T7* gene 1*);* host strain for the expression of pET-coding recombinant proteins; contains the lysogenic phage λDE3, which contains the T7-Phage-RNA-polymerase-gene under control of the *lacUV5* -Promoter.	(Studier & Moffatt, 1986)

All plasmids used or constructed during this work are listed in Table 3.

Table 3 Plasmids used or constructed in this work.

Plasmid	Relevant characteristics	Source or Reference
pAN6	Kan^R; pEKEx2 derivative for the overproduction of proteins with a C-terminal Strep-Tag II in *C. glutamicum*	(Frunzke*, et al.*, 2008)
pAN6-*whcD*	Kan^R; pAN6 derivative containing the *whcD* gene (cg0850)	This work
pJC1	Kan^R; *E. coli*//*C. glutamicum* shuttle vector ($oriV_{E.coli}$, $oriV_{C.glutamicum}$)	(Cremer, *et al*., 1990)
pJC1-6C	Kan^R; pJC1 derivative containing the *6C RNA* gene under control of its native promoter	This work
pJC1-P*recN-e2-crimson*	Kan^R, pJC1 derivative containing the promoter of *recN* (207 bp) fused to *e2-crimson*; the insert includes the promoter of *recN*, 30 bp of the coding sequence, a stop codon, and an additional ribosome binding site (pET16) in front of *e2-crimson*	(Nanda*, et al.*, 2014)
pJC1-P*dnaE2-e2-crimson*	Kan^R, pJC1 derivative containing the promoter of *dnaE2* (260 bp) fused to *e2-crimson*; the insert includes the promoter of *dnaE2*, 30 bp of the coding sequence, a stop codon, and an additional ribosome binding site (pET16) in front of *e2-crimson*	Nanda and Frunzke unpublished
pJC1-P*cglIM-e2-crimson*	Kan^R, pJC1 derivative containing the promoter of *cglIM* (530 bp) fused to *e2-crimson*; the insert includes the promoter of *cglIM*, 30 bp of the coding sequence, a stop codon, and an additional ribosome binding site (pET16) in front of *e2-crimson*	Nanda and Frunzke unpublished
pJC1-P*recA-e2-crimson*	Kan^R, pJC1 derivative containing the promoter of *recA* (260 bp) fused to *e2-crimson*; the insert includes the promoter of *recA* and an additional ribosome binding site (pET16) in front of *e2-crimson*	Nanda and Frunzke unpublished
pUCBM21	Amp^R, pUC19 derivative with extended MCS	BoehringerMannheim
pUCBM21-*6C RNA* gg	Amp^R, pUC BM21 derivative containing the 6C RNA gene (+1 to +105 bp from 6C RNA TSS) under control of the T7 promoter	This work
pK19*mobsacB*	Kan^R; vector for allelic exchange in *C. glutamicum*; (pK18 $oriV_{E.c.}$, *sacB*, *lacZ*α)	(Schäfer*, et al.*, 1994)
pK19*mobsacB*-Δ*6C*	Kan^R, pK19*mobsacB* derivative containing a 1114 bp overlap-extension PCR product which covers the flanking upstream and downstream regions (approximately 573 bp and 520 bp, respectively) of the *6C RNA* gene	This work

Plasmid	Relevant characteristics	Source or Reference
pK19*mobsacB*-ΔOP_cg0362	Kan^R, pK19*mobsacB* derivative containing a 1377 bp overlap-extension PCR product which covers the flanking upstream and downstream regions (approximately 680 bp and 676 bp, respectively) of the operon OP cg0362 (*cg0362-cg0369*)	This work
pK19*mobsacB*- Δ*whcD*	Kan^R, pK19*mobsacB* derivative containing a 713 bp overlap-extension PCR product which covers the flanking upstream and downstream regions (approximately 344 bp and 347 bp, respectively) of the *whcD* gene (*cg0850*)	This work
pET16b	Amp^R; *E. coli* vector for the overexpression of genes, PT7*lac, lacI*, His10	Novagen
pET16b-*pgk* (Cg)	Amp^R, pET16b derivative, containing the *C. glutamicum pgk* gene	(Reddy & Wendisch, 2014)
pET28a (+)	Kan^R, *E. coli* vector for the overexpression of genes, PT7*lac, lacI*, His6	Novagen
pET28a-*ramA*	Kan^R, pET28 derivative containing the *ramA* gene	(Cramer*, et al.*, 2006)

2.5 Plasmid constructions

2.5.1 Construction of pk19*mobsacB* derivatives for the deletion of genes

All pK19*mobsacB* derivatives were constructed via overlap-extension PCR. For construction of vector pK19*mobsacB*-Δ6C the region upstream (approximately 573 bp) as well as the downstream region (approximately 520 bp) of the *6C RNA* gene were amplified via oligonucleotide pairs Delta 6C-1/ Delta 6C-2 and Delta 6C-3/Delta 6C-4, respectively, from genomic DNA of *C. glutamicum* ATCC 13032. The oligonucleotides Delta 6C-2 and Delta 6C-3 had a complementary 21-bp overlap sequence (5`TGTTTAAGTTTAGTGGATGGG), which was needed for subsequent overlap-extension PCR. The amplified DNA fragments were fused in an overlap-extension PCR resulting in a 1114 bp PCR product that was amplified with oligonucleotides Delta 6C-1/Delta 6C-4. With the oligonucleotides Delta 6C-1 and Delta 6C-4 the restriction sites (5` SalI and 3`EcoRI) were added to the flanking regions to clone the fragment into vector pK19*mobsacB*. The fragment was digested with the restriction enzymes SalI and EcoRI and ligated into the vector pK19*mobsacB* cut with the same enzymes.

For the construction of vector pK19*mobsacB*-Δ6CiP the region upstream (approximately 488 bp) as well as the downstream region (approximately 518 bp) of the *6C RNA* gene and its promoter region were amplified via oligonucleotide pairs Delta 6C-1/Delta 6CiP-2 and Delta 6CiP-3/ Delta 6CiP-4, respectively, from genomic DNA of *C. glutamicum* ATCC 13032. The amplified DNA fragments were fused in an overlap-extension PCR resulting in a 1027 bp PCR product that was amplified with oligonucleotides Delta 6CiP-1/Delta 6CiP-4. This fragment was digested with the restriction enzymes SalI and EcoRI and ligated into the equally digested vector pK19*mobsacB*.

For construction of vector pK19*mobsacB*-ΔOP_cg0362 the region upstream (approximately 680 bp) as well as the downstream region (approximately 676 bp) of the operon OP_cg0362, including the codons for the first 16 aa of the first gene of the operon (*cg0362*) and the last 17 aa of the last gene in the operon (*cg0369*), were amplified via oligonucleotide pairs Delta OP_cg0362-1/Delta OP_cg0362-2 and Delta OP_cg0362-3/Delta OP_cg0362-4, respectively, from genomic DNA of *C. glutamicum* ATCC 13032. The amplified DNA fragments were fused in an overlap-extension PCR resulting in a 1377 bp PCR product that was amplified with oligonucleotides Delta OP_cg0362-1/Delta OP_cg0362-4. This fragment was digested with the restriction enzymes SbfI and EcoRI and ligated into vector pK19*mobsacB* cut with the same enzymes.

For the construction of vector pK19*mobsacB*-Δ*whcD* the region upstream (approximately 344 bp) as well as the downstream region (approximately 347 bp) of the *whcD* gene (*cg0850*), including the codons for the first 11 aa and the last 13 aa, respectively, were amplified via oligonucleotide pairs Delta whcD-1/Delta whcD-2 and Delta whcD-3/ Delta

whcD-4, respectively, from genomic DNA of *C. glutamicum* ATCC 13032. The amplified DNA fragments were fused in an overlap-extension PCR resulting in a 713 bp PCR product that was amplified with oligonucleotides Delta whcD-1/Delta whcD-4. This fragment was digested with the restriction enzymes HindI and BamHI and ligated into the equally digested vector pK19*mobsacB.*

After sequencing of the cloned overlap-extension PCR products error-free plasmids were transformed into competent *C. glutamicum* cells by electroporation.

2.5.2 Construction of pAN6 and pJC1 derivatives as expression plasmids for *C. glutamicum*

Plasmid pJC1-*6CRNA* expressing *6C RNA* from its native promoter was constructed by cloning a BamHI/SalI digested DNA fragment, obtained by PCR with genomic DNA of *C. glutamicum* ATCC 13032 as template and oligonucleotide pair 6C RNA-Prom-fw/6C RNA-Prom-rv, into BamHI/SalI digested vector pJC1.

The *whcD* gene (*cg0850*) was amplified using oligonucleotide pair whcD-fw/whcD-rv from genomic DNA of *C. glutamicum* ATCC 13032 for the construction of pAN6-*whcD*. The resulting DNA fragment was digested with restriction enzymes PstI and NheI and ligated into plasmid pAN6 cut with the same enzymes.

2.5.3 Construction of pUCBM21 derivatives as expression plasmids for *E. coli*

Plasmid pUCBM21-*6C RNA* gg expressing the *6C RNA* gene from the T7 promoter was constructed by cloning XbaI/PsiI digested DNA fragment, obtained by PCR with genomic DNA of *C. glutamicum* ATCC 13032 as template and oligonucleotide pair IV Trans 6C RNA-fw/ IV Trans 6C RNA-rv into vector pUCBM21 cut with the same enzymes. With the oligonucleotide IV Trans 6C RNA-fw the core T7 RNA polymerase binding site (5`TAATACGACTCACTATA) was introduced in front of the *6C RNA* gene. Additionally, with oligonucleotide IV Trans 6C RNA-fw a guanine was introduced between the 3`end of the T7 promoter sequence and the TSS of the 6C RNA.

2.6 Cultivation of bacteria

2.6.1 Cultivation of *E. coli*

E. coli DH5α was routinely cultivated in LB medium at 37°C. For plasmid isolation *E. coli* DH5α was routinely cultivated in 5 ml LB medium, supplemented with the appropriate antibiotic for 12 – 16 h.

2.6.2 Cultivation of *C. glutamicum*

C. glutamicum ATCC 13032 (Abe*, et al.*, 1967) and its recombinant derivatives were routinely cultivated at 30°C. For cultivation of *C. glutamicum* strains 5 ml BHI medium was inoculated with colony material from a fresh BHI agar plate and incubated for 8 h on a rotary shaker at 170 rpm. This first preculture was used to inoculate a 100 ml baffled Erlenmeyer shake flask containing 10 ml or 20 ml of CGXII minimal medium (Keilhauer*, et al.*, 1993) with 4% (w/v) glucose as sole carbon and energy source to an OD_{600} of 0.1 and incubated overnight on a rotary shaker at 130 rpm (second preculture). The cells of the first preculture were washed with 0.9% (w/v) NaCl before they were used to inoculate the second preculture. The main culture was inoculated from the second preculture after washing the cells with 0.9% (w/v) NaCl to an OD_{600} of 1 in 50 ml CGXII minimal medium (500 ml baffled Erlenmeyer shake flask) with 4% (w/v) glucose and cultivated at 120 rpm.

For RNA decay experiments *C. glutamicum* ATCC 13032 was cultivated in CGXII minimal medium with 4% (w/v) glucose to the exponential growth phase (OD_{600} of 4.5 – 5.5) and 10 ml samples were harvested at the indicated time points immediately before and after the addition of the antibiotic rifampicin (Rif) (250 µg ml^{-1}). For Staphylococcus aureus is was shown that 200 µg ml^{-1} rifampin rapidly and completely blocks *S. aureus* mRNA synthesis (Lee and Birkbeck, 1984). Rif binds in a pocket of the DNA-dependent RNA polymerase (RNAP) β subunit. The inhibitor sterically blocks the path of elongating RNA transcript at the 5`end when the transcript becomes either 2 or 3 nt in length. Therefore, RNA synthesis is inhibited and since RNA underlies a specific turnover it is degraded over time. The RNA turnover rate was assessed by Northern blotting using total RNA purified from *C. glutamicum* ATCC 13032. Ribosomal RNA (rRNA) was shown to be stable for more than 60 min post-transcriptional arrest (Roberts*, et al.*, 2006). Therefore, the 16S rRNA was used, as visible in the ethidium-bromide-stained gel, as loading control and as transfer control for the transfer of the total RNA from the agarose gel onto the nylon membrane.

2.6.3 Maintenance of bacteria

For long-term conservation *C. glutamicum* cells were cultivated in 5 ml BHI or BHIS medium overnight (12 – 16 h) at 30°C and 170 rpm. *E. coli* cells were cultured in 5 ml LB medium with the respective antibiotic overnight at 37°C and 170 rpm. The culture was centrifuged at RT for 3 min at 3,760 x *g*. The cells were resuspended in 0.7 ml of appropriate media (LB, BHI or BHIS) and mixed with 0.3 ml of sterile glycerol. The strains were stored at –80°C.

2.6.4 Determination of bacterial growth

Cell growth in liquid culture was followed by measuring the optical density at 600 nm (OD_{600}) with an UV-1800 spectrophotometer (Shimadzu, Duisburg, Germany). A water sample served as blank. Samples were diluted with water to gain absorbance values between 0.1 and 0.5 to maintain linearity between absorbance and cell concentration.

2.6.5 Determination of the cell dry weight (CDW)

For the determination of the cell dry weight (CDW) the respective strains were cultivated in 50 ml CGXII medium with 4% (w/v) glucose at 30°C and 120 rpm in shaking flasks. 10 ml of the respective cultures was harvested at different time points of cultivation at 3,760 x g for 10 min at 4°C. The cell pellet was washed in 5 ml H_2O and resuspended in 2 ml H_2O. The cell suspension was dried in small aluminium bowls at 105°C overnight. The aluminium bowls were previously incubated at 105°C for 24 h, cooled down in a desiccator and then the weight of the bowls was determined. For the determination of the CDW also the optical density of the respective aliquots was determined (see 2.6.2). For the determination of the CDW samples were taken at OD_{600} of 2, 4, 6 and 10.

2.6.6 Cultivation in microtiter scale in the BioLector system

Cultivation in microtiter scale (750 µL total volume) was performed in the BioLector system (m2p-labs; Baesweiler, Germany) (Kensy*, et al.*, 2009). *C. glutamicum* and its derivatives were precultivated in either 20 ml BHI medium (for the screening of different carbon sources) or 10 ml CGXII medium with 4% (w/v) glucose (for the testing of different reporter fusion constructs) and incubated overnight on a rotary shaker at 130 rpm. Cells of the preculture were washed in 0.9% (w/v) NaCl before using them for the inoculation of the main culture. The cultivation in 750 µl of the respective medium was started with an OD_{600} of 1 in 48-well FlowerPlates® B (m2p-labs, Baesweiler, Germany) at 30°C, 85% humidity and 1,200 rpm. For each tested strain a technical replicate was set up. The production of biomass was determined as the backscattered light intensity of sent light with a wavelength of 620 nm (signal gain factor of 9, 12, 16, 20 and 30) and for e2-crimson fluorescence measurements (610 nm excitation and 650 nm emission) gain 60 was chosen. Measurements were taken in 15 min intervals for at least 24h.

2.7 Molecular biology methods

2.7.1 Isolation of nucleic acid

2.7.1.1 Preparative plasmid DNA isolation

E. coli or *C. glutamicum* strains harbouring a plasmid were cultivated overnight in 5 ml LB or BHI media containing the appropriate antibiotic on a rotary shaker at 37°C or 30°C, respectively. Plasmid DNA from *E. coli* or *C. glutamicum* cells was isolated using the QIAprep Spin Miniprep Kit (Qiagen, Hilden, Germany) or the GeneJET Plasmid Miniprep Kit (Thermo Scientific, Schwerte, Germany) according to the corresponding manual. The isolation procedure is based on alkaline cell lysis (Bimboim & Doly, 1979). Membrane-bound DNA was eluted with sterile water.

For isolation of plasmid DNA from *C. glutamicum*, first the cell wall was disrupted by shaking the cell suspension for 2 h at 37°C at 900 rpm in a thermomixer (Eppendorf, Hamburg, Germany) in 250 ml buffer P1 (Qiagen) or Resuspension solution (Thermo Scientific) containing 15 mg lysozyme (Schwarzer and Pühler, 1991).

2.7.1.2 Preparation of total RNA

C. glutamicum strains were cultivated as described above. Cells were harvested by centrifugation at 4,000 x *g* and 4°C for 5 min in prechilled falcon tubes (in case of transcriptome analysis filled with 15 g of ice) when the desired OD_{600} was reached and immediately frozen in liquid nitrogen. Frozen samples were stored at –20°C for later preparation of total RNA. The cell pellet was resuspended in 700 µl of RLT buffer of the RNeasy kit (Qiagen, Hilden, Germany) for isolation of total RNA. Afterwards the cells were added to 0.4 g of 0.1-mm Zirconia/Silica beads (Roth, Karlsruhe, Germany) for mechanical disruption, followed by bead beating four to five times for 20 sec each with a Silamat S5 apparatus (Vivadent, Ellwangen, Germany). After centrifugation (2 min, 16,000 x *g*), the supernatant was used for RNA preparation by using the RNeasy Kit (Qiagen) with on-column DNaseI treatment according to the manufacturer's instructions. This method is based on cell lysis in the presence of dithiothreitol and guanidine isothiocyanate, which leads to inactivation of RNases and allows the isolation of intact RNA. Afterwards the RNA was absorbed in the presence of ethanol and a specific salt solution (RNeasy Kit) to a silica-gel membrane which binds selectively ss RNA molecules. The membrane-bound RNA was eluted with sterile water and stored at -20°C until use.

2.7.1.3 Preparation of genomic DNA from *C. glutamicum*

C. glutamicum strains were cultivated overnight in 5 ml LB medium at 30°C and 170 rpm on a rotary shaker. Cells were harvested at 3,760 x *g* for 5 min. The cell pellet was resuspended in 400 µl enzymatic lysis buffer containing 20 mg ml^{-1} lysozyme (freshly added). The mixture was incubated for 1 h at 37°C at 900 rpm in a thermomixer (Eppendorf, Hamburg, Germany). Subsequently, 80 µl 10% SDS and 25 µl proteinase K solution were added to the mixture and incubated for 1 h at 65°C. After proteinase K treatment 200 µl 6M NaCl was added and the mixture was centrifuged for 10 min at 16,000 x *g*. The supernatant was transferred into a fresh Eppendorf tube and mixed with 2.5 x vol of $EtOH_{abs}$. The precipitated chromosomal DNA was transferred with a recurved glass pipette into an Eppendorf tube containing 70% EtOH. Finally, the chromosomal DNA was air dried at the glass pipette tip and resolved in 100 µl TE buffer.

2.7.2 Nucleic acid gel electrophoresis

1% - 2% (w/v) agarose gels were prepared with 1x TAE buffer depending on the size of the fragment of interest. Before loading, the samples were mixed with 6x loading buffer. 7 µl of a 1 kb DNA ladder (GeneRuler™ Thermo Scientific, Schwerte, Germany) or a 100 bp DNA ladder (GeneRuler™ Thermo Scientific, Schwerte, Germany) was used for size determination of the fragments. The electrophoresis was performed in 1x TAE buffer at 75 – 95 V for 1 – 2 h. After electrophoresis the agarose gel was stained for 3 – 10 min with an ethidium bromide solution (2 µg mL^{-1}) and destained for 5 – 10 min in a water bath. The nucleic acid bands were visualized by a UV-transilluminator at 254 nm. Data documentation was done using the Quantum gel documentation system (Peqlab Biotechnologie GmbH, Erlangen, Germany).

RNA separation by size and check for the quality and purity of isolated total RNA was performed by denaturing formaldehyde (FA) agarose gel electrophoresis. RNA samples were mixed with 5x RNA loading buffer and incubated for 10 min at 65°C before they were loaded onto a 1.2 – 2% (w/v) agarose gel (0.6 – 1 g agarose, 5 ml 10x FA buffer, 45 ml H_2O; the solution was heated and cooled down to 65°C before 0.9 ml of 37% formaldehyde was added). The gel had to be equilibrated in 1x FA buffer for 30 min before loading. Denaturing FA agarose gel electrophoresis was performed at 55 – 80 V for 75 – 90 min. Gel documentation was done using Quantum gel documentation system (Peqlab Biotechnologie GmbH, Erlangen, Germany).

2.7.3 Determination of nucleic acid concentrations

The nucleic acid concentrations were determined by measuring the absorbance at 260 nm (A_{260}) with a spectrophotometer (Nanodrop® ND-1000, PeqLab Biotechnologie GmbH, Erlangen, Germany). The following conversion factors were used to calculate the DNA or RNA concentration (Sambrook & Russell, 2001):
ss DNA or RNA: A_{260} = 1 corresponds to a concentration of 40 µg/ml,
ds DNA: A_{260} = 1 corresponds to a concentration of 50 µg/ml.

The purity of DNA and RNA was displayed by the ratio of the absorbance value at A_{260} and the absorbance value at A_{280}, which should be between 1.8 – 2.0 for pure DNA and 2.0 for pure RNA.

The RNA concentration of generated 6C RNA in vitro transcript was determined with the Qubit® 2.0 fluorometer (Life technologies, Darmstadt, Germany). This method is based on the measurement of a fluorescent dye. RNA concentrations were determined using the Qubit™ RNA Broad Range (BR) Assay Kit according to the manufacturer`s instructions. With the BR Assay Kit sample concentrations in the range of 1 ng μL^{-1} – 1 µg μL^{-1} can be determined. A working solution was prepared by diluting the Qubit™ RNA BR reagent 1:200 in Qubit™ RNA BR buffer. 10 µL of each Qubit™ BR pre-diluted RNA standard (standard #1: 0 ng μL^{-1} and standard #2: 100 ng μL^{-1} in TE buffer) was added to 190 µl of working solution and mixed by vortexing for 2 – 3 sec. 1 µl of each RNA sample was added to 199 µl of the working solution and mixed. All tubes were incubated for 2 min at RT before the results were read in the fluorometer.

2.7.4 Polymerase Chain Reaction (PCR)

Polymerase chain reaction (PCR) (Mullis*, et al.*, 1986) was used for amplification of DNA fragments, for verification of cloning steps in *E. coli* DH5α cells, and for detection of desired integration or deletion mutants of *C. glutamicum* (Colony-PCR). For amplification of DNA fragments, the KOD Hot Start Polymerase (Novagen®, brand of EMD Biosciences, Inc., an affiliate of Merck KGaA, Darmstadt, Germany) was used. DreamTaq DNA polymerase (Thermo Scientific, Schwerte, Germany) was used for verification of cloning steps and for Colony-PCR. Oligonucleotides used for PCR reactions are listed in table 1. PCR reactions were performed in a T3000 thermocycler (Biometra, Göttingen, Germany). PCR setup (i.e. choice of reaction components, annealing temperature, elongation time) was done according to the manufacturer's instructions. The PCR was performed for 30 – 33 cycles. Amplification reactions were carried out in 50 µl total volume containing 50 – 300 ng template DNA, 400 nM each of the respective oligonucleotides, 1.0 – 1.5 mM $MgSO_4$, 1 U KOD Hot Start Polymerase and 200 µM dATP, dCTP, dGTP and dTTP. Initial denaturation at 95°C for 2 min was done prior to the start of the first cycle. Each cycle was defined by a 30 sec denaturation

step at 95°C, a 15 – 30 sec annealing step and a x sec polymerization step at 70°C. A final 3 – 5 min elongation step at 70°C followed. The annealing temperature was chosen 2 – 4°C below the melting temperature of the oligonucleotides. The melting temperature can be calculated using the formula TM [°C] = [(G + C) x 4] + [(A + T) x 2]. The extension time of the PCR was chosen according to the size of the DNA fragment to be amplified.

For Colony-PCR a single colony was transferred into 10 µl H_2O. 4 µl of the inoculated H_2O was used for the Colony-PCR.

For the detection of 6C RNA by Northern Blot a single-stranded (ss) digoxigenin (DIG)-labeled DNA probe (-28 bp to +139 bp relative to the 6C RNA TSS) was generated by PCR with oligonucleotide NB_rv. For amplification of ss DIG-labeled DNA probe the concentration of dTTP was reduced from 200 µM to 160 µM, 30 µM DIG-11-dUTP (Roche, Mannheim, Germany) were added to the reaction mixture, and 600 nM instead of 400 nM of the oligonucleotide NB_rv (Table 1) were used in the PCR reaction. As template a 167 bp PCR product (-28 bp to +139 bp from 6C RNA TSS) generated with the oligonucleotide pair NB_fw/NB_rv was used.

2.7.5 Purification of DNA fragments

The Omnipure-OLS® Kit (OLS® Omni Life Science GmbH & Co.KG, Bremen, Germany) was used for isolation of DNA fragments from agarose gels. Gel extraction was performed according to the manufacturer`s instructions. The DNA was eluted with sterile water and stored at –20°C.

The MinElute PCR Purification Kit (Qiagen, Hilden, Germany) was used for purification of PCR products to remove residual nucleotides and enzymes after PCR and restriction digestion according to the manufacturer's instructions.

2.7.6 Recombinant DNA techniques

All restriction endonucleases used for recombinant DNA work were "Fast Digest" (FD) enzymes and obtained from Thermo Scientific (Schwerte, Germany). Restriction endonucleases were used according to the manufacturer's instructions. Restrictions were carried out at 37° C for 30 – 60 min in "Fast Digest" buffer. A total volume of 50 µl was prepared for each digest. The reaction mixture contained 1 – 2 U of the enzymes per 1 µg of DNA. 1 µl Shrimp Alkaline Phosphatase (Thermo Scientific, Schwerte, Germany) was added to the respective samples and incubated at 37°C for 45 min to prevent religation of plasmid DNA. The Rapid DNA Ligation Kit (Thermo Scientific, Schwerte, Germany) was used according to the manufacturer's instructions for ligating DNA fragments. A total volume of

20 µl containing 5 U T4 ligase, 50 – 100 ng of digested vector DNA and three times molar excess of the PCR product was prepared and incubated for 45 min at RT.

2.7.7 DNA sequencing

DNA sequencing was performed using the single read sequencing service of Eurofins MWG Operon (Ebersfeld, Germany). The samples were premixed with gene-specific oligonucleotides or oligonucleotides binding to the plasmid backbone according to the sequencing guidelines of the company. The received sequences were compared to the in-silico sequences using the freeware tool BioEdit (Ibis Biosciences, Carlsbad, USA) or the software CloneManager 9 Professional Edition (Scientific & Educational Software, Cary, USA).

2.7.8 Generation and transformation of competent *E. coli*

5 ml LB preculture was inoculated with a single colony from a fresh LB agar plate and incubated overnight on a rotary shaker at 37°C and 170 rpm for the generation of competent *E. coli* DH5α. The 70 ml LB main culture (500 ml baffled shake flask) was inoculated with 100 µl of the preculture and was cultivated at 37°C to an OD_{600} of 0.5. The cells were chilled on ice for 10 – 15 min, transferred to a falcon tube and harvested by centrifugation at 4°C and 4,000 x *g* for 10 min. After removing the supernatant, the pellet was resuspended in 15 ml 70 mM $CaCl_2$/20 mM $MgSO_4$ and incubated for 30 min on ice and centrifuged for 10 min at 4°C. After again removing the supernatant, the pellet was resuspended in 5 ml 70 mM $CaCl_2$/20 mM $MgSO_4$ and incubated for 30 min on ice. 1.25 ml 87% glycerol were added to the suspension and the mixture was dispensed in 150 µl aliquots. The aliquots were immediately frozen in liquid nitrogen and stored at –80°C.

Competent *E. coli* DH5α cells were slowly thawed on ice. Subsequently, 10 – 100 ng of plasmid DNA or 20 µl of ligation mixture was mixed with 100 µl of competent cells and incubated for 30 min on ice, followed by a 90 sec heat shock at 42°C. Afterwards, the transformation mixture was incubated for 2 min on ice and mixed with 500 µl LB medium. The regeneration step was performed at 37°C and 300 rpm for 1 h in a thermomixer (Eppendorf, Hamburg, Germany). The cell suspension was plated on LB agar plates containing the appropriate antibiotic and incubated overnight at 37°C.

2.7.9 Generation and transformation of competent *C. glutamicum*

Generation of electro-competent *C. glutamicum* cells was performed according to the protocol of (Tauch*, et al.*, 2002). A 20 ml BHIS preculture (100 ml baffled shake flask) was inoculated with a single colony from a fresh BHIS agar plate and incubated overnight on a rotary shaker at 30°C and 130 rpm. The 60 ml BHIS main culture (500 ml baffled shake flask) was inoculated to an OD_{600} of 0.5 and was cultivated on a rotary shaker at 30°C and 120 rpm to an OD_{600} of approximately 1.75. The cells were transferred into a prechilled 50 ml falcon tube and harvested by centrifugation at 4°C and 5,000 x *g* for 20 min. After removing the supernatant, the pellet was resuspended in 10 ml ice-cold TG buffer and centrifuged for 10 min at 4°C and 5,000 x *g*. This washing step was repeated two times. Afterwards the cell pellet was resuspended in 10 ml ice-cold sterile 10% (v/v) glycerol and centrifuged for 10 min at 4°C and 5,000 x *g*. This washing step was repeated. Then the supernatant was completely removed, the cell pellet was resuspended in 0.4 – 1 ml ice-cold 10% glycerol and dispensed in 150 µl aliquots. The aliquots were immediately frozen in liquid nitrogen and stored at -80°C.

The transformation of *C. glutamicum* was performed by electroporation. Competent *C. glutamicum* cells were slowly thawed on ice. 0.1 – 5 µg of plasmid DNA was added to the competent cells and the mixture was transferred into a precooled 0.2 cm Gene Pulser cuvette (Bio-Rad Laboratories GmbH, München, Germany). 0.8 ml 10% (v/v) glycerol was carefully placed on top of the mixture. Cells were electroporated by a single-puls procedure. Electroporation was performed at 2.5 kV, 25 µF and 200 Ω at which the time constant should be between 3.5 and 4 msec. Subsequently, the cell suspension was transferred into 4 ml pre-warmed BHIS medium and incubated at 46°C for 6 min for heat-shocking the cells. A regeneration step was performed for 60 min at 30°C and 170 rpm prior to plating onto BHIS agar plates containing the appropriate antibiotic. The inoculated agar plate was incubated at 30°C for one to two days. The vector pK19*mobsac*B is not replicated in *C. glutamicum* as circular plasmid, therefore a Kanamycin resistance indicates an integration of the plasmid into the bacterial genome by homologous recombination.

2.7.10 Chromosomal gene replacement using the pK19*mobsacB* system

In-frame deletions of DNA sequences in *C. glutamicum* strains were done via two-step homologous recombination based on vector pK19*mobsacB* (Schäfer*, et al.*, 1994) and a method described by Niebisch and Bott (2001): DNA sequences to be integrated or deleted were cloned together with their >500 bp up- and downstream regions into vector pK19*mobsacB*. After transformation of the respective *C. glutamicum* strain, clones with integrated vector were selected using BHIS agar plates with 15 µg ml^{-1} Kanamycin. Since pK19*mobsacB* is a non-replicative plasmid, appearance of Kanamycin-resistant cells

depends on integration of the plasmid into the genome via homologous recombination. For excision of the vector, clones were either incubated in 5 ml BHI medium in test tubes at 30°C and 170 rpm on a rotary shaker for 3 – 5 h and plated on BHIS agar plates with 10% (w/v) sucrose or clones were incubated overnight in 5 ml BHI_{Kan25} medium at 170 rpm at 30°C and were then transferred into 5 ml CGXII medium without nitrogen and phosphate source and incubated at 30°C and 170 rpm on a rotary shaker for 6 h and plated on BHIS agar plates with 10% (w/v) sucrose. The vector pK19*mobsacB* carries the gene *sacB*. This gene codes for the enzyme levansucrase that catalyzes sucrose hydrolysis and synthesis of levan, which is lethal to *C. glutamicum* (Jäger*, et al.*, 1992). Using plates with sucrose, only clones which had excised the vector were selected. Finally, clones which showed both sucrose-resistance and Kanamycin-sensitivity were checked via Colony-PCR and DNA sequencing for proper gene integration or deletion.

2.7.11 RNA in vitro transcription

In vitro transcription to generate the full length 6C RNA transcript was performed with a linearized vector pUCBM21-*6C RNA* gg template obtained by PsiI digestion. RNA transcripts were amplified by T7 RNA polymerase, using the RiboMax Kit (Promega, Madison, USA) according to the manufacturer`s instruction. The 6C RNA in vitro transcription reaction mixture contained 7.5 mM ATP, CTP, GTP and UTP, 600 ng of linearized plasmid DNA template and 2 µl T7 Enzyme Mix (T7 RNA Polymerase, Recombinant RNasin® Ribonuclease Inhibitor Recombinant Inorganic Pyrophosphatase) in 1x T7 buffer. In vitro transcription reaction was performed in a total volume of 20 µl for 3 h at 37°C. Subsequently, a DNAse treatment (1 U of R1Q DNAse per 1 µg of DNA) was performed for 15 min at 37°C to remove DNA template. The 6C RNA transcript was purified using phenol chloroform extraction and concentrated by ethanol precipitation. RNA concentrations were determined using the Qubit Fluorometer.

2.7.12 RNA purification by phenol chloroform extraction

RNA samples were filled ad 200 µl with nuclease-free water and mixed with 200 µl acidic phenol/chloroform/isoamyl alcohol (25:24:1), pH 4.5 – 5.0. The solution was mixed until an emulsion was formed. The organic phase was separated from the aqueous phase using Phase Lock Gel tubes (Eppendorf, Hamburg, Germany). The mixture was centrifuged for 15 min at 12,000 x *g* in the Phase Lock tube. The aqueous phase (in the upper part of the Phase Look tube) was transferred into a new Eppendorf tube and mixed with 200 µl chloroform/isoamyl alcohol (24:1) to remove remaining phenol. The mixture was transferred

into a fresh Phase Lock gel tube and centrifuged for 15 min at 12,000 x *g*. The supernatant was transferred into a new Eppendorf tube and precipitated with ethanol.

2.7.13 Ethanol precipitation of RNA

RNA was mixed with 1/10 x vol of 3 M NaOAc, pH 5.0 and 2.5 – 3 x vol of $EtOH_{abs}$ for RNA precipitation and incubated either at –80°C for 1 h or at –20°C overnight, respectively. Subsequently, the RNA was centrifuged for 1 h at 16,000 x *g* at 4°C. The supernatant was carefully removed and the pellet was washed with 500 µl 75% EtOH and centrifuged for 5 min at 16,000 x *g*. The supernatant was removed and the pellet was dried for 2 – 10 min at 75°C and resuspended in nuclease – free water.

2.7.14 Northern blot analysis

For the detection of 6C RNA in total RNA of *C. glutamicum* by Northern blot a complementary single - stranded (ss) digoxigenin (DIG)-labeled specific DNA probe, generated by PCR, was used.

Total RNA was separated by size by denaturing FA agarose gel electrophoresis. The separated RNA was transferred from the agarose gel to a nylon membrane (Roche Diagnostics GmbH, Mannheim, Germany) by downward capillary transfer. The transfer was performed for 3 to 4 h in 5 x ASSC. After “blotting”, the RNA was covalently bound to the nylon membrane by UV cross-linking (1200 mJ cm^{-2}).

For the detection of 6C RNA by DIG-11-dUTP-labeled specific DNA probe first, a prehybridization of the cross-linked membrane was carried out for 30 – 60 min at 45°C in 10 ml prehybridization buffer (hybridization buffer with 0.1 mg ml^{-1} salmon sperm DNA) to block non-specific nucleic acid-binding sites on the membrane. Hybridization with the DIG-11-dUTP–labeled specific DNA probe was performed overnight at 51°C in hybridization buffer, the DNA probe was previously denatured by heating to 95°C – 100°C for 10 min in a boiling water bath. After hybridization the specific DNA probe could be detected in a chemiluminescence reaction of alkaline phosphatase, that is coupled to a DIG-specific antibody (Roche Diagnostics GmbH, Mannheim, Germany), with the substrate CDP-Star® (Roche Diagnostics GmbH, Mannheim, Germany). Unless otherwise mentioned all posthybridization steps were performed at RT. Membranes were washed twice for 5 min in 2x SSC, 0.5% SDS and twice for 15 min in 1x SSC, 0.5% SDS at 50°C to remove unbound probe. Subsequently, the membranes were stored in blocking solution for 30 min to prevent nonspecific attraction of antibody to the membrane. Afterwards, the membrane was incubated for 30 min in 20 ml antibody solution (1 µl anti-DIG-AP conjugate (Roche Diagnostics GmbH, Mannheim, Germany) in 10 ml blocking solution). Then, another washing

step, twice for 15 min, in 100 ml wash buffer was performed. Afterwards, the membrane was equilibrated for 2 – 5 min in 20 ml in detection buffer and then incubated for 5 min in CDP-Star working solution (4 drops of ready-to-use CDP-Star solution (Roche Diagnostics GmbH, Mannheim, Germany) in 10 mL detection buffer). Chemiluminescence signals were detected in a CCD camera (Image analyzer LAS-3000, Fuji Photo Film (Europe) GmbH, Düsseldorf, Germany) and quantified using the AIDA Image analyzer software (raytest Isotopenmeßgeräte GmbH, Straubenhardt, Germany).

2.7.15 Quantification of 6C RNA molecules per cell

Northern blot analysis was used to quantify the amount of 6C RNA per cell. The signal intensity of defined amounts of 6C RNA *in vitro* transcript was compared to endogenous 6C RNA quantity in defined amounts of total RNA of *C. glutamicum*. Chemiluminescence signals were detected in a CCD camera (Image analyzer LAS-3000, Fuji Photo Film (Europe) GmbH, Düsseldorf, Germany) and quantified using the AIDA Image analyzer software (raytest Isotopenmeßgeräte GmbH, Straubenhardt, Germany). With the data of the quantification the amount of 6C RNA in 1 µg of total RNA could be calculated. The number of 6C RNA molecules per cell was calculated based on the amount of total RNA per cell. The amount of total RNA per cell was calculated from the entire amount of total RNA that was isolated with the RNeasy kit (Qiagen, Hilden, Germany) from a respective amount of cells (with a known number of OD_{600} units). For the calculation of the amount of cells a conversion factor of 1.8×10^8 cells per 1 OD_{600} unit (Grünberger*, et al.*, 2012) and personal communication Nicole Paczia) was used. Then, the amount of 6C RNA per cell was calculated from the amount of total RNA per cell and the amount of 6C RNA in 1 µg of total RNA. Finally, the amount of 6C RNA was calculated into molecules per cell with the help of the web tool of “Praktische Molekularbiologie” (http://molbiol.ru/ger/scripts/01_07.html).

2.7.16 RNA-protein interaction studies

RNA-protein interactions were studied using RNA pull- down experiments. RNA pull-down experiments were performed with in vitro generated 6C RNA coupled to adipic acid dihydrazide agarose beads (Sigma Aldrich, Taufkirchen, Germany). 500 pmol (17.3 µg) of 6C RNA in a total volume of 30 µl were denatured at 75°C for 3 min and then incubated for 30 min at RT for proper refolding of the RNA. The RNA was oxidized at the 3`end using 5 mM sodium-m-periodate solution. The periodate oxidation leads to an irreversible opening of the terminal ribose, so that a double bond can be formed between the carbon and the oxygen atom. The RNA-sodium-m-periodate mixture (in a total volume of 200 µl) was incubated for 1 h at RT in the dark. Subsequently, the RNA was concentrated by ethanol

precipitation for 1 h at –80°C. After precipitation the RNA was resuspended in 100 µl 0.1 M NaOAc, pH 5.0. 200 µl of 50% adipic acid dihydrazide agarose beads solution was washed four times with 1 ml of 0.1 M NaOAc, pH 5.0. For the washing step the beads were centrifuged for 1 min at 855 x *g*, incubated for 5 – 10 min at RT to allow the beads to sink down, and then the supernatant was carefully removed. After the final washing step the beads were resuspended in 300 µl 0.1 M NaOAc, pH 5.0 and mixed with the oxidized RNA and incubated overnight at 4°C under constant shaking. Unbound RNA was removed by washing the RNA- bound- beads three times with 1 ml 2 M KCl solution and three times with 1 ml buffer D. The beads were centrifuged for 1 min at 855 x *g*, incubated for 5 – 10 min on ice to allow the beads to sink down and then the supernatant was carefully removed. After the final washing step the RNA- bound- beads were incubated with 1 mg of protein crude extract in a final volume of 500 µl with TGED buffer, 1.5 mM $MgCl_2$ and 1 U μl^{-1} RNase inhibitor (RiboLock, Fermentas, St. Leon-Rot, Germany) for 40 min at RT and constant shaking.

The protein concentration of the crude extract was determined by measuring the absorbance at 260 nm (A_{260}) and 280 nm (A_{280}) using the Nanodrop ND-1000 spectrophotometer (Peqlab, Erlangen, Germany) and calculation of the protein concentration by the following formula:

Protein concentration [mg/ml] = (1.55 x A_{280}) - (0.76 x A_{260})

After incubation with the protein crude extract the beads were washed four times with buffer D containing 1.5 mM $MgCl_2$ and two times with nuclease – free water. After the final washing step proteins were eluted with 100 µl elution buffer and incubation for 10 min at 4°C under constant shaking. For the elution the beads were centrifuged for 1 min at 855 x *g* and the supernatant, containing the eluted protein fraction, was carefully removed. A second elution step was performed by again adding 100 µl elution buffer to the beads. Each pull-down experiment was performed in a technical duplicate in parallel to increase the amount of eluted proteins. Therefore, the elution fractions of each technical duplicate were pooled, before they were precipitated with TCA overnight at 4°C. Finally, the eluted proteins were separated by SDS PAGE.

2.8 Global gene expression analysis using DNA microarrays

2.8.1 Synthesis and labeling of cDNA

For DNA microarray analysis fluorescently labeled cDNA was synthesized from total RNA isolated from *C. glutamicum* cells. The RNA samples to be compared were transcribed into Cy3-dUTP and Cy5-dUTP fluorescently labeled cDNAs by reverse transcriptase starting from 20 – 25 µg isolated total RNA.

Fluorescence labeling was performed by using the dUTP analogues Cy3-dUTP ($\lambda_{absorption\ max}$ 550 nm, $\lambda_{fluorescence\ max}$ 570 nm, green) and Cy5-dUTP ($\lambda_{absorption\ max}$ 649 nm, $\lambda_{fluorescence\ max}$ 670 nm, red). For cDNA synthesis equal amounts of isolated total RNA samples were mixed with 500 ng of random hexamer primer (Invitrogen, Karlsruhe, Germany) and filled up to a total volume of 15 µl with RNase free water. The mixtures were incubated for 10 min at 65°C followed by incubation on ice for 2 min. Afterwards the samples were either mixed with 3 µl of 1 mM Cy3-dUTP or Cy5-dUTP (GE Healthcare, München, Germany). Finally, 11.6 µl of a reverse transcriptase master mix was added to each sample.

RT Mix for two reactions:

0.1 M DTT	6.0 µl
5x first strand buffer	12.0 µl
dNTP mix*	1.2 µl
Superscript® II reverse transcriptase (200 U/µl)	4.0 µl

* dNTP mix: 25 mM dATP, 25 mM dCTP, 25 mM dGTP, 10 mM dTTP.

Reverse transcription was performed at RT for 10 min and afterwards for 110 min at 42°C. The cDNA reaction was stopped by adding 10 µl 0.1 N NaOH and incubation for 10 min at 70°C. 10 µl of 0.1 N HCl was added to neutralize the mixture.

For sample purification, to remove oligonucleotides and enzyme components and to concentrate the cDNA, Microcon YM-30 ultrafiltration devices (Millipore, Schwalbach, Germany) or Amicon Ultra 0.5 ml filters, 30k device (Merck Millipore, Merck KGaA, Darmstadt, Germany) were employed according to the manufacturer's instructions. 50 µl reaction mixtures were transferred to Microcon or Amicon filtration devices containing 450 µl nuclease- free H_2Obidist. and concentrated by centrifugation (10 min, 16,100 x *g* or 14,000 x *g*, respectively, RT). This step was repeated. The cDNA samples were pooled and the washing step was repeated one to two times by refilling the column to 500 µl with nuclease free $H_2O_{bidist.}$. The concentrated cDNA was directly used for DNA microarray hybridization.

2.8.2 *C. glutamicum* DNA microarray hybridization

The transcriptional profile of *C. glutamicum* strains was compared using DNA microarrays. For the analysis of genome-wide gene expression analysis either custom-made 4x44K 60mer DNA microarrays obtained from Agilent Technologies (Waldbronn, Germany) or 70mer DNA microarrays of the company Operon (Cologne, Germany) were used.

2.8.2.1 Hybridization of Operon microarrays

Use of the custom-made DNA microarrays for *C. glutamicum* ATCC 13032 which were obtained from Operon is described in detail by (Frunzke*, et al.*, 2008). These microarrays were printed with sequence-specific 70mer oligonucleotides and are based on the genome sequence entry NC_006958 (Kalinowski*, et al.*, 2003). On one chip, besides 3057 oligonucleotides for protein-coding genes, also 1294 oligonucleotides for intergenic regions (IGR), 60 for t-RNAs, 15 for rRNAs and 140 oligonucleotides for positive and negative controls, plasmids and resistance genes were spotted.

The concentrated Cy3- and Cy5-labeled cDNA samples (5 µl) were mixed with 50 µl OpArray Hyb Solution (Operon Biotechnologies) denatured at 95°C for 3 min and cooled to 42°C. The denatured cDNA samples were transferred into the fillport of the DNA microarray. Hybridization was performed in a MAUI® hybridization chamber (BioMicro® Systems) at 42°C for 14 – 16 h. After hybridization the array was washed three times. The first washing step was performed in wash solution A (2 % (w/v) sodium citrate, 1 % (w/v) NaCl and 0.25 % (w/v) SDS) at 42 °C. The second washing step was performed in wash solution B (2 % (w/v) sodium citrate and 1 % (w/v) NaCl) at 37 °C. In the last washing step wash solution C (0.4 % (w/v) sodium citrate and 0.2 % (w/v) NaCl) was used at RT. The arrays were dried by centrifugation (5 min, 1,000 x *g*, RT) and immediately the fluorescence of DNA microarrays was determined at 532 nm (Cy3-dUTP) and 635 nm (Cy5-dUTP) at 10 µm resolution with a GenePix 4000B laser scanner and GenePix Pro 6.0 software (Molecular Devices, Sunnyvale, USA).

2.8.2.2 Hybridization of Agilent 4–plex microarrays

Custom-made 4x44K 60mer DNA microarrays were designed using Agilent's eArray platform (https://earray.chem.agilent.com/earray). The array design included oligonucleotides for annotated protein-coding genes and structural RNA genes of the genomes from *C. glutamicum* and three other bacterial species (*Escherichia coli*, *Gluconobacter oxydans*, and *Bacillus subtilis*). For *C. glutamicum*, the genome annotation by Kalinowski, *et al*., 2003 listing 3057 protein-coding genes and 80 structural RNA genes (tRNAs and rRNAs) was used (accession number NC_006958). The custom array design comprised each of these

genes, represented by one to three oligonucleotides, and Agilent's control spots. Use of the custom-made 4x44K 60mer DNA microarrays, which were obtained from Agilent Technologies, is described in detail by (Vogt*, et al.*, 2014).

Pooled and labeled cDNAs were hybridized at 65°C for 17 h on the 4x44K arrays using Agilent's gene expression hybridization kit, Agilent's hybridization chamber, and Agilent's hybridization oven according to the manufacturer's instructions. After hybridization, the arrays were washed using Agilent's wash buffer kit according to the manufacturer's instructions. Subsequently, the fluorescence of DNA microarrays was determined at 532 nm (Cy3-dUTP) and 635 nm (Cy5-dUTP) at 5 µm resolution with a GenePix 4000B laser scanner and GenePix Pro 6.0 software (Molecular Devices, Sunnyvale, USA).

2.8.3 DNA microarray fluorescence signal measurement and data analysis

For determination of the relative mRNA level of the samples to be compared, the surface of the DNA microarrays was irradiated with monochromatic light at wavelengths of 532 nm and 635 nm to stimulate the fluorescent dyes Cy3-dUTP and Cy5-dUTP, respectively. The emitted fluorescence was registered by light sensitive cathodes at 570 nm (Cy3 fluorescence) and at 670 nm (Cy5 fluorescence) that convert the emitted fluorescence into electrical current, which was further amplified. The determined electric current correlates directly with the Cy3 and Cy5 fluorescence. Raw data files of fluorescence images were saved in TIFF format (GenePix Pro 6.0) followed by quantitative image analysis using GenePix image analysis software and gene array list (GAL) file. The ratio of Cy3- and Cy5-fluorescence correlates to the relative number of mRNA molecules in the samples and therefore it is a dimension for the relative mRNA level. The fluorescences of each spot were used to calculate the numerical values (Ratio of Medians) reflecting the relative mRNA levels and assigned to the appropriate genes of *C. glutamicum* using the Genepix Pro 6.0 software and a gene array list (GAL).

Results were saved as GPR-file (GenePix Pro 6.0) and processed using the BioConductor R-packages limma and marray (http://www.bioconductor.org) to achieve background correction of spot intensities, ratio calculation/normalization, and diagnostic-plot generation for array quality control. The calculation of signal- to- noise ratios of Cy3- and Cy5-fluorescent signals resulted from the quotient signal $\text{intensity}_{\text{spot signal}}/\text{intensity}_{\text{background}}$. For analysis, processed and loess-normalized data along with detailed information about the experiments according to the MIAME standard (Brazma, 2009) were saved in the in-house DNA microarray database (Polen and Wendisch, 2004). Analysis of differentially expressed genes was carried out by filtering processed Cy5/Cy3 ratios reflecting the relative mRNA level using the following criteria: (i) Flags ≥0; (ii) signal/noise of Cy5 (F635Median/B635Median) or Cy3 (F532Median/B532Median) ≥5. For calculation of p-

values paired Student's t-test was used comparing the relative RNA levels of a gene in the replicates to the relative RNA levels of all other genes in the replicates.

2.9 Protein biochemical methods

2.9.1 Cell disruption methods

For mechanical cell disruption a French pressure cell (SLM Aminco, Urbana, IL) was used. Cells were resuspended in 10 – 20 ml of the respective cell lysis buffer containing protease inhibitor cocktail (1 tablet Complete Mini, EDTA-free per 10 ml, Roche Diagnostics, Mannheim, Germany). *C. glutamicum* cells were disrupted at 172 MPa for five to six times. *E. coli* cells were disrupted at 108 MPa for five times. Intact cells and cell debris were removed by centrifugation at 5,087 × *g* for 40 min at 4°C. The membranes present in the resulting supernatant were separated by ultracentrifugation for 1.5 h at 229,600 × *g* and 4°C. The supernatant containing the soluble protein fraction was used for further experiments.

For enzyme activity tests with crude extract cells were disrupted by ultrasonic treatment. Cell pellets were washed twice with 20 ml 100 mM TEA pH 7.3 (5 min 3,940 x *g* 4°C). Cell extracts were prepared by resuspension in 1 ml 100 mM TEA pH 7.3 containing protease inhibitor cocktail (1 tablet Complete Mini, EDTA-free per 10 ml, Roche Diagnostics) and disruption by ultrasonic treatment (UP 200s; Dr. Hielscher GmbH, Teltow, Germany) at a duty cycle of 0.5 and an amplitude of 55% for 6 min at 4°C. The lysate was centrifuged at 16,000 × *g* for 1 h at 4°C. Immediately after centrifugation the cell-free supernatant was used for enzyme activity tests.

2.9.2 Determination of protein concentrations

Protein concentrations of crude extracts were determined either using the Bradford assay or the bicinchoninic acid (BCA) assay.

The Bradford method (Bradford, 1976) is based on a shift in absorption maximum from 465 nm to 595 nm of the dye Coomassie brilliant blue G in acidic solution by binding to proteins. 1.5 ml of Bradford reagent (Sigma-Aldrich, Taufkirchen, Germany) were mixed with 50 µl of the respective protein sample and incubated for 5 min at RT in the dark. After incubation the absorption was measured with a UV-1800 Shimadzu UV-spectrophotometer (Shimadzu Cooperation, Kyoto, Japan) at 595 nm in a plastic cuvette with a width of 1 cm. Water, instead of protein, was used as blank. The calculation of the protein concentration was based on a calibration curve with BSA in the range of 0.1–1 mg ml^{-1}. The BSA samples were treated like the protein samples.

Beside the Bradford method the BCA assay (Smith*, et al.*, 1985) was used. 25 µl of protein sample were mixed with 200 µl BCA reagent („BCA™ Protein Assay-Kit", Pierce

Biotechnology Inc., USA) and incubated for 30 min at 37 °C. Subsequently, the extinction at 562 nm was measured in a 96–well microplate in an absorbance microplate reader (SpectraMax plus, Molecular Devices, Biberach an der Riss, Germany). The calculation of the protein concentration was based on a calibration curve with BSA in the range of 0.02 – 2 mg ml^{-1}. The BSA samples were treated like the protein samples.

2.9.3 Protein precipitation

Proteins were precipitated using 1/10 x vol of TCA and incubation overnight at 4°C. Precipitated proteins were centrifuged for 30 min at 16,000 x *g* at 4°C. The supernatant was removed and the protein pellet was washed with 500 µl acetone and centrifugation for 30 min at 16,000 x *g* and 4°C. Again the supernatant was removed and the pellet was air dried before resuspending the pellet in 13 µl 50 mM Tris buffer, pH 7.6.

2.9.4 SDS polyacrylamide gel electrophoresis

SDS PAGE was used for the determination of the MW of proteins. The NuPAGE® SDS PAGE Gel System was purchased at Invitrogen and used according to the manufacturer`s instructions. NuPAGE® Bis-Tris Gels were used in combination with the NuPAGE® MES buffer. Protein samples were resuspended in 13 µl 50 mM Tris buffer pH 7.5 and mixed with 2 µl NuPAGE® Reducing Agent (10x) and 5 µl NuPAGE® LDS Sample Buffer (4x). Proteins were denatured for 10 min at 70°C before loading the entire protein sample on the pre-cast 10% Bis-Tris SDS PAGE gel. For the determination of the molecular weights the SeeBlue® Plus2 pre-stained standard (Thermo Scientific, Schwerte, Germany) was used. Protein separation was performed at constant current (80 mM per gel). Proteins were visualized by staining with Coomassie brilliant blue. First, the polyacrylamide gel was washed for at least 20 min in H_2O_{bidist}. followed by staining in GelCode ®Blue Stain Reagent (Thermo Scientific, Schwerte, Germany) for 1h. Finally, the gel was washed in $H_2O_{bidist.}$ for at least 5 x 10 min and scanned (Typhoon TRIO variable mode imager, GE Healthcare, Uppsala, Sweden).

2.9.5 Protein overexpression and purification

2.9.5.1 Heterologous overexpression of RamA in *E. coli* BL21(DE3) and protein purification

RamA-His_6 was overproduced in *E. coli* BL21(DE3) using the expression plasmid pET28a-*ramA*. *E. coli* BL21(DE3)/ pET28a-*ramA* was grown in 500 ml TB_{Kan50}. Expression was induced at an OD_{600} of 2.0 by addition of 1 mM IPTG. Two hours after induction, cells

were harvested by centrifugation, washed once with the appropriate disruption buffer, and stored at −20°C.

For purification of RamA-His_6, thawed cells were resuspended in 30 ml buffer NNG (50 mM NaH_2PO_4 (pH 8.0), 300 mM NaCl, 5% (v/v) glycerol) containing 20 mM imidazol (NNIG-20) and disrupted mechanically with a French pressure cell (SLM Aminco, Urbana, IL) at 1300 psi five times. Intact cells and cell debris were removed by centrifugation for 40 min at 5,087 x *g* and 4°C. The membranes present in the resulting supernatant were separated by ultracentrifugation for 1.5 h at 229,600 x *g* and 4°C. The soluble protein fraction was then applied to a HisTrap FF 1-ml column (GE Healthcare Germany, Munich, Germany) previously equilibrated with NNIG-20 buffer for nickel chelate affinity chromatography. Adsorbed proteins were eluted with a stepwise gradient consisting of 75, 308, and 500 mM imidazol in buffer NNG. Fractions containing RamA-His_6 collected at 308 mM imidazol were pooled, and the buffer was exchanged with storage buffer by using a 5-ml HiTrap desalting column (GE Healthcare, München, Germany) as described by the manufacturer.

2.9.5.2 Heterologous overexpression of PGK_{Cg} in *E. coli* BL21 (DE3) and protein purification

Phosphoglycerate kinase (PGK) of *C. glutamicum* was overexpressed in *E. coli* BL21(DE3) using the pET16b-pgk, which allows IPTG-inducible expression of an N-terminal tenfold His-tagged PGK_{Cg}. *E. coli* BL21(DE3)/ pET16b-pgk was grown in 500 ml LB_{Carb50} at 37°C to an OD_{600} of 0.6 and protein expression was induced by the addition of IPTG (0.5 mM). The flasks were cooled to 22°C and incubated for 4 hours at 22°C. Cells were harvested by centrifugation (15 min at 4,424 x *g*) and the cell pellet was washed with PBS buffer (5,087 x *g*, 20 min, 4°C). The cell pellet was frozen in liquid nitrogen and stored at -20°C until use.

For purification of His_{-10} PGK_{Cg}, thawed cells were resuspended in buffer TNIG-5 and were disrupted mechanically with a French pressure cell. Protein purification of His_{-10} PGK_{Cg} was performed with metal chelate affinity chromatography (Porath*, et al.*, 1975). The soluble fraction of protein crude extract was applied on a Ni^{2+}-nitrilotriacetic acid (NTA) agarose column (1 ml bed volume, Qiagen Hilden), previously equilibrated with TNIG-5 buffer. Following application of the protein extract the column was washed with at least 20 column volumes TNIG-20 buffer to remove unbound and unspecifically bound proteins. Recombinant protein was eluted stepwise with 50, 100, and 300 mM imidazol until the entire protein was eluted from the column and no absorbance at 280 nm could be detected any longer. Protein purification was checked by SDS PAGE and the elution fractions with the highest amount of purified protein were pooled. After purification and desalting the protein was buffered in 100 mM TEA pH 7.4 and stored at 4°C.

Ni^{2+}-ions were removed from the packing material by 5 column volumes stripping buffer. The column was stored in 30% ethanol at 4°C. The column was regenerated with 5 column volumes 100 mM $NiSO_4$ and equilibrated in TNIG-5.

2.9.6 Concentration and desalting of proteins

Concentration and desalting of proteins was performed by using ultra filtration devices (MWCO 30000; Amicon Ultra, Millipore, Schwalbach, Germany) at 3,256 x *g* until the sample volume was reduced to 1 ml.

2.9.7 DNA–protein interaction studies

2.9.7.1 DNA affinity chromatography

The identification of DNA-binding proteins that interact with the 6C RNA promoter region was performed by DNA affinity chromatography. The 6C RNA promoter region was amplified from chromosomal DNA of the *C. glutamicum* ATTC 13032 using oligonucleotides 6C_Promotor_fw and 6C_Promotor_rv (Tab. 1). The amplified DNA fragment extended from -336 to +23 with respect to the 6C RNA TSS. The sequence of the oligonucleotide binding to the 3` region of the DNA was extended with sequence 23 bp in size that is complementary to the sequence of the Biotin Primer. The resulting PCR product was used as template for a second PCR with oligonucleotides 6C_Promotor_fw and Biotin Primer. Oligonucleotide Biotin Primer was 5′ tagged with biotin via a TEG linker (Eurofins MWG Operon). The resulting 381 bp DNA fragment was purified by gel filtration and coupled to Streptavidin-coated magnetic beads (Dynabeads M-280 Streptavidin; Invitrogen, Darmstadt, Germany). Dynabeads M-280 Streptavidin are uniform, supramagnetic beads to which purified streptavidin is covalently bound. Biotin has a very high affinity (K_D=10^{-15} M) to streptavidin and can therefore be used to couple the DNA fragment to the Dynabeads M-280 Streptavidin. For the enrichment of proteins binding to the 6C RNA promoter region 364 pmol (91.5 µg) biotinylated 6C RNA promoter fragment were coupled to 500 µl Dynabeads M-280 Streptavidin (10 mg/ml). Before binding of the DNA to the beads, the beads were washed with 500 µl B+W buffer. Sedimentation of the magnetic beads was performed with a Dynal MPC-1 magnet. The buffer was removed by pipetting. After a second washing step the beads were resuspended in 300 µl B+W buffer, mixed with the biotinylated DNA fragment and incubated for 1 h at RT under constant shaking. Subsequently, the DNA coupled beads were washed three times with 500 µl B+W buffer, resuspended in 500 µl TGED buffer and stored at 4°C until use.

For protein interaction studies the *C. glutamicum* crude extract was mixed with the DNA coupled beads and 500 µg of chromosomal DNA in a 15 ml Falkon tube and incubated

for 45 min at RT under constant shaking. The solution was transferred stepwise into a 2 ml reaction tube and washed five times with 500 µl TGED buffer. In the second and third washing step 400 µg of chromosomal DNA was added. The bound proteins were eluted with two times 350 µl elution buffer. The elution fractions were pooled and the proteins were precipitated by TCA at 4°C overnight. Finally, the eluted proteins were resuspended in 13 µl Tris buffer, pH 7.5, and separated by SDS-PAGE, stained with Coomassie, and identified by tryptic peptide mass fingerprinting.

2.9.7.2 Gel retardation experiments

The binding of purified sixfold His-tagged RamA to the 6C RNA promoter region was tested by electromobility shift assays (EMSAs). The DNA fragments used in the EMSAs were generated by PCR. The 337 bp DNA fragment covering the promoter region of the 6C RNA gene was generated with the oligonucleotides 6C_Promotor_fw and 6C_Promotor_rv_2 (table 1). As negative control a 337 bp fragment (generated with the oligonucleotides Ppgi_Promotor_fw_JP and Ppgi_Promotor_rv_JP) covering the promoter region of the *pgi* gene was used. As positive control a 586 bp DNA fragment (generated with the oligonucleotides aceb1 and acebR4) covering the promoter region of the *aceA/B* gene was used. The concentrations of the respective DNA fragments were measured with a Nanodrop ND-1000 spectrophotometer (Peqlab, Erlangen, Germany).

In the binding assay 85 ng (0.38 pmol) of the respective DNA fragments were incubated with various amounts of RamA protein (0 – 0.76 µg) in RamA binding buffer with 0.05 µg poly [d(I - C)] in a total volume of 20 µl for 20 min at RT. Subsequently, the samples were loaded onto a native 10% polyacrylamide gel and separated by electrophoresis at 150 V for 60 to 90 min using 0.5x TBE buffer. The gel was stained with Sybr green I and visualized with a UV-transilluminator at 254 nm. Data documentation was done using the Quantum gel documentation system (Peqlab Biotechnologie GmbH, Erlangen, Germany).

2.9.8 PGK_{Cg} enzyme activity assays

The PGK activity of *C. glutamicum* was determined with purified enzyme and cell-free extracts of *C. glutamicum* ATCC 13032, *C. glutamicum* ∆6CiP, *C. glutamicum*/pJC1, *C. glutamicum*/pJC1-6C. For the measurement of the PGK activity in cell-free extracts *C. glutamicum* and the respective derivatives were cultivated in minimal and in complex medium to the exponential growth phase. Cell-free extracts were prepared by ultrasonic treatment. In vitro enzyme assays were carried out spectrophotometrically in a coupled assay in which, product of the first reaction catalyzed by PGK_{Cg}, namely 1, 3 - bisphosphoglyerate is reduced by the second enzyme glyceraldehyde-3-phosphate

dehydrogenase (GAPDH), which uses NADH. Assays were conducted in 100mM TEA buffer (pH 7.4) containing 1 mM EDTA, 2 mM $MgSO_4$, 1 mM ATP, 10 mM 3-Phosphoglycerate, 0.2 mM NADH, 10 U ml^{-1} of GAPDH (rabbit muscle). Approximately 60 ng of His-tagged PGK was used for each assay. The enzyme activity was measured by following the decrease in absorbance at 340 nm due to oxidation of NADH. All spectrophotometric measurements were carried out with an Ultrospec 3000 UV/visible spectrophotometer (Amersham Pharmacia Biotech, Freiburg, Germany) at 30°C. NAD^+ formation was followed at λ = 340 nm and an extinction coefficient of 6.22 mM^{-1} cm^{-1} for NADH was used. Enzyme activities were evaluated with the help of the SWIFT II software (Biochrom Ltd., Cambridge, UK). The Enzyme activity was calculated as follows:

$$\frac{\Delta Abs\ min^{-1} \times total\ volume\ (ml)}{6.22\ mM^{-1}\ cm^{-1} \times sample\ volume\ (ml)}$$

One unit (U) of specific enzyme activity is defined as 1 µmol × min^{-1} × mg^{-1} of protein.

2.10 MALDI ToF mass spectrometry

For peptide mass fingerprint analysis with the mass spectrometer Ultraflex III TOF/TOF (Bruker Daltonics, Bremen, Germany) protein bands were excised from Coomassie stained acrylamide gels to subject the proteins to tryptic in-gel digestion. For tryptic in-gel digestion the gel pieces were washed for 10 min with 750 µl 0.1 M ammonium bicarbonate in 30% (v/v) acetonitrile. This step was repeated until the dye was completely removed from the gel pieces. Afterwards the gel pieces were dried in a speed vac (Concentrator 5301, Eppendorf, Hamburg, Germany). Then the gel pieces were rehydratized with 6 µl 3 mM Tris-HCl buffer (pH 8.8) with 10 ng $µl^{-1}$ trypsin (Promega, Madison, WI, USA). After 30 min another 6 µl 3 mM Tris-HCl buffer (pH 8.8) were added. The tryptic digest was performed over night at RT. The tryptic peptides were eluted with 10 µl H_2Obidist. (15 min incubation at RT) and addition of 10 µl 0.2% (v/v) trifluoroacetic acid in 30% (v/v) acetonitrile (10 min incubation at RT). Samples were transferred on PACII (Prespotted Anchor Chip) targets (Bruker Daltonics, Bremen, Germany) containing prespotted α-cyano-4-hydroxycinnamic acid as matrix and a standard with a mass spectrum of 757 – 3574 Da. Samples were analyzed in the positive reflector mode and an acceleration potential of 26.3 kV. For device control and for data analysis the Bruker-Software „flexControl 3.0“ and „flexAnalysis 3.0“, respectively were used. Subsequently, the program „BioTools 3.1“., the MASCOT-Server (Matrix Science, London, UK) and the Mascot algorithm (Matrix Science, v.2.2.0) were used to compare the experimentally determined peptide mass patterns

(between 900 – 4500 Da) with those of the entire in house *C. glutamicum* protein data base. When comparing the peptide masses with the MASCOT-software and with the MS-Fit program search parameters allowed for one missed cleavage in the trypsin digest, one carbamidomethyl substitution at the cysteine as fixed modification, a variable modification due to methionine oxidation and a deviance of 50 to maximally 100 ppm. The molecular weight molmass search (MOWSE) ≥ 46 was used for unequivocal identification of proteins and peptides (Pappin*, et al.*, 1993).

2.11 Microscopy techniques

3 – 4 µl of *C. glutamicum* cultures and derivatives were pipetted onto an agarose pad on a microscope slide and observed using a Zeiss Axio Imager.M2 microscope (Zeiss, Jena, Germany). Data were acquired using AxioVision software. Images were taken at 1,000 x magnification.

For a combined staining of *C. glutamicum* cells with DAPI and Nil Red, samples of cell cultures were diluted in an appropriate volume of PBS buffer and mixed with the appropriate volume of staining solution (5 ml PBS, 1 ml DAPI and 3 µl Nil Red stock solutions), 50 µl culture and 100 µl staining solution. The mixture was incubated for 10 min in the dark.

2.12 Quantification of metabolites

2.12.1 Quantification of glucose and organic acids in culture supernatants

For quantification of substrate consumption and product formation, samples of 1 ml were taken from cultures and centrifuged twice at room temperature (6,000 x *g*, 5 min, 15,000 x *g*, 10 min). Resulting cell-free culture supernatants were analysed. The detection and quantification of organic acids and glucose in culture supernatants was performed using an Agilent 1100 liquid chromatography system (Agilent Technologies, Waldbronn, Germany) equipped with an organic acid column (300 x 8 mm polystyrol-divinylbenzol resin) from CS Chromatographie Service GmbH (Langerwehe, Germany) and a suitable guard cartridge (40 x 8 mm). Organic acids and glucose were separated by isocratic elution at 40°C with 100 mM sulfuric acid for 38 min at a flow rate of 0.4 ml min^{-1}. Samples were diluted 1:4. Organic acids were detected via an Agilent 1100 diode array detector at 215 nm, glucose was detected via an Agilent 1100 refractive index detector. Quantification was performed with the program Chemstation (Agilent) using external standards of glucose and the respective organic acids.

2.12.2 Quantification of amino acids

Reversed phase high-pressure liquid chromatography (RP-HPLC) with automatic o-phthaldialdehyde precolumn derivatization (Jones & Gilligan 1983) was used for amino acid quantification in culture supernatants using a 1290 Infinity System from Agilent Technologies (Waldbronn, Germany) equipped with a ZORBAX Eclipse AAA column (4.6 x 75 mm 3.5-Micron), a ZORBAX Analytical Guard column (4.6 x 12.5 mm 5-Micron) and a Agilent 1260 fluorescence detector. A gradient of 10 mM Na_2HPO_4/10 mM $Na_2B_4O_7$ (pH 8.2) buffer with increasing concentrations of methanol was used as eluent. Detection of the fluorescent isoindole derivatives was performed using an excitation wavelength of 230 nm and an emission wavelength of 450 nm. The concentration of the amino acids was determined by comparison with defined external standards of the respective amino acids. The program Chemstation (Agilent) was used for data evaluation. HPLC-samples were diluted 1:200-1:400.

3 Results

3.1 The 6C RNA and its expression in *C. glutamicum*

The analysis of the expression profile of the 6C RNA of *S. coelicolor* revealed an upregulation of the 6C RNA later in development, at a time that corresponds to spore formation (Swiercz*, et al.*, 2008). Therefore, it was analysed if the 6C RNA of *C. glutamicum* ATCC 13032 is expressed under standard growth conditions and if the expression level changes throughout growth. For this purpose total RNA was isolated, separated on a denaturing agarose gel and subsequently blotted from the agarose gel onto a nylon membrane.

Equal amounts of total RNA were loaded, because all 23S rRNA and 16S rRNA bands have approximately the same intensity and the transfer of the total RNA from the agarose gel onto the nylon membrane was successful (Figure 7). A specific 6C RNA signal could be detected in each RNA sample by using a complementary single-stranded (ss)-digoxigenin (DIG)-labeled specific DNA probe. The ss-DIG-labeled specific DNA probe was generated by PCR (see 2.7.4). The 6C RNA signal was not detected in total RNA samples of a Δ6C RNA mutant described later (see also 3.3.4 Figure 17), showing that the signal detected in the Northern blot is specific for the 6C RNA. It is obvious from Figure 7 C that the 6C RNA is indeed expressed in *C. glutamicum* ATCC 13032 throughout the entire cultivation period under standard conditions. Northern blot signals were quantified with the AIDA software and exhibited RNA level changes not greater than two-fold throughout the entire cultivation period.

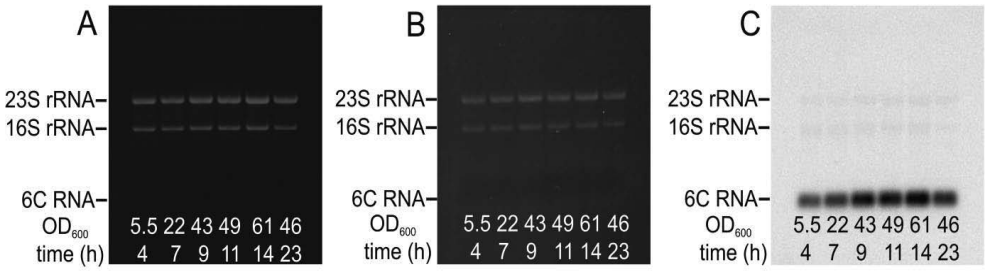

Figure 7 Northern blot experiment for the analysis of 6C RNA expression during growth. *C. glutamicum* ATCC 13032 was cultivated in CGXII medium with 4% (w/v) glucose at 30°C and 120 rpm. Samples were harvested at different time points of cultivation (after 4 to 23 h, as indicated), total RNA was isolated, separated on a denaturing agarose gel, transferred onto a nylon membrane and subsequently subjected to Northern blotting. A) Ethidium bromide-stained 1.5% denaturing agarose gel loaded with 1.2 µg of total RNA for each sample. The 23S and 16S rRNA was used to demonstrate that equal amounts of RNA have been loaded. B) Nylon membrane after blotting of the RNA from the agarose gel onto the nylon membrane. C) Northern blot for the detection of the 6C RNA transcript. The 6C RNA was visualized with a specific ss-DIG-labeled DNA probe.

3.1.1 The 6C RNA is very stable

Many sRNAs are very stable, like the 6S RNA of *E. coli* (Lee*, et al.*, 1978, Neusser*, et al.*, 2008) or RsaA and RsaH of *S. aureus* (Geissmann*, et al.*, 2009). To analyse the stability of the 6C RNA in the *C. glutamicum* wild type after 6 hours of cultivation in glucose minimal medium, the cells were treated with rifampicin to stop any further transcription initiation. Rifampicin binds in a pocket of the DNA-dependent RNA polymerase β subunit (Ezekiel & Hutchins, 1968, Matsiota-Bernard*, et al.*, 1998). The inhibitor sterically blocks the path of the elongating RNA transcript at the 5`-end when the transcript becomes either 2 or 3 nucleotides (nt) in length (Campbell*, et al.*, 2001). Therefore, RNA synthesis is completely inhibited. Since RNA underlies a specific turnover, the RNA present at the time of rifampicin addition is degraded over time, allowing the determination of the half-life. Before and after the addition of rifampicin samples were taken, total RNA was isolated and subjected to Northern blotting (Figure 8 A-C). As shown in Figure 8 C, even 240 min after the addition of rifampicin a strong 6C RNA signal could be detected. For comparison, the *gltA* mRNA transcripts encoding citrate synthase of *C. glutamicum* were used. Aliquots of the same total RNA samples as for the 6C RNA detection were separated on a denaturing agarose gel and subsequently the *gltA* mRNA was visualized with a complementary ss-DIG-labeled specific DNA probe (Figure 8 F). For *gltA* two transcripts of about 1500 bp and 1800 bp could be detected. This result is in accordance with previously published data (van Ooyen*, et al.*, 2011). Northern blot analysis revealed that the signal of the *gltA* mRNAs are no longer detectable 15 min after addition of rifampicin, showing that rifampicin is effective (Figure 8 F)

Overall, this experiment showed that the 6C RNA is a very stable RNA, with a half-life of ≥ 120 min, which is much longer compared to the half-life of *gltA* mRNAs encoding an enzyme of central metabolism (<1 min). This is also in accordance with published studies in *S. aureus*, which revealed that the majority of transcripts expressed in the exponential phase have a short half-life of < 5 min (Roberts*, et al.*, 2006). Reasons for the high stability of the 6C RNA could be its secondary structure (see also 1.3) and/or the possible binding to protein. Therefore, RNA pull-down experiments with crude extracts were conducted later to identify putative 6C RNA binding proteins (see 3.6).

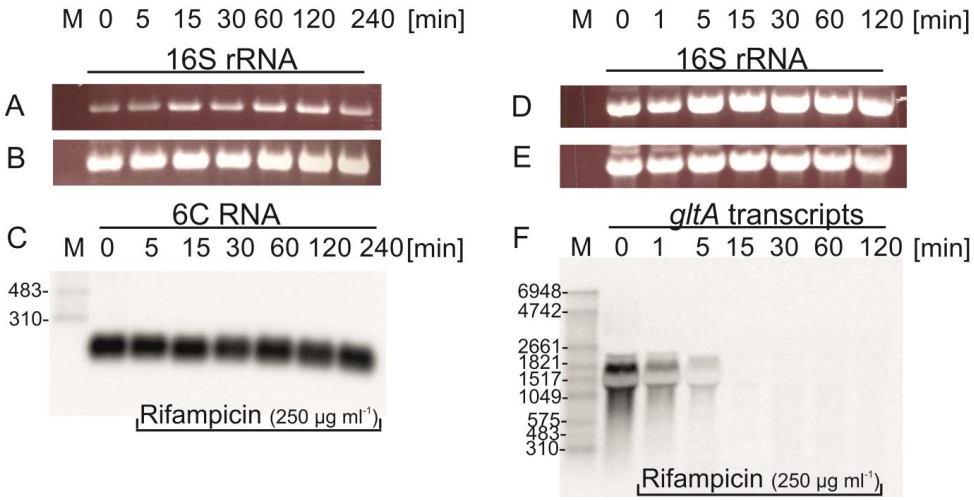

Figure 8 Northern blot analysis for the determination of the 6C RNA stability (A to C) and for comparison the stability of the *gltA* transcripts in *C. glutamicum* ATCC 13032 (D to F). *C. glutamicum* ATCC 13032 was cultivated in CGXII medium with 4% (w/v) glucose. In the exponential growth phase (after 6 hours of cultivation) the cells were treated with 250 µg ml^{-1} rifampicin and samples were taken before the addition of rifampicin (0 min) and after 1 to 240 min. A) and D) Ethidium bromide-stained 1.2% denaturing agarose gel loaded with total RNA. For the detection of the 6C RNA, 1.5 µg of total RNA was loaded for each sample. For the detection of *gltA* transcripts, 10 µg of total RNA was loaded for each sample to get an evaluable chemiluminescence signal (van Ooyen*, et al.*, 2011). The 16S rRNA was used to demonstrate that equal amounts of RNA have been loaded. B) and E) Nylon membrane after blotting of the total RNA from the denaturing agarose gel onto the nylon membrane. C) and F) Northern blot for the detection of the 6C RNA transcript and the *gltA* mRNA transcripts, respectively. The 6C RNA and the *gltA* mRNA transcripts were visualized with specific ss-DIG-labeled DNA probes, respectively. M: For 6C RNA: RNA III molecular weight marker, DIG-labeled (1517 bp, 1046 bp, 575 bp 483 bp, 310 bp); for *gltA*: RNA I molecular weight marker, DIG-labeled (6948 bp, 4742 bp, 2661 bp, 1821 bp, 1517 bp, 1046 bp, 575 bp 483 bp, 310 bp).

3.1.2 Number of 6C RNA molecules per cell

It was shown that many sRNAs, like SR1 of *B. subtilis* and 6S RNA of *E. coli* are present in high levels in the cell and that the number of sRNA molecules can be growth phase-dependent (Wassarman & Storz, 2000, Heidrich*, et al.*, 2007). To assess the abundance of the 6C RNA in *C. glutamicum*, samples were harvested in the exponential and stationary growth phase. The total RNAs of the samples were isolated, separated on a denaturing agarose gel alongside defined amounts of *in vitro* synthesized 6C RNA and subsequently subjected to Northern blotting (see in the appendix Figure A 1). 0.8 ng up to 3.2 ng of 6C RNA *in vitro* transcript was loaded for the quantification of the 6C RNA. In this range the chemiluminescence signal and the amount of *in vitro* synthesized 6C RNA showed a linear correlation (see calibration curve of signal intensity *vs*. amount of *in vitro* transcript in Figure A 1 of the Appendix). Cell numbers were determined with a conversion factor of

1.8×10^8 cells per 1 OD_{600} unit per ml cell culture (Dr. Nicole Paczia personal communication, (Grünberger*, et al.*, 2012). For details on the quantification procedure and calculation steps see 2.7.15. Using this quantification procedure, the mean amount of 6C RNA within one *C. glutamicum* cell, determined from two biological replicates, was calculated to be about 325 molecules in the exponential phase and about 260 molecules in the stationary growth phase (Table 4).

Table 4 Quantification of 6C RNA molecules per cell in *C. glutamicum* in different growth phases. Results from two biological replicates (1 and 2) are shown. For quantification of the number of 6C RNA molecules per cell, *C. glutamicum* ATCC 13032 was cultivated in CGXII medium with 4% (w/v) glucose. Samples were harvested in the exponential (exp) and stationary (stat) phase. In the first 20 ml (exp 1) and 2.1 ml (stat 1) were harvested, in the second experiment 25 ml (exp 2) and 2.9 ml (stat 2) were harvested. Total RNA was isolated, separated on a denaturing agarose gel alongside defined amounts of *in vitro* synthesized 6C RNA and subsequently subjected to Northern blotting (see Appendix Figure A 1). Northern blot signals were quantified with the AIDA software.

OD_{600}	Growth phase	Total RNA (µg)	Total RNA per cell (µg)	6C RNA (µg) in 1 µg of total RNA	6C RNA molecules per cell	6C RNA molecules per cell[1]
5.2	exp 1	237	1.27×10^{-8}	0.0018	373	
5.0	exp 2	239	1.05×10^{-8}	0.0016	277	325
49.0	stat 1	187	1.01×10^{-8}	0.0016	264	
43.2	stat 2	293	1.29×10^{-8}	0.0012	255	260

[1] Mean of two biological replicates

3.1.3 Putative transcriptional regulators of the 6C RNA

Knowledge about the transcriptional regulation of the 6C RNA might help to get a better understanding under which conditions the 6C RNA plays a physiological role in *C. glutamicum*. Therefore, DNA affinity chromatography was performed with the immobilized promoter region of the 6C RNA gene to identify potential regulators of its expression. Proteins which bound specifically to the promoter fragment ($P_{6C\ RNA}$) were eluted with buffer containing a high salt concentration and separated by SDS-PAGE (Figure 9). After staining with Coomassie, protein bands were cut out and subjected to peptide mass fingerprinting. The experiment was performed in duplicate with crude extract of two independent cultures to identify proteins that were reproducibly enriched with the 6C RNA promoter region. As shown in Figure 9 many proteins bound to $P_{6C\ RNA}$. As a negative control a DNA fragment that covers the promoter region of cg0896 (P_{cg0896}) was used (kindly provided by Dr. Abigail Koch-Koerfges), which resulted in a different protein band pattern on the 10% SDS gel (Figure 9). All proteins that could be eluted and reliably identified by peptide mass fingerprinting are listed in Table A 1in the Appendix (see also Figure A 2).

Overall, eight transcriptional regulators could be identified with the 6C RNA promoter region, indicated by arrows in Figure 9, four of them in both experiments, namely AtlR, CitB, LexA and RamA. The global transcriptional regulator GlxR, which was recently reported to bind to the intergenic region of the protein-coding gene cg0360 and the 6C RNA gene (Jungwirth*, et al.*, 2012), as well as OxyR (Teramoto*, et al.*, 2013), RamB (Gerstmeir*, et al.*, 2004) and GntR1 (Frunzke*, et al.*, 2008) could only be detected in one of two experiments. These results indicate that 6C RNA expression might indeed be regulated by one or more regulators.

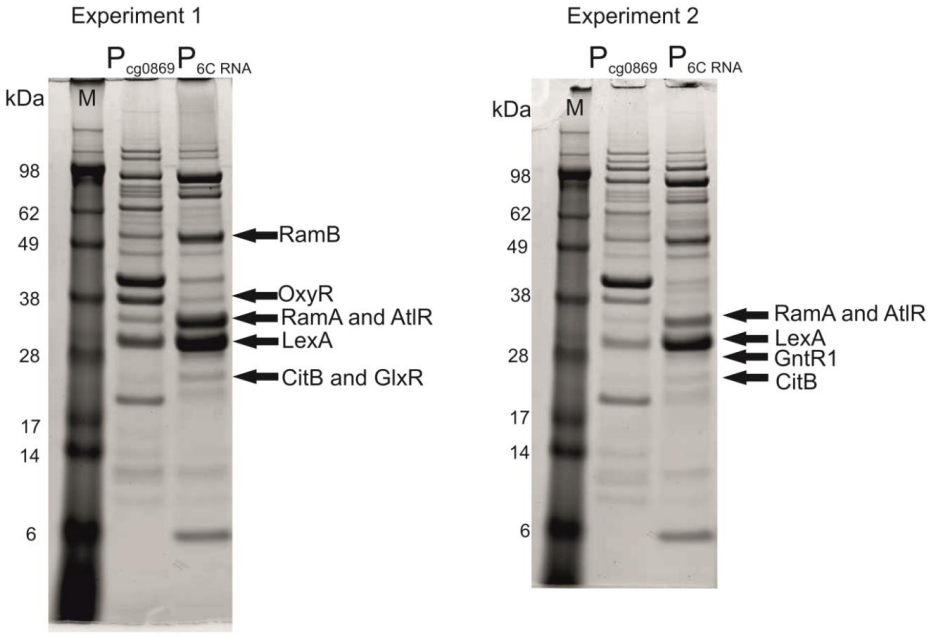

Figure 9 SDS-PAGE of eluted proteins after DNA affinity chromatography with the 6C RNA promoter region ($P_{6C\ RNA}$) of *C. glutamicum*. Shown are 10% SDS gels loaded with the elution fractions of P_{6CRNA} and of $P_{cg0896,}$ which was used as a control. The biotinylated PCR products covering the indicated promoter regions were bound to Streptavidin-coated beads and incubated with crude protein extract of *C. glutamicum* cultivated in CGXII minimal medium with 4% (w/v) glucose to an OD_{600} of 5 - 6. Unbound and weakly bound proteins were removed by several washing steps. Proteins which bound specifically to the $P_{6C\ RNA}$ and P_{cg0896} were eluted with TGED-buffer containing 2 M NaCl, precipitated by TCA, dissolved in 50 mM Tris buffer, pH 7.6 and separated by SDS-PAGE. M: SeeBlue Plus2 Pre-stained standard. Arrows indicate transcriptional regulators identified in the elution fraction of the $P_{6C\ RNA}$ by peptide mass fingerprinting. Shown are the results of two independent experiments. The 10% SDS gels were stained with Coomassie Brilliant Blue and scanned with the Typhoon scanner (GE Healthcare, Uppsala, Sweden).

A search for putative binding sites of transcriptional regulators in the 6C RNA promoter region was performed with CoryneRegNet and also by inspection based on published consensus motifs. The binding site predictions within up to -280 bp relative to the 6C RNA transcriptional start site (+1 bp) were considered. The search revealed binding sites for four different transcriptional regulators, namely RipA, RamA, LexA, and GlxR (Table 5). For RamA and RipA two binding sites are predicted. The binding sites for RamA match best with the published consensus motif, thus binding of RamA to the 6C RNA promoter region was further analysed.

Table 5 Predicted binding sites of different transcriptional regulators in *C. glutamicum* upstream of the 6C RNA TSS. The predicted binding sites, the position of the predicted binding sites, and the consensus motif of the respective transcriptional regulators are listed.

Regulator	Predicted binding site	Position relative to the 6C RNA TSS	Consensus motif 5` - 3` (Reference)
GlxR	AGTGTCATTTGCCACA	-81 to -96	TGTGANNTANNTCACA N = A/T/C/G (Jungwirth, *et al*., 2012)
LexA	TCGAATAAATAATCGG	-45 to -60	TcGAAmAnnTGTtCGA (m = A/C) (Jochmann, *et al*., 2009)
RamA	TGGGGT TGGGGGT	-128 to -133 -263 to -269	$HG_{(4-6)}Y$ or $AC_{(4-5)}D$ H = A/C/T Y = T/C D = A/G/T (Cramer, *et al,*. 2006, Schröder & Tauch, 2010)
RipA[1]	GCGTGCGGGAAGTGTCAT ATGAGATTGAAGTGACGT	-89 to -106 -136 to -153	$RRGCGN_4RYGAC$ R = A/G Y = T/C (Wennerhold, *et al.,* 2005)

[1] RipA was not identified when using $P_{6C\ RNA}$ in DNA ffinity chromatography

Gel retardation experiments were performed to confirm the direct interaction of purified RamA-His_6 with the 6C RNA promoter region. RamA was overexpressed in *E. coli* BL21(DE3) using plasmid pET28a-*ramA* (Cramer*, et al.*, 2006) kindly provided by Dr. Simon Klaffl, and purified (see 2.9.5.1). Functionality of purified RamA-His_6 was checked with a promoter fragment of the intergenic region between *aceA* and *aceB* (P_{aceAB}, positive control, Cramer*, et al.*, 2006) and the promoter region of the *pgi* gene (P_{pgi}, negative control, (Auchter*, et al.*, 2011). Functionality of the purified RamA-His_6 could be confirmed, since after incubation of the P_{aceAB} fragment with increasing molar excess of RamA-His_6 a distinct retardation of the fragment in the polyacrylamide gel could be detected (Figure 10). Since on the P_{aceAB} fragment two RamA binding site are present two retardations can be observed.

No retardation could be detected for the P_{pgi} fragment after incubation with RamA-His_6 (Figure 10).

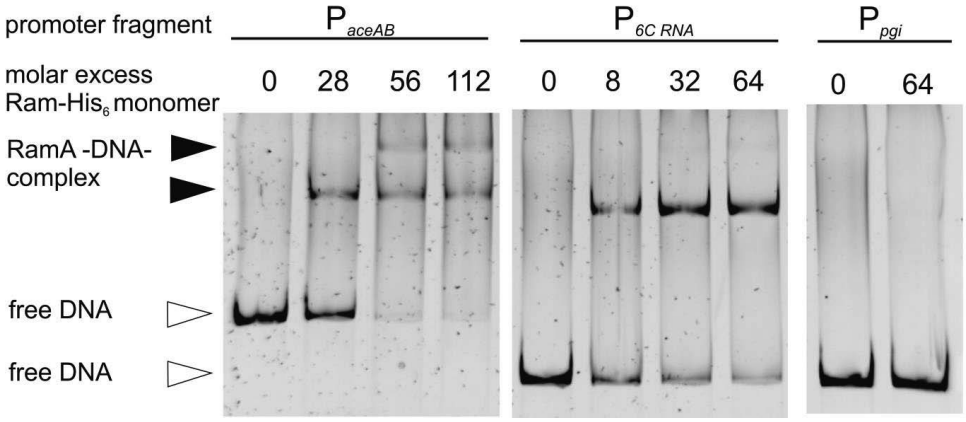

Figure 10 Gel retardation experiment with purified RamA-His_6. The fragments $P_{6C\ RNA}$, P_{aceAB} (positive control) and P_{pgi} (negative control) were incubated for 20 min at RT without and with varying molar excess of purified RamA-His_6: 8-, 32- and 64-fold molar excess in case of $P_{6C\ RNA}$; 64-fold molar excess in case of P_{pgi} fragment; and 28-, 56- and 112-fold molar excess in case of P_{aceAB}. 85 ng of DNA were used for each tested promoter fragment (19 nM of DNA for $P_{6C\ RNA}$ and P_{pgi} and 11 nM of DNA for P_{aceAB}). The analysis of the samples was performed by electrophoretic separation in a native polyacrylamide gel and subsequent staining with SYBR Green I.

In the promoter region of the 6C RNA gene two potential RamA binding sites can be found (Table 5). The direct interaction of RamA-His_6 with the promoter region of the 6C RNA could be confirmed, since after incubation of the $P_{6C\ RNA}$ fragment with increasing molar excess of RamA-His_6 a distinct retardation of the fragment in the acrylamide gel could be detected (Figure 10). However, only one distinct retardation was observed with the $P_{6C\ RNA}$ fragment, which leads to the conclusion that only one of the two predicted RamA binding sites might be relevant. Overall, the results of the DNA affinity chromatography and the electrophoretic mobility shift assays indicate that the 6C RNA might be involved in the regulatory network of the master regulator RamA.

3.2 Construction and characterization of 6C RNA deletion mutants

Two ∆6C RNA mutants were constructed to investigate if the 6C RNA is essential for *C. glutamicum* and if the presence or absence of the 6C RNA promoter sequence leads to any differences. In *C. glutamicum* ATCC 13032 the conserved 6C RNA motif is located in the intergenic region of cg0360 and cg0362. Based on these data two 6C RNA deletion mutant variants (∆6C RNA) were constructed (Figure 11) (see 2.7.6). In one ∆6C RNA mutant only the conserved 6C RNA motif was deleted (+28 to +101 bp from 6C RNA TSS), called ∆6C mutant. For further information on the conserved motif see 1.3. The second deletion mutant not only lacks the conserved 6C RNA motif, but also the upstream region, including the predicted 6C RNA promoter region (Mentz, *et al.*, 2013) (-58 to +106 bp from the 6C RNA TSS), called ∆6CiP mutant (iP: including promoter sequence).

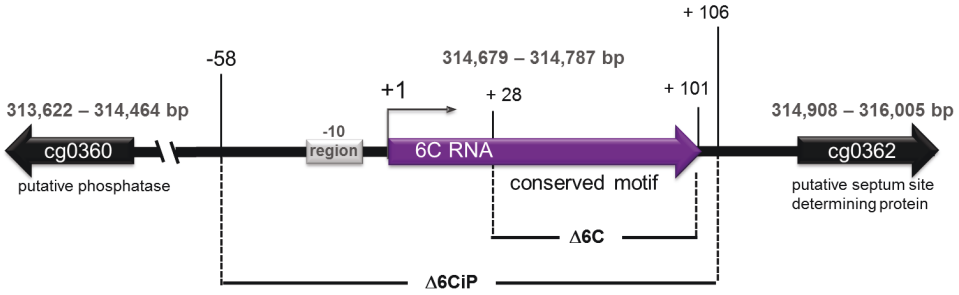

Figure 11 Map of the *C. glutamicum* genome region covering of the 6C RNA locus. The genome position of the 6C RNA gene is from 314,679 bp – 314,787 bp (Mentz, *et al.*, 2013). The 6C RNA gene is indicated by a violet arrow, the upstream and downstream genes of the 6C RNA, cg0360 (genome position from 313,622 bp – 314,464 bp) coding for a putative phosphatase and cg0362 (genome position from 314,908 bp – 316,005 bp) coding a putative septum site-determining protein, are indicated by black arrows, respectively. The genome position of the conserved 6C RNA motif is from 314,705 bp – 314,782 bp. ∆6C: genome region that was deleted in the *C. glutamicum* ∆6C mutant, ∆6CiP: genome region that was deleted in the *C. glutamicum* ∆6CiP mutant. The +/- numbers indicate positions relative to the 6C RNA TSS.

Growth of both ∆6C RNA mutant variants was compared to the *C. glutamicum* wild type in CGXII minimal medium with 4% (w/v) glucose (Figure 12). No differences with respect to the final OD_{600} or the specific growth rate were observed (Table 6). The deletion of the 6C RNA does not lead to a growth phenotype under standard conditions that could give a hint on the physiological role of the 6C RNA in *C. glutamicum*.

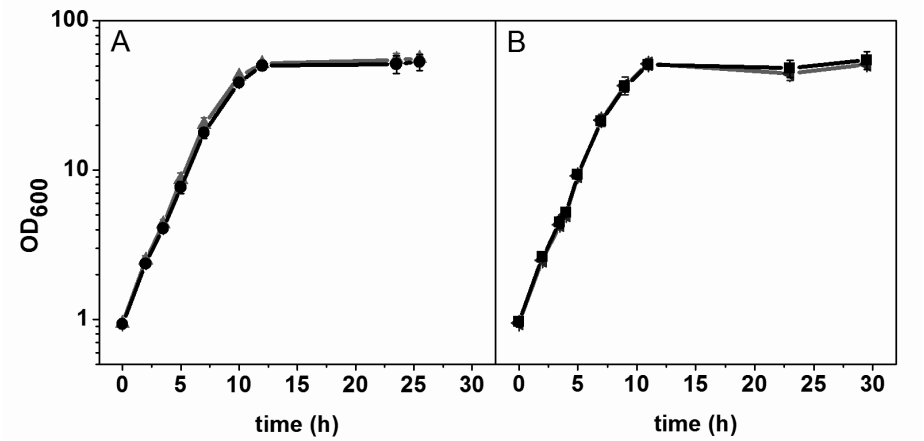

Figure 12 Growth of *C. glutamicum* ATCC 13032 and the Δ6C RNA mutant variants Δ6C and Δ6CiP. Strains were cultivated in shaking flasks in CGXII minimal medium with 4% (w/v) glucose at 30°C and 120 rpm. **A** *C. glutamicum* wild type (▲) and *C. glutamicum* Δ6C (●). **B** *C. glutamicum* wild type (◄) and *C. glutamicum* Δ6CiP (■). Average values and standard deviations of three independent cultivation experiments are shown.

Table 6 Growth parameters of *C. glutamicum* ATCC 13032 and the Δ6C RNA mutant variants Δ6C and Δ6CiP. For the construction of the Δ6CiP mutant a new ATCC 13032 batch of the DSMZ was used. Therefore, for each Δ6C RNA mutant variant the growth of the corresponding *C. glutamcim* wild type is listed. Strains were cultivated in CGXII medium with 4% (w/v) glucose at 30°C and 120 rpm. Mean values and standard deviations of three independent biological replicates are shown.

Strain	Final OD_{600}	μ (h^{-1})
C. glutamicum ATCC 13032	55.9 ±4.4	0.42 ±0.02
C. glutamicum Δ6C	53.0 ±6.6	0.41 ±0.02
C. glutamicum ATCC 13032	51.2 ±2.2	0.44 ±0.02
C. glutamicum Δ6CiP	54.5 ±7.5	0.43 ±0.01

3.2.1 Transcriptome analysis of the ∆6C mutant

Many sRNAs exhibit their regulatory function by base pairing with mRNA (see 1.2). Therefore, a global transcriptome analysis of the ∆6C mutant was performed to see whether the 6C RNA deletion has any effect on the global gene expression.

Since it is not known so far under which conditions the 6C RNA has a regulatory role in *C. glutamicum*, a transcriptome analysis was performed under standard growth conditions in which the genome-wide mRNA levels of the ∆6C mutant and the wild type were compared by using DNA microarrays. Another transcriptome analysis was performed to compare the ∆6CiP mutant and the wild type (data not shown), in which a different type of DNA microarrays (Agilent arrays instead of Operon arrays) was used. The results of the latter analysis were comparable to those of the former, indicating that the absence of the 6C RNA promoter region does not lead to additional effects on the transcriptome under the tested conditions. Therefore, in the following only the transcriptome comparison of the ∆6C mutant with the wild type is presented. In total 77 genes were found to have a significantly altered mRNA level in the ∆6C mutant, of which 40 showed a ≥ 2-fold decreased expression and 37 genes a ≥ 2-fold increased expression compared to the wild type (Table 7). Notably, three larger gene clusters have an altered expression in the ∆6C mutant, namely cg0362-cg0362, cg0808-cg0839, and cg1918-cg1934. The genes in these gene clusters had all decreased or increased mRNA ratios, respectively. The genes cg1918-cg1934 are located within the CGP3 prophage region. The genome of *C. glutamicum* contains in total three prophages (CGP1, CGP2 and CGP3), of which CGP3 is under current investigation (Frunzke*, et al.*, 2008, Baumgart*, et al.*, 2013, Nanda*, et al.*, 2014). However, the six genes within the gene cluster cg1918-cg1934 represent only a minor percentage of the entire CGP3 genes and are only moderately increased (2- to 2.47-fold). In the case of the large gene cluster cg0803-cg0839 it has to be considered that the decreased mRNA level could be “unspecific” or not be related to the gene function. Notably, the genes cg0362-cg0369 are located directly downstream of the 6C RNA and had an increased mRNA level in the ∆6C mutant, indicating that the 6C RNA could trigger the degradation of the mRNA of the downstream genes by some unknown mechanism. The genes cg0362-cg0369 are analysed in more detail in 3.5.2.

Table 7 Differentially expressed genes revealed by comparative transcriptome analysis of the Δ6C mutant and *C. glutamicum* wild type. Strains were cultivated in CGXII medium with 4% (w/v) glucose and harvested in the exponential growth phase (OD_{600} of 4-6). Given are the locus tag, the gene name, the annotation, the average mRNA ratios and *p*-values. The average mRNA ratios and *p*-values were calculated from three independent experiments.

Locus tag	Gene	Annotation	mRNA ratio Δ6C vs.WT	p-value
cg0008		putative esterase/lipase	0.17	0.00
cg0308		putative membrane protein	3.45	0.02
cg0362		putative septum site determining protein, conserved	3.04	0.01
cg0363		putative secretion ATPase protein	2.63	0.00
cg0364		putative membrane protein	2.98	0.00
cg0365		putative membrane protein	3.82	0.00
cg0368		putative secreted protein, conserved	3.32	0.02
cg0369		putative secreted protein, conserved	3.73	0.00
cg0384	*rluC1*	ribosomal large subunit pseudouridine synthase C	2.25	0.01
cg0493		hypothetical protein	0.49	0.02
cg0587	*tuf*	elongation factor Tu	0.36	0.02
cg0661		hypothetical protein, conserved	4.98	0.02
cg0665		putative serine protease	9.39	0.02
cg0671		hypothetical protein, conserved	6.71	0.04
cg0672		hypothetical protein, conserved	5.16	0.02
cg0702		putative transcriptional regulator, LysR-family	2.22	0.02
cg0803	*thtR*	thiosulfate sulfurtransferase	0.22	0.00
cg0806		hypothetical protein, conserved	0.31	0.00
cg0807		hypothetical protein, conserved	0.30	0.00
cg0808	*wbpC*	putative lipopolysaccharide biosynthesis acyltransferase, conserved	0.32	0.00
cg0809	*maf*	putative septum formation protein Maf-like protein	0.25	0.00
cg0810		hypothetical protein, conserved	0.21	0.00
cg0811	*dtsR2*	acetyl/propionyl CoA carboxylase, β chain	0.26	0.00
cg0812	*dtsR1*	acetyl/propionyl-CoA carboxylase, β chain	0.42	0.01
cg0814	*birA*	biotin-protein ligase	0.30	0.00
cg0816	*purK*	phosphoribosylaminoimidazole carboxylase	0.36	0.00
cg0817	*kup*	potassium K^+ transporter	0.32	0.00
cg0819		hypothetical protein	0.39	0.01
cg0821		hypothetical protein, conserved	0.32	0.01
cg0822		hypothetical protein, conserved	0.32	0.01
cg0823	*ntaA*	nitrilotriacetate monooxygenase component A	0.48	0.00
cg0825	*fabG*	3-ketoacyl-acyl-carrier-protein reductase	0.34	0.00
cg0826		putative membrane protein	0.28	0.00
cg0828		putative dihydrofolate reductase	0.44	0.02
cg0829		putative lactoylglutathione lyase or related lyase, glyoxylase-family, conserved	0.40	0.01
cg0830		putative membrane protein	0.30	0.00
cg0831	*tusG*	trehalose uptake system, ABC-type, permease protein	0.33	0.01
cg0832	*tusF*	trehalose uptake system, ABC-type, membrane spanning protein	0.34	0.00
cg0833		putative membrane protein, involved in trehalose uptake, conserved	0.39	0.01
cg0834	*tusE*	trehalose uptake system, ABC-type, bacterial extracellular solute-binding protein	0.41	0.00
cg0835	*tusK*	trehalose uptake system, ABC-type, component	0.34	0.00
cg0836		hypothetical protein	0.50	0.00
cg0837		hypothetical protein	0.37	0.03
cg0838		putative helicase	0.44	0.03
cg0839		hypothetical protein	0.43	0.03
cg0890		hypothetical protein, conserved	2.64	0.00

Locus tag	Gene	Annotation	mRNA ratio Δ6C vs.WT	p-value
cg1059		hypothetical protein, conserved	2.07	0.01
cg1183		putative dinucleotide-utilizing enzyme	3.11	0.04
cg1213	*tnp1a*	transposase	0.43	0.00
cg1255		putative HNH endonuclease, conserved	2.89	0.03
cg1918		putative secreted protein CGP3 region	2.42	0.01
cg1919		putative membrane protein CGP3 region	2.31	0.02
cg1921		hypothetical protein CGP3 region	2.00	0.04
cg1923		hypothetical protein CGP3 region	2.05	0.03
cg1924		hypothetical protein CGP3 region	2.41	0.01
cg1934		hypothetical protein CGP3 region	2.47	0.04
cg1980		puative MoxR-like ATPase CGP3 region	2.12	0.04
cg2183	*oppC*	ABC-type peptide transport system, permease component	0.08	0.00
cg2184	*oppD*	ATPase component of peptide ABC-type transport system, contains duplicated ATPase domains	0.10	0.02
cg2504		hypothetical protein, conserved	2.21	0.01
cg2533		hypothetical protein, conserved	2.83	0.02
cg2633		putative restriction endonuclease	3.96	0.03
cg2683		hypothetical protein, conserved	2.18	0.01
cg2725	*tnp1b*	transposase	0.49	0.02
cg2733		putative HNH nuclease	2.19	0.00
cg2893		putative cadaverine transporter, multidrug efflux permease, MFS-type	0.11	0.02
cg2894	*cgmR*	multidrugresistance-related transcription factor, TetR-family	0.23	0.03
cg2898		putative 3-ketosteroid dehydrogenase	2.67	0.02
cg2922		putative transcriptional regulator, IclR-family	3.33	0.01
cg3128		putative ABC-type transport system, ATPase component	2.17	0.00
cg3266	*tnp5c*	transposase	0.36	0.01
cg3267		putative membrane protein, putative pseudogene, C-terminal fragment	0.37	0.01
cg3284	*copS*	two component sensor kinase, copper homeostasis, horizontally transferred gene	2.23	0.04
cg3291		putative transcriptional regulator, Crp-family, horizontally transferred gene	3.16	0.02
cg3293		hypothetical protein, horizontally transferred gene	2.02	0.00
cg3354	*genH*	putative aromatic-ring hydroxylase flavoprotein monooxygenase or 3-hydroxybenzoate 6-hydroxylase	2.14	0.05

In Table 8, the genes of Table 7 were grouped into functional categories. Overall, 72% (56 genes) of all genes with an altered mRNA level are either grouped into the category of genes that encode for proteins with a predicted function or for proteins with an unknown function. As seen in Table 8 11 genes encode for transporters and make up the next largest category. This category includes the two genes with the strongest decrease in their mRNA level in the ∆6C mutant, *oppC* and *oppD* (about 10-fold). The *oppC* and *oppD* genes encode, together with *oppB* (1.5-fold regulated and therefore not listed in Table 8), for the subunits of a peptide ABC-type transport system (Pfeifer-Sancar*, et al.*, 2013) (G. Bosco, PhD Thesis). The genes *oppBCD* are part of the AmtR regulon; AmtR is the master regulator of nitrogen control in *C. glutamicum* and represses transcription of a number of genes during nitrogen surplus (Beckers*, et al.*, 2005). However, no other genes than *oppC* and *oppD* of the AmtR regulon had a ≥ 2-fold decreased mRNA ratio in the ∆6C mutant. It seems that these genes often show an altered mRNA level in DNA microarray analysis of recombinant strains (see also G. Bosco, PhD Thesis), so that it can be suggested that these alterations are rather unspecific. The functional category of other metabolic enzymes is, after the transporters, the next larger group of genes and contains ten genes. The gene with the highest increase in the mRNA level, namely cg0665 (about 10-fold), is within this group. Cg0665 was very recently reported to encode a subtilisin-like serine protease (SprA) that was isolated as an interacting partner for the global regulator GlxR (Hong*, et al.*, 2014). For details on SprA and GlxR see section 4.

The category for proteins which are involved in DNA replication and DNA repair contains six genes and the category for transcriptional regulators or parts of two-component systems contains five genes. The other functional categories only contain two genes and are not mentioned here.

Overall, the transcriptome analysis of the ∆6C mutant revealed that the deletion of the 6C RNA has some impact on global gene expression in *C. glutamicum* under standard conditions.

Table 8 Comparative transcriptome analysis of the Δ6C mutant and the *C. glutamicum* wild type. Strains were cultivated in CGXII medium with 4% (w/v) glucose and harvested in the exponential growth phase (OD_{600} of 4-6). The average mRNA ratios were calculated from three independent experiments and a *p*-value of ≤ 0.05 was set to be significant. The genes with an average mRNA ratio of ≥ 2.00 or ≤ 0.50 were grouped in functional categories. Genes with an average mRNA ratio of ≥ 4.00 or ≤ 0.25 are underlined. Genes which are grouped into two categories are labeled with an asteriks.

Functional category	mRNA ratio (Δ6C vs.WT)	
	≥2.00, ≥4.00	**≤0.50, ≤0.25**
Amino acid metabolism		*ntaA*, *thtR*
Other metabolic enzymes and proteases	*genH*, cg0665, cg2898*	*birA*, *dtsR2R1*, *fabG*, *wbpC*, cg0008*, cg0829*
Transporter	cg3128*	cg0833, *tusEFGK*, *kup*, *oppCD*, cg2893, *wbpC*
Purin metabolism	cg0866	*purK*
DNA replication/DNA repair	cg1255, cg2064, cg2633, cg2733	cg0838*
Translation	*rluC1*	*tuf*
Transcriptional regulators and Two-component systems	cg0702*, cg2922*, cg3291*, *copS*	*cgmR*
Cell division/septum formation	cg0362*	*maf*
Transposases		*tnp1a*, *tnp1b*, *tnp5c*
Proteins with a predicted function	cg0308, cg0362*, cg0363, cg0364, cg0365, cg0368, cg0369, cg0702*, cg1183, cg1255, cg1918, cg1919, cg1980, cg2534, cg2633, cg2733, cg2898*, cg2922*, cg3128*, cg3291*, cg3354	cg0008*, *wbpC*, *maf*, cg0826, cg0828, cg0829*, cg0830, cg0833, cg0838*, cg2893, cg3267
Hypothetical proteins	cg0661, cg0671, cg0672, cg0890, cg1025, cg1059, cg1921, cg1923, cg1924, cg1934, cg2504, cg2533, cg2683, cg3293	cg0493, cg0806, cg0807, cg0810, cg0819, cg0821, cg0822, cg0836, cg0837, cg0839,
CGP3 prophage genes	cg1918, cg1919, cg1921, cg1923, cg1924, cg1934, cg1980	

3.2.2 Screening for a phenotype of the Δ6C RNA mutant

C. glutamicum is able to metabolize a variety of carbohydrates, alcohols, and organic acids (Eggeling & Bott, 2005, Liebl*, et al.*, 2006, Arndt*, et al.*, 2008). Since no growth phenotype for the Δ6C RNA mutants was observed under standard growth conditions with glucose as sole carbon source, a global screening for a growth phenotype of the Δ6CiP mutant with different carbohydrates and organic acids was performed to see if the 6C RNA may play a role in the utilization of any of the tested carbon and energy sources. The CGXII main culture was supplemented with eight different carbohydrates and organic acids, namely sucrose, fructose, potassium gluconate, ribose, sodium L-lactate, sodium propionate and sodium pyruvate (100 mM, respectively), and citrate (citric acid monohydrate) (50 mM). This selection represents a variety of enery sources that require glycolytic or gluconeogenetic pathways as well as different transport mechanisms such as the PTS system or permeases. The screening for the utilization of carbon sources was performed in the BioLector. The Δ6CiP mutant and the wild type grew comparably and showed no significant differences with respect to the backscatter values throughout the entire cultivation period. This shows that the deletion of the 6C RNA did not affect growth with a variety of carbon sources and therefore is unlikely to strongly regulate any of the genes directly required for their metabolism, i.e. both catabolic and anabolic genes. Representative for the tested carbon sources, the growth of the Δ6CiP mutant and the wild type strain on fructose, pyruvate and ribose is shown (Figure 13).

Many sRNAs are involved in stress responses of bacteria (see 1.2). Therefore, in the global screening for a growth phenotype of the Δ6CiP mutant also different stress conditions were tested. Growth of the Δ6CiP mutant was compared to that of the wild type in CGXII minimal medium with 4% (w/v) glucose with a different pH, with limitation of iron and total trace elements (adapted and non adapted cells), copper excess and iron excess (Figure 13). Additionally, the growth in the presence of the SOS response-inducing agent mitomycin C was tested in the BioLector screening. The antibiotic mitomycin C (MMC) covalently cross-links complementary DNA strands, and thereby leads to the induction of the SOS response in bacteria (Tomasz, 1995, Movahedzadeh*, et al.*, 1997). The BioLector screening revealed that in the case of the trace element limitation, the Δ6CiP mutant shows a minor increase compared to the wild type with respect to the final backscatter value. However, when the cells were adapted to the trace element limitation in the preculture, no difference between the Δ6CiP mutant and the wild type could be detected any longer (Figure 13 D and E). Notably, the Δ6CiP mutant showed a higher sensitivity to MMC than the parental strain. The growth difference was concentration-dependent since the higher the MMC concentration in the medium was, the stronger was the growth defetct of the Δ6CiP mutant (Figure 13 J – L). No

growth differences of the Δ6CiP mutant compared to the wild type were observed for the other tested stress conditions.

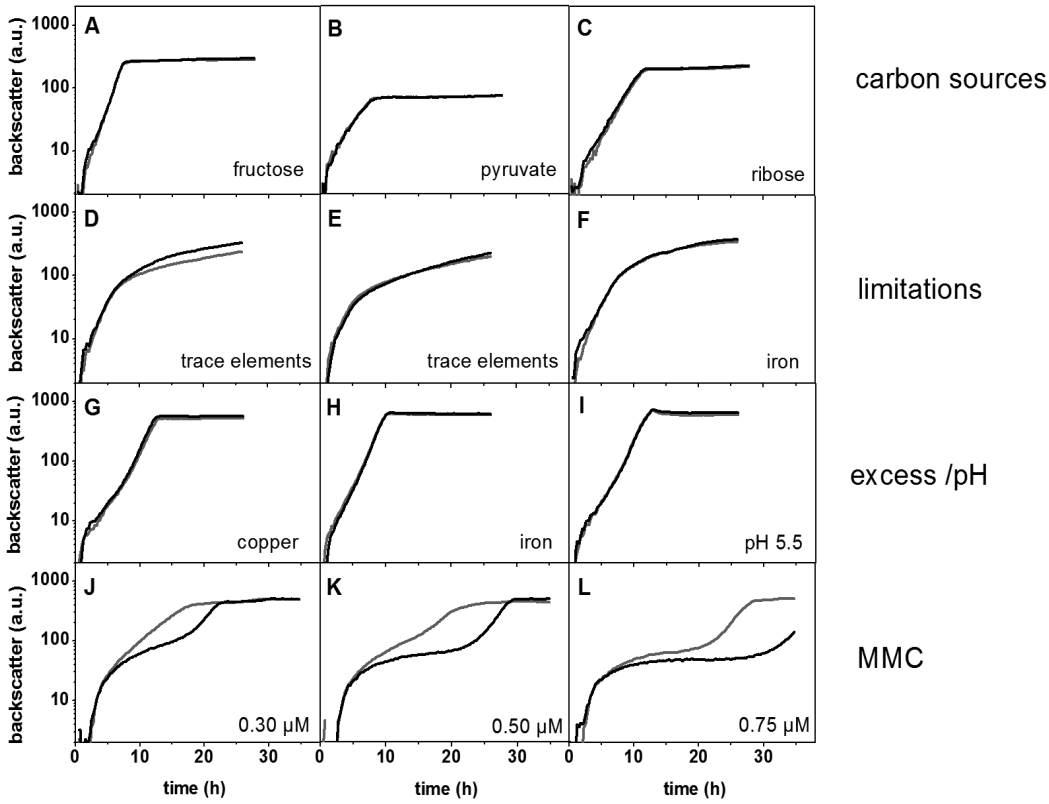

Figure 13 Growth of *C. glutamicum* wild type (grey line) and the Δ6CiP mutant (black line) with different carbon sources and under different stress conditions. For the BioLector screening the cells were precultivated in 20 ml complex BHI medium without any additional carbon source in shaking flasks at 30°C and 130 rpm. The main cultivation was performed in 48-well flowerplates in CGXII medium with (A) 100 mM fructose, (B) 100 mM pyruvate or (C) 100 mM ribose as sole carbon source, all at pH 7.0, (D) CGXII medium with 222 mM glucose and trace element limitation (1:10 diluted compared to standard medium, see section 2.2) with non-adapted cells and (E) adapted cells (precultivation in 10 ml CGXII medium with 222 mM glucose and trace element limitation (1:10) in shaking flasks), (F) iron limitation (1 µM instead of 36 µM), (G) copper excess (50 µM instead of 1.25 µM), (H) iron excess (100 µM instead of 36 µM), (I) pH 5.5 instead of pH 7.0. Moreover, the growth in CGXII medium with 222 mM glucose with 0.3 µM (J) 0.5 µM (K) and 0.75 µM (L) mitomycin C (MMC), added at the start of the cultivation, is depicted. The strains were cultivated in 750 µl of the respective medium in the BioLector system (m2p labs) at 30°C and 1,200 rpm. Mean values of two technical replicates are shown. Please note that the fluctuations of backscatter values below 10 result from technical limitations and the logarithmic presentation.

3.3 Properties of the Δ6CiP mutant in the presence of mitomycin C (MMC)

3.3.1 Growth and cell shape of Δ6CiP mutant cultivated with MMC

Growth experiments in shaking flasks were performed to confirm the results of the BioLector screening (see above). The cultivation was performed with 0.75 µM MMC, the highest concentration tested in the BioLector, because with this concentration the strongest growth phenotype for the 6C RNA deletion mutant could be observed. Indeed, when 0.75 µM MMC was added to the medium at the the start of the cultivation, the Δ6CiP mutant grows differently from the wild type (Figure 14). The Δ6CiP mutant had a similar initial growth rate as the wild type (0.30 ± 0.01 h^{-1} *vs*. 0.32 ± 0.01 h^{-1}). However, after about six hours of cultivation the cells ceased to grow and entered a lag phase for about 18 h. After about 24 h of cultivation the Δ6CiP mutant started to grow again and after 30 h reached 70% of the final OD_{600} of the wild type (25.2 ± 8.8 *vs*. 39.9 ± 0.3) (Figure 14). Notably, the growth rate and the final biomass of the wild type in the presence of 0.75 µM MMC were reduced by 26% and 30%, respectively, compared to growth in the absence of MMC (Table 10).

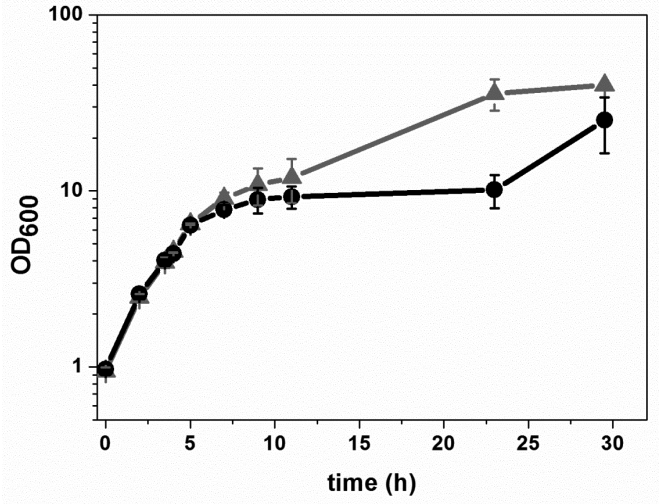

Figure 14 Growth of *C. glutamicum* wild type (▲) and *C. glutamicum* Δ6CiP (●) in CGXII minimal medium with 4% (w/v) glucose and 0.75 µM MMC. Cells were cultivated in 50 ml cultures at 30°C and 120 rpm. Average values and standard deviations of three independent cultivation experiments are shown.

Microscopic analysis revealed that MMC-treated cells (Figure 15 C and D) have an elongated cell morphology compared to untreated *C. glutamicum* cells (Figure 15 A and B). No significant differences between the morphology of deletion mutant and the wild type could be observed, neither under standard growth conditions nor under SOS response-inducing conditions. This indicates that the differences in the OD_{600} measurement are not caused by a different cell morphology.

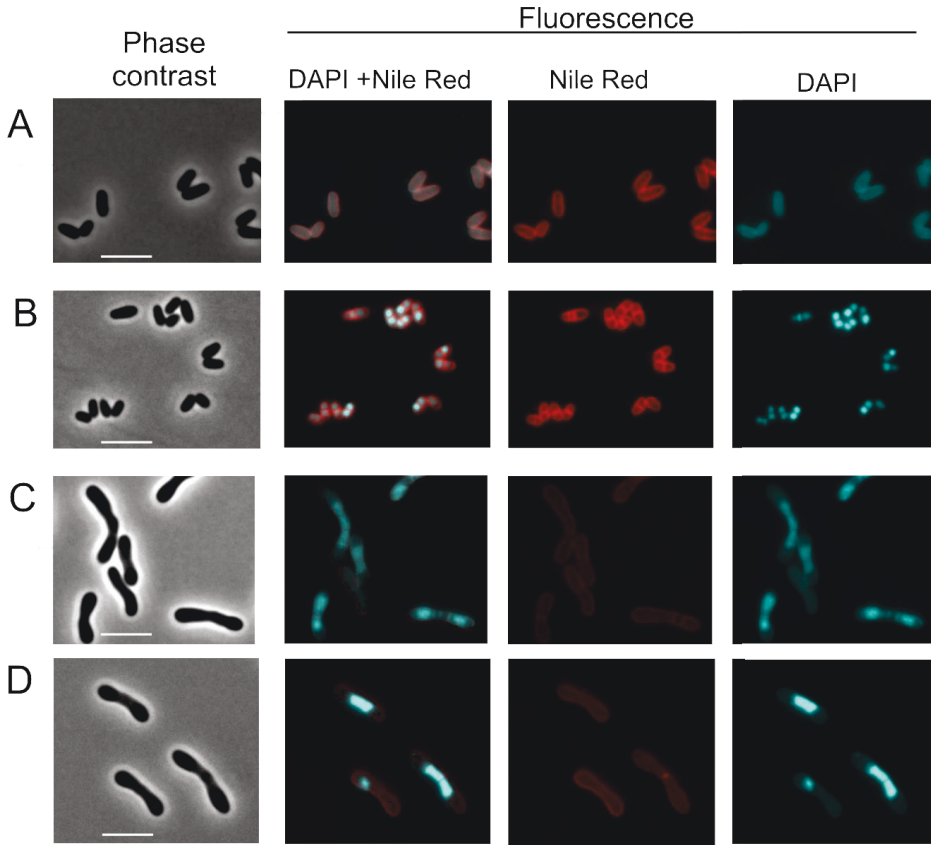

Figure 15 Microscopy images of *C. glutamicum* wild type (A and C) and the Δ6CiP mutant (B and D). Strains were cultivated in CGXII minimal medium with 4% (w/v) glucose either without MMC (A and B) or with 0.75 µM MMC (C and D). Samples were taken in the exponential growth phase. DNA was stained with 4',6-diamidino-2-phenylindole (DAPI) (cyan) and lipophilic regions with nile red (red). The white scale bar is 5 µm in length.

3.3.2 Transcriptome analysis of the ∆6CiP mutant cultivated with MMC

For the ∆6CiP mutant a strong growth deffect was observed in the presence of MMC (Figure 14). This result indicates that the 6C RNA might have a role under SOS response-inducing conditions in *C. glutamicum*. Therefore, the gene expression differences under SOS response-inducing conditions were investigated by comparing the ∆6CiP mutant and the wild type in the presence of 0.75 µM MMC using DNA microarray analysis. In total, 92 genes showed ≥2-fold altered mRNA levels (using total RNA from cells harvested in the exponential growth phase at an OD_{600} of 5). These genes are listed in Table 9 and were grouped into functional categories. For details on the average mRNA ratios, *p*-values and the annotated functions see Table A 2 in the Appendix. From these 92 genes 50 had an increased mRNA level in the ∆6CiP mutant. The majority of up-regulated genes (43 genes, 86%) are located within the CGP3 prophage region. However, these genes represent only 25% of the entire CGP3 genes and are only moderately increased (2- to 3-fold). The remaining CGP3 prophage genes with a *p*-value of ≤ 0.05 had mRNA ratios between 1.11 and 1.98. Notably, although the ∆6CiP mutant has a strong growth defect under SOS response-inducing conditions, genes like *lexA*, *recA* and *divS,* encoding for key players of the SOS response, namley the transcriptional regulator LexA, the recombinase A (RecA) and the cell division suppressor DivS, have mRNA levels which are similar to the wild type (data not shown). Seven genes with an increased mRNA level are not located within the CGP3 region. All of them were grouped into different functional categories. This shows that the genes with an increased mRNA level in the ∆6CiP mutant do not have an obvious functional relation to each other. Among these seven genes is cg2633, which had the highest increased mRNA level (10-fold) and codes for a putative restriction endonuclease. Since this gene had already a 4-fold increased mRNA level in the transcriptome analysis under standard growth conditions, it could be a possible 6C RNA target. Other genes, that showed MMC-independent alteration in their mRNA level in the ∆6CiP mutant, are discussed in more detail elsewhere (see 4.).

The remaining 42 genes (of 92) had a significantly more than 2-fold decreased mRNA level in the ∆6CiP mutant. These genes code for proteins of various functions. Three genes encode enzymes of central metabolism, namely isocitrate lyase (*aceA*), which is part of the glyoxylate shunt, acetate kinase (*ackA*) and phosphotransacetylase (*pta*), which are both involved in the acetate metabolism. Another gene codes for the elongation factor EF-Tu involved in protein synthesis. The altered mRNA level of these genes could be a consequence of the retarded growth of the ∆6CiP mutant in the presence of MMC. The genes *nadA*, *nadC* and *nadS* were also more than 2-fold down-regulated in the ∆6CiP mutant under SOS response-inducing conditions. *NadA* and *nadC* are involved in NAD *de novo* biosynthesis and are broadly conserved in the genomes of numerous bacterial species

(Teramoto*, et al.*, 2010). *NadS* codes for a cysteine desulfurase-like protein which is involved in Fe-S cluster assembly, required for maturation of NadA. *NadA*, *nadC*, and *nadS* were shown to be essential for growth in the absence of an exogenous source of NAD (Teramoto*, et al.*, 2010). The decreased mRNA level of these genes could also be involved in the retarded growth of the ∆6CiP mutant, since deletion of each of the three genes resulted in a growth defect (Teramoto*, et al.*, 2010). Surprisingly, the gene encoding NdnR, which acts as a transcriptional repressor of the NAD *de novo* biosynthesis genes (Teramoto*, et al.*, 2010), was also down-regulated.

Furthermore, some genes involved in the assimilatory reduction of inorganic sulfur compounds, like *cysIJNYZ*, also had decreased mRNA levels in the ∆6CiP mutant compared to the wild type. The genes *cysINYZ* are organized in an operon together with *cysDHX*. The latter three genes also had significantly decreased mRNA values in the deletion mutant (0.51 to 0.56) but they did not fulfil the chosen cut-off (≤ 0.50) and are therefore not listed in Table 9.

The global transcriptome analysis revealed that the absence of the 6C RNA has no influence in the presence of MMC on the transcriptional level of genes which are involved in the SOS response of *C. glutamicum*, although the ∆6CiP mutant shows a strong growth defect. The potential effect of the 6C RNA could rather be on the translational or posttranslational level and not affect mRNA levels. However, this transcriptome analysis is specific only to the defined time point during cultivation. Therefore, the SOS response in the ∆6CiP mutant in the presence of MMC was investigated further in the following.

Table 9 Differentially expressed genes revealed by comparative transcriptome analysis of the Δ6CiP mutant and the *C. glutamicum* wild type. Strains were cultivated in CGXII medium with 4% (w/v) glucose and 0.75 µM MMC and harvested in the exponential growth phase (OD_{600} of 5) shortly before growth of the Δ6CiP mutant faded to a lag phase. The average mRNA ratio was calculated from three biological replicates and a *p*-value of ≤ 0.05 was set to be significant. The genes with an average mRNA ratio of ≥ 2.00 or ≤ 0.50 and a *p*-value of ≤ 0.05 were grouped in functional categories. Genes with an average mRNA ratio of ≥ 4.00 or ≤ 0.25 are underlined. Genes labeled with an asterisk are grouped into two categories.

Functional category	mRNA ratio (Δ6C vs. WT)	
	≥2.00, ≥4.00	**≤0.50, ≤0.25**
Amino acid metabolism		*metE*
Glyoxylate shunt		*aceA*
Acetate and ethanol catabolism		*ackA, pta, adhA*
Sulfate metabolism		*cysIJNYZ*
ß-ketoadipate pathway	*pcaH*	*catA1*
Biosynthesis of cofactors		*nadACS,*
Transport		cg0507*,cg0508*, *tusEFG,* cg0833*, *mctC, gluA, oppBCD,* cg2470*, *vanK,* cg2703*, cg2704*, *msiK1,* cg2937*, *porH*
DNA replication/DNA repair	cg1255*, cg2633*	
Translation		*tuf*
Transcriptional regulators		*cgmR, ndnR*
CGP3 prophage genes	cg1897, cg1903, cg1910, cg1911, cg1917, cg1936, cg1937, cg1940, cg1941, cg1954, cg1961, cg1962, cg1967, cg1975, cg1999, cg2005, cg2006, cg2007, cg2008-cg2011, cg2014-cg2017, cg2018-cg2020, cg2022, cg2028, cg2032, cg2034, cg2037, cg2051, cg2053, cg2055-cg2057, cg2062, cg2064, cg2069, cg2071	
Proteins with a predicted function	cg1255*, cg1897, cg1903, cg1910, cg1911, cg1936, cg1937, cg1940, cg1941, cg1962, cg2005, cg2007, cg2008-cg2011, cg2018-cg2020, cg2022, cg2032, cg2053, cg2055-cg2057, cg2062, cg2064, cg2069, cg2071,cg2633*, cg2828	cg0507*, cg0508*,cg0833*, cg0952, cg2470*, cg2701, cg2703*, cg2704*, cg2937, cg3195, cg3212, cg3390
Hypothetical proteins	cg1917, cg1954, cg1961, cg1967, cg1975, cg1999, cg2006, cg2014-cg2017, cg2028, cg2034, cg2037, cg2051, cg2080, cg2106	cg2707, cg3016

3.3.3 The SOS response is altered in the ∆6CiP mutant

The ∆6CiP mutant showed a growth phenotype in the presence of the SOS response-inducing antibiotic MMC without a strong alteration in expression of SOS response-related genes (see above). Since the DNA microarray analysis is limited to one defined time point of gene expression, the induction of the SOS response in the ∆6CiP strain was analysed using the promoters of four different SOS genes (P_{recA}, P_{recN}, P_{dnaE2} and P_{cglIM}) fused to the coding sequence of the autofluorescent protein E2-crimson in the plasmid pJC1 (see 2.4). For all of these genes a binding of LexA was shown by DNA band shift assays (Jochmann*, et al.*, 2009). The reporter fusion constructs allow a monitoring of the activity of these promoters during the course of cultivation and may help to find a reason for the growth phenotype of the ∆6CiP mutant. Analysis of the P_{recA} -, P_{recN} -, P_{dnaE2} - and P_{cglIM} - e2-crimson constructs revealed that for all tested promoters comparable results were observed, which are depicted in the Appendix (Figure A 3 and Figure A 4). In the following only P_{recA} is described in detail, representative for all tested promoters.

No significant difference regarding growth or fluorescence output between strain ∆6CiP/pJC1-P_{recA}-e2-crimson and WT/pJC1-P_{recA}-e2-crimson was observed during cultivation in the absence of MMC. The ∆6CiP mutant derivative showed comparable growth as the corresponding wild type and reached slightly higher backscatter values in the stationary growth phase (Figure 16 A). The fluorescence output for both strains was much lower in the cultivation without MMC than with MMC (Figure 16 C *vs*. Figure 16 D), confirming induction of the SOS response by MMC. In the presence of MMC differences between the ∆6CiP mutant and the wild type were observed for the backscatter values, the E2-crimson fluorescence, and the specific fluorescence (Figure 16 B, D, F). In the presence of MMC the ∆6CiP derivative needed longer time to reach the stationary growth phase than the corresponding wild-type strain (Figure 16 B). The delayed entry of the ∆6CiP mutant into the stationary phase in the presence of MMC was not due to a decreased maximal growth rate, but to a slow linear growth in the first 15 hours of cultivation. Once this phase ended, possibly by a degradation of the MMC or other yet unknown reasons, the ∆6CiP mutant started to grow exponentially again and finally also reached somewhat higher backscatter values than the corresponding wild-type strain (Figure 16 B). The fluorescence output was lower in the ∆6CiP mutant during the entire cultivation period with MMC (Figure 16 D). It could be observed that the maximal peak of specific fluorescence signal was reached after about 8 to 12 hours of cultivation, independent of the strain in which the promoter activity was tested (Figure 16 F). These findings correspond to the mRNA ratios of *recA* (and also *dnaE2*, *recN*, and *cglIM*) in the comparative transcriptome analysis (see 3.3.2), because the mRNA levels of these genes showed no difference to the wild type in the exponential growth phase. In the ∆6CiP strain, the peak of the specific fluorescence was much broader than in

the wild type (Figure 16 F). This is most likely due to a higher oxygen availability during the cultivation. Since the ∆6CiP strain showed a phase of linear growth presumably more oxygen was present than in the wild type culture, which already grew exponentially during this time period. In the transition from the exponential to the stationary phase, oxygen is limited so that E2-crimson fluorescence proteins can not fully mature and the specific fluorescence signal decreases. In the stationary phase the cells cease to grow, the oxygen supply increases again and the E2-crimson fluorescence protein can fully mature and the fluorescence signal increases again. When both strains reached the stationary phase, the final level of specific fluorescence was much lower in the ∆6CiP mutant than in the wild type (Figure 16 F, see also Figure A 3 and Figure A 4). This result indicates that less fluorescence protein was expressed in the ∆6CiP mutant during oxygen limitation conditions, which in the stationary phase matured to a fully fluorescent protein. This leads to the suggestion that the SOS response in the ∆6CiP mutant is indeed altered.

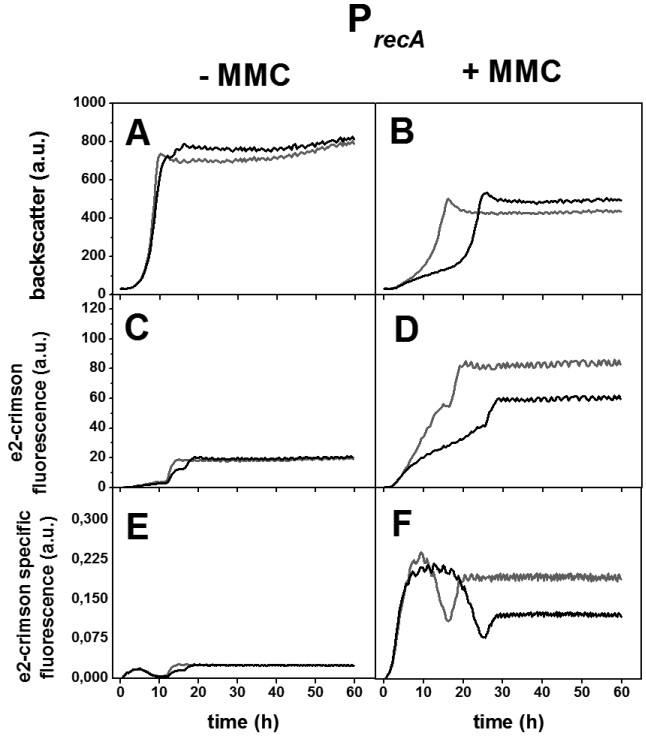

Figure 16 E2-crimson expression analysis under the control of P_{recA} (A – F) in the absence (A, C, E) or presence (B, D, F) of 0.4 µM MMC. Shown are the growth (backscatter signal of 620 nm light) (A, B), the E2-crimson fluorescence (C, D) and the specific fluorescence (E, F) of recombinant *C. glutamicum*/pJC1-P_{recA}-*e2-crimson* (grey line A – F) and ∆6CiP/pJC1-P_{recA}-*e2-crimson* (black line A – F). The specific fluorescence was calculated as the ratio of fluorescence signal to the backscatter signal (given in arbitrary units, a.u.). Cells were inoculated to an OD_{600} of 1 and cultivated in 750 µl of CGXII minimal medium with 4% (w/v) glucose at 30°C and 1,200 rpm. Average values of two technical replicates are shown representative for two independent biological experiments giving comparable results.

3.3.4 Complementation of the Δ6CiP mutant MMC-phenotype

Complementation studies were performed to check if plasmid-born 6C RNA expression from its native promoter can reverse the growth phenotype of the deletion mutant in the presence of MMC (Figure 14). For the complementation a pJC1 derivative containing the 6C RNA gene under the control of its native promoter was constructed and transformed into competent *C. glutamicum* Δ6CiP cells (see 2.4 and 2.5.2). The growth of the complementation strain *C. glutamicum* Δ6CiP/pJC1-6C was compared to the growth of the Δ6CiP mutant and the wild type, both harboring the empty vector as control, in the presence of MMC. The final OD_{600} values as well as the specific growth rates of *C. glutamicum*/pJC1, Δ6CiP/pJC1, and Δ6CiP/pJC1-6C were reduced in glucose minimal medium with 25 µg ml^{-1} kanamycin and 0.75 µM MMC compared to standard conditions (Table 10). As a result of the growth experiment, a kind of complementation was observed, yet growth behavior of the complemented strain in the exponential phase was surprisingly different compared to the wild type or the deletion mutant (Figure 17 A). The Δ6CiP/pJC1-6C strain showed wild type-like growth in the first four hours of cultivation in the presence of MMC. Then, the cells ceased to grow for about three hours and the OD_{600} of about 2.5 even decreased. After about seven hours of cultivation the complementation strain started to grow again. After 24 hours, the final OD_{600} of the Δ6CiP/pJC1-6C strain was comparable to that of *C. glutamicum*/pJC1 (Figure 17 A).

Northern blot analysis was used to analyze the amount of 6C RNA in strain Δ6CiP/pJC1-6C compared to the empty vector controls and revealed one 6C RNA transcript, expressed in the Δ6CiP/pJC1-6C (Figure 17 B, lane 2). In the Δ6CiP mutant with the empty vector, as expected, no 6C RNA signal could be detected. However, in the complementation strain the 6C RNA level was about five-fold higher than in the wild type with the empty vector (analyzed by using the AIDA image analyzer software). Thus, Northern blot analysis revealed that with the plasmid-born expression it was not possible to reach the physiological 6C RNA level, due to the medium copy number of pJC1 (Menkel*, et al.*, 1989, Cremer*, et al.*, 1990). Instead, the Δ6CiP/pJC1-6C strain can rather be considered as an overexpression strain. The effect of 6C RNA overexpression will be discussed in more detail in the next chapter (see 3.7).

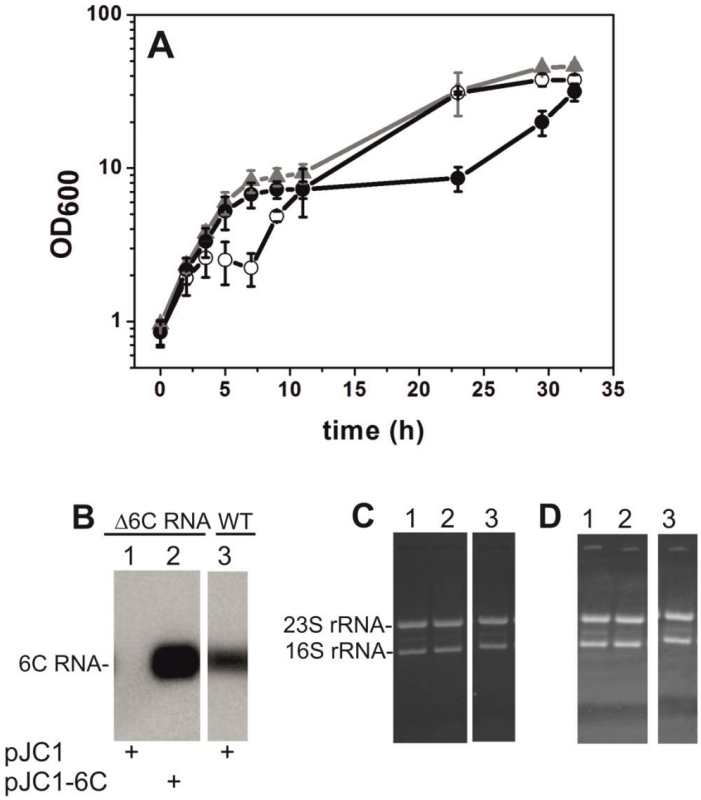

Figure 17 Growth (A) and Northern blot analysis (B-D) of *C. glutamicum*/pJC1 (▲), *C. glutamicum* Δ6CiP/pJC1 (●) and *C. glutamicum* Δ6CiP/pJC1-6C (○). Strains were cultivated in CGXII minimal medium with 4% (w/v) glucose, 25 µg ml^{-1} kanamycin and 0.75 µM MMC at 30°C and 120 rpm. Average values and standard deviations of three independent experiments are shown. During cultivation samples were harvested in the exponential phase (after 5 hours of cultivation) and total RNA was isolated and subjected to Northern blotting. B: Northern blot for the detection of the 6C RNA transcript, lane 1: total RNA from *C. glutamicum* Δ6CiP/pJC1, lane 2: total RNA from *C. glutamicum* Δ6CiP/pJC1-6C, lane 3: total RNA from *C. glutamicum*/pJC1. 1.2 µg of total RNA was loaded for each sample. The 16S rRNA was used as loading and transfer control (C and D). C: 1.2% FA agarose gel; lanes 1, 2, 3 as in B. D: Nylon membrane after blotting; lane 1, 2, 3: as in B.

3.4 Overexpression of the 6C RNA in *C. glutamicum* pJC1-6C (+/-MMC)

3.4.1 Growth and cell shape of *C. glutamicum* pJC1-6C (+/-MMC)

The complementation study of the growth defect of the ∆6CiP mutant under SOS response -inducing conditions revealed an exceptional growth phenotype. This is most likely due to the higher amount of 6C RNA compared to the wild type as a consequence of the medium pJC1 copy number (Menkel*, et al.*, 1989, Cremer*, et al.*, 1990). Therefore, the consequences of 6C RNA overexpression in the wild type by plasmid pJC1-6C were studied in more detail.

In the absence of MMC *C. glutamicum* pJC1-6C reached about the same final OD_{600} as the reference strain and had a similar growth rate in glucose minimal medium (Table 10, Figure 18 A). However, in the presence of MMC growth was different compared to the reference strain (Figure 18 B). The wild type with pJC1-6C showed a very similar growth behavior as strain ∆6CiP/pJC1-6C described above in the presence of MMC (see Figure 17).

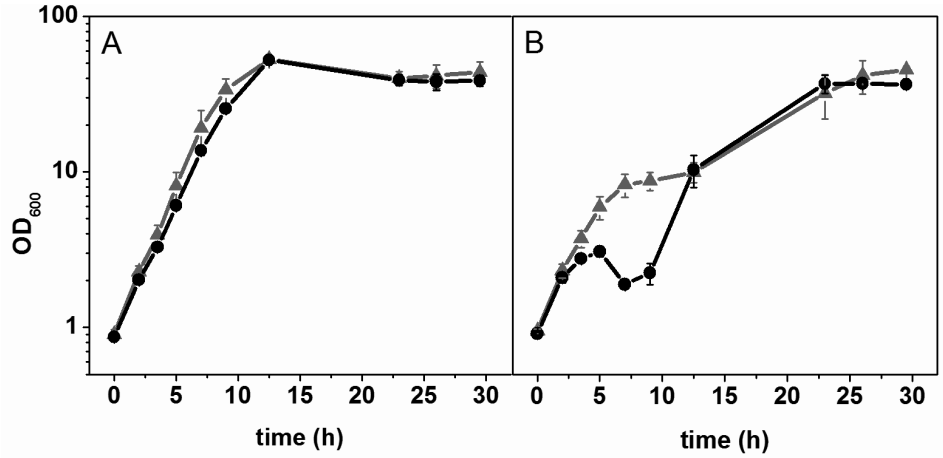

Figure 18 Growth of *C. glutamicum*/pJC1 and *C. glutamicum*/pJC1-6C. *C. glutamicum*/pJC1 (▲) and *C. glutamicum*/pJC1-6C (●) cultivated in CGXII medium with 4% (w/v) glucose and 25 µg ml^{-1} kanamycin without MMC (A) and with 0.75 µM MMC (B). Strains were cultivated at 30°C and 120 rpm. Average values and standard deviations of three independent cultivation experiments are shown.

Table 10 Growth parameters of *C. glutamicum*, *C. glutamicum* Δ6CiP, *C. glutamicum*/pJC1, *C. glutamicum*/pJC1-6C, *C. glutamicum* Δ6CiP/pJC1 and *C. glutamicum* Δ6CiP/pJC1-6C. The strains were cultivated in CGXII medium with 4% (w/v) glucose and 25 µg ml^{-1} kanamycin in the absence and in the presence of 0.75 µM MMC. Final OD_{600} = after 30 h of cultivation. Average values and standard deviations of three independent experiments are shown. N.d. not determined because no exponential growth observed.

Strain	**CGXII medium with 4% glucose**			
	-MMC		**+MMC**	
	Final OD_{600}	**µ (h^{-1})**	**Final OD_{600}**	**µ (h^{-1})**
C. glutamicum[1]	51.2 ±2.2	0.42 ±0.02	39.9 ±0.3	0.32 ±0.01
C. glutamicum Δ6CiP[1]	54.5 ±7.5	0.43 ±0.01	25.2 ±8.8	0.30 ±0.01
C. glutamicum/pJC1	43.9 ±7.0	0.43 ±0.05	45.3 ±0.9	0.31 ±0.02
C. glutamicum/pJC1-6C	38.6 ±3.2	0.39 ±0.02	36.5 ±1.7	n.d
C. glutamicum Δ6CiP/pJC1[2]	59.4 ±2.4	0.43 ±0.03	31.5 ±4.1	0.29 ±0.02
C. glutamicum Δ6CiP/pJC1-6C[2]	37.1 ±1.8	0.41 ±0.03	37.4 ±3.3	n.d

[1] strains were cultivated without kanamycin in the medium

[2] final OD_{600} = 32 h

Microscopic investigation revealed that the cells of strain *C. glutamicum*/pJC1-6C have an elongated cell shape under standard conditions (samples were taken in the exponential growth phase after 6 h of cultivation at an OD_{600} of 12-14). Moreover, free DNA was found in the extracellular space (highlighted with red circles in Figure 19), indicating cell envelope damage or spontaneous cell lysis. In the presence of MMC *C. glutamicum*/pJC1-6C revealed a strongly altered morphology compared to the reference strain with pJC1, in particular branched cells were observed (samples were taken after 6 h of cultivation at an OD_{600} of 3 for *C. glutamicum*/pJC1-6C and 8 for the reference strain with pJC1) (Figure 19). Moreover, microscopic investigation showed that many cells were lysed and only the empty cell envelopes were left (cells without DNA content). The observed cell lysis could be a reason for the decreased OD_{600} in the exponential growth phase (after 5-10 hours of cultivation). Additionally, in *C. glutamicum*/pJC1-6C the septum sites were irregularly distributed and partly condensed to “knob-like” structures and the cells failed to divide properly, which could result in the observed branched cell morphology.

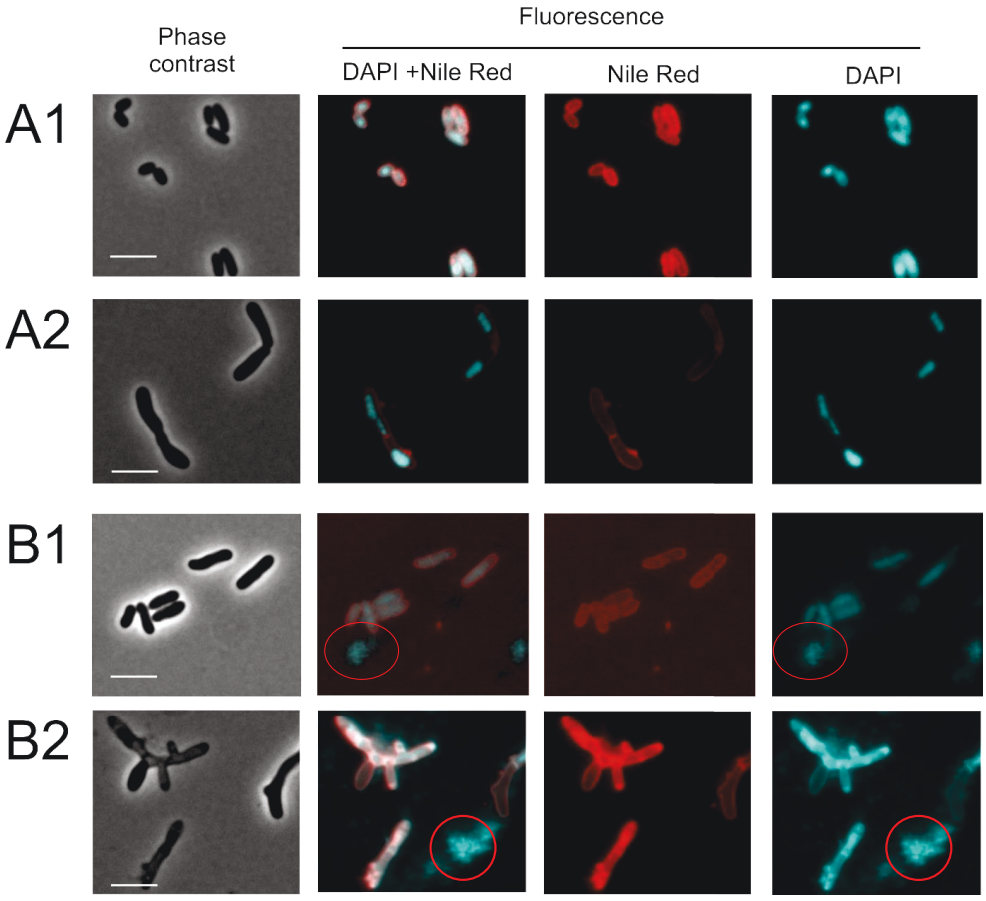

Figure 19 Microscopy images of *C. glutamicum*/pJC1 (A1 and A2) and *C. glutamicum*/pJC1-6C (B1 and B2). Strains were cultivated in CGXII minimal medium with 4% (w/v) glucose and 25 µg ml^{-1} kanamycin without MMC (A1 and B1) and with 0.75 µM MMC (A2 and B2) at 30°C and 120 rpm. Samples were taken in the exponential growth phase after 6 h of cultivation (*C. glutamicum*/pJC1 without MMC OD_{600} of 14, *C. glutamicum*/pJC1-6C without MMC OD_{600} of 12, *C. glutamicum*/pJC1 with 0.75 µM MMC OD_{600} of 8 and *C. glutamicum*/pJC1-6C with 0.75 µM MMC OD_{600} of 3. DNA was stained with 4',6-diamidino-2-phenylindole (DAPI) (cyan) and lipophilic regions with nile red (red). Red circles highlight free DNA. The white scale bar is 5 µm in length.

3.4.2 Transcriptome analysis of *C. glutamicum* pJC1-6C (+/- MMC)

A comparative transcriptome analysis of the strains wild type/pJC1-6C and wild type/pJC1 was performed to investigate the effect of an increased 6C RNA level on global gene expression under standard conditions. Overall, 28 genes had a more than 2-fold altered mRNA level and are listed in Table 11. The genes were also grouped into functional categories (Table 12).

Only three genes had an increased mRNA ratio (average mRNA ratios between 2.15 and 2.57), namely *ald* encoding an aldehyde dehydrogenase, *adhA* encoding a Zn-

dependent alcohol dehydrogenase, and cg3195 encoding a putative flavin-containing monooxygenase FMO.

Table 11 Differentially expressed genes revealed by comparative transcriptome analysis of *C. glutamicum*/pJC1-6C and *C. glutamicum*/ pJC1. Strains were cultivated in CGXII medium with 4% (w/v) glucose and 25 µg ml^{-1} kanamycin and harvested in the exponential growth phase (OD_{600} of 5-6). The average mRNA ratios and *p*-values were calculated from three independent experiments and mRNA ratios with a *p*-value ≤0.05 were set as significant. For each gene the locus tag, the gene name, the annotation, the average mRNA ratio and the *p*-value are given.

Locus tag	Gene	Annotation	mRNA ratio WT/pJC1-6C vs. WT/pJC1	p-value
cg0044	*rbsB*	putative periplasmic D-ribose-binding protein	0.45	0.00
cg0045		putative ABC transport protein, sugar transport, membrane component	0.44	0.00
cg0275	*mgtE2*	Mg^{2+} transporter, MgtE-family	0.48	0.01
cg0850	*whcD*	transcription factor, whmD homolg, not involved in oxidative stress	0.43	0.01
cg1336		putative secreted protein	0.43	0.00
cg1636		putative secreted protein	0.39	0.01
cg1897		putative secreted protein CGP3 region	0.12	0.01
cg1918		putative secreted protein CGP3 region	0.19	0.01
cg1934		hypothetical protein CGP3 region	0.44	0.05
cg1967		hypothetical protein CGP3 region	0.47	0.02
cg1968		hypothetical protein CGP3 region	0.49	0.02
cg1969		hypothetical protein CGP3 region	0.48	0.02
cg1970		hypothetical protein CGP3 region	0.49	0.03
cg1974		putative protein, contains peptidoglycan-binding LysM domain CGP3 region	0.33	0.01
cg1975		hypothetical protein, conserved CGP3 region	0.28	0.01
cg1977		putative secreted protein CGP3 region	0.26	0.01
cg1980		putative MoxR-like ATPase CGP3 region	0.44	0.04
cg2008		putative membrane protein CGP3 region	0.28	0.04
cg2014		hypothetical protein CGP3 region	0.21	0.02
cg2017		hypothetical protein CGP3 region	0.28	0.02
cg2063		putative membrane protein CGP3 region	0.31	0.03
cg2089		hypothetical protein, conserved	0.45	0.01
cg2376		putative secreted protein	0.40	0.01
cg2377	*mraW*	S-adenosyl-methyltransferase	0.29	0.00
cg3096	*ald*	aldehyde dehydrogenase	2.57	0.01
cg3107	*adhA*	Zn-dependent alcohol dehydrogenase	2.29	0.04
cg3195		putative flavin-containing monooxygenase FMO	2.15	0.05
cg3348		putative plasmid maintenance system antidote protein, HigA homolog	0.47	0.01

25 genes had a more than 2-fold decreased mRNA ratio in *C. glutamicum*/pJC1-6C compared to the reference strain. 15 of these genes are located within the CGP3 region and encode mainly proteins of unknown function. These 15 genes represent 8% of all CGP3 genes and were moderately decreased (2- to 3-fold). The remaining 40% of genes with a decreased mRNA level were grouped into different functional categories. One gene to mention here is *mraW* (cg2377 coding for an S-adenosyl-methyltransferase). This gene is

located within the *dcw* cluster, which comprises cell division- and cell wall-related genes (Valbuena*, et al.*, 2006). *mraW* is transcribed as part of a polycistronic mRNA, which includes at least *mraZ, mraW, cg2376* (*ftsL*)*, ftsI* (penicillin binding protein 3, PBP3), and *murE*, from a promoter that is located upstream of *mraZ* (Valbuena*, et al.*, 2006). The other genes which are transcribed as part of this polycistronic mRNA had, like *mraW*, down-regulated mRNA levels in the 6C RNA overexpression strain (cg2376 (*ftsL*) had an mRNA ratio of 0.4 (Table 11) and the other genes had ratios between 0.51 and 0.7 and are therefore not listed in Table 11). The genes *murE* and *ftsI,* involved in peptidoglycan synthesis, were reported to be essential for *C. glutamicum* (Wijayarathna*, et al.*, 2001). The reduced mRNA levels of these genes might be a reason for the elongated cell shape of the 6C RNA overexpression strain.

Overall, this transcriptome analysis showed that also an increased level of the 6C RNA has some influence on the global transcriptome of *C. glutamicum* under standard conditions.

Table 12 Differentially expressed genes revealed by comparative transcriptome analysis of *C. glutamicum*/pJC1-6C and *C. glutamicum*/pJC1. Strains were cultivated in CGXII medium with 4% (w/v) glucose and 25 µg ml^{-1} kanamycin and harvested in the exponential growth phase (OD_{600} of 5-6). The average mRNA ratio was calculated from three biological replicates and mRNA ratios with a *p*-value ≤0.05 were set as significant. The genes with an average mRNA ratio ≥2.00 or ≤0.50 and a *p*-value of ≤0.05 were grouped into functional categories. Genes with an average mRNA ratio ≤0.25 are underlined. Genes labeled with an asterisk are grouped into two categories.

Functional category	mRNA ratio (WT/pJC1-6C vs.WT/pJC1) ≥2.00	≤0.50, ≤0.25
Acetate and ethanol catabolism	*ald, adhA*	
Transporter		*rbsB, mgtE2, cg0045**
Cell division/cell wall		*mraW,* cg2376 (ftsL)*
Transcriptional regulators		*whcD*
CGP3 prophage genes		cg1897*, cg1918*, cg1934*, cg1967-cg1970*, cg1974*, cg1975*, cg1977*, cg1980*, cg2008*, cg2014*, cg2017*, cg2063*
Proteins with a predicted function	cg3195	cg0044, cg0045*, cg1336, cg1636, cg1897*, cg1918*, cg1974*, cg1977*, cg1980*, cg2008*, cg2063*, cg2376 (ftsL)*, cg3348
Hypothetical proteins		cg1934*, cg1967-cg1969*, cg1970*, cg1975*, cg2014*, cg2017*, cg2089

In contrast to standard conditions the global transcriptome analysis in the presence of MMC revealed that more than 400 genes had an at least two-fold altered mRNA level in the 6C RNA overexpression strain (Table 13 and Table A 3 in the appendix). 123 genes had a ≥2-fold increased mRNA level in *C. glutamicum*/pJC1-6C compared to the empty vector control. The genes with the highest increased mRNA level were *benA* (14.78-fold)*, benB* (16.66-fold), and *benC* (9.78-fold) coding for enzymes involved in benzoate degradation in

C. glutamicum (Shen & Liu, 2005, Brinkrolf*, et al.*, 2006). In *C. glutamicum* benzoate degradation requires the *ben* genes for converting benzoate into catechol and the three *cat* genes for degrading the resulting catechol into ß-ketoadipate enol-lactone. Also the mRNA ratios of the *cat* genes *catA* (6.51-fold), *catB* (2.03-fold), and *catC* (1.84-fold, below 2.00 and therefore not listed in Table 13) were increased. Transcriptional regulation of the genes belonging to the *ben*- and *cat*-clusters is assumed to be under the control of the regulator BenR (Brune*, et al.*, 2005). The *benR* gene (cg2641) was significantly 1.5-fold increased in *C. glutamicum*/pJC1-6C. Since LuxR-type regulators like BenR are generally regarded to act as transcriptional activators (Cramer*, et al.*, 2006, Hansmeier*, et al.*, 2006), an increased mRNA level of *benR* could indeed lead to an up-regulation of the genes within the *ben*- and *cat*-clusters. Additionally, benzoate and/or *cis*, *cis*-muconic acids would be required for the activation as known from *Pseudomonas* sp. and *Acinetobacter* sp. (Collier*, et al.*, 1998, McFall*, et al.*, 1998).

Also genes of the protocatechuate branch of the ß-ketoadipate pathway showed increased mRNA levels in *C. glutamicum*/pJC1-6C. 4-Hydroxybenzoate hydroxylase activity, necessary for the conversion of 4-hydroxybenzoate into protocatechuate, is encoded by *pobA*. The *pobA* gene is located in a transcription unit along with *pcaK*, encoding a putative 4-hydroxybenzoate transporter (Shen & Liu, 2005). Both genes had an increased mRNA ratio (2.85-fold and 2.35-fold, respectively) (Table 13). The subunits of the protocatechuate 3,4-dioxygenase are encoded by *pcaG* and *pcaH*, which also had an increased mRNA level (2.00-fold and 2.01-fold, respectively). Moreover, *pcaB* and *pcaC,* necessary for the conversion of ß-carboxy-*cis*-*cis*-muconate into ß-ketoadipate enol-lactone, had an increased mRNA ratio (Table 13) (*pcaB* 2.11-fold, *pcaC* 1.44-fold). A possible reason for the increased mRNA level of the genes of the protocatechuate branch of the ß-ketoadipate pathway remains to be elucidated. Interestingly, also the genes of the vanillate metabolism in *C. glutamicum*, including *vanA*, *vanB*, and *vanK* and the divergently transcribed *vanR* had an increased mRNA ratio (2.15 to 2.25-fold) (Merkens*, et al.*, 2005). *VanA* and *vanB* code for enzymes that convert vanillate into protocatechuate. The protocatechuate is then, as described above, converted to ß-ketoadipate enol-lactone and finally to succinyl-CoA and acetyl-CoA (Brinkrolf et al. 2006). VanR negatively controls *vanABK* transcription (Brinkrolf*, et al.*, 2006). The mRNA ratio of *vanR* was not altered, nevertheless this does exclude that the VanR activity is somehow altered.

Moreover, genes coding for proteins involved in glutamate (*gluABC*), citrate (*tctBC*) and ribose/xylose (*rbsACBD*) uptake, including the transcriptional repressor RbsR (*rbsR*) had an increased mRNA level in the *C. glutamicum*/pJC1-6C. A second transcriptional regulator is involved in the control of the *rbs* operon, namely UriR (Brinkrolf*, et al.*, 2008, Nentwich*, et al.*, 2009). It could be shown that RbsR and UriR recognize the same cognate *cre*-like DNA

sequences in the operators of their target genes (Brinkrolf*, et al.*, 2008). Further targets of UriR are the genes of the *uriR* operon (*uriR-rbsK1-uriT-uriH*) (Brinkrolf*, et al.*, 2008), which also had an increased mRNA level in *C. glutamicum*/pJC1-6C in the presence of MMC (except for *uriH*, ratios between 1.49 and 1.58). The question comes up if the altered mRNA ratios of all these genes coding for proteins of transport systems is due to a general effect, which is related with the different growth behaviour of *C. glutamicum*/pJC1-6C, or if it is directly related to the 6C RNA.

Overall, 289 genes had a decreased mRNA ratio in *C. glutamicum*/pJC1-6C in the presence of MMC (Table 13). 163 genes (54%) of these are located within the CGP3 region, which in total comprises 174 genes. This means that 93% of the CGP3 region genes had a decreased mRNA level in *C. glutamicum*/pJC1-6C. Notably, an opposing trend was observed in the ∆6CiP mutant, in which 86% of the 50 genes with an increased mRNA ratio in the presence of MMC were located within the CGP3 region (Table 9, section 3.6.2). These results lead to the suggestion that the level of 6C RNA directly or indirectly could have an influence on the expression of genes located within the CGP3 region or on the copy number of the prophage (Frunzke*, et al.*, 2008).

Three genes with a decreased mRNA level in *C. glutamicum*/pJC1-6C in the presence of MMC are involved in cell division and cell wall synthesis, namely *murE, ftsI, and mraW*. Detailed information about the latter three genes was given above in the transcriptome comparison under standard conditions. Additionally, cg1325, encoding a putative stress-responsive transcriptional regulator, had a decreased mRNA ratio. Possibly, the decreased mRNA level of this predicted transcriptional regulator could be involved in the different growth behaviour of *C. glutamicum*/pJC1-6C in the presence of MMC.

Interestingly, in the group of genes for transcriptional regulators was cg0850 coding for the transcription factor WhcD (WhiB2). *C. glutamicum* possesses overall four *whiB*-like genes known as *whcA (whiB4), whcB (whiB3), whcD (whiB2),* and *whcE (whiB1).* Except for *whcD*, the *whc* genes have already been intensively studied in *C. glutamicum*. The *whcE* gene plays a positive role in survival of cells exposed to oxidative and heat stress (Kim*, et al.*, 2005) whereas the *whcA* gene plays a negative role in the expression of genes responding to oxidative stress (Choi*, et al.*, 2009). WhcD (WhiB2) showed 88% sequence identity to WhmD of *M. smegmatis*, which is an essential mycobacterial protein required for proper septation and cell division (Gomez & Bishai, 2000). The decreased level of *whcD* in *C. glutamicum*/pJC1-6C could lead to an altered cell morphology both in the absence and in the presence of MMC (Figure 19 B1 and B2). Therefore, WhcD from *C. glutamicum* was further analysed (3.5.1). If the 6C RNA is directly or indirectly involved in the regulation of *whcD* expression or stability needs further investigation.

Table 13 Differentially expressed genes revealed by comparative transcriptome analysis of *C. glutamicum*/pJC1-6C and *C. glutamicum*/pJC1 in the presence of MMC. Strains were cultivated in CGXII medium with 4% (w/v) glucose and 25 µg ml^{-1} kanamycin in the presence of 0.75 µM MMC and harvested in the exponential growth phase (OD_{600} of 3 for *C. glutamicum*/pJC1-6C and OD_{600} of 5 for *C. glutamicum*/pJC1). The genes with an average mRNA ratio ≥2.00 or ≤0.50 and a *p*-value of ≤0.05 were grouped into functional categories. Genes with an average mRNA ratio ≥10.00 and ≤0.10 are underlined; genes with an average mRNA ratio ≥4.00 and ≤0.25 are shown in bold. Some genes are grouped into two functional categories and are marked by an asterisk.

Functional category	mRNA ratio (WT/pJC1-6C vs.WT/pJC1)	
	≥2.00, ≥4.00, ≥10.00	**≤0.50, ≤0.25, ≤0.10**
Amino acid metabolism	*metE*	*gltBD, msrB, msrA,*
TCA cycle, acetate, propionate and ethanol metabolism	***ald, adhA,*** *prp**D2B2**C2, prpD1B1, sucCD*	
Aromatic compound metabolism	*benAB**C**, **catA1**B, vanAB, pobA, pcaB, pcaH, pcaG, benK*, pcaK**	
Other metabolic enzymes	***fabG2**, rolH, rolM, lplA, glpQ2, uriH*	*cmk, idhA3, trmU, seuC,*
Metabolism of cofactors, trace elements and electron carriers	*nadSCA, ndnR*,* ***cytP,*** *ripA*, fdxB*	*fdxA, copO*
Transport	*benK*, benE, gntP, oppABC, phnB, rbsACD, gluABC, vanK, tctBC, putP, pcaK**	*rbsB, amt, mgtE2*
DNA replication/DNA repair		*sigA*, ssb, recO, dnaB,* ***dnaE2,*** *recJ*, cglIM*, cglIR*, cglR*, cglIR**
Translation		*rplI, rpsF*
Transcriptional regulators, regulatory proteins and two-component systems	*ndnR*, rbsR, ripA*, esrS*,glnD*	*whcE*, cg2922*, whcD, cg3303*, cgtR2, cgtS2, glnX, sigA*, gntR2**
Cell wall/ cell division related and fatty acid metabolism	*ufaA*	*murE, ftsI,* ***mraW,***
Resistance related		*lmbR*
Stess related	*uspA2, cspA, betB, hmp, esrS**	*cspB, qor2, whcE*, arnA* (sRNA)*
Transposases	*tnp23a*	*tnp17a, tnp19a, tnp4a,*
CGP3 prophage genes		cg1890-cg2071 (163 of 174 genes), including *alpC, alpA, res, arnA* (sRNA), gntR2*, recJ*, cglIM*, cglIR*, cglR*, cglIR**

Functional category	mRNA ratio (WT/pJC1-6C vs.WT/pJC1)	
	≥2.00, ≥4.00, ≥10.00	**≤0.50, ≤0.25, ≤0.10**
Proteins with a predicted function	cg0340, cg0637, cg0638, cg0639, cg0642, cg0644, cg0921, cg0922, cg0961, cg0962, cg1077, cg1080, cg1081, cg1087, cg1100, cg1159, cg1203, cg1205, cg1237, cg1332, cg1454, cg1498, cg1514, cg1541, cg1542, cg1572, cg1612, cg1619, cg1640, cg1657, cg1665, cg1682, cg2336, cg2435, cg2440, cg2467, cg2557,cg2610, cg2674, cg2675, cg2676, cg2677, cg2678, cg2927, cg2959, cg2965, cg2966, cg3067, cg3195, cg4005	cg0031, cg0044, cg0045, cg0046, **cg0078**, cg0079, cg0083, cg0183, cg0252, cg0291, cg0308, cg0455, cg0578, cg0706, cg0714, cg0753, cg0772, cg0905, cg0998, cg1232, cg1255, cg1291, cg1307, cg1325, cg1440, **cg1508**, cg1628, cg1864, **cg1881**, **cg1883**, **cg1884**, cg2110, cg2125, cg2312, cg2349, **cg2376**, cg2380, cg2449, cg2556, cg2633, cg2699, cg2719, cg2733, cg2739, cg2750, cg2828, cg2884, cg2922*, cg3020, cg3074, cg3134, cg3135, cg3138, cg3140, cg3143, cg3211, cg3234, cg3260, cg3272, cg3274, cg3286, cg3303*, cg3330, cg3338, **cg3348**, cg3382, cg3405
Hypothetical proteins	cg0974, cg1097, cg1202, cg1221, cg1548, cg1618, cg2089, cg2283, cg2324, cg2392, cg2430, cg2438, cg2481, cg2487, cg2666, cg2667	**cg0077**, cg0096, cg0269, cg0676, cg0851, cg0852, **cg0875**, **cg0907**, **cg1059**, cg1091,cg1523, cg1567, cg2080, cg2088, cg2263, **cg2504**, cg2564, **cg2683**, cg3139, cg3319, **cg3329**

3.5 Putative mRNA targets of the 6C RNA

3.5.1 Deletion and Overexpression of *whcD*

A Δ*whcD* mutant was constructed to investigate the physiological role of WhcD in *C. glutamicum*. In the transcriptome analysis of *C. glutamicum*/pJC1-6C the *whcD* mRNA level was decreased (Table 12 and Table 13), therefore the constructed Δ*whcD* mutant should also aid to analyse a possible relation between the 6C RNA and the transcriptional regulator WhcD and the observed changes in the cell morphology of *C. glutamicum*/pJC1-6C. Moreover, the WhcD homologue in *M. smegmatis* (WhmD) was shown to be involved in cell septation (Gomez & Bishai, 2000). Therefore, the characterization of the *whcD* gene should elucidate if the homologous proteins are functionally equivalent in both actinobacteria.

Single colonies of the Δ*whcD* mutant appeared less glossy compared to *C. glutamicum* wild type after cultivation on BHI+10% sucrose agar plates at 30°C for three days. Furthermore, the surface of the Δ*whcD* mutant colonies appeared to be rough (Figure A 7) suggesting a change in the composition of the cell envelope. Moreover, the Δ*whcD* mutant had a 47% reduced final OD_{600} (29.7 ± 4.7 *vs* 55.9 ± 4.4) and a 22% reduced growth rate (0.33 ± 0.03 h^{-1} vs 0.42 ± 0.05 h^{-1}) compared to the wild type (Figure 20 A). In contrast to the *whcD* deletion, increased expression of this gene using plasmid pAN6-*whcD* in the wild-type background did not lead to a growth phenotype (Figure 20 B). The strong effect of the *whcD* deletion on growth leads to the suggestion that WhcD might play an important regulatory role in *C. glutamicum*.

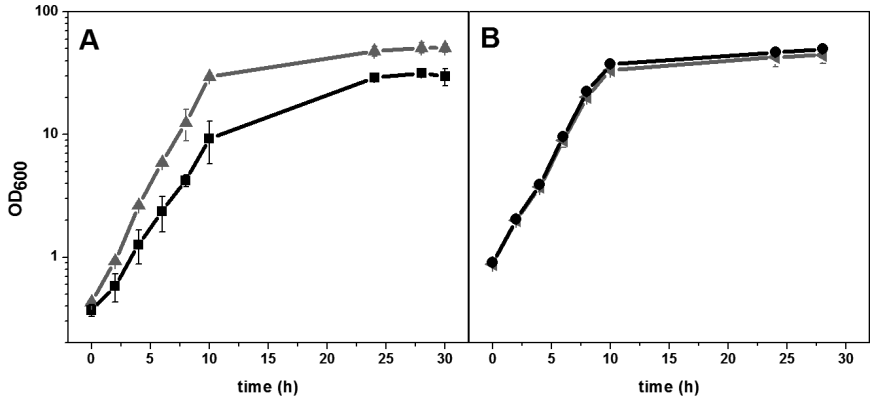

Figure 20 Growth of *C. glutamicum* wild type and *C. glutamicum* Δ*whcD* (A) and *C. glutamicum*/pAN6 and *C. glutamicum*/pAN6-*whcD* (B). A *C. glutamicum* (▲) and *C. glutamicum* Δ*whcD* (■) cultivated in CGXII minimal medium with 4% (w/v) glucose. **B** *C. glutamicum*/pAN6 (◀) and *C. glutamicum*/pAN6-*whcD* (●) cultivated in CGXII minimal medium with 4% (w/v) glucose, 25 µg ml^{-1} kanamycin and 0.5 mM IPTG. All strains were cultivated at 30°C and 120 rpm. Average values and standard deviations of three independent cultivations are shown.

Microscopic investigation of Δ*whcD* cells in the exponential growth phase revealed that the cells have a branched and elongated cell morphology (Figure 21), resembling the morphology of *C. glutamicum*/pJC1-6C cells in the presence of MMC (Figure 19 B2). Like for the 6C RNA overexpression strain, microscopic invetsigation revealed that free DNA is present in the extracellular space, indicating a severe damage of the cell membrane and/or the cell wall. Additionally, in the Δ*whcD* mutant the septum sites are irregularly distributed and partly condensed to "knob-like" structures and the cells failed to divide properly, which results in the observed branched and elongated cell morphology of the Δ*whcD* cells.

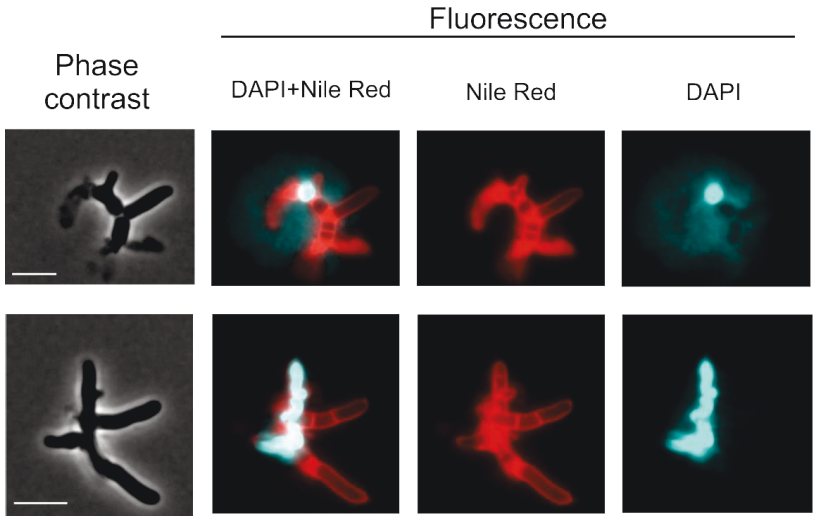

Figure 21 Microscopy images of *C. glutamicum* Δ*whcD*. The Δ*whcD* mutant was cultivated in 50 ml CGXII minimal medium with 4% (w/v) glucose at 30°C and 120 rpm. Samples were taken in the exponential growth phase. DNA was stained with 4',6-diamidino-2-phenylindole (DAPI) (cyan) and lipophilic regions with nile red (red). The white scale bar is 5 µm in length.

Taken together, *whcD* is crucial for *C. glutamicum*, although the data show that *whcD* seems not essential under standard cultivation conditions in glucose minimal medium. However, it can not be excluded that suppressor mutantions compensate the absence of *whcD*. Therefore, a genome resequencing of the Δ*whcD* mutant should be performed to get information about suppressor mutations. The altered cell morphology of the Δ*whcD* cells strongly resembles the cell morphology of *C. glutamicum/*pJC1-6C cells when cultivated in the presence of MMC (see 3.4.1), which is an indication for a potential connection between the 6C RNA and WhcD *in C. glutamicum.* Furthermore, the determination of the cell dry weight (CDW) of the Δ*whcD* mutant and the wild type revealed a different correlation between optical density and CDW (OD_{600} = 1 corresponds to 0.43 ± 0.03 g CDW l^{-1} for strain Δ*whcD vs.* 0.30 ± 0.01 g CDW l^{-1} for the wild type). The CDW was determined for OD_{600} values between 2 and 10 and a linear correlation between the CDW and the OD_{600} could be

shown for both strains (see in the appendix Figure A 6). This result reveals that the altered cell morohology of the Δ*whcD* mutant has consequences for the CDW/OD_{600} ratio. Apparently, the Δ*whcD* mutant scatters light less than the wild type.

The strongly altered cell morphology of the Δ*whcD* under standard conditions indicates that WhcD might play a role in the regulation of the cell wall metabolism and/or cell division in *C. glutamicum*. Therefore, it was investigated whether the *whcD* deletion has an influence on global gene expression. In *C. glutamicum* and in *M. smegmatis* the regulons of the transcriptional regulators WhcD and WhmD, respectively, are not known yet.

Comparative transcriptome analysis of the Δ*whcD* mutant and *C. glutamicum* wild type revealed 42 genes which had a more than 2-fold altered mRNA ratio (Table 14). 15 genes had an increased mRNA level in the Δ*whcD* mutant. The genes with the highest mRNA ratio were *mraZ* (4.67-fold) and *mraW* (2.74-fold). Both genes are located within the *dcw* cluster, which comprises cell division- and cell wall-related genes (Valbuena*, et al.*, 2006). The genes *mraW* and *mraZ are* transcribed as part of a polycistronic mRNA, which includes at least *mraZ, mraW, cg2376* (*ftsL*) (2.32-fold), *ftsI* (1.8-fold) and *murE* (1.57-fold, ratios below 2.00 are not listed in Table 14). The increased mRNA level of these genes could be a reason for the altered cell morphology of the Δ*whcD* mutant. Moreover, two genes with a decreased mRNA level in the Δ*whcD* mutant, namely cg3187 and cg2077 code for arabinofuranosyltransferases (Afts). These enzymes are involved in the biosynthesis of arabinogalactan, which is part of the corynebacterial cell envelope. Another gene associated with cell wall biogenesis, *cop1*, which encodes a trehalose corynomycolyl transferase, also had a decreased mRNA level in the Δ*whcD* mutant. The deletion of corynomycolyl transferases in *C. glutamicum* can lead to segmentation defects (Kacem*, et al.*, 2004). Moreover, Cop1 was found to play an additional role in the control of cell shape (Brand*, et al.*, 2003). Therefore, the decrease in the *cop1* level could be involved in the morphological phenotype of Δ*whcD*. Moreover, cg2199 coding for a penicillin-binding protein (PBP2a) had a decreased mRNA level. The PBP2a is a member of the HMW-PBPs and is involved in peptidoglycan synthesis (Valbuena*, et al.*, 2007). The altered mRNA levels of the genes described above could be, at least partly, the reason of the altered cell morphology of the Δ*whcD* mutant.

The neighbouring genes of *whcD,* namely cg0851 and the convergently transcribed cg0852, both coding for proteins with unknown function, had mRNA ratios of 1.34 and 0.55, respectively. Thus, a regulatory influence of WhcD on its downstream genes cannot be excluded.

Table 14 Differentially expressed genes revealed by comparative transcriptome analysis of Δ*whcD* mutant and *C. glutamicum* wild type. Strains were cultivated in CGXII medium with 4% (w/v) glucose and harvested in the exponential growth phase (OD_{600} 4.5 – 6.0). The average mRNA ratio was calculated from four biological replicates. Average mRNA ratios with a *p*-value ≤0.05 were set to be significant. Genes with an average mRNA ratio ≥2.00 or ≤0.50 and a *p*-value of ≤0.05 are listed.

Locus tag	Gene	Annotation	mRNA ratio (Δ*whcD* vs.WT)
cg2378	*mraZ*	putative MraZ protein	4.67
cg2377	*mraW*	S-adenosyl-methyltransferase	2.74
cg2379		hypothetical protein	2.72
cg3169	*pck*	phosphoenolpyruvate carboxykinase	2.48
cg0077		hypothetical protein	2.35
cg2376		putative secreted protein	2.32
cg0012	*ssuR*	sulphonate sulphur utilization transcriptional regulator SsuR	2.31
cg0762	*prpC2*	2-methylcitrate synthase, involved in propionate catabolism	2.28
cg2833	*cysK*	O-acetylserine thiol-lyase, cysteine synthase	2.24
cg0760	*prpB2*	2-methylisocitrate lyase	2.19
cg3378		hypothetical protein	2.19
cg2102	*sigB*	RNA polymerase sigma factor	2.11
cg0078		putative membrane protein	2.07
cg3119	*cysJ*	sulfite reductase flavoprotein, ferredoxin-$NADP^+$ reductase	2.04
cg0759	*prpD2*	2-methycitrate dehydratase	2.03
cg2707		hypothetical protein	0.50
cg0624		putative secreted oxidoreductase	0.49
cg2118	*fruR*	transcriptional regulator of sugar metabolism, DeoR-family	0.49
cg0623		putative cobalamin ECF transporter	0.49
cg1604		putative porin	0.48
cg3182	*cop1*	trehalose corynomycolyl transferase Cop1	0.48
cg1579		putative secreted protein	0.48
cg2925	*ptsS*	sucrose-specific EIIABC component EIISuc of PTS	0.48
cg0848	*wbbL*	putative rhamnosyl transferase WbbL	0.47
cg3187	*aftB*	arabinofuranosyltransferase	0.47
cg3181		putative secreted protein	0.47
cg0622		putative cobalamin ECF transporter, duplicated ATPase component	0.46
cg2199	*pbp*	penicillin-binding protein, putative D-alanyl-D-alanine carboxypeptidase	0.46
cg0675	*mrsA*	phosphoglucosamine mutase	0.45
cg1091		hypothetical protein	0.44
cg2229		putative exconuclease ATPase subunit or CTP synthase UTP-ammonia lyase	0.43
cg1636		putative secreted protein	0.41
cg1578		putative membrane protein, acyltransferase-family	0.40
cg0955		putative secreted protein	0.40
cg3197	*psp5*	putative secreted protein	0.39
cg2077		putative arabinofuranosyltransferase or membrane protein	0.38
cg2519		hypothetical protein	0.35
cg1577		putative secreted hydrolase	0.34
cg1007		putative membrane protein	0.33
cg2080		hypothetical protein	0.18
cg1603		hypothetical protein	0.12
cg0850	*whcD*	transcription factor WhcD	0.04

3.5.2 Characterization of the downstream genes of the 6C RNA

Notably, the genes from cg0362 to cg0369, which are located directly downstream of the 6C RNA gene, had an increased mRNA level in the Δ6C mutant (3.2.1). A read-through from the 6C RNA promoter leading to the increased expression of cg0362-cg0369 can be excluded since in the Δ6CiP mutant, which also lacks the 6C RNA promoter, these genes also had an increased mRNA ratio (data not shown). Among this group of genes is cg0362, encoding a putative septum site-determining protein. An increased expression of cg0362 could lead to morphological changes or alterations in septation, yet in the microscopic investigation of the Δ6CiP strains no differences in morphology and septum formation could be observed (Figure 15 A and B). However, *C. glutamicum*/pJC1-6C which overexpresses the 6C RNA from its native promoter had an altered cell morphology under standard conditions, which became even more prominent in the presence of MMC. If the 6C RNA would trigger the degradation of the mRNA of the downstream genes, an increased 6C RNA level could even lead to a higher level of mRNA degradation. However, the mRNA level of the downstream genes was only moderately decreased in *C. glutamicum*/pJC1-6C (without MMC mRNA ratios between 0.76 and 1.18; with 0.75 µM MMC mRNA ratios between 0.59 and 1.17).

The mutant ΔOP_cg0362 was constructed, in which the nine genes from cg0362 to cg0369 were deleted, to investigate if the deletion of the downstream genes of the 6C RNA has any consequence on growth or cell morphology of *C. glutamicum*. Neither growth nor morphology of *C. glutamicum* ΔOP_cg0362 was altered under standard conditions (Figure 22) (see also in appendix Figure A 5). Since the alteration in the cell morphology of *C. glutamicum*/pJC1-6C was even stronger in the presence of MMC, *C. glutamicum* ΔOP_cg0362 was also cultivated in the presence of MMC. However, also in the presence of MMC neither growth nor morphology of the ΔOP_cg0362 mutant was different to the wild type (Figure 22) (see also in appendix Figure A 5). Further investigations are necessary to elucidate the physiological role of the downstream genes of the 6C RNA. However, the results show that the absence of cg0362 and the following genes up to cg0369 seem not to be responsible for the altered cell morphology of *C. glutamicum*/pJC1-6C. Nevertheless, a regulation of the mRNA level of the downstream genes by the 6C RNA can not be excluded yet. Moreover, increased expression of the genes cg0362-cg0369 using plasmid pAN6-OP_cg0362 in the wild-type background should be investigated to see if the overexpression of the genes has any effect on cell morphology.

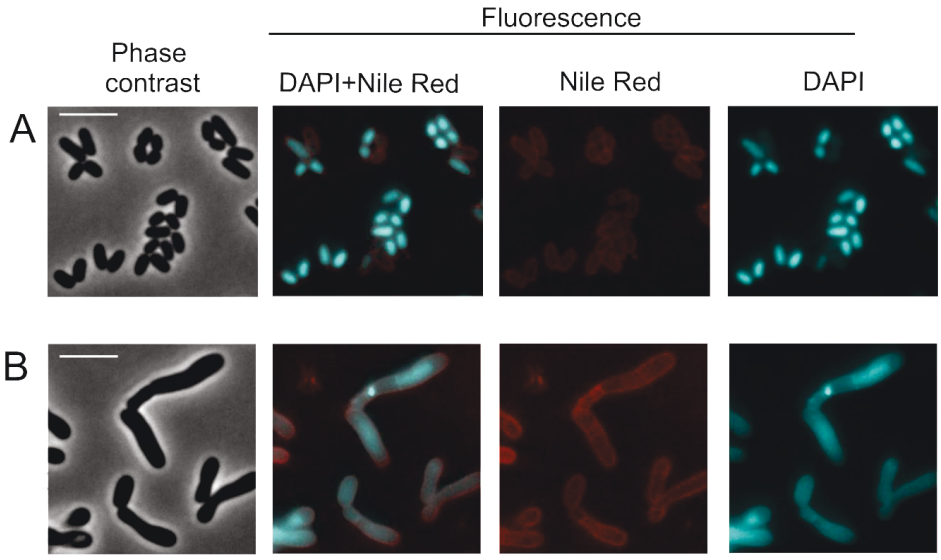

Figure 22 Microscopic images of *C. glutamicum* ΔOP_cg0362. ΔOP_cg0362 was cultivated in CGXII medium with 4% (w/v) glucose (A) and with 0.75 µM MMC (B) at 30°C and 120 rpm. DNA was stained with 4',6-diamidino-2-phenylindole (DAPI) (cyan) and lipophilic regions with nile red (red). The white scale bar is 5 µm in length.

3.6 Putative protein interaction partners of the 6C RNA

Basically, sRNAs can target mRNA and/or protein interaction partners, thereby accomplishing their regulatory functions (see 1.2). RNA pull-down experiments were performed to investigate if the 6C RNA of *C. glutamicum* has protein interaction partners. For these experiments *in vitro* generated 6C RNA was coupled to adipic acid dihydrazide agarose beads and incubated with crude protein extract generated from *C. glutamicum* Δ6CiP (see 2.7.16). The Δ6CiP strain was chosen to prevent binding of a putative protein target to the *in vivo* generated 6C RNA. SDS-PAGE analysis revealed several proteins that could be eluted from the *in vitro* generated 6C RNA (Figure 23 A). After the final washing step (W6) all unbound or weakly bound proteins were successfully removed (Figure 23 A and B). As a negative control uncoupled beads were used, which were also incubated with crude protein extract. Several proteins could be eluted from both, the RNA-coupled and the uncoupled agarose beads, indicating that some proteins in the crude extract bind unspecifically to the agarose beads (Figure 23 A). However, one protein band on the SDS gel was most prominent compared to the other protein bands in the elution fractions (marked with an asterisk in Figure 23 A and B). This protein band was only visible in the elution fraction of the pull-down with the 6C RNA-coupled beads and not in the negative control with the uncoupled beads (Figure 23 A). The protein was identified by peptide mass fingerprinting as phosphoglycerate kinase of *C. glutamicum* (PGK_{Cg}) (Table 15). In a second RNA-pull

down experiment, 75 ng µl^{-1} of heparin was added as competitor to the mixture of RNA-coupled beads and the crude extract (Figure 23 B). This experiment revealed that even in the presence of competitor PGK_{Cg} binds to the 6C RNA (Table 15). Thus, PGK_{Cg} could reproducibly be eluted from the 6C RNA and since it was not eluted in the negative control it seems that the binding of the PGK to the 6C RNA is rather specific.

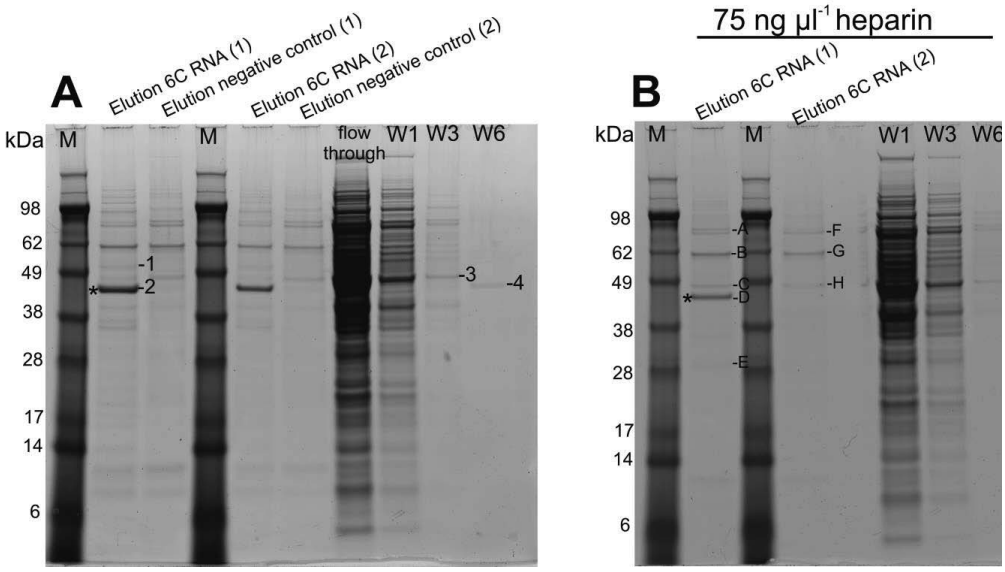

Figure 23 SDS-gel analysis of proteins obtained by RNA pull-down experiments with *in vitro* synthesized 6C RNA coupled to adipic acid dihydrazide agarose beads. Crude extract was prepared from *C. glutamicum* ΔCiP cultivated in CGXII minimal medium with 4% (w/v) glucose and harvested in the exponential growth phase. As negative control uncoupled beads were used. Proteins were eluted with 2 M NaCl from RNA-coupled or uncoupled beads. The elution was performed in two consecutive steps, indicated by (1) and (2), each with 2 M NaCl. M: SeeBlue Plus2 Pre-stained standard. Numbers and letters indicate proteins that were identified by peptide mass fingerprinting (Table 15). Shown are the results of two independent pull-down experiments (A and B). B: RNA pull-down with the addition of 75 ng µl^{-1} of heparin as competitor. The 10% SDS-polyacrylamide gels were stained with Coomassie Brilliant Blue and scanned with the Typhoon scanner.

Table 15 Proteins obtained in RNA pull-down experiments with 6C RNA *in vitro* transcript and identified by peptide mass fingerprinting. Proteins are sorted by locus tag.

Protein band	Locus tag		Annotation	Theoretical MW
E	cg0237		short chain dehydrogenase	26.7 kDa
3	cg0587	Tuf	tuf elongation factor	43.8 kDa
3, C, H	cg1111	Eno	enolase phosphopyruvate hydratase	44.9 kDa
C, H	cg1133	GlyA	serine hydroxymethyltransferase	46.5 kDa
A, F	cg1290	MetE	5-methyltetrahydropteroyltriglutamate-homocysteine methyltransferase	81.3 kDa
B	cg1531	RpsA	30S ribosomal protein S1	53.9 kDa
2, 4, D	cg1790	PGK	phosphoglycerate kinase	42.8 kDa
1	cg2964	GuaB1	inosine-5-monophosphate DH	50.9 kDa
B, G	cg3011	GroEL	chaperonin GroEL	57.3 kDa

Electrophoretic mobility shift assays (EMSAs) were used to characterize and specify the complex formation of the 6C RNA with PGK_{Cg}. The EMSAs were performed in cooperation with Sabine Schneider of the group of Prof. Wagner (HHU Düsseldorf). For the EMSAs PGK_{Cg} was overexpressed in *E. coli* BL21(DE3) using plasmid pET16b-pgk (Cg) and subsequently purified as described previously (Reddy & Wendisch, 2014). The functionality of purified His_{10}-PGK_{Cg} was tested in *in vitro* enzyme activity assays as described previously (Reddy and Wendisch, 20014). An enzyme activity of 165 ± 38 U mg^{-1} could be determined for the purified His_{10}-PGK_{Cg}, which is the range of the recently published maximal activity of 220 U mg^{-1} (Reddy & Wendisch, 2014). After confirming the functionality of PGK_{Cg} it was used in EMSAs. After incubation of the *in vitro* generated and radioactively labeled 6C RNA with increasing molar excess of PGK_{Cg} no retardation of the 6C RNA was obsereved (Figure 24 A). Since in the first EMSA no retardation was observed, buffer D was exchanged with TGED buffer. However, also with TGED buffer no complex formation of the protein and the RNA could be detected (Figure 24 B, lane 1, 2 and 3). Since PGK has an ATP/ADP-binding domain (Flachner*, et al.*, 2004), ATP was added to the reaction mixture. Notably, in the case of the addition of 1 mM ATP to 10 µM PGK_{Cg} the signal of unbound 6C RNA seems to fade on the autoradiogram (Figure 24 B, lane 3 and 4). However, any signal of retarded 6C RNA could be detected in the upper part of the autoradiogram, which would indicate complex formation of 6C RNA and PGK_{Cg}. Conclusively, the EMSA experiments could not confirm an interaction of PGK_{Cg} with 6C RNA under the conditions tested. Possibly, further factors (e.g. a specific metabolite) could be required for an interaction, that are present in the crude extract but not in the EMSA setup. Moreover, it should be investigated whether PGK binds unspecifically to RNA, by testing a control RNA in pull-down experiments.

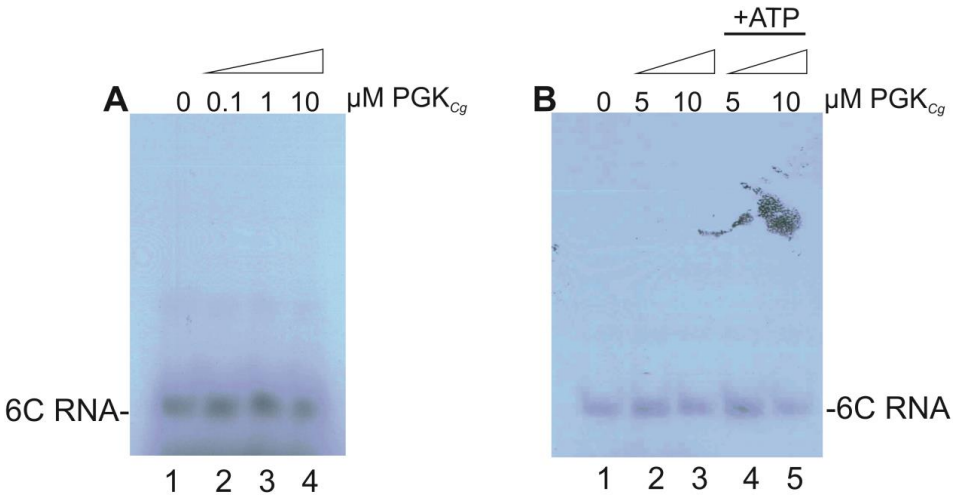

Figure 24 EMSAs with 6C RNA and PGK$_{Cg}$. For gel retardation experiments 20 nM radioactively labeled 6C RNA was incubated with increasing amounts of PGK$_{Cg}$ in buffer D (A) or TGED buffer (B) and 1 mM $MgCl_2$ for 10 min at 30°C. Subsequently, 20 ng µl^{-1} of heparin was added as competitor and the mixture was incubated for 5 min at 30°C. Samples were separated on a 5% polyacrylamide gel. Radioactively labeled 6C RNA was visualised by autoradiography. **A** lane 1 to 4: 20 nM 6C RNA with 0, 0.1, 1 and 10 µM PGK, respectively. **B** lane 1 to 3: 20 nM 6C RNA with 0, 5 and 10 µM PGK, respectively, lane 4 and 5: 20 nM 6C RNA with 5 and 10 µM PGK and 1 mM ATP, respectively. For retardation analysis with ATP, at first, the protein was incubated with 1 mM ATP, then radioactively labeled 6C RNA was added, and the mixture was incubated for 10 min.

3.7 Effect of 6C RNA on amino acid production in *C. glutamicum*

C. glutamicum has a very high biotechnological relevance. However, the potential impact of sRNAs on production was not considered, yet. It was speculated that 6C RNA could be involved in a kind of metabolic slow-down response (Swiercz*, et al.*, 2008). Therefore, in the course of this work the influence of 6C RNA overexpression on amino acid synthesis by L-lysine and L-leucine/ L-valine production strains of *C. glutamicum* was tested. Moreover, ethambutol (EMB)-induced L-glutamate efflux into the supernatant was analysed for *C. glutamicum*/pJC1-6C in comparison to the wild type empty vector control. L-glutamate efflux can be triggered, among others, by the addition of the antituberculosis drug EMB (Radmacher*, et al.*, 2005), which inhibits arabinogalactan synthesis (Takayama & Kilburn, 1989). The 6C RNA overexpression strain reached only about 10% of the final OD_{600} of the *C. glutamicum* empty vector control (4.2 ± 0.6 *vs*. 41.1 ± 2.5) and the specific L-glutamate concentration in the supernatant of *C. glutamicum*/pJC1-6C was increased (5.55 ± 1.29 *vs*. 1.31 ± 1.85 mM). Thus, *C. glutamicum*/pJC1-6C showed a strongly increased sensitivity towards EMB. The cells doubled only once and then ceased to grow (see in the appendix Figure A 8). Notably, *C. glutamicum*/pJC1-6C cells have a different cell morphology compared to the empty vector control in the presence of EMB (Figure 25). It was already

published that the exposure to EMB causes alterations of the cell morphology, as *C. glutamicum* wild-type cells were more coccoid in their shape (Radmacher*, et al.*, 2005). This could also be observed in this experiment (Figure 25 A and B). The cells overexpressing the 6C RNA also decreased in length, but still were twice as large as the reference strain. Moreover, the cell morphology appeared very irregular. It was suggested that the 6C RNA could be involved in cell division and/or cell wall synthesis in *C. glutamicum*, as indicated by an elongated and branched morphology (see 3.4). If an increased 6C RNA level indeed disturbs cell division and/or cell wall synthesis, it could explain the dramatically increased sensitivity to EMB, which inhibits the cell wall arabinogalactan synthesis, and which finally leads to a complete growth delay of *C. glutamicum*/pJC1-6C in the presence of EMB (see Appendix Figure A 8 A).

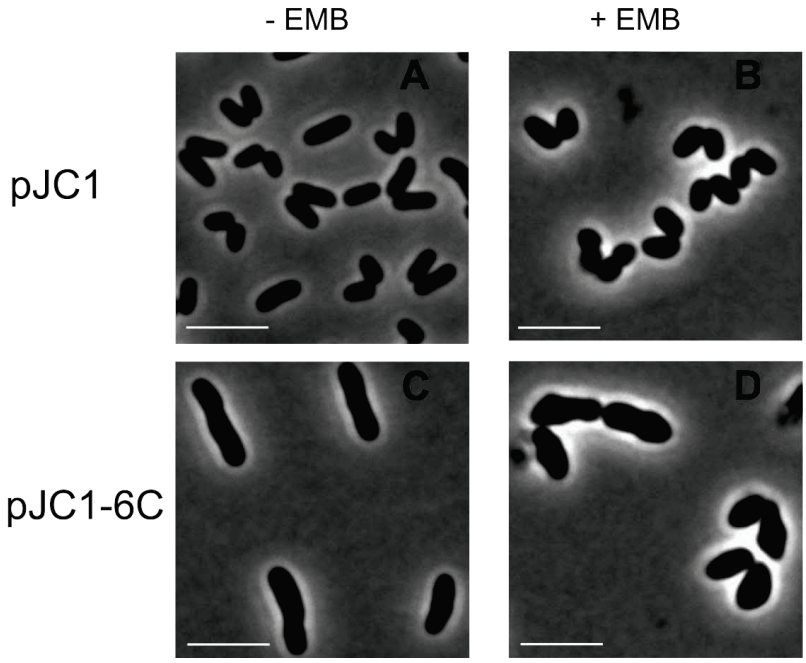

Figure 25 Microscopic images of *C. glutamicum*/pJC1 (A and B) and *C. glutamicum*/pJC1-6C (C and D). Strains were cultivated at 30°C and 120 rpm in CGXII medium with 4% (w/v) glucose and 25 µg ml^{-1} kanamycin without (A and C) or with 500 µg ml^{-1} ethambutol (B and D). Images were taken after 5 h of cultivation. The white scale bar is 5 µm in length.

Overall, it could be observed that an increased 6C RNA level always seems to have a negative effect on growth of *C. glutamicum* in glucose minimal medium (see Appendix Figure A 8 A).

An increased biomass-specifc production of amino acids in the tested producer strains, namely the L-lysine producer *C. glutamicum* DM1800 (Georgi*, et al.*, 2005) and the

L-leucine producer *C. glutamicum* MV-ValLeu33, which also accumulates L-valine as by-product (Vogt*, et al.*, 2014), could be measured. It was observed that the biomass-specific production of L-lysine was higher in *C. glutamicum* DM1800/pJC1-6C compared to the empty vector control (Table 16). The L-leucine producer *C. glutamicum* MV-ValLeu33/pJC1-6C produced more L-leucine and less L-valine after 48 h of cultivation (Table 16). These results indicate that an increased level of 6C RNA, probably by slowed-down growth and reduced biomass formation, has a positive effect on product formation, but the underlying mechanisms need to be elucidated. An improved export of amino acids can lead to higher productivity, as shown for example for L-isoleucine production (Xie*, et al.*, 2012). The potential effect of the 6C RNA overexpression on the cell wall composition could possibly have a positive influence on the export of amino acids.

Table 16 Final OD_{600}, amino acid concentration and biomass-specific amino acid concentration in the supernatants of *C. glutamicum* strains DM1800/pJC1-6C and MV-ValLeu33/pJC1-6C and the corresponding empty vector controls after 48 h of cultivation. Average values and standard deviations of three independent experiments in CGXII medium with 4% (w/v) glucose and 25 µg ml^{-1} kanamycin are shown.

Strain	OD_{600}	Amino acid concentration (mM)	Biomass-specific production (mmol (g CDW)$^{-1}$)
		Lysine	
DM1800/pJC1	44.47 ± 5.26	23.8 ± 0.9	2.5 ± 0.0
DM1800/pJC1-6C	31.33 ± 5.20	23.9 ± 1.9	3.6 ± 0.4
		Leucine	
MV-ValLeu33/pJC1	38.87 ± 9.24	34.5 ± 3.0	4.4 ± 0.1
MV-ValLeu33/pJC1-6C	33.07 ± 8.29	42.9 ± 2.3	6.3 ± 0.2
		Valine	
MV-ValLeu33/pJC1	38.87 ± 9.24	21.8 ± 0.9	2.8 ± 0.3
MV-ValLeu33/pJC1-6C	33.07 ± 8.29	6.0 ± 0.8	0.89 ± 0.2

4 Discussion

4.1 The 6C RNA is an abundant and very stable sRNA in *C. glutamicum*

In this study the 6C RNA of *C. glutamicum* was characterized. Northern blot analysis revealed that the 6C RNA is present throughout growth. The determination of 6C RNA levels in *C. glutamicum* revealed about 325 molecules per cell in the exponential phase and about 260 molecules per cell in the stationary phase. These levels are similar to those of some other sRNAs, for example the SR1 of *B. subtilis,* which is involved in the regulation of arginine catabolism (Heidrich*, et al.*, 2006). Like some other sRNAs, the SR1 of *B. subtilis* is abundant in the cell and expressed in a growth phase-dependent manner. The amount of SR1 within one *B. subtilis* cell was calculated to be about 20 molecules in the exponential phase and 200–250 molecules in the stationary phase (Heidrich*, et al.*, 2007). The levels of 6S RNA from *E. coli* were estimated to change from 1,000 to 10,000 copies per cell during the transition from the exponential to the stationary phase (Wassarman & Storz, 2000). In contrast to SR1 and 6S RNA, the 6C RNA of *C. glutamicum* is present constitutively throughout all growth phases under standard conditions, exhibiting RNA level changes not greater than two-fold. The amount of 6C RNA per cell is much lower than the amount determined for 6S RNA of *E. coli* (see above) and, for example, the 4,500 molecules measured for OxyS of *E. coli* under oxidative stress conditions (Altuvia*, et al.*, 1997). However, in comparison to the levels of individual mRNAs, which were estimated in to be in the range of 0.05 to 5 copies per cell (Taniguchi*, et al.*, 2010, Maier*, et al.*, 2011), the 6C RNA is highly abundant.

RNA -decay analysis using rifampicin revealed that the 6C RNA is very stable with a half-life of ≥ 120 min. The stability of different sRNAs varies. Many of them have a half-life in the range of less than one hour: for the OyxS RNA of *E. coli* strain-dependent half-lifes between 12 and 30 min were determined (Altuvia*, et al.*, 1997). For RsaA and RsaH of *S. aureus* half-lives greater 60 min were determined (Geissmann*, et al.*, 2009). However, the half-life determined for the 6C RNA exceeded the data published so far by a factor of two or more. Reasons for the high stability of the 6C RNA could be its secondary structure containing two prominent stem-loops and one minor stem-loop (see also 1.3) and/or the possible binding to protein. In general, stem-loop structures stabilize RNA folding and can also protect from degradation by RNases. Most natural antisense RNAs display a high degree of secondary structure with stem-loops as their most prominent feature (Hjalt & Wagner, 1992). In *S. coelicolo*r and *M. tuberculosis* stems with C-rich loops within the sRNA structure were found (Arnvig & Young, 2009, Vockenhuber*, et al.*, 2011). These are assumed to act as alternative termination structures to known Rho-independent termination (Pánek*, et al.*, 2008). Also other sRNAs like RsaE of *S. aureus* and *B. subtilis* have C-rich sequences (Geissmann*, et al.*, 2009, Bohn*, et al.*, 2010). In *S. aureus,* for example, these act as an

initial binding site to the mRNA target (Boisset*, et al.*, 2007). If a C-rich loop yields enough target specificity in a high-GC organism, remains to be experimentally validated.

The abundance of the 6C RNA possibly indicates interaction with several mRNA and/or protein targets. Although the 6C RNA is very stable and present in high amounts, it is not essential for *C. glutamicum*, as its gene can be deleted without problems. No growth phenotype of the ∆6C mutant was observed under standard cultivation conditions compared to the wild type, indicating a physiological role under particular conditions.

4.2 The potential role of the 6C RNA under SOS response-inducing conditions

In bacteria many sRNAs are involved in stress responses, e.g. to iron limitation (RyhB) (Geissmann & Touati, 2004, Massé*, et al.*, 2005), oxidative stress (OxyS) (Altuvia*, et al.*, 1998), sugar-phosphate stress (SgrS) (Vanderpool & Gottesman, 2004, Kawamoto*, et al.*, 2005), acid stress (GadY) (Tramonti*, et al.*, 2008) or temperature stress (DsrA) (Sledjeski*, et al.*, 1996). In this study a global screening for the growth behaviour of the ∆6CiP mutant during cultivation with different carbon sources and under different stress conditions revealed no phenotype except when cultivated with mitomycin C (MMC). The ∆6CiP mutant showed a higher sensitivity to MMC than the parental strain. MMC is an antibiotic agent that covalently cross-links complementary DNA strands, and thereby leads to the induction of the SOS response in bacteria (Tomasz, 1995, Movahedzadeh*, et al.*, 1997). Therefore, the 6C RNA of *C. glutamicum* could be involved in the SOS response.

In *E. coli* the SOS response system, which is an inducible DNA repair system, has been studied intensively (Little & Mount, 1982, Markham*, et al.*, 1984, Friedberg, 1995). In the case of DNA damage, RecA is activated and leads to the autocleavage of LexA and thereby to a derepression of SOS genes (Figure 26).

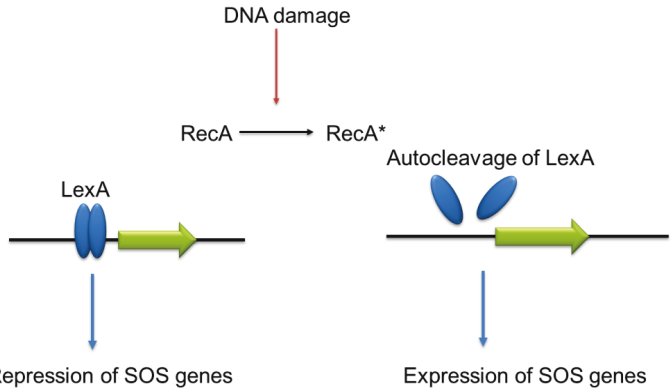

Figure 26 Schematic overview of the SOS response in *E. coli*. The SOS response is triggered by the DNA damage-induced conversion of the recombinase A (RecA) into its activated state, RecA*, which serves as co-protease to stimulate the autocleavage of the LexA repressor (Little, 1991). The autocleavage of LexA generates two polypeptides, thereby preventing DNA binding of LexA and enabling derepression of the SOS response-regulon.

In *M. tuberculosis recA* and *lexA* homologs have been identified and the LexA regulon has been determined (Davis*, et al.*, 1991, Durbach*, et al.*, 1997, Movahedzadeh*, et al.*, 1997, Davis*, et al.*, 2002). However, in *M. tuberculosis* many of the DNA repair genes have been shown to be DNA-damage-inducible in a LexA/RecA-independent manner, revealing the existence of an overlapping stress response system in mycobacteria (Brooks*, et al.*, 2001, Rand*, et al.*, 2003). Homologs of the transcriptional regulator LexA, which is the key component of the SOS repair pathway, and RecA, which is a key component in DNA repair and recombination, are also present in *C. glutamicum*. The *C. glutamicum* LexA regulon was already deduced from comparative transcriptomics and band shift assays (Jochmann*, et al.*, 2009). Overall, the expression of 48 genes was found to be controlled by LexA, many of unknown function (Jochmann*, et al.*, 2009). DNA inspection revealed a potential LexA-binding site also in front of the 6C RNA gene and in DNA affinity chromatography experiments LexA was enriched with the 6C RNA promoter region (see 3.1.3). This indicates that the 6C RNA may indeed be involved in the SOS response of *C. glutamicum*. However, further studies are required to confirm a direct influence of LexA on 6C RNA expression, e.g. by showing the in vitro binding of purified LexA to the 6C RNA promoter region and by analysing the 6C RNA level in a Δ*lexA* deletion mutant.

Microscopic analysis of the *C. glutamicum* wild type and the Δ6CiP mutant revealed that both MMC-treated strains have an elongated cell morphology compared to untreated cells. This cell elongation following DNA damage is due to DivS-dependent suppression of cell division in *C. glutamicum* (Ogino*, et al.*, 2008). No significant differences between the morphology of the deletion mutant and the wild type could be observed, neither under

standard growth conditions nor under SOS response-inducing conditions. This indicates that the differences in the OD_{600} measurement are not caused by a different cell morphology.

Notably, although the ∆6CiP mutant showed a growth phenotype under SOS response-inducing conditions, the majority of genes of the LexA regulon, i.e. *lexA, recA*, *divS, recN,* and *dnaE2* (Jochmann*, et al.*, 2009) had no significantly altered mRNA ratio. This indicates that the mRNA level of these genes in the ∆6CiP mutant was similar to that in the wild type in the exponential growth phase, or at least at the time point of growth at which the samples were harvested for the transcriptome analysis. It has to be considered that the transcriptome analysis is restricted to one defined time point during growth and only gives results for that restricted time point, a kind of “snap shot” of the mRNA level. Furthermore, it cannot be excluded that the 6C RNA (i) plays a time/growth-dependent role in the SOS response on the transcriptional level and (ii) might act on the translational level or protein activity, which might lead to the altered growth behaviour of the ∆6CiP mutant in the presence of MMC. The 6C RNA level should be investigated in the presence of MMC and compared to the level in the absence of MMC by Northern blot analysis to see if the 6C RNA level exhibits SOS response-dependent changes.

To investigate the potential role of the 6C RNA in the SOS response in *C. glutamicum* in more detail, experiments with LexA-regulated promoters of four different genes were performed (*cglIM*, *dnaE2*, *recA* and *recN*) using E2-crimson as reporter. For all of these genes a binding of LexA was shown by DNA band shift assays (Jochmann*, et al.*, 2009). CglIM was identified to be responsible for the methylation of cytosine residues in DNA (Schäfer*, et al.*, 1997) and belongs to a restriction modification system (CglIM, CglIR, and CglIIM) of *C. glutamicum*. The *dnaE2* gene encodes for a protein which is a paralogue of the major replicative DNA polymerase subunit DnaE. The homologous DnaE2 protein of *M. tuberculosis* is also regulated by LexA (Davis*, et al.*, 2002) and is postulated to participate in error-prone DNA repair synthesis, resulting in SOS-induced mutagenesis (Boshoff*, et al.*, 2003) and *recN* encodes for a DNA repair protein.

The ∆6CiP mutant revealed a reduced E2-crimson fluorescence output for all tested promoters in the stationary phase, indicating that the SOS response level in the ∆6CiP mutant is lower compared to the wild type in the stationary phase. A possible reason for this result could be that the 6C RNA positively affects the mRNA of the SOS response genes with respect to stability or translation when cells enter the stationary phase, which is the time period of growth when the ∆6CiP mutant slows down growth and enters the observed plateau phase. The absence of the 6C RNA would then lead to less stable mRNA of the SOS response genes and possibly to mRNA degradation. A global transcriptome analysis should be performed with total RNA samples of the ∆6CiP mutant and the wild type in the stationary phase, to see whether the mRNA levels of the SOS response genes are decreased in the

∆6CiP mutant. In any case, a time/growth-dependent decrease of the promoter activity of all tested promoters would likely lead to a deficiency of the cells to cope with the SOS response-induced DNA repair.

Another reason for the growth phenotype of the ∆6CiP mutant under SOS response-inducing conditions could be an impaired sulfur metabolism. Sulfur is essential for microbial growth because it is a constituent of e.g. cysteine, methionine, iron-sulfur proteins, coenzyme A, mycothiol, biotin and tRNAs (Rückert & Kalinowski, 2008).The genes of the *cys*-operon are known to be responsible for the reduction of sulfate and sulfite to sulfide. In the ∆6CiP mutant all genes of the *cys*-operon had a decreased mRNA level, which could indicate that the 6C RNA stabilizes the mRNA of these genes. The cysteine-derived compound mycothiol was demonstrated to protect against alkylating agents, like certain antibiotics (Rawat*, et al.*, 2002). MMC can be regarded as such an alkylating agent because it crosslinks DNA and this is accomplished by reductive activation followed by two N-alkylations. Both alkylations are sequence specific for a guanine nucleoside in the sequence 5'-CpG-3' (Tomasz, 1995). So it can be suggested that an imbalance in the sulfur metabolism and the resulting imbalance of sulfur-containing compounds, such as mycothiol, could indeed lead to an increased sensitivity against alkylating agents like MMC, which could explain the retarded growth of the ∆6CiP mutant.

One example for a bacterial sRNA involved in the SOS response is IstR-1 (inhibitor of SOS-induced toxicity by RNA) of *E. coli*, which is about 75 nt in size (Vogel*, et al.*, 2004). In the abscence of the SOS response IstR-1 inhibits the synthesis of an SOS-induced toxic peptide, namely TisB. Base-pairing of IstR-1 to *tisAB* mRNA enables RNase III-dependent cleavage, thereby inactivating the mRNA for translation. SOS-induced *tisAB* mRNA gradually accumulates over IstR-1 resulting in toxic TisB expression which possibly is still limited by IstR-1 (Vogel*, et al.*, 2004) (Figure 27). It is suggested that the inhibitory sRNA IstR-1 prevents inadvertent TisB synthesis during normal growth and, possibly, also limits SOS response-induced toxicity.

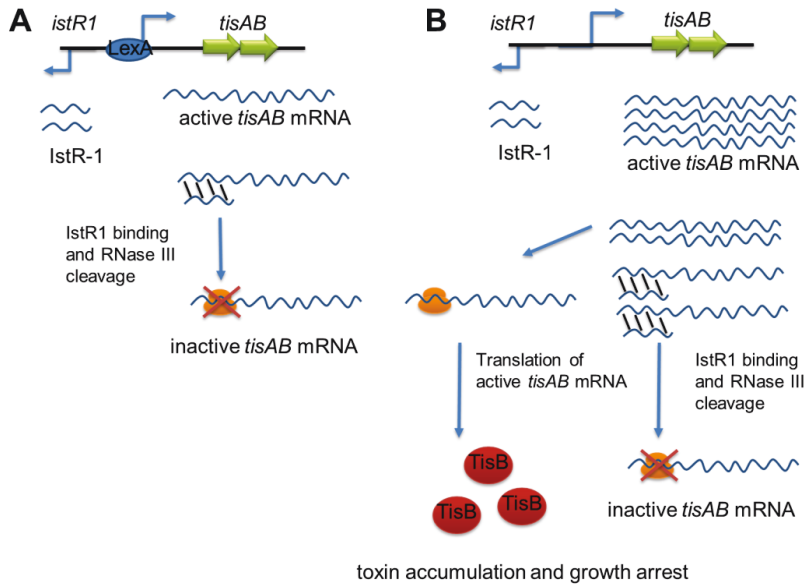

Figure 27 Model of IstR-1 dependent *tisAB* expression. (A) The IstR-1 is constitutively expressed in *E. coli* throughout growth. The divergently orientated bicistronic *tisAB* (toxicity -induced by SOS) operon was shown to be controlled by LexA. Under noninducing conditions IstR-1 is present in high excess over its target, *tisAB* mRNA, which is present only in low levels due to the incomplete repression of LexA. IstR-1 base pairs within a 23 bp region of the *tisAB* mRNA and entails RNaseIII-dependent cleavage, thus inhibiting translation. **(B)** Under SOS response-inducing conditions the transcription of *tisAB* is induced and *tisAB* mRNA level increases, whereas IstR-1 level remains almost constant. The increase of *tisAB* mRNA results in an almost complete cleavage of IstR-1 due RNaseIII-dependent cleavage upon binding and the *tisAB* mRNA can gradually accumulate. Under these conditions the toxic peptide is formed and exerts its effect and slows down growth. Image modified from Vogel*, et al.*, 2004.

Based on this model one could speculate whether 6C RNA might repress the expression of a yet unknown toxic peptide in *C .glutamicum* under SOS-induced conditions. The absence of the 6C RNA could lead to a gradual accumulation of such a peptide which results in the temporary growth arrest of the ∆6CiP mutant in the presence of MMC. If so, global transcriptome analysis of the ∆6CiP mutant when it slows down growth and enters the growth arrest phase could help to identify such a putative gene for a toxic peptide. During this time the mRNA level of the "toxic peptide" should be increased, if there is a similar system as observed for IstR-1/*tisAB* mRNA of *E. coli*. However, toxins have not yet been identified in *C. glutamicum*. A LC-MS-based global proteome analysis should also help to identify increased peptide levels of such a "toxic peptide" in *C. glutamicum* under SOS response-inducing conditions.

Global gene expression analysis by DNA microarrays revealed that overall ten genes exhibited an altered mRNA level in the ∆6C mutant independent of the presence or absence of MMC. In this group cg2633 and cg1255 are the genes with the highest increased

mRNA level in the ∆6CiP mutant when cultivated with MMC (10-fold and 4-fold, respectively) and also had an increased mRNA level (4-fold and 3-fold, respectively) under standard conditions. Both genes code for proteins involved in DNA repair, namely a putative restriction endonuclease and a HNH endonuclease. Cg1255 was reported to be part of the *C. glutamicum* LexA regulon (Jochmann*, et al.*, 2009). The increased mRNA levels could indicate that the genes are less repressed in the ∆6C mutant independent of an SOS-induced state. A destabilizing effect on the mRNAs upon binding of the 6C RNA could fine-tune expression and possibly prevent an overexpression of these genes, which in turn could have an adverse effect in the cell under SOS stress. Thus, the possible regulatory role of the 6C RNA in the SOS response could be more versatile.

Moreover, the group of genes exhibiting an altered mRNA level independent of MMC contains *cgmR* encoding a multidrug resistance-related transcription factor of the TetR-family. The *cgmR* gene exhibited a five-fold decreased mRNA level in the ∆6CiP mutant, both in the absence and in the presence of MMC. The upstream gene of *cgmR,* cg2893, which encodes a multidrug efflux permease, also exhibited a decreased mRNA ratio under standard growth conditions. CgmR was reported to function as a transcriptional repressor responsible for the antimicrobial resistance system and of the upstream gene cg2893 (Itou*, et al.*, 2005). The decreased mRNA level of this multidrug resistance-related transcription factor could be involved in the increased sensitivity against the antibiotic MMC. Whether the 6C RNA is directly or indirectly involved in the regulation of *cgmR* in *C. glutamicum* remains to be elucidated and is an interesting target for further studies.

Finally, the question comes up why sRNAs shoud be recruited to be regulators in the SOS response or in a stress response at all. One hypothesis is that the relatively low input of energy and the short time required to synthesize sRNAs make them ideal regulators of rapid responses to changing environmental conditions. Secondly, the ability of sRNAs to act at posttranscriptional levels provides greater regulatory flexibility by permitting the repression or activation of genes that have already been transcribed (Altuvia*, et al.*, 1997).

4.3 Potential mRNA targets of the 6C RNA

Beside a potential role of the 6C RNA in the SOS response, global transcriptome analysis gave first hints that the 6C RNA may also be responsible for the regulation of some other genes which are not related to the SOS response. For example the gene with the strongest increased mRNA level (9-fold) in the *C. glutamicum* ∆6C mutant under standard cultivation conditions was *sprA* (cg0665). The serine protease SprA was recently identified as an interacting partner of GlxR and preferentially functions in the exponential phase. Purified His_6-SprA protein underwent self-proteolysis and also proteolyzed purified GlxR, the

latter one presumably only in the absence of its ligand cAMP (Hong*, et al.*, 2014). In addition, the self-proteolytic activity of SprA suggests that the immediate and timely removal of SprA is also important to ensure precise regulatory control (Hong*, et al.*, 2014). It was also published that GlxR binds to the 6C RNA promotor region. However, the relevance of this finding remains to be elucidated (Jungwirth*, et al.*, 2012). It is suggested that SprA performs a novel regulatory role, not only in GlxR-mediated gene expression, but also in other areas of cell physiology, since in an *sprA*-overexpression strain proteins involved in diverse cellular functions such as energy and carbon metabolism, nitrogen metabolism, methylation reactions, and peptidoglycan biosynthesis, were affected and showed decreased transcription (Hong*, et al.*, 2014). Whether the 6C RNA directly or indirectly influences the mRNA level of *sprA* and thereby perhaps influences GlxR-mediated gene expression or other processes in *C. glutamicum* is not clear yet. However, if the 6C RNA is involved in GlxR-mediated regulation processes, it might be expected that the 6C RNA deletion would lead to a growth phenotype. Nevertheless, sRNAs are involved in fine-tuning processes and their deletion or overexpression often does not lead to a severe phenotype.

Another gene which showed an increased mRNA ratio (3-fold) in the ∆6C mutant under standard cultivation conditions was cg2922, encoding a putative transcriptional regulator of the IclR-family. Members of the IclR-family act as repressors, activators and proteins with a dual role (Molina-Henares*, et al.*, 2006). The genes controlled by IclR-type regulators are very diverse and involved for example in multidrug resistance, degradation of aromatics, inactivation of quorum-sensing signals, or sporulation (Molina-Henares*, et al.*, 2006). One example for a member of this regulator family is SsgR, which activates *ssgA,* a gene that plays an important role in sporulation-specific cell division and morphogenesis of *S. coelicolor* (Traag*, et al.*, 2004). Notably, cg2922 had a decreased mRNA level in the strain *C. glutamicum*/pJC1-6C in the presence of MMC, which had a branched morphology. Thus, cg2922 could also be a candidate mRNA target of the 6C RNA, since cg2922 mRNA levels showed an opposing trend depending on the 6C RNA level. In *C. glutamicum* cg2922 has not been characterized so far and is predicted to be located in an operon together with cg2923-cg2929 (Pfeifer-Sancar*, et al.*, 2013). However, none of the other genes of this putative operon showed an altered mRNA ratio, neither in the transcriptome comparison of *C. glutamicum*/pJC1-6C and *C. glutamicum*/pJC1 nor in the transcriptome comparison of the ∆6C mutant and the wild type. Therefore, it could be suggested that the the transcription of the genes terminates before all genes are transcribed, or that the genes in the predicted operon are transcribed from a separate promoter and if so, it could be that the mRNAs have a different stability. Nevertheless, the context of 6C RNA and cg2922 requires further investigation.

A transcriptome analysis was performed in which the genome-wide mRNA levels of the strain *C. glutamicum*/pJC1-6C and *C. glutamicum*/pJC1 in the absence and in the presence of MMC were compared. The global gene expression changes in response to 6C RNA overexpression (*C. glutamicum*/pJC1-6C) were determined to get further hints regarding potential mRNA targets of the 6C RNA. Under SOS response-inducing conditions by addition of MMC over 90% of the CGP3 prophage genes exhibited decreased mRNA levels in the 6C RNA overexpression strain. In *C. glutamicum* CGP3 prophage gene expression is induced by the addition of MMC in a time-dependent manner (PhD thesis Antonia Heyer, 2013). It seems that the CGP3 prophage genes are less induced by MMC in the *C. glutamicum*/pJC1-6C. The prophage CGP3 makes up ~ 6% of the *C. glutamicum* ATCC 13032 genome covering the genes from cg1890 to cg2071 (Frunzke*, et al.*, 2008). It was already reported from cases in which genes within the CGP3 region exhibited increased mRNA levels due to an increased phage copy number, i.e. in the *dtxR* deletion mutant, which lacks the master regulator DtxR for iron homeostasis (Wennerhold & Bott, 2006, Frunzke*, et al.*, 2008). The phage copy number should be determined in *C. glutamicum*/pJC1-6C under SOS response-inducing to investigate if it is decreased.

Two genes had a decreased mRNA level in *C. glutamicum*/pJC1-6C, independent of MMC, namely *whcD* and *mraW. WhcD* is discussed in more detail below. *MraW* is located within the *dcw* (division cell wall) cluster, which comprises cell division- and cell wall-related genes and is transcribed as part of a polycistronic mRNA, which includes at least *mraZ, mraW, cg2376 (ftsL), ftsI* and *murE*, from a promoter that is located upstream of *mraZ* (Valbuena*, et al.*, 2006, Letek*, et al.*, 2008). Cell division in *C. glutamicum* is different from that of other bacteria, not only because of the absence of homologues of spatial and temporal regulators of cell division, like the FtsZ-interacting protein FtsA (reviewed in (Letek*, et al.*, 2008, Donovan & Bramkamp, 2014). *C. glutamicum* lacks MreB, which is required in most rod-shaped bacteria, like *E. coli* or *B. subtilis*, for proper cell elongation/cell division (Wachi & Matsuhashi, 1989, Levin*, et al.*, 1992). MreB assembles into wire-like structures along the cell that support elongation of the lateral cell wall. In contrast, *Corynebacterium* as well as *Streptomyces* species were found to elongate in an MreB-independent manner by peptidoglycan synthesis at the cell poles (Daniel & Errington, 2003).

In *C. glutamicum*/pJC1-6C the *mraW* mRNA level was decreased under standard conditions and was even more decreased in the presence of MMC as the morphology of the cells changes more dramatically. The genes *murE* and *ftsI* coding for UDP-N-acetylmuramoyl-L-alanyl-D-glutamate:meso-diaminopimelate ligase and penicillin-binding protein 3 (PBP3), respectively, are both involved in peptidoglycan synthesis and were reported to be essential for *C. glutamicum* (Wijayarathna*, et al.*, 2001). They also had a decreased mRNA level (ratios of 0.48 and 0.38, respectively) in strain *C. glutamicum*/pJC1-

6C in the presence of MMC. This could be a reason for the altered cell morphology of the 6C RNA overexpression strain and as well for the assumed damage to the cell membrane and/or the cell wall.

Finally, it can be concluded that the 6C RNA might play a role in cell division and/or cell wall metabolism of *C. glutmicum*, which would add a new level of complexity to the outstanding cell division process.

4.3.1 The downstream genes of the 6C RNA (cg0362 to cg0369)

Downstream of the 6C RNA a putative cell divison-related gene is located, namely cg0362 encoding a putative septum site-determining protein, in a putative operon (cg0362-cg0369). The genes cg0362–cg0369 are highly conserved among actinobacteria (Figure 28). This indicates that the genes most likely encode for proteins with a central function in many actinobacteria. Notably, these genes exhibited an increased mRNA level in the ∆6C mutant. This observation could have several reasons. One possibility would be that the 6C RNA triggers the degradation of the mRNA of the downstream genes by some mechanism. For the 6C RNA a promoter which is recognised by the primary sigma factor σ^A was identified from RNA sequencing data (Pfeifer-Sancar*, et al.*, 2013), whereas for the downstream genes no σ^A -dependent promoter could be found. So it remains to be identified whether an alternative sigma factor-dependent promoter is present in front of the downstream genes of the 6C RNA. Possibly, the increased level of the downstream genes could also be due to a read-through from the 6C RNA promoter. However, a read-through can rather be excluded because in the ∆6CiP mutant variant, which lacks not only the conserved motif but also the 6C RNA promoter sequence, the mRNA levels of the genes were still increased.

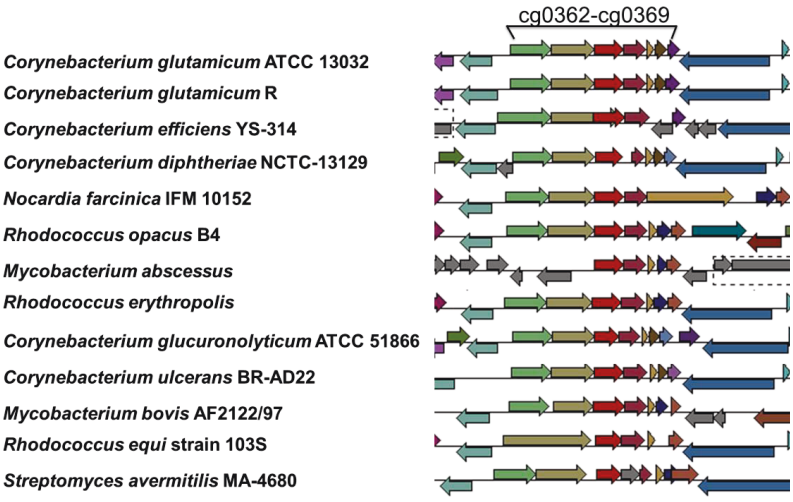

Figure 28 Genomic organisation of the genes cg0362-cg0369 in different actinobacteria.

So far the genes cg0362-cg0369 have not been characterized in *C. glutamicum*. Characterization of a ΔOP_cg0362 mutant (see 3.5.2) showed that the genes cg0362-cg0369 are not essential for *C. glutamicum* and that their absence does not lead to a growth phenotype, neither under standard conditions nor in the presence of MMC (see 3.5.2). Moreover, cg0362 seems not to play a crucial role in septum site determination under the conditions tested, since no alterations in septum formation or septum placement could be observed for the ΔOP_cg0362 deletion mutant. If the 6C RNA is assumed to pair with the mRNA of its downstream genes, resulting in mRNA degradation, it would be expected that the mRNA level of the downstream genes in the 6C RNA overexpression strain is decreased. However, this was not the case. This could be due to the detection limit of the DNA microarray. The mRNA level of these genes in the wild type is already very low, so that a further decrease might be hardly detectable. Nevertheless, a potential regulatory function of the 6C RNA on its downstream genes, for example as a kind of attenuator, cannot be excluded so far. To analyse the function of the genes from cg0362 to cg0369 and the possible connection to the 6C RNA further experimental effort is needed.

4.3.2 The WhcD regulator of *C. glutamicum*

Another potential target of the 6C RNA identified during this study is *whcD*. Its expression level was significantly decreased in *C. glutamicum*/pJC1-6C overexpressing the 6C RNA, in the absence as well as in the presence of MMC, indicating that the 6C RNA could trigger the degradation of the mRNA of *whcD* by some mechanism, independently from the SOS response. All organisms that belong to the Actinomycetales apparently possess

whiB-like genes that function in diverse cellular processes, including cell division, differentiation, pathogenesis, starvation survival, and stress responses (Hutter & Dick, 1999, Gomez & Bishai, 2000, Molle*, et al.*, 2000, Geiman*, et al.*, 2006, Raghunand & Bishai, 2006, Smith*, et al.*, 2012). *C. glutamicum* possesses overall four *whiB*-like genes annotated as *whcE (whiB1), whcD (whiB2), whcB (whiB3),* and *whcA (whiB4). WhcD* transcription was published to be rather low and constitutive during all growth phases, whereas the other *whc* genes are preferentially transcribed during the stationary phase (Kim*, et al.*, 2005, Choi*, et al.*, 2009, Lee*, et al.*, 2012, Lee*, et al.*, 2013). Except for *whcD*, the *whc* genes have already been intensively studied in *C. glutamicum*. The *whcE* gene plays a positive role in survival of cells exposed to oxidative and heat stress (Kim*, et al.*, 2005), whereas the *whcA* gene plays a negative role in the expression of genes responding to oxidative stress (Choi*, et al.*, 2009). The *whcB* gene plays a regulatory role during stationary phase growth, particularly in electron transfer reactions (Lee*, et al.*, 2012). However, the *whcD* gene was not characterized in *C. glutamicum* so far. Notably, WhcD showed 88% sequence identity to WhmD of *M. smegmatis*. *M. smegmatis whmD* gene is an essential mycobacterial gene required for proper septation and cell division (Gomez & Bishai, 2000). In *M. smegmatis* the chromosomal *whmD* gene could be disrupted only in the presence of a plasmid-borne *whmD* copy. A plasmid that allowed chemically regulated expression of the WhmD protein was used to generate a conditional *whmD* mutant. On withdrawal of the inducer, the conditional whmD mutant exhibited filamentous, branched cell growth with diminished septum formation and aberrant septal placement, whereas *whmD* overexpression resulted in growth retardation and hyperseptation (Gomez & Bishai, 2000). It has been shown that *M. smegmatis whmD* and its homologue *whiB2* in *M. tuberculosis* are functionally equivalent (Raghunand & Bishai, 2006). Comparable to the findings in *M. smegmatis*, a decreased mRNA level of *whcD* in *C. glutamicum*/pJC1-6C could lead to an altered septum formation, which in turn could explain the changed cell morphology of *C. glutamicum*/pJC1-6C in the absence as well in the presence of MMC. Indeed, a Δ*whcD* mutant of *C. glutamicum* showed an altered morphology resembling the one of *C. glutamicum*/pJC1-6C in the presence of MMC (see 3.4.1). These results show that WhcD of *C. glutamicum* and WhmD of *M. smegmatis* indeed seem to have a comparable physiological relevance in some aspects of cell division/cell septation for both actinobacteria.

The regulon of WhmD of *M. smegmatis* was not published yet. First attempts to identify the regulon of WhcD in *C. glutamicum* were performed in this study by global transcriptome analysis using a Δ*whcD* mutant. It appears that WhcD of *C. glutamicum* seems to regulate mainly genes involved in cell division, namely *mraW* and *mraZ*, as well as in cell wall synthesis, namely *aftB*, *cop1* and cg2077 and cg2199. The cell wall structure of *C. glutamicum* and other corynebacteria and mycobacteria is unique because in addition to a

peptidoglycan layer they contain an outer membrane composed of mycolic acids that is covalently linked to the peptidoglycan via a polysaccharide arabinogalactan network (for review (Hett & Rubin, 2008, Favrot & Ronning, 2012). Cg2077 codes for a putative arabinosyltransferase (Aft) and cg2199 codes for PBP2a, a member of the HMW-PBPs class B, which are suggested to be involved in the cell division process (Valbuena*, et al.*, 2007). Single colonies of the Δ*whcD* mutant appeared less glossy compared to *C. glutamicum* wild type on solid media. Furthermore, the surface of the Δ*whcD* mutant colonies appeared even rough (Figure A 7), suggesting a change in the composition of the cell envelope. Notably, such observations could also be made for a Δ*aftB* deletion mutant of *C. glutamicum* (Seidel*, et al.*, 2007). This result supports the suggestion that *aftB* could be part of the WhcD regulon in *C. glutamicum*.

The next steps in the analysis of the WhcD regulon would be the confirmation of the binding of purified WhcD protein to the promoter regions of the putative target genes via EMSAs and the definition of a consensus binding motif of WhcD.

4.4 3-phosphoglycerate kinase – a candidate protein interaction partner of the 6C RNA

The phosphoglycerate kinase of *C. glutamicum* (PGK_{Cg}), which is a major enzyme in glycolysis, could reproducibly and specifically be eluted with the 6C RNA in RNA pull-down experiments (see 3.6). However, this binding could not be confirmed in RNA band shift assays under the conditions tested. This could indicate that a further factor is required for interaction, which is present in crude extract, but not in the defined EMSA condition. As a protein as additional factor should have been co-purified in the RNA pull-down exeriments, a metabolite as cofactor appears to be more likely. Alternatively, the heterologous overproduction of PGK_{Cg} in *E. coli* could possibly lead to problems in proper protein folding. Therefore, also PGK_{Cg} which was overexpressed in *C. glutamicum* should be used in further EMSAs. Moreover, EMSAs together with the PGK_{Cg} substrate (3-Phosphoglyceric acid) should be performed, to analyse if a substrate-bound state of PGK_{Cg} leads to a binding of the 6C RNA.

Another reason could be that the binding of PGK_{Cg} to the 6C RNA in RNA pull-down experiments is rather unspecific. This assumption is supported by the finding that in RNA-pull down experiments with *E. coli* 6S RNA (provided by Sabine Schneider, HHU Düsseldorf) and protein crude extract of *C. glutamicum* PGK_{Cg} could also be enriched. Moreover, for the 6S RNA and PGK of *E. coli* (PGK_{Ec}) also a complex formation was observed (Dissertation Sabine Schneider, 2014, Research group of Prof. Wagner HHU Düsseldorf). It could be suggested that in the RNA pull-down experiments the 6C RNA *in vitro* transcript does not

have the same secondary structure as *in vivo* and may change its conformation due to the m-periodate oxidation and subsequent binding to the agarose beads. If the secondary structure of the 6C RNA is lost and changed into another form, this could possibly enable or force the binding of PGK_{Cg} to the 6C RNA. In EMSAs the secondary structure of the 6C RNA *in vitro* transcript is possibly more close to the native secondary structure, which includes also double stranded regions, and this could prevent the binding of purified PGK to 6C RNA to some extent.

Additionally, when considering the amount of PGK in the cell (estimated from specific PGK_{Cg} activities in crude extract and from purified enzyme, data not shown) in relation to the amount of 6C RNA molecules, a regulatory role of the 6C RNA on PGK_{Cg} can rather be excluded since PGK_{Cg} appears to be present in much higher amounts than 6C RNA (approximately 230 times more, data not shown). Moreover, no obvious differences in the specific PGK activities were observed in enzyme assays with crude extract of *C. glutamicum* wild type, the Δ6C mutant and the 6C RNA overproducer, indicating that the 6C RNA has no influence on the PGK_{Cg} activity. Alternatively, PGK in excess could be involved in a kind of regulation by conditional binding of the 6C RNAs in a cell, thereby enabling a localization effect to effectively prevent the binding of 6C RNA to other targets. The conditional binding should be triggered by some signal, for example, the presence of the PGK substrate or its product and/or ATP/ADP.

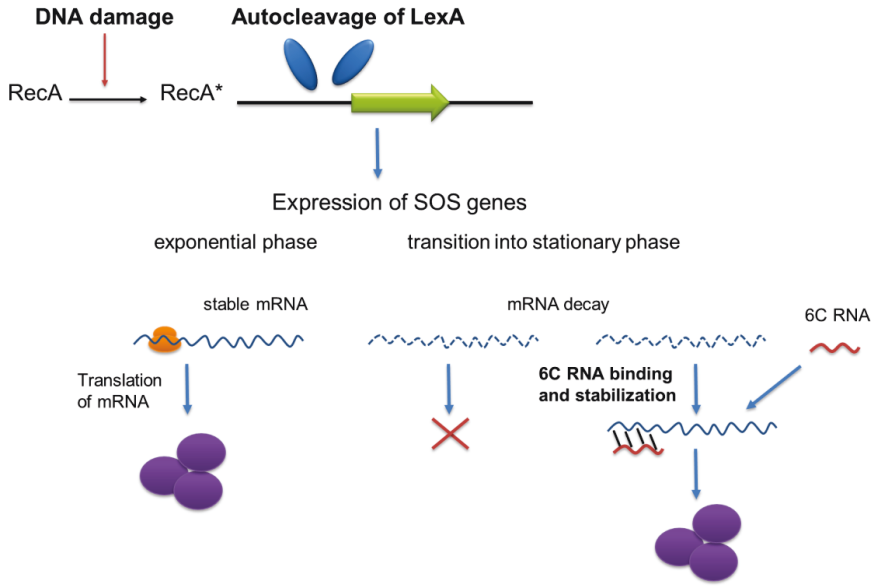

Figure 29 A hypothetical scenario how the 6C RNA could be involved in the fine-tuning/regulation of the SOS response in *C. glutamicum*. Upon DNA damage expression of SOS genes is derepressed by activated autocleavage of LexA. In the exponential phase the mRNAs of the SOS genes underlie a certain turned-over but are newly synthesized thus, enabling translation to some extent. During and after transition into the stationary phase, mRNA synthesis is shut down and mRNA decay increasingly determines the levels of intact, translation-competent mRNAs. In this situation base pairing of 6C RNA to the mRNAs has a stabilizing effect, by which translation of the mRNAs is lasting longer than in the absence of the 6C RNA to support the SOS response.

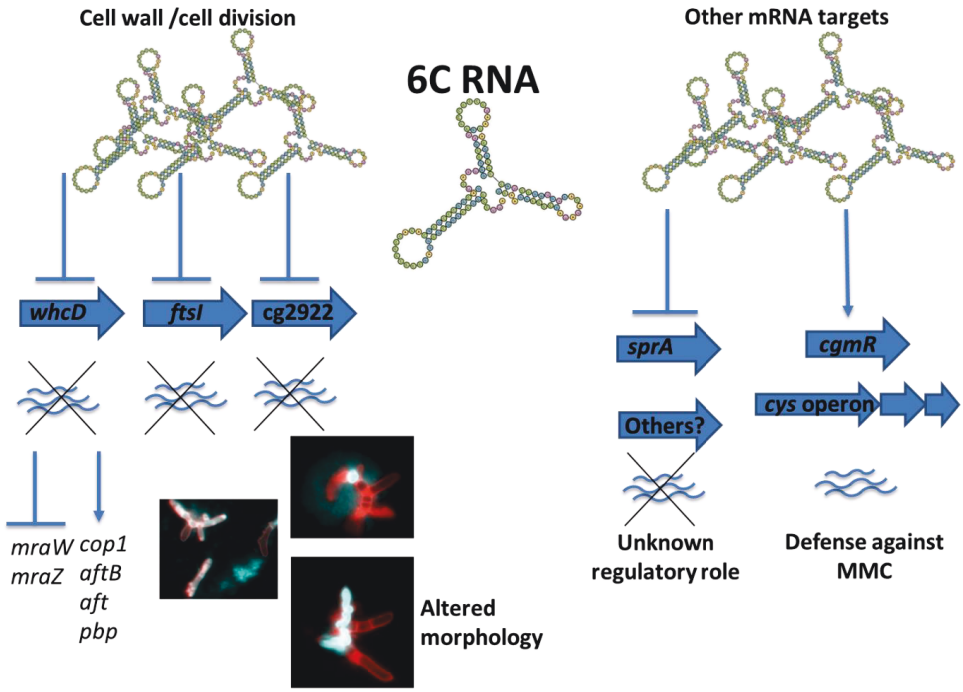

Figure 30 Overview on potential mRNA targets of the 6C RNA in *C. glutamicum*. The 6C RNA might have several mRNA targets, the majority of which are involved in some aspects of cell septation or cell wall synthesis. Thus, it can be speculated that the 6C RNA plays a role in the cell division of *C. glutamicum*, so that altered 6C RNA levels lead to a dramatically altered cell morphology under SOS response-inducing conditions. Beside the potential role in some aspects of cell division, the 6C RNA is suggested to have other mRNA targets of which the regulatory role remains to be elucidated.

Taken together, what is the function of the 6C RNA in *C. glutamicum*? Data of this study led to the assumption that the 6C RNA most probably is involved in some aspects of the SOS repsonse and/or the cell division/cell wall synthesis of *C. glutamicum.* It remains to be studied if the 6C RNA mediates its functions via a base pairing with candidate target mRNAs and whether a hitherto unidentified Hfq-like protein is involved.

5 References

Abe S, Takayama K & Kinoshita S (1967) Taxonomical studies on glutamic acid producing bacteria. *J. Gen. Appl. Microbiol.* **13**: 279-301.

Altuvia S, Weinstein-Fischer D, Zhang A, Postow L & Storz G (1997) A small, stable RNA induced by oxidative stress: role as a pleiotropic regulator and antimutator. *Cell* **90**: 43-53.

Altuvia S, Zhang A, Argaman L, Tiwari A & Storz G (1998) The *Escherichia coli* OxyS regulatory RNA represses *fhlA* translation by blocking ribosome binding. *EMBO J.* **17**: 6069-6075.

Arndt A, Auchter M, Ishige T, Wendisch VF & Eikmanns BJ (2008) Ethanol catabolism in *Corynebacterium glutamicum*. *J. Mol. Microbiol. Biotechnol.* **15**: 222-233.

Arnvig KB & Young DB (2009) Identification of small RNAs in *Mycobacterium tuberculosis*. *Mol. Microbiol.* **73**: 397-408.

Auchter M, Cramer A, Huser A*, et al.* (2011) RamA and RamB are global transcriptional regulators in *Corynebacterium glutamicum* and control genes for enzymes of the central metabolism. *J. Biotechnol.* **154**: 126-139.

Babitzke P, Baker CS & Romeo T (2009) Regulation of translation initiation by RNA binding proteins. *Annu. Rev. Microbiol.* **63**: 27-44.

Barrangou R, Fremaux C, Deveau H*, et al.* (2007) CRISPR provides acquired resistance against viruses in prokaryotes. *Science* **315**: 1709-1712.

Baumgart M, Unthan S, Rückert C*, et al.* (2013) Construction of a prophage-free variant of *Corynebacterium glutamicum* ATCC 13032 for use as a platform strain for basic research and industrial biotechnology. *Appl. Environ. Microbiol.* **79**: 6006-6015.

Beckers G, Strösser J, Hildebrandt U, Kalinowski J, Farwick M, Krämer R & Burkovski A (2005) Regulation of AmtR-controlled gene expression in *Corynebacterium glutamicum*: mechanism and characterization of the AmtR regulon. *Mol. Microbiol.* **58**: 580-595.

Bimboim HC & Doly J (1979) A rapid alkaline extraction procedure for screening recombinant plasmid DNA. *Nucleic acids research* **7**: 1513-1523.

Blombach B, Riester T, Wieschalka S, Ziert C, Youn JW, Wendisch VF & Eikmanns BJ (2011) *Corynebacterium glutamicum* tailored for efficient isobutanol production. *Appl. Environ. Microbiol.* **77**: 3300-3310.

Bohn C, Rigoulay C, Chabelskaya S*, et al.* (2010) Experimental discovery of small RNAs in *Staphylococcus aureus* reveals a riboregulator of central metabolism. *Nucleic Acids Res.* **38**: 6620-6636.

Boisset S, Geissmann T, Huntzinger E*, et al.* (2007) *Staphylococcus aureus* RNAIII coordinately represses the synthesis of virulence factors and the transcription regulator Rot by an antisense mechanism. *Genes Dev.* **21**: 1353-1366.

Boshoff HI, Reed MB, Barry CE, 3rd & Mizrahi V (2003) DnaE2 polymerase contributes to in vivo survival and the emergence of drug resistance in *Mycobacterium tuberculosis*. *Cell* **113**: 183-193.

Bott M & Brocker M (2012) Two-component signal transduction in *Corynebacterium glutamicum* and other corynebacteria: on the way towards stimuli and targets. *Appl. Microbiol. Biotechnol.* **94**: 1131-1150.

Bradford MM (1976) A rapid and sensitive method for the quantitation of microgram quantities of protein utilizing the principle of protein-dye binding. *Analytical Biochemistry* **72**: 248-254.

Brand S, Niehaus K, Pühler A & Kalinowski J (2003) Identification and functional analysis of six mycolyltransferase genes of *Corynebacterium glutamicum* ATCC 13032: the genes *cop1, cmt1, and cmt2* can replace each other in the synthesis of trehalose dicorynomycolate, a component of the mycolic acid layer of the cell envelope. *Arch. Microbiol.* **180**: 33-44.

Brantl S (2007) Regulatory mechanisms employed by *cis*-encoded antisense RNAs. *Curr. Opin. Microbiol.* **10**: 102-109.

Brennan RG & Link TM (2007) Hfq structure, function and ligand binding. *Curr. Opin. Microbiol.* **10**: 125-133.

Brinkrolf K, Brune I & Tauch A (2006) Transcriptional regulation of catabolic pathways for aromatic compounds in *Corynebacterium glutamicum*. *Genet. Mol. Res.* **5**: 773-789.

Brinkrolf K, Schröder J, Pühler A & Tauch A (2010) The transcriptional regulatory repertoire of *Corynebacterium glutamicum*: reconstruction of the network controlling pathways involved in lysine and glutamate production. *J. Biotechnol.* **149**: 173-182.

Brinkrolf K, Ploger S, Solle S*, et al.* (2008) The LacI/GalR family transcriptional regulator UriR negatively controls uridine utilization of *Corynebacterium glutamicum* by binding to catabolite-responsive element (*cre*)-like sequences. *Microbiology* **154**: 1068-1081.

Brooks PC, Movahedzadeh F & Davis EO (2001) Identification of some DNA damage-inducible genes of *Mycobacterium tuberculosis*: apparent lack of correlation with LexA binding. *J. Bacteriol.* **183**: 4459-4467.

Brouns SJ, Jore MM, Lundgren M*, et al.* (2008) Small CRISPR RNAs guide antiviral defense in prokaryotes. *Science* **321**: 960-964.

Brune I, Brinkrolf K, Kalinowski J, Pühler A & Tauch A (2005) The individual and common repertoire of DNA-binding transcriptional regulators of *Corynebacterium glutamicum, Corynebacterium efficiens, Corynebacterium diphtheriae and Corynebacterium jeikeium* deduced from the complete genome sequences. *BMC Genomics* **6**: 86.

Burge SW, Daub J, Eberhardt R*, et al.* (2013) Rfam 11.0: 10 years of RNA families. *Nucleic Acids Res.* **41**: D226-232.

Campbell EA, Korzheva N, Mustaev A, Murakami K, Nair S, Goldfarb A & Darst SA (2001) Structural mechanism for rifampicin inhibition of bacterial RNA polymerase. *Cell* **104**: 901-912.

Cavanagh AT, Klocko AD, Liu X & Wassarman KM (2008) Promoter specificity for 6S RNA regulation of transcription is determined by core promoter sequences and competition for region 4.2 of sigma70. *Mol. Microbiol.* **67**: 1242-1256.

Choi WW, Park SD, Lee SM, Kim HB, Kim Y & Lee HS (2009) The *whcA* gene plays a negative role in oxidative stress response of *Corynebacterium glutamicum*. *FEMS Microbiol. Lett.* **290**: 32-38.

Collier LS, Gaines GL, 3rd & Neidle EL (1998) Regulation of benzoate degradation in *Acinetobacter* sp. strain ADP1 by BenM, a LysR-type transcriptional activator. *J. Bacteriol.* **180**: 2493-2501.

Cramer A, Gerstmeir R, Schaffer S, Bott M & Eikmanns BJ (2006) Identification of RamA, a novel LuxR-type transcriptional regulator of genes involved in acetate metabolism of *Corynebacterium glutamicum*. *J. Bacteriol.* **188**: 2554-2567.

Cremer J, Eggeling L & Sahm H (1990) Cloning the *dapA* and *dapB* cluster of the lysine-secreting bacterium *Corynebacterium glutamicum*. *Mol. Gen.Genet.* **220**: 478-480.

Daniel RA & Errington J (2003) Control of cell morphogenesis in bacteria: two distinct ways to make a rod-shaped cell. *Cell* **113**: 767-776.

Davis EO, Sedgwick SG & Colston MJ (1991) Novel structure of the *recA* locus of *Mycobacterium tuberculosis* implies processing of the gene product. *J. Bacteriol.* **173**: 5653-5662.

Davis EO, Dullaghan EM & Rand L (2002) Definition of the mycobacterial SOS box and use to identify LexA-regulated genes in *Mycobacterium tuberculosis*. *J. Bacteriol.* **184**: 3287-3295.

Donovan C & Bramkamp M (2014) Cell division in *Corynebacterineae*. *Front. Microbiol.* **5**: 132.

Durbach SI, Andersen SJ & Mizrahi V (1997) SOS induction in mycobacteria: analysis of the DNA-binding activity of a LexA-like repressor and its role in DNA damage induction of the *recA* gene from *Mycobacterium smegmatis*. *Mol. Microbiol.* **26**: 643-653.

Eggeling L & Bott M (2005) *Handbook of Corynebacterium glutamicum. Taylor & Francis, Boca Raton.*

Ezekiel DH & Hutchins JE (1968) Mutations affecting RNA polymerase associated with rifampicin resistance in *Escherichia coli*. *Nature* **220**: 276-277.

Favrot L & Ronning DR (2012) Targeting the mycobacterial envelope for tuberculosis drug development. *Expert Rev. Anti Infect. Ther.* **10**: 1023-1036.

Fiuza M, Canova MJ, Zanella-Cléon I*, et al.* (2008a) From the characterization of the four serine/threonine protein kinases (PknA/B/G/L) of *Corynebacterium glutamicum* toward the role of PknA and PknB in cell division. *J. Biol. Chem.* **283**: 18099-18112.

Fiuza M, Letek M, Leiba J*, et al.* (2010) Phosphorylation of a novel cytoskeletal protein (RsmP) regulates rod-shaped morphology in *Corynebacterium glutamicum*. *J. Biol. Chem.* **285**: 29387-29397.

Fiuza M, Canova MJ, Patin D*, et al.* (2008b) The MurC ligase essential for peptidoglycan biosynthesis is regulated by the serine/threonine protein kinase PknA in *Corynebacterium glutamicum*. *J. Biol. Chem.* **283**: 36553-36563.

Flachner B, Kovári Z, Varga A, Gugolya Z, Vonderviszt F, Náray-Szabó G & Vas M (2004) Role of phosphate chain mobility of MgATP in completing the 3-phosphoglycerate kinase catalytic site: binding, kinetic, and crystallographic studies with ATP and MgATP. *Biochemistry* **43**: 3436-3449.

Franze de Fernandez MT, Eoyang L & August JT (1968) Factor fraction required for the synthesis of bacteriophage Qbeta-RNA. *Nature* **219**: 588-590.

Friedberg EC (1995) Out of the shadows and into the light: the emergence of DNA repair. *Trends Biochem. Sci.* **20**: 381.

Fröhlich KS & Vogel J (2009) Activation of gene expression by small RNA. *Curr. Opin. Microbiol.* **12**: 674-682.

Frunzke J, Bramkamp M, Schweitzer JE & Bott M (2008) Population Heterogeneity in *Corynebacterium glutamicum* ATCC 13032 caused by prophage CGP3. *J. Bacteriol.* **190**: 5111-5119.

Frunzke J, Engels V, Hasenbein S, Gätgens C & Bott M (2008) Co-ordinated regulation of gluconate catabolism and glucose uptake in *Corynebacterium glutamicum* by two functionally equivalent transcriptional regulators, GntR1 and GntR2. *Mol. Microbiol.* **67**: 305-322.

Gao B & Gupta RS (2012) Phylogenetic framework and molecular signatures for the main clades of the phylum *Actinobacteria*. *Microbiol. Mol. Biol. Rev.* **76**: 66-112.

Gardner PP, Daub J, Tate JG*, et al.* (2009) Rfam: updates to the RNA families database. *Nucleic Acids Res.* **37**: D136-140.

Geiman DE, Raghunand TR, Agarwal N & Bishai WR (2006) Differential gene expression in response to exposure to antimycobacterial agents and other stress conditions among seven *Mycobacterium tuberculosis whiB*-like genes. *Antimicrob. Agents Chemother.* **50**: 2836-2841.

Geissmann T, Chevalier C, Cros MJ*, et al.* (2009) A search for small noncoding RNAs in *Staphylococcus aureus* reveals a conserved sequence motif for regulation. *Nucleic Acids Res.* **37**: 7239-7257.

Geissmann TA & Touati D (2004) Hfq, a new chaperoning role: binding to messenger RNA determines access for small RNA regulator. *EMBO J.* **23**: 396-405.

Georgi T, Rittmann D & Wendisch VF (2005) Lysine and glutamate production by *Corynebacterium glutamicum* on glucose, fructose and sucrose: roles of malic enzyme and fructose-1,6-bisphosphatase. *Metab. Eng.* **7**: 291-301.

Gerdes K & Molin S (1986) Partitioning of plasmid R1. Structural and functional analysis of the parA locus. *J. Mol. Biol.* **190**: 269-279.

Gerdes K, Jacobsen JS & Franch T (1997) Plasmid stabilization by post-segregational killing. *Genet. Eng. (N Y)* **19**: 49-61.

Gerstmeir R, Cramer A, Dangel P, Schaffer S & Eikmanns BJ (2004) RamB, a novel transcriptional regulator of genes involved in acetate metabolism of *Corynebacterium glutamicum*. *J. Bacteriol.* **186**: 2798-2809.

Gildehaus N, Neusser T, Wurm R & Wagner R (2007) Studies on the function of the riboregulator 6S RNA from *E. coli*: RNA polymerase binding, inhibition of in vitro transcription and synthesis of RNA-directed de novo transcripts. *Nucleic Acids Res.* **35**: 1885-1896.

Gomez JE & Bishai WR (2000) *whmD* is an essential mycobacterial gene required for proper septation and cell division. *Proc. Natl. Acad. Sci. U S A* **97**: 8554-8559.

Grünberger A, Paczia N, Probst C*, et al.* (2012) A disposable picolitre bioreactor for cultivation and investigation of industrially relevant bacteria on the single cell level. *Lab. Chip.* **12**: 2060-2068.

Hanahan D (1983) Studies on transformation of *Escherichia coli* with plasmids. *J. Mol. Biol.* **166**: 557-580.

Hansmeier N, Albersmeier A, Tauch A*, et al.* (2006) The surface (S)-layer gene *cspB* of *Corynebacterium glutamicum* is transcriptionally activated by a LuxR-type regulator and located on a 6 kb genomic island absent from the type strain ATCC 13032. *Microbiology* **152**: 923-935.

Heidrich N, Moll I & Brantl S (2007) In vitro analysis of the interaction between the small RNA SR1 and its primary target *ahrC* mRNA. *Nucleic Acids Res.* **35**: 4331-4346.

Heidrich N, Chinali A, Gerth U & Brantl S (2006) The small untranslated RNA SR1 from the *Bacillus subtilis* genome is involved in the regulation of arginine catabolism. *Mol. Microbiol.* **62**: 520-536.

Hett EC & Rubin EJ (2008) Bacterial growth and cell division: a mycobacterial perspective. *Microbiol. Mol. Biol. Rev.* **72**: 126-156.

Hjalt T & Wagner EG (1992) The effect of loop size in antisense and target RNAs on the efficiency of antisense RNA control. *Nucleic Acids Res.* **20**: 6723-6732.

Hong EJ, Park JS, Kim Y & Lee HS (2014) Role of *Corynebacterium glutamicum sprA* encoding a Serine Protease in *glxR*-Mediated Global Gene Regulation. *PLoS One* **9**: e93587.

Hutter B & Dick T (1999) Molecular genetic characterisation of *whiB3*, a mycobacterial homologue of a *Streptomyces* sporulation factor. *Res. Microbiol.* **150**: 295-301.

Ikeda M & Nakagawa S (2003) The *Corynebacterium glutamicum* genome: features and impacts on biotechnological processes. *Appl. Microbiol. Biotechnol.* **62**: 99-109.

Inui M, Kawaguchi H, Murakami S, Vertes AA & Yukawa H (2004) Metabolic engineering of *Corynebacterium glutamicum* for fuel ethanol production under oxygen-deprivation conditions. *J. Mol. Microbiol. Biotechnol.* **8**: 243-254.

Itou H, Okada U, Suzuki H, Yao M, Wachi M, Watanabe N & Tanaka I (2005) The CGL2612 protein from *Corynebacterium glutamicum* is a drug resistance-related transcriptional repressor: structural and functional analysis of a newly identified transcription factor from genomic DNA analysis. *J. Biol. Chem.* **280**: 38711-38719.

Jäger W, Schäfer A, Pühler A, Labes G & Wohlleben W (1992) Expression of the *Bacillus subtilis* sacB gene leads to sucrose sensitivity in the gram-positive bacterium *Corynebacterium glutamicum* but not in *Streptomyces lividans*. *J. Bacteriol.* **174**: 5462-5465.

Jochmann N, Kurze AK, Czaja LF*, et al.* (2009) Genetic makeup of the *Corynebacterium glutamicum* LexA regulon deduced from comparative transcriptomics and in vitro DNA band shift assays. *Microbiology* **155**: 1459-1477.

Jungwirth B, Sala C, Kohl TA*, et al.* (2012) High-resolution detection of DNA binding sites of the global transcriptional regulator GlxR in *Corynebacterium glutamicum*. *Microbiology* **159(Pt 1):**: 12-22.

Kacem R, De Sousa-D'Auria C, Tropis M*, et al.* (2004) Importance of mycoloyltransferases on the physiology of *Corynebacterium glutamicum*. *Microbiology* **150**: 73-84.

Kalinowski J, Bathe B, Bartels D*, et al.* (2003) The complete *Corynebacterium glutamicum* ATCC 13032 genome sequence and its impact on the production of L-aspartate-derived amino acids and vitamins. *J. Biotechnol.* **104**: 5-25.

Kawamoto H, Morita T, Shimizu A, Inada T & Aiba H (2005) Implication of membrane localization of target mRNA in the action of a small RNA: mechanism of post-transcriptional regulation of glucose transporter in *Escherichia coli*. *Genes Dev.* **19**: 328-338.

Keilhauer C, Eggeling L & Sahm H (1993) Isoleucine synthesis in *Corynebacterium glutamicum*: molecular analysis of the ilvB-ilvN-ilvC operon. *J. Bacteriol.* **175**: 5595-5603.

Kensy F, Zang E, Faulhammer C, Tan RK & Büchs J (2009) Validation of a high-throughput fermentation system based on online monitoring of biomass and fluorescence in continuously shaken microtiter plates. *Microb. Cell Fact.* **8**: 31.

Kim TH, Park JS, Kim HJ, Kim Y, Kim P & Lee HS (2005) The *whcE* gene of *Corynebacterium glutamicum* is important for survival following heat and oxidative stress. *Biochem. Biophys. Res. Commun.* **337**: 757-764.

Kinoshita S, Udaka, S., and Shimono, M. (1957) Studies on the amino acid fermentation I. Production of L-glutamic acid by various microorganisms. *J. Gen. Appl. Microbiol.* **3**: 193-205.

Kohl TA & Tauch A (2009) The GlxR regulon of the amino acid producer *Corynebacterium glutamicum*: Detection of the corynebacterial core regulon and integration into the transcriptional regulatory network model. *J. Biotechnol.* **143**: 239-246.

Küberl A, Fränzel B, Eggeling L, Polen T, Wolters DA & Bott M (2014) Pupylated proteins in *Corynebacterium glutamicum* revealed by MudPIT analysis. *Proteomics* **doi: 10.1002/pmic.201300531 ahead of print**.

Lee JY, Park JS, Kim HJ, Kim Y & Lee HS (2012) *Corynebacterium glutamicum whcB*, a stationary phase-specific regulatory gene. *FEMS Microbiol. Lett.* **327**: 103-109.

Lee JY, Kim HJ, Kim ES, Kim P, Kim Y & Lee HS (2013) Regulatory interaction of the *Corynebacterium glutamicum whc* genes in oxidative stress responses. *J. Biotechnol.* **168**: 149-154.

Lee SY, Bailey SC & Apirion D (1978) Small stable RNAs from *Escherichia coli*: evidence for the existence of new molecules and for a new ribonucleoprotein particle containing 6S RNA. *J. Bacteriol.* **133**: 1015-1023.

Letek M, Fiuza M, Ordóñez E, Villadangos AF, Ramos A, Mateos LM & Gil JA (2008) Cell growth and cell division in the rod-shaped actinomycete *Corynebacterium glutamicum*. *Antonie Van Leeuwenhoek* **94**: 99-109.

Levin PA, Margolis PS, Setlow P, Losick R & Sun D (1992) Identification of *Bacillus subtilis* genes for septum placement and shape determination. *J. Bacteriol.* **174**: 6717-6728.

Liebl W, Dworkin M, Falkow S, Rosenberg E, Schleifer KH & Stackebrandt E (2006) *The Prokaryotes. 3rd edn. Vol. 3. New York, USA: Springer; 2006* The genus *Corynebacterium* - nonmedical; pp. 796–818. Vol.

Litsanov B, Brocker M & Bott M (2012) Toward homosuccinate fermentation: metabolic engineering of *Corynebacterium glutamicum* for anaerobic production of succinate from glucose and formate. *Appl. Environ. Microbiol.* **78**: 3325-3337.

Litsanov B, Kabus A, Brocker M & Bott M (2012) Efficient aerobic succinate production from glucose in minimal medium with *Corynebacterium glutamicum*. *Microb. Biotechnol.* **5**: 116-128.

Little JW (1991) Mechanism of specific LexA cleavage: autodigestion and the role of RecA coprotease. *Biochimie* **73**: 411-421.

Little JW & Mount DW (1982) The SOS regulatory system of *Escherichia coli*. *Cell* **29**: 11-22.

Liu JM & Camilli A (2010) A broadening world of bacterial small RNAs. *Curr. Opin. Microbiol.* **13**: 18-23.

Liu MY & Romeo T (1997) The global regulator CsrA of *Escherichia coli* is a specific mRNA-binding protein. *J. Bacteriol.* **179**: 4639-4642.

Maier T, Schmidt A, Güell M, Kühner S, Gavin AC, Aebersold R & Serrano L (2011) Quantification of mRNA and protein and integration with protein turnover in a bacterium. *Mol. Syst. Biol.* **7**: 511.

Majdalani N, Cunning C, Sledjeski D, Elliott T & Gottesman S (1998) DsrA RNA regulates translation of RpoS message by an anti-antisense mechanism, independent of its action as an antisilencer of transcription. *Proc. Natl. Acad. Sci. U S A* **95**: 12462-12467.

Markham BE, Harper JE, Mount DW*, et al.* (1984) Analysis of mRNA synthesis following induction of the *Escherichia coli* SOS system. *J. Mol. Biol.* **178**: 237-248.

Massé E & Gottesman S (2002) A small RNA regulates the expression of genes involved in iron metabolism in *Escherichia coli*. *Proc. Natl. Acad. Sci. U S A* **99**: 4620-4625.

Massé E, Vanderpool CK & Gottesman S (2005) Effect of RyhB small RNA on global iron use in *Escherichia coli*. *J. Bacteriol.* **187**: 6962-6971.

Mathews DH, Sabina J, Zuker M & Turner DH (1999) Expanded sequence dependence of thermodynamic parameters improves prediction of RNA secondary structure. *J. Mol. Biol.* **288**: 911-940.

Matsiota-Bernard P, Vrioni G & Marinis E (1998) Characterization of *rpoB* mutations in rifampin-resistant clinical *Mycobacterium tuberculosis* isolates from Greece. *J. Clin. Microbiol.* **36**: 20-23.

McFall SM, Chugani SA & Chakrabarty AM (1998) Transcriptional activation of the catechol and chlorocatechol operons: variations on a theme. *Gene* **223**: 257-267.

Meissner D, Vollstedt A, van Dijl JM & Freudl R (2007) Comparative analysis of twin-arginine (Tat)-dependent protein secretion of a heterologous model protein (GFP) in three different Gram-positive bacteria. *Appl. Microbiol. Biotechnol.* **76**: 633-642.

Menkel E, Thierbach G, Eggeling L & Sahm H (1989) Influence of increased aspartate availability on lysine formation by a recombinant strain of *Corynebacterium glutamicum* and utilization of fumarate. *Appl. Environ. Microbiol.* **55**: 684-688.

Mentz A, Neshat A, Pfeifer-Sancar K, Pühler A, Rückert C & Kalinowski J (2013) Comprehensive discovery and characterization of small RNAs in *Corynebacterium glutamicum* ATCC 13032. *BMC Genomics* **14**: 714.

Merkens H, Beckers G, Wirtz A & Burkovski A (2005) Vanillate metabolism in *Corynebacterium glutamicum*. *Curr. Microbiol.* **51**: 59-65.

Molina-Henares AJ, Krell T, Eugenia Guazzaroni M, Segura A & Ramos JL (2006) Members of the IclR family of bacterial transcriptional regulators function as activators and/or repressors. *FEMS Microbiol. Rev.* **30**: 157-186.

Molle V, Palframan WJ, Findlay KC & Buttner MJ (2000) WhiD and WhiB, homologous proteins required for different stages of sporulation in *Streptomyces coelicolor* A3(2). *J. Bacteriol.* **182**: 1286-1295.

Møller T, Franch T, Udesen C, Gerdes K & Valentin-Hansen P (2002) Spot 42 RNA mediates discoordinate expression of the *E. coli* galactose operon. *Genes Dev.* **16**: 1696-1706.

Mondragón V, Franco B, Jonas K, Suzuki K, Romeo T, Melefors O & Georgellis D (2006) pH-dependent activation of the BarA-UvrY two-component system in *Escherichia coli*. *J. Bacteriol.* **188**: 8303-8306.

Morita T, Maki K & Aiba H (2005) RNase E-based ribonucleoprotein complexes: mechanical basis of mRNA destabilization mediated by bacterial noncoding RNAs. *Genes Dev.* **19**: 2176-2186.

Movahedzadeh F, Colston MJ & Davis EO (1997) Determination of DNA sequences required for regulated *Mycobacterium tuberculosis* RecA expression in response to DNA-damaging agents suggests that two modes of regulation exist. *J. Bacteriol.* **179**: 3509-3518.

Mullis K, Faloona F, Scharf S, Saiki R, Horn G & Erlich H (1986) Specific enzymatic amplification of DNA in vitro: the polymerase chain reaction. *Cold Spring Harb. Symp. Quant. Biol.* **51 Pt 1,** : 263-273.

Nanda AM, Heyer A, Krämer C, Grünberger A, Kohlheyer D & Frunzke J (2014) Analysis of SOS-induced spontaneous prophage induction in *Corynebacterium glutamicum* at the single-cell level. *J. Bacteriol.* **196**: 180-188.

Nentwich SS, Brinkrolf K, Gaigalat L*, et al.* (2009) Characterization of the LacI-type transcriptional repressor RbsR controlling ribose transport in *Corynebacterium glutamicum* ATCC 13032. *Microbiology* **155**: 150-164.

Neusser T, Gildehaus N, Wurm R & Wagner R (2008) Studies on the expression of 6S RNA from *E. coli*: involvement of regulators important for stress and growth adaptation. *Biol. Chem.* **389**: 285-297.

Neusser T, Polen T, Geissen R & Wagner R (2010) Depletion of the non-coding regulatory 6S RNA in E. coli causes a surprising reduction in the expression of the translation machinery. *BMC Genomics* **11**: 165.

Niebisch A, Kabus A, Schultz C, Weil B & Bott M (2006) Corynebacterial protein kinase G controls 2-oxoglutarate dehydrogenase activity via the phosphorylation status of the OdhI protein. *J. Biol. Chem.* **281**: 12300-12307.

Nielsen AK, Thorsted P, Thisted T, Wagner EG & Gerdes K (1991) The rifampicin-inducible genes *srnB* from F and *pnd* from R483 are regulated by antisense RNAs and mediate plasmid maintenance by killing of plasmid-free segregants. *Mol. Microbiol.* **5**: 1961-1973.

Novick RP, Iordanescu S, Projan SJ, Kornblum J & Edelman I (1989) pT181 plasmid replication is regulated by a countertranscript-driven transcriptional attenuator. *Cell* **59**: 395-404.

Ogino H, Teramoto H, Inui M & Yukawa H (2008) DivS, a novel SOS-inducible cell-division suppressor in *Corynebacterium glutamicum*. *Mol. Microbiol.* **67**: 597-608.

Okino S, Noburyu R, Suda M, Jojima T, Inui M & Yukawa H (2008) An efficient succinic acid production process in a metabolically engineered *Corynebacterium glutamicum* strain. *Appl. Microbiol. Biotechnol.* **81**: 459-464.

Opdyke JA, Kang JG & Storz G (2004) GadY, a small-RNA regulator of acid response genes in *Escherichia coli*. *J. Bacteriol.* **186**: 6698-6705.

Pánek J, Bobek J, Mikulik K, Basler M & Vohradsky J (2008) Biocomputational prediction of small non-coding RNAs in *Streptomyces*. *BMC Genomics* **9**: 217.

Papenfort K & Vogel J (2009) Multiple target regulation by small noncoding RNAs rewires gene expression at the post-transcriptional level. *Res. Microbiol.* **160**: 278-287.

Pappin DJ, Hojrup P & Bleasby AJ (1993) Rapid identification of proteins by peptide-mass fingerprinting. *Curr. Biol.* **3**: 327-332.

Pátek M & Nešvera J (2011) Sigma factors and promoters in *Corynebacterium glutamicum*. *J. Biotechnol.* **154**: 101-113.

Pearce MJ, Mintseris J, Ferreyra J, Gygi SP & Darwin KH (2008) Ubiquitin-like protein involved in the proteasome pathway of *Mycobacterium tuberculosis*. *Science* **322**: 1104-1107.

Pfeifer-Sancar K, Mentz A, Rückert C & Kalinowski J (2013) Comprehensive analysis of the *Corynebacterium glutamicum* transcriptome using an improved RNAseq technique. *BMC Genomics* **14**: 888.

Porath J, Carlsson J, Olsson I & Belfrage G (1975) Metal chelate affinity chromatography, a new approach to protein fractionation. *Nature* **258**: 598-599.

Radmacher E, Stansen KC, Besra GS*, et al.* (2005) Ethambutol, a cell wall inhibitor of *Mycobacterium tuberculosis*, elicits L-glutamate efflux of *Corynebacterium glutamicum*. *Microbiology* **151**: 1359-1368.

Raghunand TR & Bishai WR (2006) *Mycobacterium smegmatis whmD* and its homologue *Mycobacterium tuberculosis whiB2* are functionally equivalent. *Microbiology* **152**: 2735-2747.

Rand L, Hinds J, Springer B, Sander P, Buxton RS & Davis EO (2003) The majority of inducible DNA repair genes in *Mycobacterium tuberculosis* are induced independently of RecA. *Mol. Microbiol.* **50**: 1031-1042.

Rawat M, Newton GL, Ko M, Martinez GJ, Fahey RC & Av-Gay Y (2002) Mycothiol-deficient *Mycobacterium smegmatis* mutants are hypersensitive to alkylating agents, free radicals, and antibiotics. *Antimicrob. Agents Chemother.* **46**: 3348-3355.

Reddy GK & Wendisch VF (2014) Characterization of 3-phosphoglycerate kinase from *Corynebacterium glutamicum* and its impact on amino acid production. *BMC Microbiol.* **14**: 54.

Roberts C, Anderson KL, Murphy E*, et al.* (2006) Characterizing the effect of the *Staphylococcus aureus* virulence factor regulator, SarA, on log-phase mRNA half-lives. *J. Bacteriol.* **188**: 2593-2603.

Romeo T (1998) Global regulation by the small RNA-binding protein CsrA and the non-coding RNA molecule CsrB. *Mol. Microbiol.* **29**: 1321-1330.

Rückert C & Kalinowski J (2008) Sulfur Metabolism in *Corynebacterium glutamicum*. *Burkovski A, ed. Corynebacteria: Genomics and Molecular Biology. Norfolk, UK: Caister Academic Press* 217-240.

Sambrook J & Russell DW (2001) Molecular cloning: a laboratory manual. *Cold Spring Harbor Laboratory Press , Cold Spring Harbor, N.Y.*

Schäfer A, Tauch A, Droste N, Pühler A & Kalinowski J (1997) The *Corynebacterium glutamicum cglIM* gene encoding a 5-cytosine methyltransferase enzyme confers a specific DNA methylation pattern in an McrBC-deficient *Escherichia coli* strain. *Gene* **203**: 95-101.

Schäfer A, Tauch A, Jäger W, Kalinowski J, Thierbach G & Pühler A (1994) Small mobilizable multi-purpose cloning vectors derived from the *Escherichia coli* plasmids pK18 and pK19: selection of defined deletions in the chromosome of *Corynebacterium glutamicum*. *Gene* **145**: 69-73.

Schneider S (2014) Charakterisierung zellulärer Interaktionspartner der 6S RNA aus *Escherichia coli* und Analyse des 6S RNA Regulationsnetzwerkes. Dissertation. Heinrich-Heine-Universität Düsseldorf.

Schröder J & Tauch A (2010) Transcriptional regulation of gene expression in *Corynebacterium glutamicum*: the role of global, master and local regulators in the modular and hierarchical gene regulatory network. *FEMS Microbiol. Rev.* **34**: 685-737.

Schultz C, Niebisch A, Schwaiger A, Viets U, Metzger S, Bramkamp M & Bott M (2009) Genetic and biochemical analysis of the serine/threonine protein kinases PknA, PknB, PknG and PknL of *Corynebacterium glutamicum*: evidence for non-essentiality and for phosphorylation of OdhI and FtsZ by multiple kinases. *Mol. Microbiol.* **74**: 724-741.

Seidel M, Alderwick LJ, Birch HL, Sahm H, Eggeling L & Besra GS (2007) Identification of a novel arabinofuranosyltransferase AftB involved in a terminal step of cell wall arabinan biosynthesis in Corynebacterianeae, such as *Corynebacterium glutamicum* and *Mycobacterium tuberculosis*. *J. Biol. Chem.* **282**: 14729-14740.

Shen X & Liu S (2005) Key enzymes of the protocatechuate branch of the beta-ketoadipate pathway for aromatic degradation in *Corynebacterium glutamicum*. *Sci. China C. Life Sci.* **48**: 241-249.

Silvaggi JM, Perkins JB & Losick R (2005) Small untranslated RNA antitoxin in *Bacillus subtilis*. *J. Bacteriol.* **187**: 6641-6650.

Sledjeski D & Gottesman S (1995) A small RNA acts as an antisilencer of the H-NS-silenced rcsA gene of *Escherichia coli*. *Proc. Natl. Acad. Sci. U S A* **92**: 2003-2007.

Sledjeski DD, Gupta A & Gottesman S (1996) The small RNA, DsrA, is essential for the low temperature expression of RpoS during exponential growth in *Escherichia coli*. *EMBO J.* **15**: 3993-4000.

Sledjeski DD, Whitman C & Zhang A (2001) Hfq is necessary for regulation by the untranslated RNA DsrA. *J. Bacteriol.* **183**: 1997-2005.

Smith KM, Cho KM & Liao JC (2010) Engineering *Corynebacterium glutamicum* for isobutanol production. *Appl. Microbiol. Biotechnol.* **87**: 1045-1055.

Smith LJ, Stapleton MR, Buxton RS & Green J (2012) Structure-function relationships of the *Mycobacterium tuberculosis* transcription factor WhiB1. *PLoS One* **7**: e40407.

Smith PK, Krohn RI, Hermanson GT*, et al.* (1985) Measurement of protein using bicinchoninic acid. *Analytical Biochemistry* **150**: 76-85.

Sorek R, Kunin V & Hugenholtz P (2008) CRISPR--a widespread system that provides acquired resistance against phages in bacteria and archaea. *Nat. Rev. Microbiol.* **6**: 181-186.

Steuten B & Wagner R (2012) A conformational switch is responsible for the reversal of the 6S RNA-dependent RNA polymerase inhibition in *Escherichia coli*. *Biol. Chem.* **393**: 1513-1522.

Steuten B, Setny P, Zacharias M & Wagner R (2013) Mapping the spatial neighborhood of the regulatory 6S RNA bound to *Escherichia coli* RNA polymerase holoenzyme. *J. Mol. Biol.* **425**: 3649-3661.

Storz G, Vogel J & Wassarman KM (2011) Regulation by small RNAs in bacteria: expanding frontiers. *Mol. Cell.* **43**: 880-891.

Striebel F, Imkamp F, Özcelik D & Weber-Ban E (2014) Pupylation as a signal for proteasomal degradation in bacteria. *Biochim. Biophys. Acta.* **1843**: 103-113.

Studier FW & Moffatt BA (1986) Use of bacteriophage T7 RNA polymerase to direct selective high-level expression of cloned genes. *J. Mol. Biol.* **189**: 113-130.

Sun X, Zhulin I & Wartell RM (2002) Predicted structure and phyletic distribution of the RNA-binding protein Hfq. *Nucleic Acids Res.* **30**: 3662-3671.

Swiercz JP, Hindra, Bobek J, Haiser HJ, Di Berardo C, Tjaden B & Elliot MA (2008) Small non-coding RNAs in *Streptomyces coelicolor*. *Nucleic Acids Res.* **36**: 7240-7251.

Takayama K & Kilburn JO (1989) Inhibition of synthesis of arabinogalactan by ethambutol in *Mycobacterium smegmatis*. *Antimicrob. Agents Chemother.* **33**: 1493-1499.

Taniguchi Y, Choi PJ, Li GW*, et al.* (2010) Quantifying *E. coli* proteome and transcriptome with single-molecule sensitivity in single cells. *Science* **329**: 533-538.

Tauch A, Götker S, Pühler A, Kalinowski J & Thierbach G (2002) The alanine racemase gene alr is an alternative to antibiotic resistance genes in cloning systems for industrial *Corynebacterium glutamicum* strains. *J. Biotechnol.* **99**: 79-91.

Teramoto H, Inui M & Yukawa H (2013) OxyR acts as a transcriptional repressor of hydrogen peroxide-inducible antioxidant genes in *Corynebacterium glutamicum* R. *FEBS J.* **280**: 3298-3312.

Teramoto H, Suda M, Inui M & Yukawa H (2010) Regulation of the expression of genes involved in NAD de novo biosynthesis in *Corynebacterium glutamicum*. *Appl. Environ. Microbiol.* **76**: 5488-5495.

Tomasz M (1995) Mitomycin C: small, fast and deadly (but very selective). *Chem. Biol.* **2**: 575-579.

Tomizawa J (1986) Control of ColE1 plasmid replication: binding of RNA I to RNA II and inhibition of primer formation. *Cell* **47**: 89-97.

Tomizawa J, Itoh T, Selzer G & Som T (1981) Inhibition of ColE1 RNA primer formation by a plasmid-specified small RNA. *Proc. Natl. Acad. Sci. U S A* **78**: 1421-1425.

Toyoda K, Teramoto H, Inui M & Yukawa H (2011) Genome-wide identification of in vivo binding sites of GlxR, a cyclic AMP receptor protein-type regulator in *Corynebacterium glutamicum*. *J. Bacteriol.* **193**: 4123-4133.

Traag BA, Kelemen GH & Van Wezel GP (2004) Transcription of the sporulation gene *ssgA* is activated by the IclR-type regulator SsgR in a *whi*-independent manner in *Streptomyces coelicolor* A3(2). *Mol. Microbiol.* **53**: 985-1000.

Tramonti A, De Canio M & De Biase D (2008) GadX/GadW-dependent regulation of the *Escherichia coli* acid fitness island: transcriptional control at the *gadY-gadW* divergent promoters and identification of four novel 42 bp GadX/GadW-specific binding sites. *Mol. Microbiol.* **70**: 965-982.

Trotochaud AE & Wassarman KM (2004) 6S RNA function enhances long-term cell survival. *J. Bacteriol.* **186**: 4978-4985.

Udaka S (1960) Screening method for microorganisms accumulating metabolites and its use in the isolation of *Micrococcus glutamicus*. *J. Bacteriol.* **79**: 754-755.

Valbuena N, Letek M, Ordóñez E, Ayala J, Daniel RA, Gil JA & Mateos LM (2007) Characterization of HMW-PBPs from the rod-shaped actinomycete *Corynebacterium glutamicum*: peptidoglycan synthesis in cells lacking actin-like cytoskeletal structures. *Mol. Microbiol.* **66**: 643-657.

Valbuena N, Letek M, Ramos A*, et al.* (2006) Morphological changes and proteome response of *Corynebacterium glutamicum* to a partial depletion of *FtsI*. *Microbiology* **152**: 2491-2503.

Valentin-Hansen P, Eriksen M & Udesen C (2004) The bacterial Sm-like protein Hfq: a key player in RNA transactions. *Mol. Microbiol.* **51**: 1525-1533.

van der Oost J, Jore MM, Westra ER, Lundgren M & Brouns SJ (2009) CRISPR-based adaptive and heritable immunity in prokaryotes. *Trends Biochem. Sci.* **34**: 401-407.

van Ooyen J, Emer D, Bussmann M, Bott M, Eikmanns BJ & Eggeling L (2011) Citrate synthase in *Corynebacterium glutamicum* is encoded by two *gltA* transcripts which are controlled by RamA, RamB, and GlxR. *J. Biotechnol.* **154**: 140-148.

Vanderpool CK & Gottesman S (2004) Involvement of a novel transcriptional activator and small RNA in post-transcriptional regulation of the glucose phosphoenolpyruvate phosphotransferase system. *Mol. Microbiol.* **54**: 1076-1089.

Vockenhuber MP, Sharma CM, Statt MG*, et al.* (2011) Deep sequencing-based identification of small non-coding RNAs in *Streptomyces coelicolor*. *RNA Biol.* **8**: 468-477.

Vogel J & Papenfort K (2006) Small non-coding RNAs and the bacterial outer membrane. *Curr. Opin. Microbiol.* **9**: 605-611.

Vogel J, Argaman L, Wagner EG & Altuvia S (2004) The small RNA IstR inhibits synthesis of an SOS-induced toxic peptide. *Curr. Biol.* **14**: 2271-2276.

Vogt M, Haas S, Klaffl S, Polen T, Eggeling L, van Ooyen J & Bott M (2014) Pushing product formation to its limit: metabolic engineering of *Corynebacterium glutamicum* for L-leucine overproduction. *Metab. Eng.* **22**: 40-52.

Wachi M & Matsuhashi M (1989) Negative control of cell division by *mreB*, a gene that functions in determining the rod shape of *Escherichia coli* cells. *J. Bacteriol.* **171**: 3123-3127.

Wassarman KM & Storz G (2000) 6S RNA regulates *E. coli* RNA polymerase activity. *Cell* **101**: 613-623.

Wassarman KM & Saecker RM (2006) Synthesis-mediated release of a small RNA inhibitor of RNA polymerase. *Science* **314**: 1601-1603.

Waters LS & Storz G (2009) Regulatory RNAs in bacteria. *Cell* **136**: 615-628.

Weilbacher T, Suzuki K, Dubey AK*, et al.* (2003) A novel sRNA component of the carbon storage regulatory system of *Escherichia coli*. *Mol. Microbiol.* **48**: 657-670.

Wennerhold J & Bott M (2006) The DtxR regulon of *Corynebacterium glutamicum*. *J. Bacteriol.* **188**: 2907-2918.

Wieschalka S, Blombach B, Bott M & Eikmanns BJ (2013) Bio-based production of organic acids with *Corynebacterium glutamicum*. *Microb. Biotechnol.* **6**: 87-102.

Wijayarathna CD, Wachi M & Nagai K (2001) Isolation of *ftsI* and *murE* genes involved in peptidoglycan synthesis from *Corynebacterium glutamicum*. *Appl. Microbiol. Biotechnol.* **55**: 466-470.

Wurm R, Neusser T & Wagner R (2010) 6S RNA-dependent inhibition of RNA polymerase is released by RNA-dependent synthesis of small de novo products. *Biol. Chem.* **391**: 187-196.

Xie X, Xu L, Shi J, Xu Q & Chen N (2012) Effect of transport proteins on L-isoleucine production with the L-isoleucine-producing strain *Corynebacterium glutamicum* YILW. *J. Ind. Microbiol. Biotechnol.* **39**: 1549-1556.

Zemanová M, Kaderábková P, Pátek M, Knoppová M, Silar R & Nesvera J (2008) Chromosomally encoded small antisense RNA in *Corynebacterium glutamicum*. *FEMS Microbiol. Lett.* **279**: 195-201.

Zhang A, Altuvia S, Tiwari A, Argaman L, Hengge-Aronis R & Storz G (1998) The OxyS regulatory RNA represses rpoS translation and binds the Hfq (HF-I) protein. *EMBO J.* **17**: 6061-6068.

6 Appendix

6.1 Number of 6C RNA molecules per cell

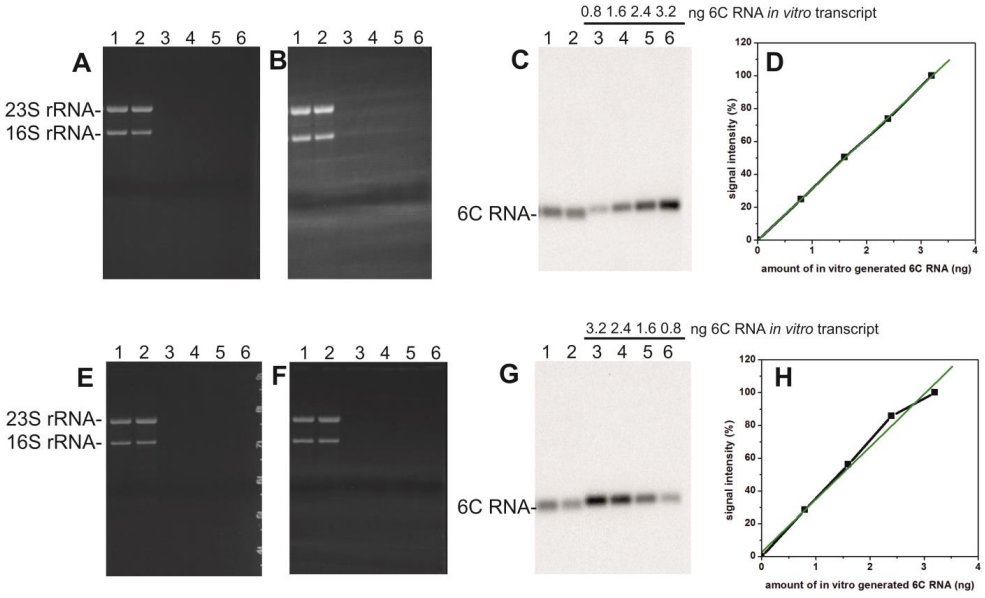

Figure A 1 Northern blot analysis for the quantification of the 6C RNA in *C. glutamicum*. Two independent experiments are shown (A to D and E to H). For the first experiment (A to D) *C. glutamicum* ATCC 13032 was cultivated in CGXII medium with 4% (w/v) glucose to OD_{600} = 5.2 (exponential phase) or OD_{600} = 49.0, (stationary phase), respectively. Then, 20 ml or 2.1 ml culture, respectively, were withdrawn and used for the preparation of total RNA. For the second experiment (E to H) *C. glutamicum* ATCC 13032 was cultivated in CGXII medium with 4% (w/v) glucose to OD_{600} = 5.0 (exponential phase) or OD_{600} = 43.2, (stationary phase), respectively. Then, 25 ml or 2.9 ml culture, respectively, were withdrawn and used for the preparation of total RNA. Total RNA was separated on a 1.5% agarose gel alongside purified 6C RNA *in vitro* transcript (A and E), transferred from the agarose gel onto a nylon membrane (B and F) and subsequently the 6C RNA in the total RNA samples, as well as the 6C RNA *in vitro* transcript, was visualized by a complementary ss-DIG-labeled specific DNA probe (C and G). The 16S rRNA was used as loading control on the agarose gel and as transfer control from the agarose gel onto the nylon membrane. Lanes 1 and 2: 1.0 µg of total RNA isolated from *C. glutamicum*, in the exponential and stationary phase, respectively, lanes 3 to 6: 0.8 ng to 3.2 ng of *in vitro* synthesized and purified 6C RNA. The signal intensities of the 6C RNA bands were determined with the AIDA software. The highest amount of *in vitro* transcript was set to 100%. From the signal intensities and the respective amounts of 6C RNA *in vitro* transcript a calibration curve was prepared (D and H).

6.2 Putative transcriptional regulators of the 6C RNA

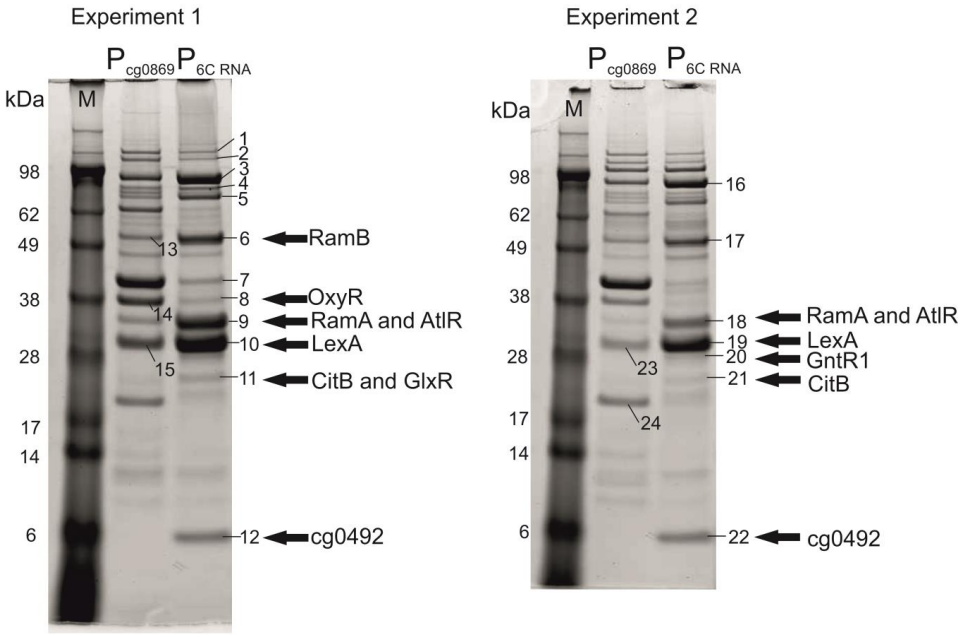

Figure A 2 SDS-gel analysis of eluted proteins after DNA affinity chromatography with the 6C RNA promoter region ($P_{6C\ RNA}$) of *C. glutamicum*. Shown are 10% SDS gels loaded with the elution fractions of $P_{6C\ RNA}$ and of P_{cg0896} which was used as a control. The biotinylated bead-bound PCR products of the respective promoter region were incubated with protein crude extract of *C. glutamicum* cultivated in CGXII minimal medium with 4% (w/v) glucose to an OD_{600} of 5 - 6. Unbound or weakly bound proteins were removed by several washing steps. Proteins which bound specifically to the $P_{6C\ RNA}$ and P_{cg0896} were eluted with TGED-buffer with 2 M NaCl, precipitated by TCA and separated by SDS PAGE. M: SeeBlue Plus2 Pre-stained standard. Arrows indicate transcriptional regulators identified in the elution fraction of the $P_{6C\ RNA}$ by peptide mass fingerprinting. Shown are the results of two independent experiments. The 10% SDS gels were stained with Coomassie Brilliant Blue and scanned with the Typhoon scanner.

Table A 1 Proteins which could be reliably identified by peptide mass fingerprinting in the elution fractions of $P_{6C\ RNA}$ and P_{cg0896} in DNA affinity chromatography experiments. Results with a MOWSE score ≥ 46 were regarded as significant, in case of scores <46, at least 25% of the respective protein sequence had to be covered with the identified peptides. Proteins are sorted by spot number (Figure A 2). Proteins labeled with an asterisk are transcriptional regulators that could be eluted with the $P_{6C\ RNA}$ and identified by peptide mass fingerprint in two independent DNA affinity chromatography experiments.

Protein band	Locus tag		Annotation	Theoretical MW
1	cg0577	RpoC	DNA-directed RNA polymerase β' subunit	147.9 kDa
2	cg0576	RpoB	DNA-directed RNA polymerase β subunit	128.8 kDa
1,2	cg0373	TopA	DNA topoisomerase I	109.6 kDa
3, 16	cg1525	PolA	DNA polymerase I	96.8 kDa
4	cg2064		putative DNA topoisomerase I omega-protein	84.0 kDa
4	cg1290	MetE	5-methyltetrahydropteroyltriglutamate--homocysteine methyltransferase	81.6 kDa
5	cg1805	PriA	primosome assembly protein PriA or N' replication factor Y, helicase superfamily II-type	75.0 kDa
5	cg0889		putative DNA helicase RecQ	75.4 kDa
6	cg0444	RamB	transcriptional regulator, involved in acetate metabolism, MerR-family	54.0 kDa
6,13,17	cg2321		putative DNA polymerase III ε subunit or related 3'-5' exonuclease	51.4 kDa
7	cg1997	CglIR	type II restriction endonuclease	39.9 kDa
8,14	cg2109	OxyR	hydrogen peroxide sensing regulator, Lys-family	35.0 kDa
9,15,18	cg2831	RamA*	transcriptional regulator, acetate metabolism, LuxR-family	31.0 kDa
9,18	cg0146	AltR*	transcriptional regulator for arabitol metabolism, DeoR-family	31.0 kDa
10,19,23	cg3307	Ssb	single-strand DNA-binding protein	23.3 kDa
10,19	cg2114	LexA*	transcriptional repressor/regulator, involved in SOS/stress response, LexA-family	27.3 kDa
11,21	cg0090	CitB*	two component response regulator, citrate homeostasis	23.4 kDa
11	cg0350	GlxR	cAMP-dependent global transcriptional regulator, Crp-family	25.0 kDa
12,22	cg0492	Cg0492*	putative DNA-binding excisionase protein, extremely conserved	7.0 kDa
20	cg2783	GntR1	gluconate-responsive repressor 1, repressor of genes involved in gluconate catabolism and the pentose phosphate pathway, GntR-family	27.2 kDa
24	cg1870	RuvA	holliday junction DNA helicase motor protein	21.6 kDa

6.3 The SOS response is altered in the ∆6CiP mutant

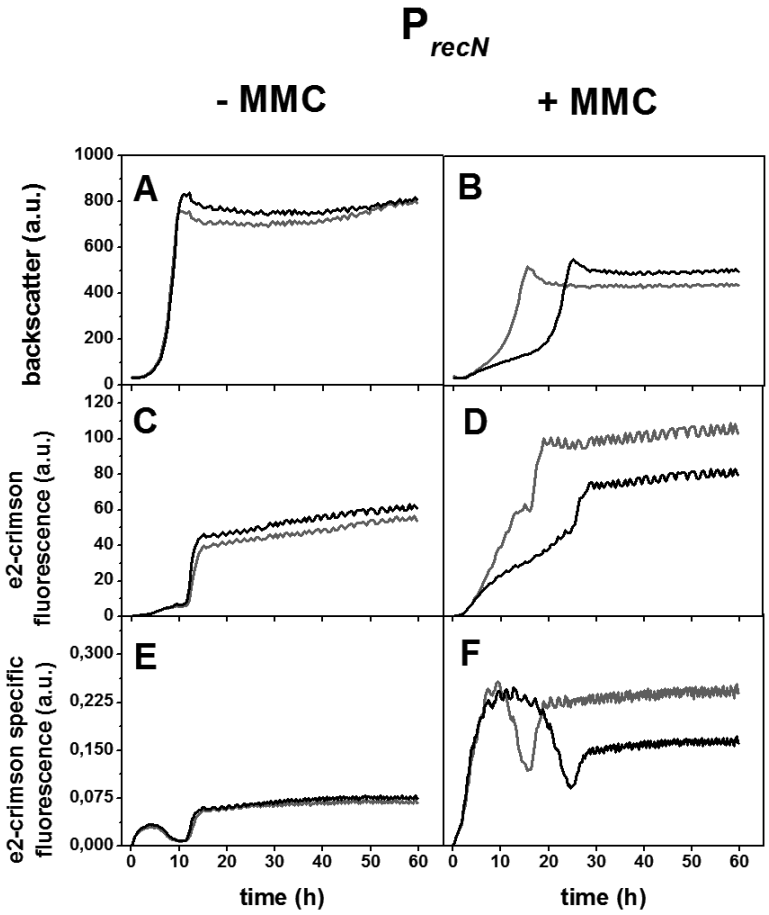

Figure A 3 E2-crimson expression analysis under the control of P_{recN} (A – F) in the absence (A, C, E) or presence (B, D, F) of 0.4 µM MMC. Shown are the growth (backscatter signal of 620 nm light) (A, B), the E2-crimson fluorescence (C, D) and the specific fluorescence (E, F) of recombinant *C. glutamicum*/pJC1-P_{recN}-*e2-crimson* (grey line A – F) and ∆6CiP/pJC1-P_{recN}-*e2-crimson* (black line A – F). The specific fluorescence was calculated as the ratio of fluorescence signal to the backscatter signal (given in arbitrary units, a.u.). Cells were inoculated to an OD_{600} of 1 and cultivated in 750 µl of CGXII minimal medium with 4% (w/v) glucose at 30°C and 1,200 rpm. Shown are the average values of two technical replicates representative for two independent biological experiments giving comparable results.

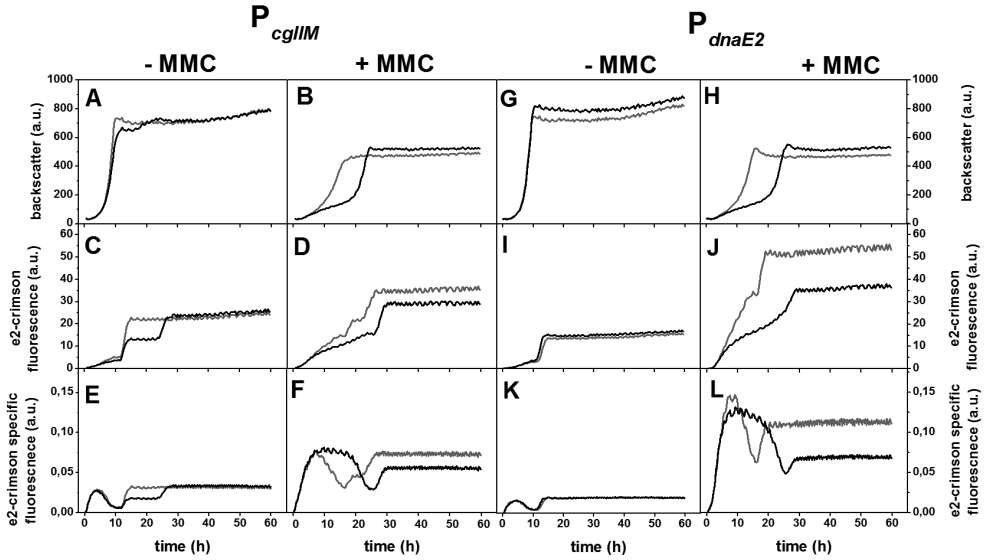

Figure A 4 E2-crimson expression analysis under the control of P_{cglIM} (A – F) in the absence (A, C, E) or presence (B, D, F) of 0.4 µM MMC and E2-crimson expression analysis under the control of P_{dnaE2} (G – L) in the absence (G, I, K) or presence (H, J, L) of 0.4 µM MMC. Shown are the growth (backscatter signal of 620 nm light) (A, B, G, H), the E2-crimson fluorescence (C, D, I, J) and the specific fluorescence (E, F, K, L) of recombinant *C. glutamicum*/pJC1-P_{cglIM}-*e2-crimson* (grey line A – F) and Δ6CiP/pJC1-P_{dnaE2}-*e2-crimson* (black line A – F) and recombinant *C. glutamicum*/pJC1-P_{dnaE2}-*e2-crimson* (grey line G – L) and Δ6CiP/pJC1-P_{dnaE2}-*e2-crimson* (black line G – L). The specific fluorescence was calculated as the ratio of fluorescence signal to the backscatter signal (given in arbitrary units, a.u.). Cells were inoculated to an OD_{600} of 1 and cultivated in 750 µl of CGXII minimal medium with 4% (w/v) glucose at 30°C and 1,200 rpm. Shown are the average values of two technical replicates representative for two independent biological experiments giving comparable results.

6.4 Characterization of the downstream genes of the 6C RNA

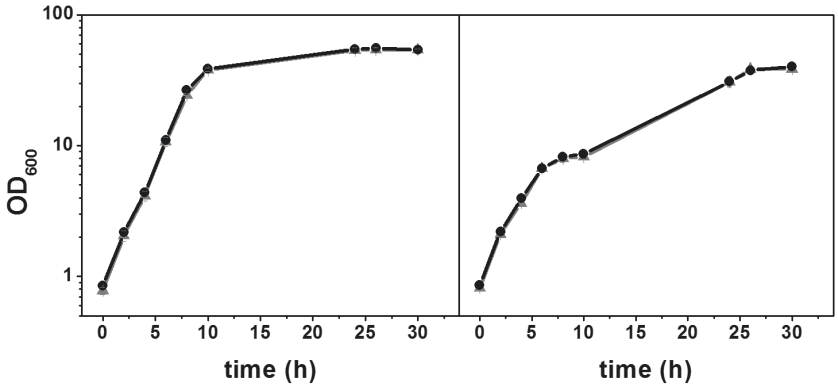

Figure A 5 Growth of *C. glutamicum* ATCC 13032 and ΔOP_cg0362. Strains were cultivated in shaking flasks in CGXII minimal medium with 4% (w/v) glucose at 30°C and 120 rpm. **A** *C. glutamicum* wild type (▲) and *C. glutamicum* Δ**OP_cg0362** (●). **B** *C. glutamicum* wild type (▲) and *C. glutamicum* Δ**OP_cg0362** (●) with 0.75 µM MMC. Average values and standard deviations of three independent cultivation experiments are shown.

6.5 Deletion and overexpression of *whcD*

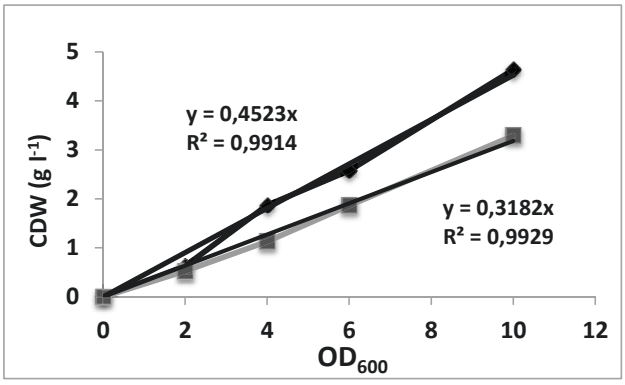

Figure A 6 Analysis of the relation between CDW and optical density for *C. glutamicum* wild type (grey) and *C. glutamicum* Δ*whcD* (black).

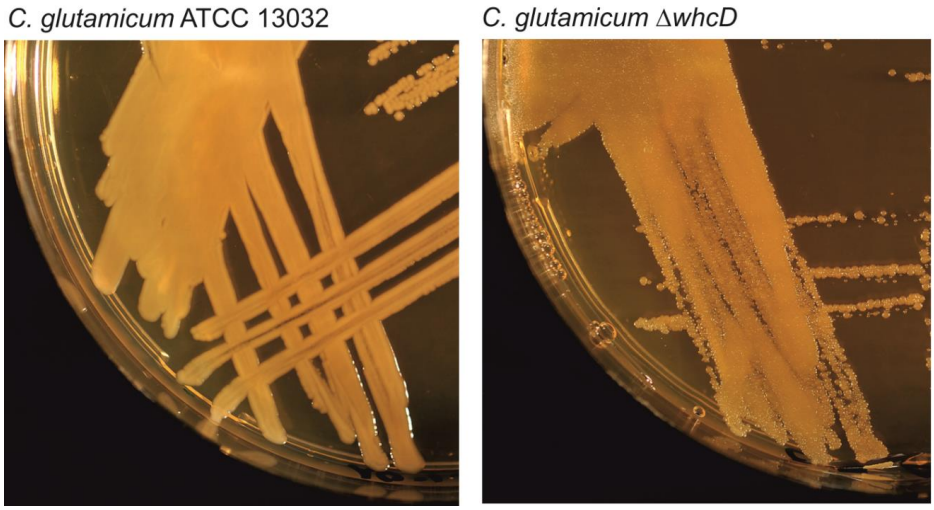

Figure A 7 BHI+10% sucrose agar plates after cultivation for three days at 30°C with *C. glutamicum* ATCC 13032 (left) and *C. glutamicum* Δ*whcD* (right).

6.6 Effect of 6C RNA on amino acid production in *C. glutamicum*

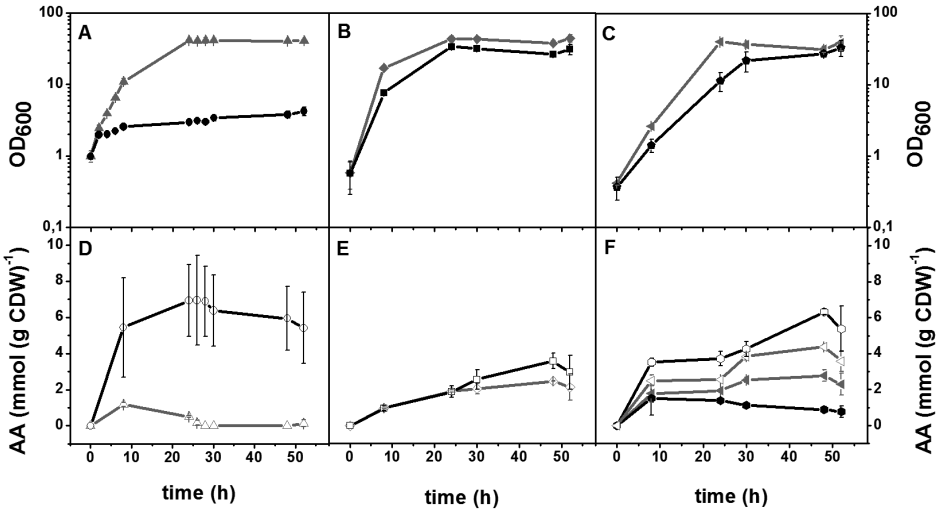

Figure A 8 Growth (closed symbols) and biomass specific amino acid production (open symbols) of different *C. glutamicum* derivatives. Strains were cultivated in CGXII medium with 4% (w/v) glucose, 25 µg ml^{-1} kanamycin at 30°C and 120 rpm. The average values and the standard deviation of three independent experiments are shown. A Growth of *C. glutamicum*/ pJC1 (▲) and *C. glutamicum*/ pJC1-6C (●) in the presence of 500 µg ml^{-1} ethambutol. B Growth of *C. glutamicum* DM1800/ pJC1 (♦) and *C. glutamicum* DM1800/ pJC1-6C (■). C Growth of *C. glutamicum* MV-ValLeu33/ pJC1 (◄) and *C. glutamicum* MV-ValLeu33/ pJC1-6C (●). D Biomass-specific L-glutamate production of *C. glutamicum* pJC1 and *C. glutamicum*/ pJC1-6C. E Biomass-specific L-lysine production of *C. glutamicum* DM1800/ pJC1 and *C. glutamicum* DM1800/ pJC1-6C. F Biomass-specific L-valine (closed symobols) and L-leucine (open symbols) production of *C. glutamicum* MV-ValLeu33/ pJC1 and *C. glutamicum* MV-ValLeu33/ pJC1-6C.

6.7 Transcriptome analysis

Table A 2 Differentially expressed genes revealed by comparative transcriptome analysis of the Δ6CiP mutant and *C. glutamicum* wild type with 0.75 µM MMC. Given are the locus tag, the gene name, the annotation, the average mRNA ratios and *p*-values. The average mRNA ratio and *p*-value were calculated from three independent experiments.

Locus tag	Gene	Annotation	mRNA ratio Δ6CiP vs. WT	p-value
cg0507		putative ABC-type putative spermidine/putrescine/ironIII transporter, permease subunit	0.41	0.03
cg0508		putative ABC-type putative spermidine/putrescine/ironIII transporter, substrate-binding lipoprotein	0.45	0.00
cg0587	*tuf*	elongation factor Tu	0.39	0.04
cg0831	*tusG*	trehalose uptake system, ABC-type, permease protein	0.44	0.00
cg0832	*tusF*	trehalose uptake system, ABC-type, membrane spanning protein	0.48	0.01
cg0833		putative membrane protein, involved in trehalose uptake, conserved	0.50	0.01
cg0834	*tusE*	trehalose uptake system, ABC-type, bacterial extracellular solute-binding protein	0.47	0.01
cg0952		putative integral membrane protein	0.46	0.02
cg0953	*mctC*	monocarboxylic acid transporter	0.42	0.00
cg1214	*nadS*	cysteine desulfurase-like protein involved in Fe-S cluster assembly, required for maturation of NadA	0.36	0.03
cg1215	*nadC*	quinolinate phosphoribosyltransferase	0.38	0.02
cg1216	*nadA*	quinolinate synthetase	0.38	0.01
cg1218	*ndnR*	transcriptional repressor of NAD de novo biosynthesis genes ndnR-nadA-nadC-nadS operon, NrtR-family	0.46	0.01
cg1255		putative HNH endonuclease, conserved	4.65	0.00
cg1290	*metE*	5-methyltetrahydropteroyltriglutamate--homocysteine methyltransferase	0.32	0.00
cg1897		putative secreted protein CGP3 region	2.70	0.01
cg1903		putative ABC-type multidrug transport system, ATPase component CGP3 region	2.04	0.00
cg1910		putative secreted or membrane protein CGP3 region	2.15	0.00
cg1911		putative secreted protein CGP3 region	2.37	0.01
cg1917		hypothetical protein CGP3 region	2.48	0.00
cg1936		putative secreted protein CGP3 region	2.51	0.01
cg1937		putative secreted protein CGP3 region	2.23	0.02
cg1940		putative secreted protein CGP3 region	2.38	0.02
cg1941		putative secreted protein CGP3 region	2.23	0.02
cg1954		hypothetical protein CGP3 region	2.94	0.05
cg1961		hypothetical protein CGP3 region	2.01	0.04
cg1962		putative membrane protein CGP3 region	2.27	0.01
cg1967		hypothetical protein CGP3 region	2.22	0.02
cg1975		hypothetical protein, conserved CGP3 region	2.25	0.04
cg1999		hypothetical protein CGP3 region	2.66	0.01
cg2005		putative protein-plasmid encoded, conserved CGP3 region	2.15	0.01
cg2006		hypothetical protein CGP3 region	2.08	0.00
cg2007		putative membrane protein CGP3 region	2.01	0.00
cg2008		putative membrane protein CGP3 region	2.04	0.01
cg2009		putative CLP-family ATP-binding protease CGP3 region	2.35	0.01
cg2010		putative permease of the major facilitator superfamily CGP3 region	2.04	0.00
cg2011		putative membrane protein CGP3 region	2.01	0.00
cg2014		hypothetical protein CGP3 region	2.27	0.01
cg2015		hypothetical protein CGP3 region	2.12	0.00
cg2016		hypothetical protein CGP3 region	2.08	0.00
cg2017		hypothetical protein CGP3 region	2.65	0.01
cg2018		putative membrane protein CGP3 region	2.84	0.01
cg2019		putative membrane protein CGP3 region	2.19	0.01
cg2020		putative membrane protein CGP3 region	3.10	0.00
cg2022		putative secreted protein CGP3 region	3.01	0.01
cg2028		hypothetical protein CGP3 region	2.22	0.01

cg2032		putative membrane protein CGP3 region	2.38	0.02
cg2034		hypothetical protein CGP3 region	2.64	0.00
cg2037		hypothetical protein, conserved CGP3 region	2.64	0.02
cg2051		hypothetical protein CGP3 region	2.90	0.00
cg2053		putative membrane protein CGP3 region	2.03	0.01
cg2055		putative membrane protein CGP3 region	2.09	0.00
cg2056		putative membrane protein CGP3 region	2.96	0.01
cg2057		putative secreted protein CGP3 region	3.21	0.00
cg2062		putative protein, similar to plasmid-encoded protein PXO2.09 CGP3 region	2.51	0.00
cg2064		putative DNA topoisomerase I omega-protein CGP3 region	2.15	0.01
cg2069	*psp1*	putative secreted protein CGP3 region	3.12	0.01
cg2071	*int2'*	putative phage integrase N-terminal fragment, CGP3 region	2.10	0.01
cg2080		hypothetical protein, conserved	2.30	0.00
cg2106		hypothetical protein, conserved	2.16	0.00
cg2136	*gluA*	glutamate uptake system, ABC-type, ATP-binding protein	0.49	0.01
cg2157	*terC*	tellurium resistance membrane protein	2.38	0.01
cg2182	*oppB*	ABC-type peptide transport system, permease component	0.32	0.00
cg2183	*oppC*	ABC-type peptide transport system, permease component	0.05	0.01
cg2184	*oppD*	ATPase component of peptide ABC-type transport system, contains duplicated ATPase domains	0.04	0.01
cg2470		putative secreted branched-chain amino acid ABC transporter substrate-binding protein	0.47	0.01
cg2560	*aceA*	isocitrate lyase	0.35	0.02
cg2618	*vanK*	transporter vanillate/protocatechuate	0.38	0.01
cg2631	*pcaH*	protocatechuate dioxygenase β subunit	3.57	0.00
cg2633		putative restriction endonuclease	10.37	0.00
cg2636	*catA1*	catechol 1,2-dioxygenase	0.36	0.00
cg2701		putative membrane protein	0.41	0.03
cg2703		putative ABC-type putative sugar transporter, permease subunit	0.32	0.03
cg2704		putative ABC-type putative sugar transporter, permease subunit	0.45	0.00
cg2707		hypothetical protein, conserved	0.46	0.01
cg2708	*msiK1*	ABC-type sugar transport system, ATPase component	0.45	0.00
cg2828		putative membrane protein	2.06	0.04
cg2894	*cgmR*	multidrugresistance-related transcription factor, TetR-family	0.20	0.04
cg2937		putative ABC-type dipeptide/oligopeptide/nickel transport system, secreted component	0.44	0.01
cg3009	*porH*	main cell wall channel protein	0.49	0.04
cg3016		hypothetical protein	0.45	0.04
cg3047	*ackA*	acetate kinase	0.42	0.03
cg3048	*pta*	phosphotransacetylase, phosphate acetyltransferase	0.44	0.01
cg3107	*adhA*	Zn-dependent alcohol dehydrogenase	0.43	0.00
cg3112	*cysZ*	Sulfate transporter, loss causes sulfide/cysteine auxotrophy ((info from genome reduction project))	0.41	0.00
cg3113	*cysY*	Sirohydrochlorin ferrochelatase	0.49	0.00
cg3114	*cysN*	sulfate adenyltransferase subunit 1	0.49	0.00
cg3118	*cysI*	sulfite reductase hemoprotein, ferredoxin-sulfite reductase	0.48	0.02
cg3119	*cysJ*	sulfite reductase flavoprotein, Ferredoxin-NADP+ reductase	0.46	0.02
cg3195		putative flavin-containing monooxygenase FMO	0.27	0.02
cg3212		putative carboxymuconolactone decarboxylase subunit	0.44	0.02
cg3390		putative myo-Inositol catabolism, sugar phosphate isomerase/epimerase	0.40	0.04

Table A 3 Differentially expressed genes revealed by comparative transcriptome analysis of *C. glutamicum*/pJC1-6C and *C. glutamicum*/ pJC1 with 0.75 µM MMC. Given are the locus tag, the gene name, the annotation, the average mRNA ratios and *p*-values. The average mRNA ratio and *p*-value were calculated from three independent experiments.

Locus tag	Gene	Annotation	mRNA ratio WT/pJC1-6C vs. WT/pJC1	p-value
cg0031		putative reductase, related to diketogulonate reductase	0.26	0.01
cg0044	*rbsB*	putative periplasmic D-ribose-binding protein	0.45	0.01
cg0045		putative ABC transport protein, sugar transport, membrane component	0.46	0.00
cg0046		putative ABC transport protein, ATP-binding component	0.36	0.01
cg0077		hypothetical protein, VTC domain, conserved	0.19	0.01
cg0078		putative membrane protein	0.21	0.01
cg0079		putative secreted protein, CotH homolog	0.32	0.00
cg0083		putative nicotinamide mononucleotide uptake permease, nicotinamide mononucleotide NMN uptake permease, PnuC-family	0.47	0.01
cg0096		hypothetical protein, conserved	0.50	0.01
cg0183		putative LysE-type translocator, threonine efflux transporter, resistance to homoserine/threonine RhtB-family	0.44	0.00
cg0229	*gltB*	glutamine 2-oxoglutarate aminotransferase NADPH large subunit, also glutamate synthase	0.45	0.01
cg0230	*gltD*	glutamine 2-oxoglutarate aminotransferase NADPH small subunit, also glutamate synthase	0.40	0.01
cg0252		putative membrane protein	0.33	0.01
cg0269		hypothetical protein, conserved	0.26	0.00
cg0275	*mgtE2*	Mg^{2+} transporter, MgtE-family	0.29	0.00
cg0291		putative 3,4-dioxygenase β subunit	0.48	0.04
cg0308		putative membrane protein	0.48	0.00
cg0340		putative sugar/metabolite permease, MFS-type	2.41	0.00
cg0426	*tnp17a*	transposase fragment	0.49	0.00
cg0455		putative permease, major facilitator superfamily	0.50	0.00
cg0578		putative membrane protein	0.47	0.03
cg0637	*betB*	putative βine aldehyde dehydrogenase BADH oxidoreductase	3.31	0.00
cg0638		putative HD superfamily hydrolase	4.00	0.00
cg0639		putative ferredoxin reductase	4.70	0.00
cg0640	*fdxB*	ferredoxin no. 2, 2Fe-2S	3.88	0.00
cg0641	*fabG2*	probable short-chain dehydrogenase, secreted	5.07	0.00
cg0642		putative PEP-utilizing enzyme, probably DNA binding, conserved	5.48	0.00
cg0644		putative pyruvate phosphate dikinase, PEP/pyruvate binding	5.50	0.00
cg0645	*cytP*	cytochrome P450	5.61	0.00
cg0676		hypothetical protein, conserved	0.47	0.00
cg0706		putative membrane protein, conserved	0.40	0.01
cg0707	*esrS*	two component sensor kinase	0.48	0.01
cg0714		putative polymerase involved in DNA repair	0.41	0.01
cg0738	*dnaE2*	DNA polymerase III subunit α	0.24	0.00
cg0753		putative secreted protein	0.45	0.01
cg0756	*cspA*	carbon starvation protein A	2.06	0.01
cg0759	*prpD2*	2-methycitrate dehydratase	4.43	0.00
cg0760	*prpB2*	2-methylisocitrate lyase	4.23	0.01
cg0762	*prpC2*	2-methylcitrate synthase,	3.76	0.01
cg0772		putative sugar efflux permease, MFS-type	0.47	0.00
cg0796	*prpD1*	2-methycitrate dehydratase	2.67	0.00
cg0797	*prpB1*	2-methylisocitrate lyase	3.12	0.00
cg0850	*whcD*	transcription factor,	0.31	0.01
cg0851		hypothetical protein	0.32	0.01
cg0852		hypothetical protein, conserved	0.50	0.01
cg0875		hypothetical protein, conserved	0.16	0.00
cg0878	*whcE*	transcriptional regulator	0.46	0.00

cg0905	*psp2*	putative secreted protein	0.45	0.01
cg0907		hypothetical protein	0.24	0.00
cg0921		putative cytoplasmic siderophore-interacting protein	3.21	0.00
cg0922		putative secreted siderophore-binding lipoprotein	3.51	0.00
cg0938	*cspB*	cold shock protein	0.44	0.01
cg0961		putative homoserine O-acetyltransferase	5.85	0.00
cg0962		putative secreted protein	2.00	0.00
cg0974		hypothetical protein, conserved	2.31	0.00
cg0996	*cgtR2*	two component response regulator	0.45	0.03
cg0997	*cgtS2*	two component sensor kinase	0.36	0.02
cg0998		putative trypsin-like serine protease PepD,	0.39	0.03
cg1059		hypothetical protein, conserved	0.14	0.00
cg1077		putative permease of the major facilitator superfamily	2.45	0.00
cg1080		putative multicopper oxidase	2.01	0.01
cg1081		putative ABC-type multidrug transport system, ATPase component	2.03	0.00
cg1087		putative membrane protein	2.38	0.00
cg1090	*ggtB*	probable γ-glutamyltranspeptidase precursor PR	2.00	0.00
cg1091		hypothetical protein	0.30	0.01
cg1097		hypothetical protein	2.04	0.00
cg1100		putative ABC transporter transmembrane component	2.00	0.00
cg1120	*ripA*	transcriptional regulator of iron proteins and repressor of aconitase, AraC-family	2.10	0.01
cg1153	*seuC*	FMNH2-dependent monooxygenase	0.40	0.00
cg1159		putative secreted protein	2.43	0.00
cg1202		hypothetical protein, conserved	3.21	0.00
cg1203		putative Mg-chelatase subunit ChlI	2.15	0.00
cg1205		putative protein	2.10	0.00
cg1214	*nadS*	cysteine desulfurase-like protein involved in Fe-S cluster assembly	2.75	0.00
cg1215	*nadC*	quinolinate phosphoribosyltransferase	2.39	0.00
cg1216	*nadA*	quinolinate synthetase	2.71	0.00
cg1218	*ndnR*	transcriptional repressor of NAD de novo biosynthesis genes ndnR-nadA-nadC-nadS operon, NrtR-family	2.77	0.00
cg1221		hypothetical protein, conserved	2.02	0.00
cg1222	*lplA*	lipoate-protein ligase A	2.09	0.01
cg1224	*pPhnB*	similarity to alkylphosphonate uptake operon protein PhnB-Escherichia coli, conserved	2.45	0.00
cg1225	*benK3*	putative benzoate transport transmembrane protein	2.35	0.00
cg1226	*pobB*	4-hydroxybenzoate 3-monooxygenase	2.85	0.00
cg1232		putative protein, conserved, LmbE-family	0.49	0.05
cg1237		putative membrane protein	2.35	0.00
cg1255		putative HNH endonuclease, conserved	0.26	0.00
cg1290	*metE*	5-methyltetrahydropteroyltriglutamate--homocysteine methyltransferase	2.01	0.00
cg1291		putative membrane protein	0.29	0.00
cg1307		putative superfamily II DNA and RNA helicase	0.50	0.02
cg1309	*rolH*	3-3-hydroxyphenylpropionate hydroxylase or 2-polyprenyl-6-methoxyphenol hydroxylase and related FAD-dependent oxidoreductase	2.73	0.00
cg1310	*rolM*	maleylacetate reductase	2.38	0.01
cg1314	*putP*	proline transport system	2.11	0.00
cg1325		putative stress-responsive transcriptional regulator, conserved	0.44	0.02
cg1332		putative secreted hydrolase	2.49	0.00
cg1397	*trmU*	tRNA 5-methylaminomethyl-2-thiouridylate-methyltransferase	0.45	0.03
cg1410	*rbsR*	transcriptional repressor of of the ribose importer RbsACBD, LacI-family	2.11	0.00
cg1411	*rbsA*	ribose/xylose transporter, ABC-type sugar aldose transport system, ATPase component	2.06	0.00
cg1412	*rbsC*	ribose/xylose transporter, ABC-type transport system, permease component	2.17	0.00
cg1413	*rbsB*	ribose/xylose transport, secreted sugar-binding protein	2.44	0.00
cg1414	*rbsD*	ribose/xylose transport system, ABC-type transport system,	2.27	0.00

		uncharacterized component		
cg1440		putative ABC-type nitrate/sulfonate/taurine/bicarbonate transport system, ATPase component N-terminal fragment	0.10	0.04
cg1454		putative aliphatic sulfonates uptake ABC transporter secreted solute-binding protein	2.32	0.00
cg1498		putative RecG-like helicase	2.55	0.00
cg1508		putative pseudogene - similar to Psp1 CGP1 region	0.23	0.01
cg1509		hypothetical protein CGP1 region	0.30	0.02
cg1513	*tnp23a*	transposase, putative pseudogene CGP1 region	2.07	0.00
cg1514		putative secreted protein CGP1 region	2.31	0.03
cg1523		hypothetical protein, conserved CGP1 region	0.43	0.02
cg1541		putative pseudogene, conserved protein	2.41	0.00
cg1542		putative membrane protein	2.97	0.00
cg1543	*uriH*	inosine-uridine preferring nucleoside hydrolase	2.04	0.00
cg1548		hypothetical protein, conserved	2.07	0.00
cg1553	*qor2*	Quinone oxidoreductase, involve in disulfide stress response	0.42	0.00
cg1567		hypothetical protein	0.46	0.03
cg1572	*glpQ2*	putative glycerophosphoryl diester phosphodiesterase 2	2.06	0.01
cg1595	*uspA2*	universal stress protein no. 2, nucleotide-binding protein	2.26	0.01
cg1612		putative acetyltransferase	4.35	0.00
cg1616	*cmk*	cytidylate kinase	0.49	0.01
cg1618		hypothetical protein, conserved	2.47	0.00
cg1619		putative DNA gyrase inhibitor or transcriptional regulator, AraC-family	2.17	0.00
cg1628		putative hydrolase of the α/β superfamily	0.44	0.03
cg1640		putative membrane protein containing CBS domain	2.00	0.02
cg1657	*ufaA*	putative cyclopropane fatty acid synthase cyclopropane-fatty-acyl-phospholipid synthase	2.02	0.00
cg1665		putative secreted protein	2.75	0.00
cg1682		putative trypsin-like serine protease	2.26	0.00
cg1785	*amtA*	high-affinity ammonia permease	0.32	0.02
cg1864		putative ABC-type dipeptide/oligopeptide/nickel transport systems, secreted component	0.34	0.01
cg1881		putative iron-dependent peroxidase, secreted protein, conserved	0.21	0.00
cg1883		putative secreted protein	0.20	0.01
cg1884		putative copper resistance protein C	0.21	0.01
cg1890	*alpC*	actin-like protein CGP3 region	0.02	0.00
cg1891	*alpA*	putative phage DNA adapter protein CGP3 region	0.01	0.00
cg1892		hypothetical protein, conserved CGP3 region	0.45	0.00
cg1893		putative N-acetyltransferase CGP3 region	0.40	0.00
cg1895		putative secreted protein CGP3 region	0.07	0.00
cg1896		putative secreted protein CGP3 region	0.01	0.01
cg1897		putative secreted protein CGP3 region	0.00	0.00
cg1898		hypothetical protein CGP3 region	0.05	0.00
cg1899		hypothetical protein CGP3 region	0.03	0.00
cg1900		hypothetical protein CGP3 region	0.04	0.00
cg1901		hypothetical protein CGP3 region	0.23	0.00
cg1902		putative secreted protein CGP3 region	0.28	0.01
cg1903		putative ABC-type multidrug transport system, ATPase component CGP3 region	0.39	0.04
cg1909		hypothetical protein CGP3 region	0.35	0.01
cg1910		putative secreted or membrane protein CGP3 region	0.34	0.03
cg1911		putative secreted protein CGP3 region	0.46	0.04
cg1912		hypothetical protein CGP3 region	0.27	0.01
cg1913		hypothetical protein CGP3 region	0.09	0.00
cg1914		hypothetical protein CGP3 region	0.04	0.00
cg1915		hypothetical protein CGP3 region	0.04	0.00
cg1916		hypothetical protein CGP3 region	0.04	0.00
cg1917		hypothetical protein CGP3 region	0.14	0.00
cg1918		putative secreted protein CGP3 region	0.01	0.01
cg1919		putative membrane protein CGP3 region	0.03	0.00
cg1920		hypothetical protein CGP3 region	0.03	0.00

cg1921		hypothetical protein CGP3 region	0.03	0.00
cg1922		hypothetical protein CGP3 region	0.03	0.00
cg1923		hypothetical protein CGP3 region	0.03	0.00
cg1924		hypothetical protein CGP3 region	0.03	0.00
cg1925		hypothetical protein CGP3 region	0.11	0.00
cg1926		hypothetical protein CGP3 region	0.07	0.00
cg1927		putative molecular chaperone CGP3 region	0.07	0.00
cg1928		hypothetical protein CGP3 region	0.05	0.00
cg1929	*res*	resolvase,-family recombinase CGP3 region	0.05	0.00
cg1930		putative secreted hydrolase CGP3 region	0.11	0.01
cg1931		putative secreted protein CGP3 region	0.11	0.01
cg1932	*ppp2*	putative protein phosphatase CGP3 region	0.04	0.00
cg1934		hypothetical protein CGP3 region	0.02	0.00
cg1935	*gntR2*	gluconate-responsive repressor 2, repressor of genes involved in gluconate catabolism and the pentose phosphate pathway CGP3 region, GntR-family	0.13	0.00
cg1936		putative secreted protein CGP3 region	0.01	0.00
cg1937		putative secreted protein CGP3 region	0.03	0.00
cg1938		hypothetical protein CGP3 region	0.07	0.00
cg1940		putative secreted protein CGP3 region	0.05	0.00
cg1941		putative secreted protein CGP3 region	0.03	0.00
cg1942		putative secreted protein CGP3 region	0.48	0.02
cg1944		hypothetical protein CGP3 region	0.20	0.00
cg1945		hypothetical protein, conserved CGP3 region	0.22	0.01
cg1946		hypothetical protein CGP3 region	0.29	0.01
cg1947		hypothetical protein CGP3 region	0.27	0.02
cg1948		hypothetical protein CGP3 region	0.18	0.00
cg1949		hypothetical protein CGP3 region	0.28	0.01
cg1950	*tnp14b*	transposase fragment CGP3 region	0.23	0.01
cg1951	*tnp14a*	transposase fragment CGP3 region	0.20	0.01
cg1954		hypothetical protein CGP3 region	0.03	0.00
cg1955		putative secreted protein CGP3 region	0.01	0.00
cg1956	*recJ*	single-stranded-DNA-specific exonuclease CGP3 region	0.02	0.00
cg1957		hypothetical protein CGP3 region	0.02	0.00
cg1959	*priP*	prophage DNA primase CGP3 region	0.03	0.00
cg1960		hypothetical protein CGP3 region	0.02	0.00
cg1961		hypothetical protein CGP3 region	0.05	0.00
cg1962		putative membrane protein CGP3 region	0.36	0.00
cg1963		putative superfamily II DNA/RNA helicase CGP3 region	0.05	0.00
cg1964		hypothetical protein CGP3 region	0.05	0.00
cg1965		putative protein, similarity to gp57-phage N15 CGP3 region	0.12	0.00
cg1966		hypothetical protein CGP3 region	0.10	0.00
cg1967		hypothetical protein CGP3 region	0.01	0.00
cg1968		hypothetical protein CGP3 region	0.01	0.00
cg1969		hypothetical protein CGP3 region	0.01	0.00
cg1970		hypothetical protein CGP3 region	0.01	0.00
cg1971		hypothetical protein CGP3 region	0.02	0.00
cg1972		putative translation elongation factor, GTPase CGP3 region	0.07	0.01
cg1974		putative protein, contains peptidoglycan-binding LysM domain CGP3 region	0.01	0.01
cg1975		hypothetical protein, conserved CGP3 region	0.01	0.00
cg1976		hypothetical protein CGP3 region	0.02	0.00
cg1977		putative secreted protein CGP3 region	0.05	0.00
cg1978		hypothetical protein CGP3 region	0.07	0.00
cg1980		puative MoxR-like ATPase CGP3 region	0.05	0.00
cg1981		hypothetical protein CGP3 region	0.06	0.00
cg1982		putative ATPase with chaperone activity, ATP-binding subunit CGP3 region	0.05	0.00
cg1983		hypothetical protein CGP3 region	0.05	0.00
cg1984		hypothetical protein CGP3 region	0.05	0.00
cg1985		putative superfamily I DNA or RNA helicase CGP3 region	0.04	0.00

cg1986	hypothetical protein CGP3 region	0.05	0.00
cg1987	hypothetical protein CGP3 region	0.06	0.00
cg1988	hypothetical protein CGP3 region	0.05	0.00
cg1989	hypothetical protein CGP3 region	0.06	0.00
cg1990	putative NUDIIX hydrolase CGP3 region	0.11	0.00
cg1991	putative protein CGP3 region	0.07	0.00
cg1992	hypothetical protein CGP3 region	0.08	0.00
cg1993	hypothetical protein CGP3 region	0.02	0.00
cg1994	hypothetical protein CGP3 region	0.01	0.00
cg1995	hypothetical protein CGP3 region	0.01	0.00
cg1999	hypothetical protein CGP3 region	0.01	0.00
cg2000	putative membrane protein CGP3 region	0.24	0.01
cg2001	hypothetical protein, conserved CGP3 region	0.47	0.02
cg2002	hypothetical protein CGP3 region	0.35	0.00
cg2003	hypothetical protein, conserved CGP3 region	0.07	0.00
cg2004	puative protein, conserved CGP3 region	0.03	0.00
cg2005	putative protein-plasmid encoded, conserved CGP3 region	0.02	0.00
cg2006	hypothetical protein CGP3 region	0.06	0.00
cg2007	putative membrane protein CGP3 region	0.02	0.00
cg2008	putative membrane protein CGP3 region	0.01	0.00
cg2009	putative CLP-family ATP-binding protease CGP3 region	0.01	0.00
cg2010	putative permease of the major facilitator superfamily CGP3 region	0.01	0.01
cg2011	putative membrane protein CGP3 region	0.01	0.00
cg2012	putative secreted protein CGP3 region	0.01	0.02
cg2014	hypothetical protein CGP3 region	0.01	0.00
cg2015	hypothetical protein CGP3 region	0.03	0.00
cg2016	hypothetical protein CGP3 region	0.01	0.00
cg2017	hypothetical protein CGP3 region	0.01	0.00
cg2018	putative membrane protein CGP3 region	0.00	0.00
cg2019	putative membrane protein CGP3 region	0.01	0.00
cg2020	putative membrane protein CGP3 region	0.01	0.00
cg2021	putative protein, CGP3 region	0.01	0.01
cg2022	putative secreted protein CGP3 region	0.00	0.01
cg2023	putative membrane protein CGP3 region	0.03	0.00
cg2024	putative nuclease subunit of the excinuclease complex CGP3 region	0.12	0.01
cg2025	hypothetical protein CGP3 region	0.44	0.01
cg2026	hypothetical protein CGP3 region	0.29	0.01
cg2027	hypothetical protein CGP3 region	0.27	0.01
cg2028	hypothetical protein CGP3 region	0.25	0.00
cg2029	hypothetical protein CGP3 region	0.16	0.01
cg2030	hypothetical protein CGP3 region	0.14	0.01
cg2031	hypothetical protein, conserved CGP3 region	0.15	0.00
cg2032	putative membrane protein CGP3 region	0.01	0.00
cg2033	putative secreted protein CGP3 region	0.07	0.00
cg2034	hypothetical protein CGP3 region	0.21	0.00
cg2035	putative methyltransferase CGP3 region	0.25	0.01
cg2036	putative secreted protein CGP3 region	0.21	0.01
cg2037	hypothetical protein, conserved CGP3 region	0.18	0.00
cg2038	hypothetical protein CGP3 region	0.25	0.00
cg2039	hypothetical protein CGP3 region	0.39	0.01
cg2040	putative transcriptional regulator, HTH_3-family CGP3 region	0.44	0.00
cg2041	hypothetical protein CGP3 region	0.27	0.01
cg2042	putative secreted protein CGP3 region	0.30	0.01
cg2043	hypothetical protein, conserved CGP3 region	0.30	0.02
cg2044	putative secreted protein CGP3 region	0.30	0.01
cg2045	hypothetical protein CGP3 region	0.24	0.00
cg2046	hypothetical protein CGP3 region	0.34	0.01
cg2047	putative secreted protein CGP3 region	0.11	0.00
cg2048	hypothetical protein CGP3 region	0.07	0.01

cg2049		hypothetical protein CGP3 region	0.14	0.00
cg2050		hypothetical protein CGP3 region	0.14	0.01
cg2051		hypothetical protein CGP3 region	0.22	0.00
cg2052		putative secreted protein CGP3 region	0.29	0.00
cg2053		putative membrane protein CGP3 region	0.24	0.01
cg2054		putative membrane protein CGP3 region	0.21	0.01
cg2055		putative membrane protein CGP3 region	0.22	0.00
cg2056		putative membrane protein CGP3 region	0.17	0.00
cg2057		putative secreted protein CGP3 region	0.15	0.00
cg2058		hypothetical protein CGP3 region	0.16	0.00
cg2059		putative secreted protein CGP3 region	0.23	0.00
cg2060		hypothetical protein CGP3 region	0.26	0.01
cg2061	*psp3*	putative secreted protein CGP3 region	0.38	0.02
cg2062		putative protein, similar to plasmid-encoded protein PXO2.09 CGP3 region	0.01	0.00
cg2063		putative membrane protein CGP3 region	0.01	0.00
cg2064		putative DNA topoisomerase I omega-protein CGP3 region	0.00	0.00
cg2065		putative superfamily II DNA or RNA helicase CGP3 region	0.04	0.00
cg2066		putative low-complexity protein	0.10	0.01
cg2068		hypothetical protein CGP3 region	0.25	0.03
cg2069	*psp1*	putative secreted protein CGP3 region	0.15	0.00
cg2070	*' int2*	putative phage integrase C-terminal fragment, CGP3 region	0.02	0.00
cg2071	*int2'*	putative phage integrase N-terminal fragment, CGP3 region	0.02	0.00
cg2078	*msrB*	peptide methionine sulfoxide reductase-related protein	0.41	0.00
cg2080		hypothetical protein, conserved	0.35	0.03
cg2088		hypothetical protein	0.33	0.00
cg2089		hypothetical protein, conserved	0.30	0.02
cg2092	*SigA*	RNA polymerase sigma factor	0.50	0.03
cg2110		putative membrane protein	0.35	0.00
cg2125	*uraA*	putative uracyl permease	0.47	0.02
cg2136	*gluA*	glutamate uptake system, ABC-type, ATP-binding protein	2.32	0.00
cg2137	*gluB*	glutamate uptake system, secreted glutamate-binding protein	2.29	0.01
cg2138	*gluC*	glutamate uptake system, ABC-type, permease subunit 1	2.26	0.00
cg2181	*oppA*	ABC-type peptide transport system, secreted component	2.59	0.01
cg2182	*oppB*	ABC-type peptide transport system, permease component	2.74	0.00
cg2183	*oppC*	ABC-type peptide transport system, permease component	2.21	0.01
cg2258	*glnD*	PII uridylyl-transferase	2.05	0.00
cg2263		hypothetical protein	0.49	0.01
cg2283		hypothetical protein	2.17	0.04
cg2312	*gip*	putative hydroxypyruvate isomerase	0.46	0.01
cg2313	*idhA3*	myo-inositol 2-dehydrogenase	0.46	0.00
cg2324		hypothetical protein, conserved	2.07	0.00
cg2336		putative secreted protein	2.03	0.01
cg2349		putative ATPase component of ABC transporter for antiobiotics with duplicated ATPase domains	0.44	0.03
cg2374	*murE*	UDP-N-acetylmuramoylalanyl-D-glutamate-2,6-diaminopimelate ligase	0.48	0.03
cg2375	*ftsI*	penicillin-binding protein 2X	0.38	0.01
cg2376		putative secreted protein	0.24	0.01
cg2377	*mraW*	S-adenosyl-methyltransferase	0.20	0.00
cg2380		putative membrane protein	0.32	0.03
cg2392		hypothetical protein, conserved	2.01	0.00
cg2430		hypothetical protein	2.46	0.00
cg2435		putative protein synthesis inhibitor, putative ss-mRNA endonuclease	2.17	0.00
cg2438		hypothetical protein	2.68	0.00
cg2440		putative permease of the major facilitator superfamily	2.31	0.00
cg2449		putative protein	0.46	0.00
cg2461	*tnp4a*	transposase	0.28	0.00
cg2467		putative branched-chain amino acid ABC transporter ATP-binding protein	2.34	0.00
cg2481		hypothetical protein, conserved	2.20	0.00

cg2487		hypothetical protein, conserved	2.03	0.00
cg2504		hypothetical protein, conserved	0.14	0.00
cg2509	*recO*	DNA repair protein	0.44	0.00
cg2556		putative iron-regulated membrane protein	0.48	0.02
cg2557		putative secondary Na+/bile acid symporter, bile acid:Na+ symporter BASS-family	2.62	0.01
cg2564		hypothetical protein	0.48	0.01
cg2610		putative ABC-type dipeptide/oligopeptide/nickel transport system, secreted component	6.11	0.00
cg2616	*vanA*	vanillate demethylase, oxygenase subunit	2.15	0.01
cg2617	*vanB*	vanillate demethylase, subunit	2.15	0.00
cg2618	*vanK*	transporter vanillate/protocatechuate	2.25	0.00
cg2629	*pcaB*	β-carboxy-cis,cis-muconate cycloisomerase	2.11	0.01
cg2630	*pcaG*	protocatechuate dioxygenase α subunit	2.00	0.01
cg2631	*pcaH*	protocatechuate dioxygenase β subunit	2.01	0.01
cg2633		putative restriction endonuclease	0.07	0.00
cg2635	*catB*	chloromuconate cycloisomerase	2.03	0.00
cg2636	*catA1*	catechol 1,2-dioxygenase	6.51	0.01
cg2637	*benA*	benzoate 1,2-dioxygenase α subunit aromatic ring hydroxylation dioxygenase A	14.79	0.03
cg2638	*benB*	benzoate dioxygenase small subunit	16.66	0.03
cg2639	*benC*	benzoate 1,2-dioxygenase ferredoxin reductase subunit	9.78	0.02
cg2642	*benK*	putative benzoate transport protein	13.42	0.02
cg2643	*benE*	benzoate membrane transport protein, benzoate:H+ symporter BenE-family	2.95	0.02
cg2666		hypothetical protein	2.27	0.00
cg2667		hypothetical protein	2.01	0.00
cg2674		putative alkylhydroperoxidase AhpD-family core domain	2.26	0.00
cg2675		putative ATPase component of ABC-type transport system, contains duplicated ATPase domains	2.80	0.00
cg2676		putative ABC-type dipeptide/oligopeptide/nickel transport systems, permease component	2.73	0.00
cg2677		putative ABC-type dipeptide/oligopeptide/nickel transport system, permease component	2.67	0.01
cg2678		putative ABC-type dipeptide/oligopeptide/nickel transport systems, secreted component	2.39	0.02
cg2683		hypothetical protein, conserved	0.14	0.00
cg2699		putative copper resistance protein D	0.44	0.04
cg2719		putative enterochelin esterase	0.46	0.03
cg2733		putative HNH nuclease	0.49	0.00
cg2739		putative permease of the major facilitator superfamily	0.33	0.00
cg2750		putative membrane protein, conserved	0.35	0.00
cg2828		putative membrane protein	0.29	0.01
cg2836	*sucD*	succinyl-CoA synthetase α subunit, ADP-forming	2.53	0.00
cg2837	*sucC*	succinyl-CoA synthetase subunit β, ADP-forming	2.53	0.00
cg2884		putative dipeptide/tripeptide permease	0.44	0.00
cg2922		putative transcriptional regulator, IclR-family	0.31	0.00
cg2927	*scrB*	putative sucrose-6-phosphate hydrolase, β-fructofuranosidase	2.27	0.00
cg2959		putative secreted protein	2.21	0.00
cg2965		putative transcriptional regulator, AraC-type	2.17	0.01
cg2966		putative phenol 2-monooxygenase	4.41	0.00
cg2971	*lmrb*	lincomycin resistance protein	0.47	0.04
cg3020		putative membrane protein	0.47	0.01
cg3044	*glnX*	glutamine uptake or metabolism	0.50	0.01
cg3067		putative membrane protein	2.45	0.00
cg3074		putative transcriptional regulator, conserved	0.50	0.00
cg3096	*ald*	aldehyde degyhdrogenase	4.86	0.00
cg3107	*adhA*	Zn-dependent alcohol dehydrogenase	4.23	0.01
cg3126	*tctB*	citrate uptake transporter, membrane subunit	2.16	0.00
cg3127	*tctC*	citrate uptake transporter, substrate binding protein	2.01	0.00
cg3134		putative ABC-type putative cobalt/sugar, queuosine-regulated ECF transporter, transmembrane component STY3231 of energizing module	0.37	0.01

cg3135		putative ABC-type putative cobalt/sugar, queuosine-regulated ECF transporter, substrate-specific component STY3230	0.49	0.01
cg3138	*ppmA*	putative membrane-bound protease modulator	0.36	0.02
cg3139		hypothetical protein, conserved	0.32	0.03
cg3140	*tagA1*	putative DNA-3-methyladenine glycosylase I protein	0.35	0.01
cg3141	*hmp*	flavohemoprotein	0.37	0.00
cg3143		putative secreted protein, conserved	0.47	0.02
cg3195		putative flavin-containing monooxygenase FMO	7.67	0.00
cg3211		putative secreted protein	0.29	0.01
cg3216	*gntP*	gluconate permease, gluconate:H+ symporter GntP-family	2.87	0.00
cg3234		putative metal-dependent amidase/aminoacylase/carboxypeptidase	0.43	0.03
cg3236	*msrA*	peptide methionine sulfoxide reductase	0.40	0.02
cg3260		putative membrane protein	0.29	0.01
cg3272		putative membrane protein	0.39	0.05
cg3274		putative site-specific recombinases, DNA invertase Pin homolog-fragment, putative pseudogene	0.32	0.02
cg3275	*fdxA*	ferredoxin no. 1	0.50	0.00
cg3286		putative secreted protein of unknown function	0.29	0.01
cg3287	*copO*	secreted multicopper oxidase	0.43	0.03
cg3297	*tnp19a*	transposase fragment, putative pseudogene	0.37	0.00
cg3303		putative transcriptional regulator, PadR-like-family	0.30	0.01
cg3304	*dnaB*	replicative DNA helicase	0.32	0.01
cg3306	*rplI*	50S ribosomal protein L9	0.44	0.03
cg3307	*ssb*	single-strand DNA-binding protein	0.41	0.04
cg3308	*rpsF*	30S ribosomal protein S6	0.41	0.04
cg3319		hypothetical protein, conserved	0.50	0.01
cg3329		hypothetical protein, conserved	0.19	0.00
cg3330		putative secreted protein	0.47	0.01
cg3338		putative membrane protein	0.40	0.02
cg3348		putative plasmid maintenance system antidote protein, HigA homolog	0.23	0.00
cg3382		putative dipeptide/tripeptide permease	0.45	0.00
cg3405		putative NADPH quinone reductase or Zn-dependent oxidoreductase	0.38	0.00
cg4005		putative secreted protein	2.31	0.00
cg4007		hypothetical protein	0.24	0.00

Erklärung

Ich versichere an Eides Statt, dass die Dissertation von mir selbständig und ohne unzulässige fremde Hilfe unter Beachtung der „Grundsätze zur Sicherung guter wissenschaftlicher Praxis an der Heinrich-Heine-Universität Düsseldorf“ erstellt worden ist. Die Dissertation wurde in der vorgelegten oder ähnlichen Form noch bei keiner anderen Institution eingereicht. Ich habe bisher keine erfolglosen Promotionsversuche unternommen.

Jennifer Pahlke

Acknowledgements

I like to thank Prof. Michael Bott for giving me the opportunity to perform my PhD thesis in the Institute of Bio and Geosciences, IBG-1: Biotechnology.

I also like to thank Prof. Rolf Wagner for being my second referee.

I thank Dr. Tino Polen for giving me the opportunity to work in his research group in a perfect equipped working environment and for being my supervisor.

I thank CLIB-GC and the Ministry of Innovation Science and Research of NRW for financial support.

Special thanks go to Sabine Schneider for being such a friendly cooperation partner.

Moreover, I thank my colleagues Nadine, Markus, Sabrina, Ulli, Jan, Nicolai, Andi and Michael for the pleasant working atmosphere, for the fun in the coffee breaks, their patience and for answering every of my questions.

My special thanks go to Abigail who was always open for discussion and for her never ending motivation and ethusiasm.

I also thank Meike for always being there for helpful discussions and always having a good advice.

I thank Doris for introducing me into the fascinating world of yoga.

Finally, I like to thank my brothers Alexander and Markus, my sister Stefanie and especially my parents Marina and Alfred, for being the most important persons in my life, for giving me love and fortitude to overcome any hurdle on my way and for always believing in me and my work.

Band / Volume 62
Regulatorische Aspekte der Expression und Sekretion heterologer Proteine in *Corynebacterium glutamicum*
A. R. Chattopadhyay (2013), VIII, 195 pp
ISBN: 978-3-89336-845-7

Band / Volume 63
***Gluconobacter oxydans* strain development: Studies on central carbon metabolism and respiration**
J. Richhardt (2013), III, 181 pp
ISBN: 978-3-89336-851-8

Band / Volume 64
Metabolic Engineering von *Corynebacterium glutamicum* für die Produktion einer Dicarbonsäure
A. Otten (2013), 98 pp
ISBN: 978-3-89336-860-0

Band / Volume 65
Rapid Development of Small-Molecule producing Microorganisms based on Metabolite Sensors
S. Binder (2013), 138 pp
ISBN: 978-3-89336-872-3

Band / Volume 66
Increasing the NADPH supply for whole-cell biotransformation and development of a novel biosensor
S. Solvej (2013), 130 pp
ISBN: 978-3-89336-900-3

Band / Volume 67
Expression, purification and biophysical characterization of human Presenilin 2
G. Yang (2013), 159 pp
ISBN: 978-3-89336-928-7

Band / Volume 68
Modifikationen der Atmungskette in *Corynebacterium glutamicum* und Rolle des Flavohämoproteins Hmp
L. Platzen (2013), IV, 119 pp
ISBN: 978-3-89336-931-7

Band / Volume 69
L-Cystein-Bildung mit *Corynebacterium glutamicum* und optische Sensoren zur zellulären Metabolitanalyse
K. Hoffmann (2014),vi, 83 pp
ISBN: 978-3-89336-939-3

Band / Volume 70
Metabolic engineering of Corynebacterium glutamicum for production of the adipate precursor 2-oxoadipate
M. Spelberg (2014), 118 pp
ISBN: 978-3-89336-954-6

Band / Volume 71
Design and application of metabolite sensors for the FACS-based isolation of feedback-resistant enzyme variants
G. Schendzielorz (2014), 129 pp
ISBN: 978-3-89336-955-3

Band / Volume 72
The development and application of a single cell biosensor for the detection of L-methionine and branched-chain amino acids
N. Mustafi (2014), 137 pp
ISBN: 978-3-89336-956-0

Band / Volume 73
Metabolic engineering of *Corynebacterium glutamicum* for production of L-leucine and 2-ketoisocaproate
M. Vogt (2014), VI, 92 pp
ISBN: 978-3-89336-968-3

Band / Volume 74
Pupylierung in *Corynebacterium glutamicum*
A. Küberl (2014), VI, 163 pp
ISBN: 978-3-89336-969-0

Band / Volume 75
Tat-translocase composition in *Corynebacterium glutamicum* and the effect of TorD coexpression
D. Oertel (2014), v, 117 pp
ISBN: 978-3-89336-996-6

Band / Volume 76
The 6C RNA of *Corynebacterium glutamicum*
J. Pahlke (2014), II, 144 pp
ISBN: 978-3-95806-003-6

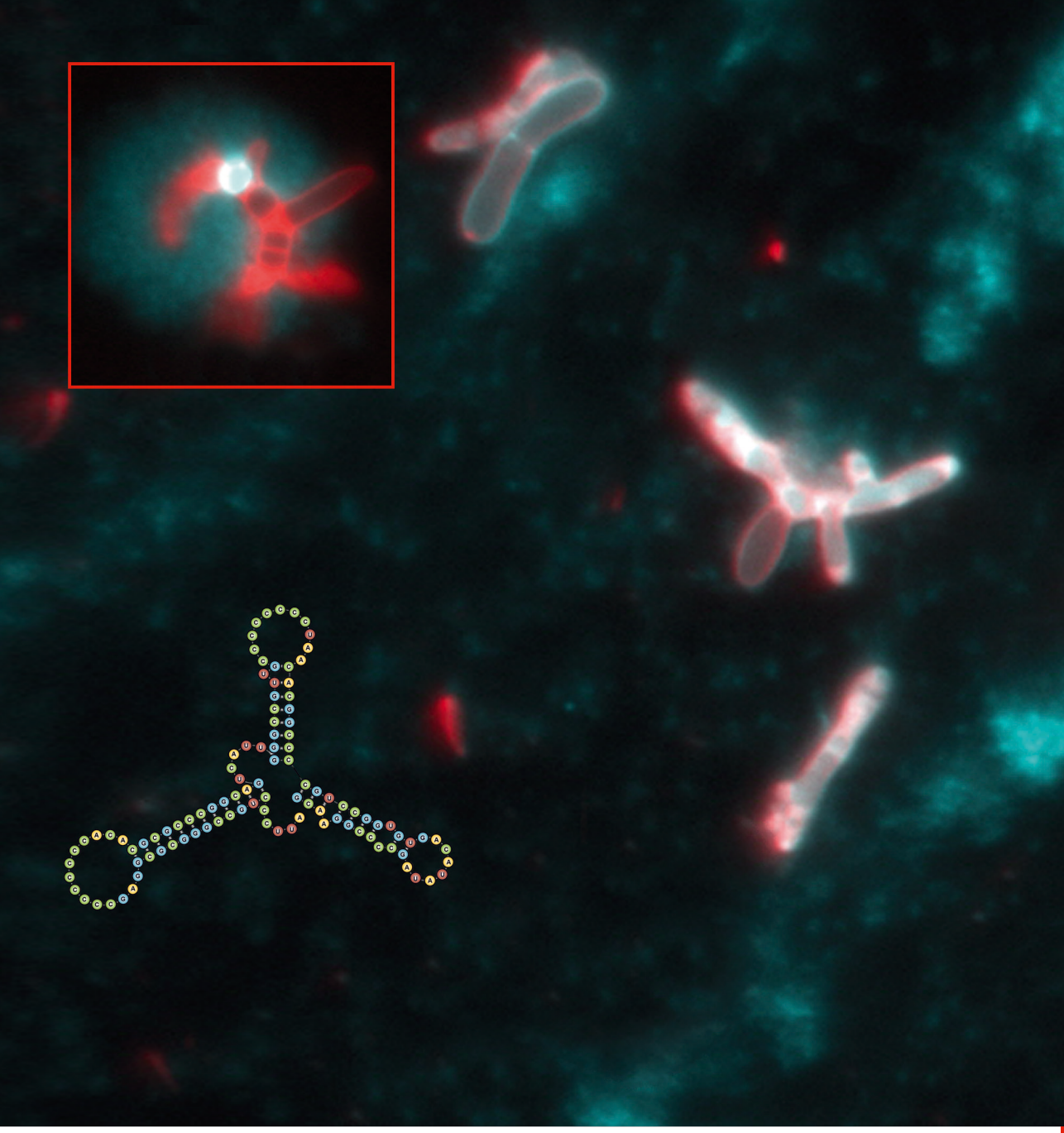

Gesundheit / Health
Band / Volume 76
ISBN 978-3-95806-003-6

JÜLICH
FORSCHUNGSZENTRUM